UNIVERSIDADE DE LISBOA
FACULDADE DE MEDICINA DE LISBOA

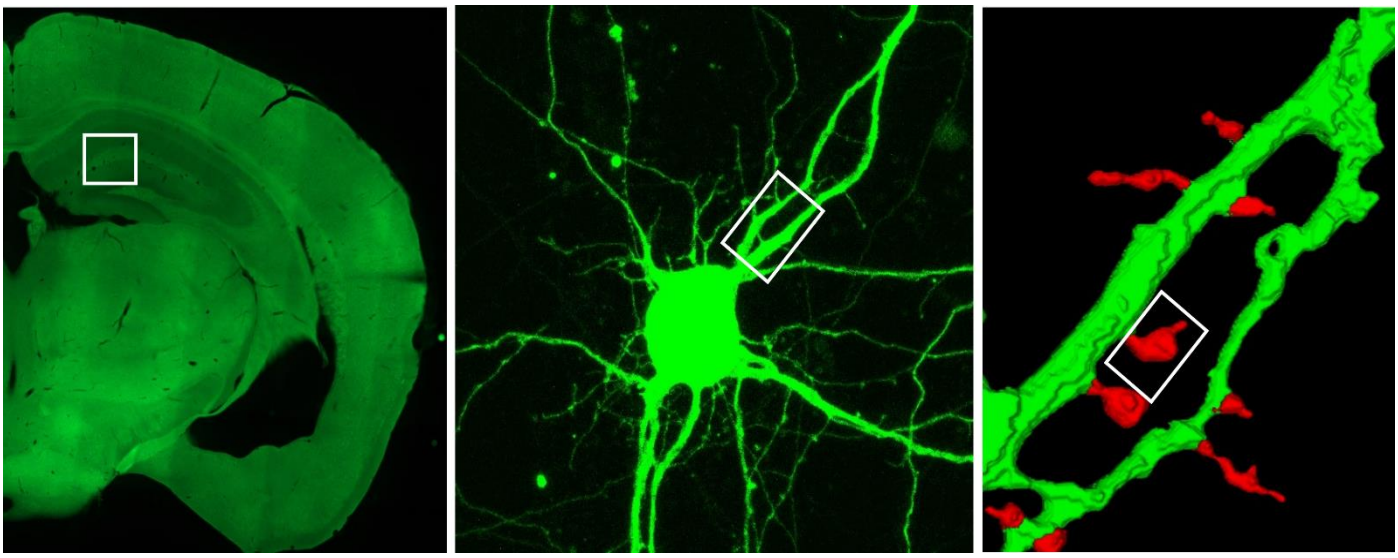

MECHANISMS UNDERLYING THE PHYSIOLOGICAL ROLE OF AMYLOID PRECURSOR PROTEIN IN GLUTAMATERGIC SYNAPSES

JOANA ISABEL RAJÃO SARAIVA

Orientadores: Prof. Doutora Luísa Maria Vaqueiro Lopes

Prof. Doutora Paula Antunes Pousinha

Tese especialmente elaborada para obtenção do grau de Doutor em Ciências Biomédicas, Especialidade em Neurociências

2023

UNIVERSIDADE DE LISBOA
FACULDADE DE MEDICINA DE LISBOA

MECHANISMS UNDERLYING THE PHYSIOLOGICAL ROLE OF AMYLOID PRECURSOR PROTEIN IN GLUTAMATERGIC SYNAPSES

JOANA ISABEL RAJÃO SARAIVA

Orientadores: Prof. Doutora Luísa Maria Vaqueiro Lopes
Prof. Doutora Paula Antunes Pousinha
Tese especialmente elaborada para obtenção do grau de Doutor em Ciências Biomédicas, Especialidade em Neurociências

Júri:

Presidente: Doutor Mário Nuno Ramos de Almeida Ramirez, Professor Associado com Agregação e Vice-Presidente do Conselho Científico da Faculdade de Medicina da Universidade de Lisboa

Vogais:
- PhD David Blum, Senior Research Director da Université de Lille (France);

- Doutora Ana Luísa Monteiro de Carvalho, Professora Associada da Faculdade de Ciências e Tecnologia da Universidade de Coimbra;

- Doutor Alexandre Valério de Mendonça, Professor Catedrático Convidado da Faculdade de Medicina da Universidade de Lisboa;

- Doutora Luísa Maria Vaqueiro Lopes, Professora Associada Convidada com Agregação da Faculdade de Medicina da Universidade de Lisboa (Orientadora);

- Doutor Domingos Manuel Pinto Henriques, Investigador Auxiliar da Faculdade de Medicina da Universidade de Lisboa.

This work was supported by Santa Casa da Misericórdia (MB-7-2018). JR Saraiva is a FCT/PhD fellow (iMM Lisbon BioMed PhD Program): PD/BD/135516/2018 and COVID/BD/152606/2022, funded by FCT and República Portuguesa/Ciência, Tecnologia e Ensino Superior.

The experimental work herein described was performed at:

Instituto de Medicina Molecular João Lobo Antunes, Faculdade de Medicina da Universidade de Lisboa

University Côte d' Azur, Centre National de la Recherche Scientifique (CNRS) UMR 7275, Institut de Pharmacologie Moléculaire et Cellulaire (IPMC), 06560 Valbonne, France

The work has been discussed and evaluated by the Thesis Committee members: Prof. Doutora Ana Luísa Carvalho, Prof. Doutor Sérgio de Almeida and Prof. Doutora Vanessa Morais.

As opiniões expressas nesta publicação são da exclusiva responsabilidade do seu autor, não cabendo qualquer responsabilidade à Faculdade de Medicina da Universidade de Lisboa pelos conteúdos nele apresentados.

A impressão desta dissertação foi aprovada pelo Conselho Científico da Faculdade de Medicina de Lisboa em reunião de 21 de março de 2023.

Agradecimentos

Há quem diga que fazer o Doutoramento é como andar de montanha-russa, devido aos momentos altos e baixos por que passamos. Eu diria que fazer o Doutoramento com uma pandemia pelo meio é mais parecido com uma queda livre: de repente perdemos o nosso chão e não sabemos como aterrar em segurança. Por isso, quero agradecer a todos os que foram o meu paraquedas durante esta viagem. Sou uma sortuda por estar rodeada de pessoas fantásticas que me guiaram e apoiaram durante estes anos.

Quero agradecer às minhas orientadoras Luísa e Paula por me terem dado a oportunidade de participar neste projeto, por tudo o que me ensinaram e pela preocupação e disponibilidade que sempre demonstraram, do início ao final da tese. Além disso, quero agradecer aos dois grupos onde trabalhei no iMM e no IPMC por me terem acolhido da melhor forma possível e por contribuírem todos os dias para um ambiente de trabalho fantástico.

Às minhas queridas mentoras Mariana e Joana Coelho: foi um privilégio poder aprender e trabalhar convosco. Não só são cientistas brilhantes, como pessoas incríveis e uma grande inspiração para mim.

Às minhas coleguinhas de casa (Bárbara, Inês e Joana): que sorte que foi partilhar estes anos convosco. Obrigada por todas as vezes em que rimos às gargalhadas (mas também pelas vezes em que choramos) todas juntas na cozinha. Vocês são as maiores!

Ao Carlitos, por ser um amigo gigante, que tantas vezes me salvou as experiências e ouviu os meus desabafos nas viagens de carro, mas também por todas as ideias que tivemos juntos e pela nossa dupla imbatível como representantes.

À Ana, pela ajuda preciosa que me deu quando mais precisei e por me fazer crescer como cientista e como pessoa.

Aos meus queridos BioMeds: parece que foi ontem que nos encontramos pela primeira vez na sala de aula prontos para começar o doutoramento. Obrigada pelos jantares e conversas, foi fantástico partilhar este percurso convosco.

Quero também enviar um ‘merci’ ao grupinho dos almoços no IPMC, que me acolheu em França e me fez sentir mais em casa.

A todos os que me ajudaram quando as técnicas no laboratório não estavam a funcionar e me deram força para continuar, em especial à Dalila, Isaura, Bia, Luís e João e aos vários grupos do iMM que tanto me apoiaram (ASebastiao, LSaude, VMorais, SAlmeida) e que certamente vão ter saudades dos meus imm-gerais. Foi incrível fazer parte da comunidade do iMM, pela união, boa disposição e disponibilidade que todos têm.

Um agradecimento muito grande às ‘facilities’ incríveis que temos no iMM, incluindo as unidades de Bioimaging e Rodents, que me deram um apoio essencial durante este projeto. Queria também agradecer à Filipa Nunes e ao training hub, pela ajuda incansável que dão aos alunos de Doutoramento. Por fim, um agradecimento enorme ao meu comité de tese, que me deu input valioso e sempre se mostrou disponível para ajudar.

Não posso deixar de agradecer às pessoas fantásticas que conheci na Champalimaud e que tanto me ajudaram nesta fase final do Doutoramento. Um beijinho muito especial à Teresa, pela compreensão e generosidade.

Gostava ainda de agradecer aos meus professores e orientadores de Mestrado, por todos os ensinamentos, orientação e por me transmitiram esta paixão pelo mundo da investigação.

Aos meus queridos amigos: os que tenho a sorte de ter há mais de 10 anos, o grupo maravilhoso que se juntou no mestrado e os que conheci durante o Doutoramento, muito obrigada por me aturarem e me darem tanta força!

Ao Miguel: mal sabias no que te estavas a meter quando me conheceste e eu te disse que estava a fazer o Doutoramento! Foste tu a dar-me força quando saía tarde do laboratório, a dar-me um abracinho quando as experiências não corriam bem e a dizer ‘está quase’ quando parecia que não ia conseguir acabar. Obrigada por tudo.

Por fim: à minha família. Aos meus pais e às minhas irmãs: por serem o meu paraquedas todos os dias, com a vossa força, apoio incondicional e conselhos sábios. Se cheguei até aqui, foi por causa de vocês.

Ao meu avô por todas as vezes que me ligou quando saía tarde do laboratório e à minha avó por me ter ensinado que o importante é gostarmos do que fazemos.

Esta tese não é só minha. É vossa também.

Table of Contents

Abbreviation list i
Abstract iv
Resumo vi
Publications ix
1 Introduction 1
1.1 Prologue 2
1.2 Literature review 7
1.2.1 NMDA receptors properties 8
A) How do ionotropic NMDA receptors become activated? 8
B) Which synaptic responses are mediated by NMDAR activation? 9
C) How does the NMDAR structure relate to its synaptic functions? 10
D) Does subunit composition influence NMDAR synaptic function? 13
E) Does the GluN2B/A ratio change with age? 15
F) Are there age-dependent alterations in NMDAR functions and properties? 18
G) Which factors regulate NMDAR synaptic content? 27
1.2.2 APP as a putative regulator of NMDARs 32
A) Integrating APP domains with its functions 35
B) APP binding partners modulate its function 37
C) APP is located at synaptic terminals 39
D) APP trafficking and processing 40
E) Why is it challenging to study APP physiological roles at the synapse? 43
F) Which mouse models have been used to study APP physiological functions? 48
G) APP regulates synaptic adhesion and synaptogenesis 52
H) APP regulates glutamatergic transmission, synaptic plasticity and memory 55
I) Which are the physiological/pathological roles of APP-derived fragments? 60
J) Is AICD a transcription regulator? 63
1.3 Hypothesis and aims 65
2 Methods 68
2.1 Models 69
2.2 Protocols 71
A) Human and mouse samples 71
B) Patch Clamp electrophysiology 72
C) Protein analysis 74

D) APP knockdown in primary neuronal cultures 78
E) Statistical Analysis 83
2.3 Supplementary Protocols 84
A) Prediction of aminoacid disorder in the structure of APP and NMDAR subunits 84
B) AICD incubation in mouse primary neuronal cultures 84
C) AAV-shAPP production and validation 87
2.4 Supporting information 89
A) Patch-Clamp electrophysiology 89
B) Fractionation into PSD-enriched fractions 92
C) Western Blotting (APP and APP-derived fragments) 93
3 Results 96
3.1 Does APP regulate NMDARs in immature and mature synapses? 98
A) APP interacts with the predominant NMDAR subtypes in immature and mature synapses 98
B) APP is highly abundant in immature synapses, where it regulates NMDAR currents through the intracellular domain 103
C) APP modulates the NMDAR synaptic content in immature synapses 107
3.2 Does APP regulate NMDARs in aged synapses? 111
A) APP interaction with NMDARs is maintained upon aging 111
B) Aged mice exhibit an increase in the relative contribution of GluN2B-NMDAR synaptic currents 115
C) APP processing contributes to the increase in GluN2B-NMDAR relative currents upon aging 117
D) Interfering with APP intracellular signaling normalizes the GluN2B-NMDAR contribution in aged mice 121
E) APP interacts with NMDARs in humans and tends to be more processed upon aging 123
3.3 Summary 128
3.4 Supplementary Results 130
A) Prediction of aminoacid disorder in the structure of APP and NMDAR subunits 130
B) Transcriptional effects of AICD in primary neuronal cultures 131
C) Production and validation of a viral vector to knockdown APP *in vivo* 133
4 Conclusions 135
4.1 Discussion 136
4.2 Future perspectives 149
4.3 Graphical Abstracts 152
5 References 154

6 Appendix.. 190

Abbreviation list

3xTg-AD - Triple transgenic mouse model of Alzheimer's Disease
AAV – Adeno-associated virus
ABD - Agonist-binding domain
AC - Adenylate cyclase
AD – Alzheimer's Disease
ADAM10 - Disintegrin and metalloproteinase domain-containing protein 10
AICD - APP intracellular domain
AMPA – α-Amino-3-hydroxy-5-methyl-4isoxazolepropionic acid
AMPAR – α-Amino-3-hydroxy-5-methyl-4isoxazolepropionic acid receptor
ANOVA – Analysis of variance
AP5 - 2-Amino-5-phosphonopentanoic acid
APLP1 - Amyloid precursor-like protein 1
APLP2 - Amyloid precursor-like protein 2
APP - Amyloid precursor protein
APPswe - amyloid precursor protein with Swedish mutation
Aslow - amplitude of the slow component
ATD - Amino-terminal domain
Aβ – amyloid beta
BACE1 - β-site APP-cleaving enzyme 1
BI – BACE1 inhibitor
BSA – Bovine serum albumin
C57BL6/J – "Black Six" or B6 Strain Mice
CA1 – Cornu ammonis 1
CA2 – Cornu ammonis 2
Ca^{2+} - Calcium
CA3 – Cornu ammonis 3
CaMKII – Calcium calmodulin dependent protein kinase II
cAMP – 3'-5'-cyclic adenosine monophosphate
cDKO - Double conditional knockout
CTD - C-terminal domain
CTFs - APP C-terminal fragments
CTFα – APP C-terminal fragment α
CTFβ – APP C-terminal fragment β
cTKO - Triple conditional knockout
CTR – Control
CypA – Cyclophilin A
DG – Dentate gyrus

DIV - Days *in vitro*

DM - Double mutant

DMEM – Dulbecco's modified Eagle's medium

DNQX - 6,7-Dinitro-1,4-dihydroquinoxaline-2,3-dione

DTT – Ditiotreitol

E (n) - Embryonic day (n)

EDTA – Ethylenediaminetetraacetic acid

EPSCs - Excitatory postsynaptic currents

ER - Endoplasmic reticulum

fAD - Familial Alzheimer's Disease

FBS – Fetal bovine serum

fEPSP – Field Excitatory postsynaptic potential

GABA – Gamma-aminobutyric acid

GAPDH - Glyceraldehyde 3-phosphate

GSK3β - Glycogen synthase kinase 3β

HBSS – Hank's balanced salt solution

HEK293 - Human embryonic kidney 293 cells

HRP – Horseradish peroxidase

Ifen - Ifenprodil

IPTG - Isopropyl β-D-1-thiogalactopyranoside

KD - Knockdown

KDa – Kilodaltons

KI - Knock-in

KO - Knockout

LRP1 - Low-density lipoprotein receptor-related protein 1

LTD – Long-term depression

LTP – Long-term potentiation

MAGUK - Membrane-associated guanylate kinase

MAPT- Microtubule-associated protein tau

mRNA - Messenger RNA

MWM – Morris water maze

NaCl – Sodium chloride

NMDA - N-Methyl-D-aspartate

NMDAR - N-methyl-D-aspartate receptors

NS1 – Non-silencing sequence

P(n) – Postnatal day (n)

PBS – Phosphate buffered saline

PFA – Paraformaldehyde

pGluN2B – Phosphorylated GluN2B

PKA – Protein kinase A

PSD – Postsynaptic density

PSD-95 - Postsynaptic density protein 95

PSEN - Presenilin

PSEN1 - presenilin-1

PTB1-p – PTB1 peptide

PTB2-p - PTB2 peptide

PTMs - Posttranslational modifications

PVDF -Polyvinylidene fluoride

RIPA – Radioimmunoprecipitation assay buffer

ROI - Region of interest

RT – Room temperature

RT-qPCR - Real-time quantitative polymerase chain reaction

SAP-102 - Synapse-associated protein 102

sAPPα - Secreted APP α

sAPPβ - Secreted APP β

SCR - Scramble

SDS – Sodium dodecyl sulfate

SEM – Standard error of mean

shAPP - Short-hairpin RNA against APP

shCTR – Short-hairpin RNA control

shRNA - Short-hairpin RNA

TBS – Tris buffered saline

TGN - Trans-Golgi network

Tip60 - Tat-interactive protein 60

TMD - Transmembrane domain

WT – Wild-type

Zn^{2+} - Zinc

τweighted - weighted component

Abstract

N-methyl-D-aspartate receptors (NMDARs) are glutamatergic ionotropic receptors essential for synaptic maturation during development and synaptic plasticity in adult stages, whose properties are known to change depending on the life stage.

In particular, the subunit composition of synaptic NMDARs has important implications for NMDAR function. In the hippocampus, NMDARs are mainly composed by GluN2A or GluN2B subunits, with GluN2B-NMDARs being associated with slower kinetics, more calcium charge transfer and higher mobility.

GluN2B-NMDARs are predominant in immature synapses during development, contributing to the synaptic maturation process, which involves a GluN2B to GluN2A shift. Thus, GluN2A-NMDARs are the most abundant subtype in adult stages, when most synapses are in the mature state. Much less is known about the subunit contribution in aged synapses. However, previous reports showed age-related alterations in NMDAR properties, such as slower responses, lower current amplitudes and a negative correlation between GluN2B levels and memory performance.

These alterations in NMDAR properties, from development to aging, might be caused by different regulation mechanisms. The amyloid precursor protein (APP), which is mainly known to be involved in Alzheimer's Disease, has emerged as a putative regulator of NMDARs. Although the physiological role of APP is not fully understood, it is known to regulate synaptogenesis and synaptic plasticity and might have different effects when acting through the full-length protein or its derived fragments. Additionally, APP has shown to interact and regulate NMDAR surface levels and currents but the functional relevance of this interaction at different life stages, as well as the underlying mechanisms of regulation have not been explored so far.

Thus, we hypothesized that APP regulates NMDARs in an age-dependent manner and defined as the main aims of this work to study APP-NMDAR regulation mechanisms in immature, mature and aged synapses. To address these questions in physiological conditions, we used as our experimental models the hippocampus of wild-type C57Bl/6 mice at different life stages (infant (7-10 days), adults (10-16 weeks) and aged (18 – 20 months), as well as postmortem brain tissue from human subjects with different ages (18-89 years old) and rodent hippocampal primary neuronal cultures.

By combining patch-clamp electrophysiology and molecular approaches, we have unraveled a dual mechanism by which APP controls GluN2B-NMDARs, depending on

the life stage. In the present study, we show that APP is highly abundant at the post synapse in infant mice, where it interacts with GluN2B-NMDARs, controlling its mediated currents. Moreover, APP knockdown in primary neuronal cultures caused a reduction in GluN2B-NMDAR synaptic content, suggesting that APP might be important to stabilize the receptors at the synapse. Considering the crucial role of GluN2B-NMDAR in synapse maturation, this mechanism might potentially be important to achieve functional, mature synapses during development.

Although this interaction is maintained in adult/aged synapses, NMDAR-mediated currents showed to be unaltered when interfering with the APP C-terminal during a short period at these ages, contrary to the results obtained in infant mice. Thus, we concluded that the APP-NMDAR regulatory mechanisms are different in adult/aged mice when compared to infants.

We hypothesize that alterations in the APP-NMDAR regulation could be the underlying mechanism for age-related alterations in NMDAR properties. Accordingly, we found that aged mice exhibit an increase in GluN2B-NMDAR relative currents, which does not correlate with alterations in subunit levels. Moreover, we found an increase in APP processing into intracellular fragments upon aging. Importantly, when we inhibited APP processing or interfered with APP intracellular signaling in aged mice, we were able to normalize GluN2B-NMDAR synaptic contribution to adult-like levels. Thus, we propose that signaling pathways mediated by APP intracellular fragments induce an increase in GluN2B-NMDAR relative currents upon aging. Additionally, we show that APP processing into intracellular fragments also tends to increase in aged humans, suggesting that a similar mechanism might occur in mice and humans. Considering the impact of NMDAR on synaptic plasticity, this increase in GluN2B-NMDAR relative currents can potentially contribute to age-related synaptic and memory impairments.

Key words: APP (amyloid precursor protein), NMDA receptor, aging, postnatal development, glutamatergic synapse

Resumo

Os recetores N-metil-D-aspartato (NMDARs) são recetores glutamatérgicos ionotrópicos, que desempenham um papel fundamental na maturação e plasticidade sinápticas, sendo que as suas propriedades são influenciadas pela composição das subunidades e sofrem alterações ao longo da idade.

No hipocampo, os recetores NMDA sinápticos pertencem maioritariamente ao subtipo GluN2A ou GluN2B, sendo que o subtipo GluN2B-NMDA está associado a uma cinética mais lenta, maior transferência de carga por cálcio e uma maior mobilidade.

Os recetores GluN2B-NMDA são abundantes nas sinapses imaturas durante o desenvolvimento e contribuem para o processo de maturação sináptica, fase na qual os recetores GluN2A-NMDAR passam a ser predominantes. Apesar da informação em relação à contribuição relativa destas subunidades para o funcionamento neuronal no envelhecimento ser limitada, já se comprovou que as propriedades dos recetores NMDA se alteram em idades mais avançadas. Em modelos de roedores, os recetores respondem de forma mais lenta e apresentam menor amplitude de correntes. Além disso, existe uma correlação negativa entre os níveis de GluN2B e as capacidades de memória/ aprendizagem em ratinhos envelhecidos.

Estas alterações que ocorrem ao longo da idade podem ser causadas por modificações nos mecanismos de regulação dos NMDARs. Em particular, a proteína precursora de amiloide (PPA), extensivamente estudada por estar envolvida na Doença de Alzheimer, pode funcionar como reguladora dos NMDARs. Apesar de a função fisiológica desta proteína não ser ainda totalmente compreendida, sabe-se que a PPA desempenha um papel importante na sinaptogénese e plasticidade sináptica. Sabe-se ainda que a PPA atua não só na sua forma integral, mas também através dos fragmentos que se geram quando é clivada. Além disso, foi previamente demonstrado que a PPA interage com os recetores NMDA e tem a capacidade de regular os seus níveis na membrana plasmática e as suas correntes. No entanto, a relevância funcional desta interação, bem como os mecanismos de regulação ao longo da idade são ainda desconhecidos.

Assim sendo, a nossa hipótese é que a PPA regula os recetores NMDA de uma forma dependente da idade. Logo, definimos como o principal objetivo deste trabalho estudar os mecanismos de regulação dos recetores NMDA pela PPA em sinapses imaturas, maduras e envelhecidas. De forma a explorar estes mecanismos em condições fisiológicas, utilizamos como modelos experimentais o hipocampo de ratinhos C57Bl/6

‘wild-type’ com diferentes idades (período pós-natal (7-10 dias), idade adulta (10-16 semanas) e idade avançada (18 – 20 meses), culturas primárias de neurónios de rato do hipocampo, bem como amostras de tecido cerebral (córtex) humano obtidas postmortem de indivíduos com idades compreendidas entre 18 e 89 anos.

Neste trabalho utilizamos uma combinação de métodos de eletrofisiologia Patch-Clamp e estudos moleculares, levando à conclusão de que a modulação exercida pela PPA na função dos recetores GluN2B-NMDA apresenta mecansimos diferentes consoante a idade.

Os nossos resultados em ratinhos durante o desenvolvimento pós-natal mostraram que a PPA é muito abundante na pós-sinapse, onde interage com os recetores GluN2B-NMDA e controla as suas correntes. Além disso, quando induzimos o silenciamento da PPA em culturas primárias de neurónios, observamos uma redução na percentagem de subunidades GluN2B que se encontram na pós-sinapse, sugerindo que a PPA pode estabilizar estes recetores na sinapse. Tendo em conta o papel fundamental dos recetores GluN2B-NMDA para a maturação sináptica, é possível que este mecanismo seja importante para obter sinapses funcionais e maduras durante o desenvolvimento.

Apesar da interação entre a PPA e os NMDAR se manter em sinapses de ratinhos adultos e envelhecidos, nestas idades não observamos alterações nas correntes mediadas por NMDARs quando interferimos de forma aguda com o C-terminal da PPA, ao contrário do que observamos durante o desenvolvimento pós-natal. Logo, concluímos que os mecanismos de regulação PPA-NMDAR são diferentes em idades adultas/envelhecidas, quando comparadas com fases de desenvolvimento.

De acordo com a nossa hipótese, o envelhecimento poderá levar a alterações na regulação PPA-NMDAR, contribuindo para alterações nas propriedades dos NMDARs em idades avançadas. De facto, verificamos que os ratinhos nestas idades apresentam um aumento na contribuição relativa das correntes sinápticas mediadas por GluN2B-NMDARs. Nestas mesmas idades, observamos um aumento do processamento da PPA, gerando níveis mais elevados de fragmentos intracelulares. Quando inibimos o processamento da PPA ou interferimos com a sinalização mediada pelo domínio intracelular da PPA em ratinhos envelhecidos, observamos a normalização das correntes relativas mediadas por GluN2B-NMDARs para valores semelhantes aos registados em idade adulta.

Assim sendo, os nossos dados indicam que as vias de sinalização induzidas pelos fragmentos intracelulares derivados da PPA levam a um aumento das correntes

relativas GluN2B-NMDARs em idades avançadas. Uma vez que provamos que o processamento da PPA está também aumentado com o envelhecimento em amostras de tecido cerebral humano, podemos especular que o mecanismo poderá ocorrer de forma semelhante em ambas as espécies. Além disso, tendo em conta o papel crucial dos NMDARs na plasticidade sináptica, é possível que este aumento nas correntes relativas GluN2B-NMDA possa contribuir para os défices sinápticos e de memória associados ao envelhecimento.

Palavras-chave: PPA (proteína precursora de amiloide), recetor NMDA, envelhecimento, desenvolvimento pós-natal, sinapse glutamatérgica

Publications

Publications related to this dissertation

Rajão-Saraiva, J., Dunot, J., Ribera, A., Temido-Ferreira, M., Coelho, J. E., König, S., Moreno, S., Enguita, F. J., Willem, M., Kins, S., Marie, H., Lopes, L. V., & Pousinha, P. A. (2022). Age-dependent NMDA receptor function is regulated by the amyloid precursor protein. *Aging Cell*, *00*, e13778. https://doi.org/10.1111/acel.13778
*(In the appendix, **Section 6**)*

Other publications (during the PhD)

Pousinha PA, Mouska X, Bianchi D, Temido-Ferreira M, Rajão-Saraiva J, Gomes R, Fernandez SP, Salgueiro-Pereira AR, Gandin C, Raymond EF, Barik J, Goutagny R, Bethus I, Lopes LV, Migliore M, Marie H. (2019) The Amyloid Precursor Protein C-Terminal Domain Alters CA1 Neuron Firing, Modifying Hippocampus Oscillations and Impairing Spatial Memory Encoding. Cell Rep. 29:317-331.e5. doi: 10.1016/j.celrep.2019.08.103. PMID: 31597094.

1 Introduction

1.1 Prologue

“All ideas in science were born in the dramatic conflict between reality and our attempts to understand it.”

Albert Einstein

From synaptic plasticity to NMDA receptors

One of the most important and fascinating properties of the mammalian brain is its plasticity, i.e. its ability to constantly adapt depending on our experiences (Costandi, 2016). We can consider the communication between neurons as a dynamic combination of conversations (synapses) happening at the same time, as illustrated in **Figure 1.1**. Using this analogy, the plasticity of the synapses would be the ability to 'initiate or stop a certain conversation' or 'adjust the volume of each conversation', depending on the context.

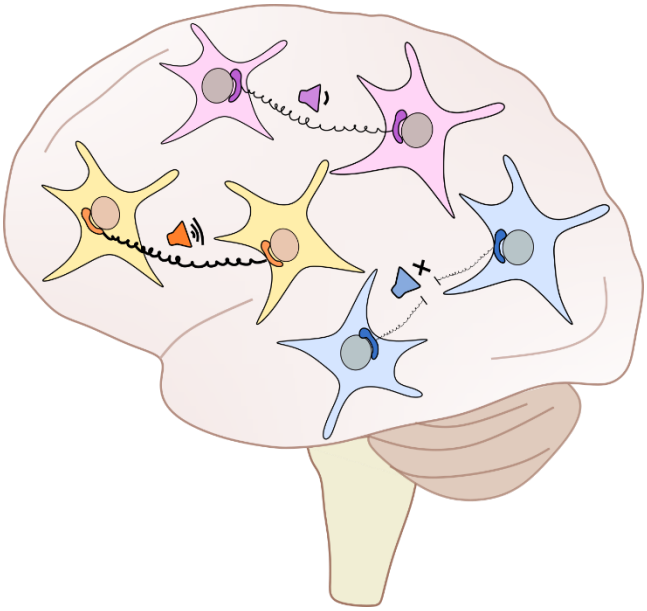

Figure 1.1 – Illustration of synapses as dynamic 'conversations' between neurons. The volume settings illustrate the synaptic strength of each connection. Adapted from (Ludwig, 2017).

This plasticity might occur at the structural level, by forming new connections (synaptogenesis) and eliminating others. Although synaptogenesis occurs throughout a healthy person's lifespan, it is more predominant during early brain development, as shown in **Figure 1.2** (Huttenlocher & Dabholkar, 1997). In fact, during our first years of life, we are highly sensitive to all types of environmental stimuli and experience, we absorb and process a great amount of information and ultimately learn complex skills (sensory processing, language ang cognitive functions) (Berardi et al., 2000, Goldman-Rakic, 1987). This is why the formation of new synaptic connections is so important at this stage, leading to the establishment of neuronal networks. Thus, we can consider the

synaptogenic stage as the phase when the brain ‘initiates multiple conversations’ at the same time.

To make these networks functional, the most active connections are selected for reinforcement and maturation, while the weaker ones disappear (Huttenlocher et al., 1982). Thus, the synaptic maturation stage involves the selection of “conversations” that should be maintained in the brain.

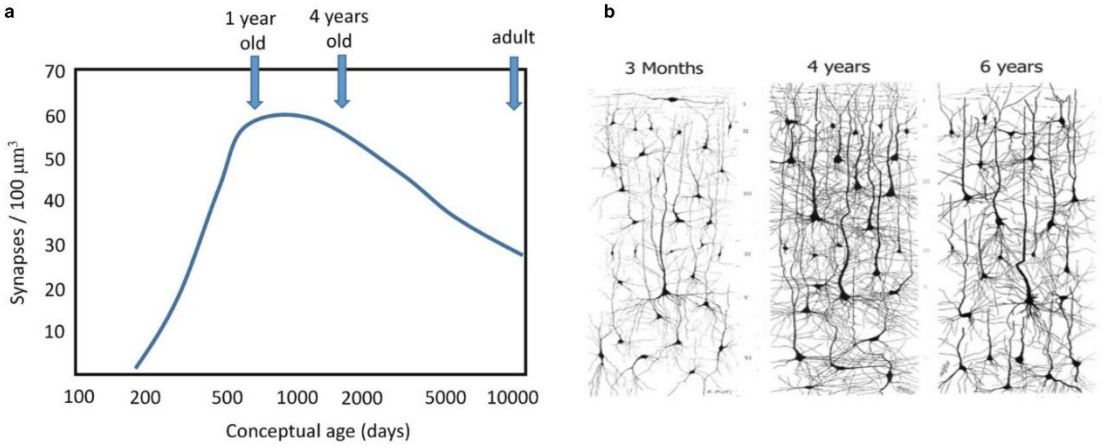

Figure 1.2 – **Alterations in synaptic density from development to adulthood**.

a) The temporal profile of synapse density in the human neocortex. The synapse density reaches the peak at 1–4 years after birth and declines gradually after that. Adapted from (Okabe, 2020),

b) Golgi-impregnated neurons in the primary auditory cortex from children at different postnatal ages. Adapted from (Kral & Pallas, 2011).

When we become adults, most of our synapses are in the mature state, but maintain their plasticity at the functional level. The ability of synapses to be strengthened or weakened in response to increasing or decreasing activity levels is called synaptic plasticity and is essential for our adaptation, learning and memory skills (Citri & Malenka, 2008). The synaptic strength can be seen as the volume settings of each ‘conversation’, which are not static. Increasing or decreasing the synaptic strength is like ‘tuning up or down the volume control’, thus helping to determine which ‘conversations’ are more important and should be ‘heard’ at a given time.

If synaptic plasticity mechanisms become dysregulated, then it might be harder to distinguish the ‘important conversations from the overall noise’. This is likely what happens upon aging. Contrary to what was initially thought, the cognitive decline associated with normal aging is not attributed to significant neuronal loss but is rather a result from changes in synaptic connectivity and plasticity (Burke & Barnes, 2006).

The mechanisms that govern the synaptic maturation process during development, the synaptic plasticity in mature synapses and its age-associated impairments are still not completely understood. When these processes occur in glutamatergic synapses, the main excitatory synapses in the brain, they depend on an important molecular player: the NMDA receptors (NMDARs). These postsynaptic receptors are activated upon glutamate release and consist of ion channels permeable to calcium (Ca^{2+}). They are crucial for synaptic maturation and plasticity since they convert patterns of neuronal activity into synaptic alterations (Pérez-Otaño & Ehlers, 2004).

In fact, NMDARs act as coincidence detectors during synaptic maturation stages, being activated when pre and postsynaptic activity occur at the same time. Therefore, NMDAR activation works as a signal for synaptic maturation and stabilization, leading to alterations in their composition and function, as illustrated in **Figure 1.3** (Shi et al., 1999, Durand & Konnerth, 1996).

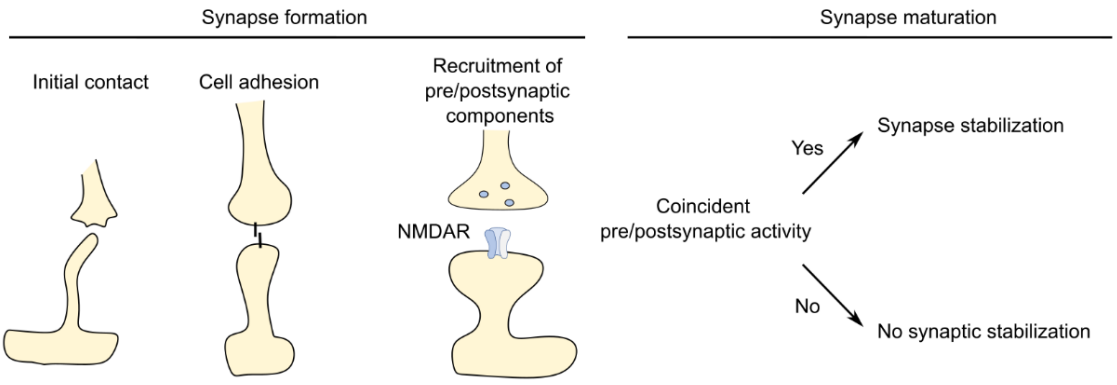

Figure 1.3 – Mechanisms of synapse stabilization.

Once the initial synapse is established, activities of the pre- and postsynaptic membrane need to be synchronized, i.e., the postsynaptic membrane needs to respond to presynaptic neurotransmitter release. Synchronization stabilizes the synapse, whereas failure to synchronize leaves the postsynaptic membrane unstable, which leads to a retraction and elimination of the synapse. Adapted from (Konradi & Heckers, 2003)

In mature synapses, the stimulation frequency and the consequent NMDAR-mediated Ca^{2+} influx, determines which synapses become potentiated or depressed, as shown in **Figure 1.4**. Potentiation is a persistent synaptic strengthening leading to a long-lasting increase in signal transmission between neurons, whereas depression is a long-lasting reduction in synaptic strength (Citri & Malenka, 2008).

In response to high-frequency stimulation, the calcium influx through NMDARs is maximal, which activates intracellular signaling cascades that ultimately lead to long-term synaptic potentiation (LTP), which involves receptor insertion at the post-synapse.

In contrast, low-frequency stimulation causes modest increases in postsynaptic calcium, triggering the removal of receptors from the post-synapse and inducing long-term depression (LTD).

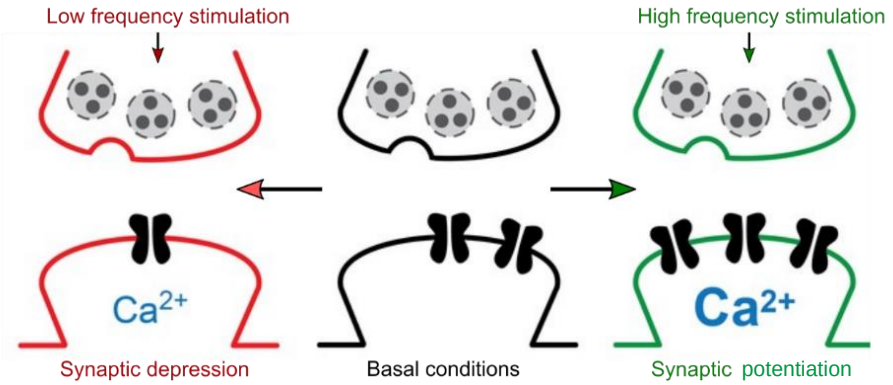

Figure 1.4 – Different patterns of electrical stimulation induce bidirectional changes in synaptic efficacy.

High-frequency stimulation induces long-term synaptic potentiation (LTP), leading to an increase in signal transmission. In contrast, prolonged low-frequency stimulation induces long-term synaptic depression (LTD), i.e. a decrease in synaptic transmission. These changes in synaptic efficacy are mediated, in part, by changes in levels of intracellular calcium through NMDARs. Adapted from (Plasticity lab, n.d.).

Considering the crucial role of NMDARs for synaptic maturation and plasticity, we hypothesize that NMDAR properties, functions and regulation mechanisms might suffer alterations throughout our life, possibly becoming dysregulated upon aging.

1.2 Literature review

1.2.1 NMDA receptors properties

A) How do ionotropic NMDA receptors become activated?

N-methyl-D-aspartate receptors (NMDARs) belong to the glutamatergic ionotropic receptor family, consisting of ion channels whose opening is favored by glutamate binding. The family of ionotropic glutamatergic receptors can be subdivided into three types named after their selective agonists: NMDA, α-amino-3-hydroxy-5-methyl-4-isoxazole propionic acid (AMPA) and kainate (KA) receptors (Kew & Kemp, 2005), as depicted in **Figure 1.5**.

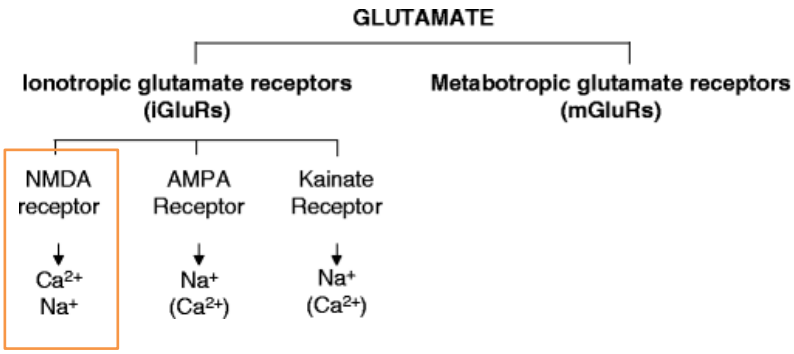

Figure 1.5 – Schematic representation of the different types of glutamatergic receptors.

Adapted from (Kew & Kemp, 2005).

NMDAR activation is ligand and voltage-dependent, since it requires the binding of glutamate (agonist) and a co-agonist (glycine/D-serine) (Oliet & Mothet, 2009), as well as sufficient cell depolarization. Accordingly, at resting potential, the extracellular magnesium (Mg^{2+}) ions work as a break, by binding to the receptor and blocking ion flux through the channel. Depolarization of the cell removes the Mg^{2+} break, thus allowing current flow (Nowak et al., 1984).

Therefore, NMDARs act as coincidence detectors for pre- and postsynaptic activity since receptor activation requires glutamate release (at the pre-synaptic terminal) and strong membrane depolarization (post-synaptic cell). The current-voltage curves for the NMDA receptor at normal Mg^{2+} concentrations and in the absence of this ion are represented in **Figure 1.6**.

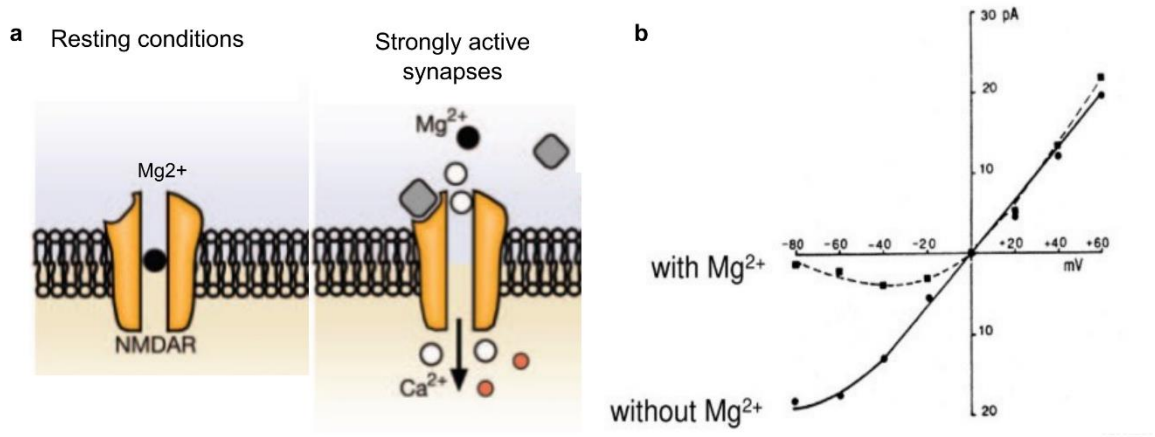

Figure 1.6 - NMDAR voltage-dependent block by magnesium (Mg^{2+})

a) Under conditions of rest or low levels of input activity, the channel of the NMDA receptor is blocked by magnesium ions (Mg^{2+}). High concentrations of glutamate released at a strongly active synapse produce strong depolarization of the post-synaptic membrane, resulting in the expulsion of Mg^{2+} ions from the NMDAR channel, allowing ion influx. Adapted from (Cooke & Bliss, 2006).

b) Glutamate-induced currents in the whole-cell recordings. The current-voltage curve for the NMDAR at normal Mg^{2+} concentrations (0.5 mM), is non-linear, contrary to the condition in the absence of Mg^{2+}. At resting potentials (-70mV) NMDARs are largely blocked by Mg^{2+}. Adapted from (Nowak et al., 1984).

B) Which synaptic responses are mediated by NMDAR activation?

When the necessary conditions for NMDAR activation occur, the receptors suffer a conformation change, leading to channel opening, a strong influx of sodium (Na^{+}) and calcium (Ca^{2+}) and small efflux of potassium (K^{+}) ions. Therefore, the net effect is the depolarization of the postsynaptic neuron (Lüscher & Malenka, 2012).

Compared to other glutamatergic ionotropic receptors, NMDARs exhibit high Ca^{2+} permeability (Burnashev, 1998). Accordingly, a substantial fraction of the current through NMDARs is carried by Ca^{2+} ions (fractional Ca^{2+} current, ~10%) (Garaschuk et al., 1996) and can lead to large Ca^{2+} accumulations in dendritic spines (Sobczyk et al., 2005).

Therefore, besides contributing to depolarization, NMDARs couple electrical synaptic activity to biochemical signaling via activation of Ca^{2+}-dependent enzymes and downstream signaling pathways. For example, high frequency stimulation causes a large influx of calcium through NMDARs, leading to the activation of kinases (such as calcium/calmodulin kinase II (CaMKII)) and the downstream insertion of AMPARs into the synapse (Sanhueza et al., 2011). In contrast, low frequency stimulation and the consequent calcium entry through NMDARs leads to the activation of phosphatases

including the calcium/calmodulin dependent phosphatase (calcineurin), inducing the endocytosis of AMPARs (Mulkey et al., 1994).

The high affinity for glutamate and slow kinetics of NMDARs allow them to decode synaptic input patterns over prolonged periods (Patneau & Mayer, 1990, Traynelis et al., 2010). Accordingly, NMDARs can remain open for hundreds of milliseconds after presynaptic release of glutamate (Vicini et al., 1998, Lester et al., 1990), whereas AMPARs current decays much faster (a few milliseconds) (Mosbacher et al., 1994). Thus, calcium influx through NMDARs can lead to long-term changes in synaptic strength, through LTP of LTD and contribute to learning and memory processes. The synaptic processes that occur upon NMDAR activation are summarized in **Figure 1.7**.

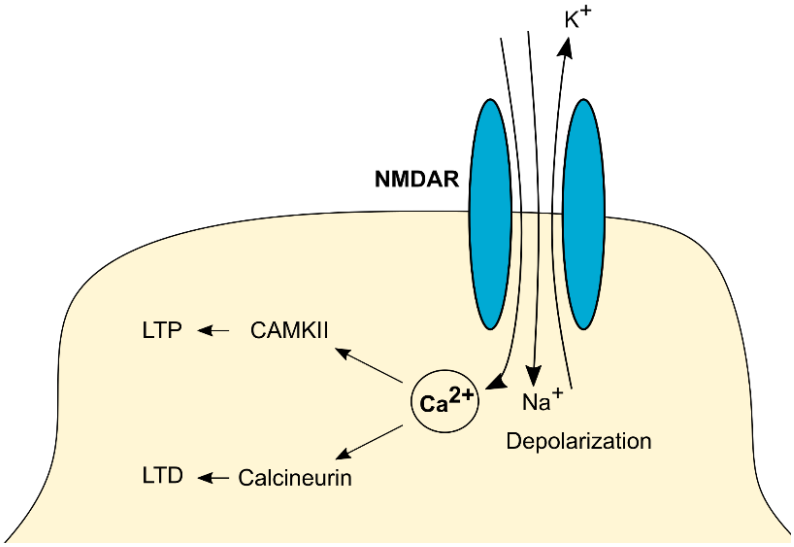

Figure 1.7 – Synaptic responses mediated by NMDAR activation. The ionotropic function of NMDARs causes depolarization through monovalent cation flux and through calcium influx, which activates downstream calcium-dependent pathways, including LTP and LTD.

C) How does the NMDAR structure relate to its synaptic functions?

NMDARs consist of large complexes of four homologous subunits, which belong to one of these families: GluN1 (8 isoforms due to alternative splicing), GluN2 (subunits A-D) and GluN3 (subunits A and B) (Paoletti & Neyton, 2007), as depicted in **Figure 1.8a**. Most NMDARs in the brain are heteromeric receptors usually consisting of two GluN1 (obligatory subunit) and two GluN2 subunits (regulatory subunit), as represented in **Figure 1.8b**.

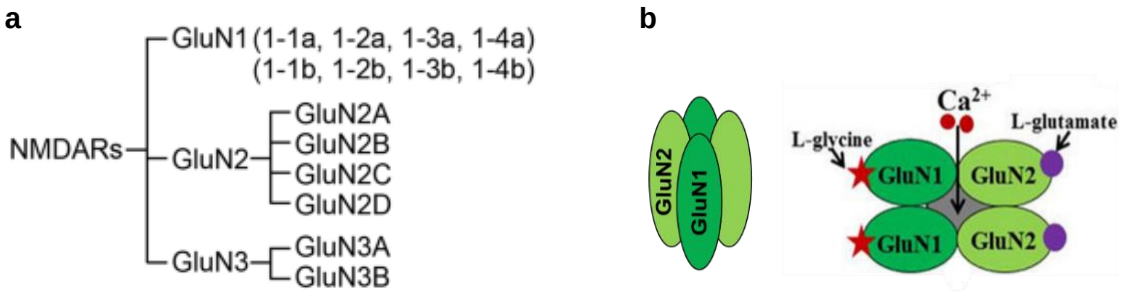

Figure 1.8 – NMDAR subunits and their organization into heteromeric receptors.

a) List of different NMDAR subunits. Adapted from (W. Zhang et al., 2022).

b) Organization of NMDAR subunits into heteromeric receptors, usually containing two GluN1 and two GluN2 subunits. Adapted from (Kumar, 2015).

All NMDAR subunits share a structure composed of four distinct domains as illustrated in **Figure 1.9**:

- Amino-terminal domain (ATD) - important for subunit assembly
- Ligand-binding domain (LBD) or agonist-binding domain – glutamate, glycine and D-serine binding sites
- Transmembrane domain (TMD) - contains the ion channel, composed by 3 membrane-spanning domains (M1, M3, M4) and a re-entrant pore loop (M2) which form the ion channel.
- C-terminal domain (CTD) - involved in receptor trafficking, anchoring and intracellular signaling.

X-ray crystallography and cryogenic electron microscopy (cryo-EM) have revealed the atomic structures of the extracellular (ATD and LBD) and transmembrane domains (Karakas & Furukawa, 2014, Lü et al., 2017). In contrast, the CTDs do not contain any known domains beyond short recognition motifs, involved in binding to other proteins (Warnet et al., 2021), as illustrated in **Figure 1.9**.

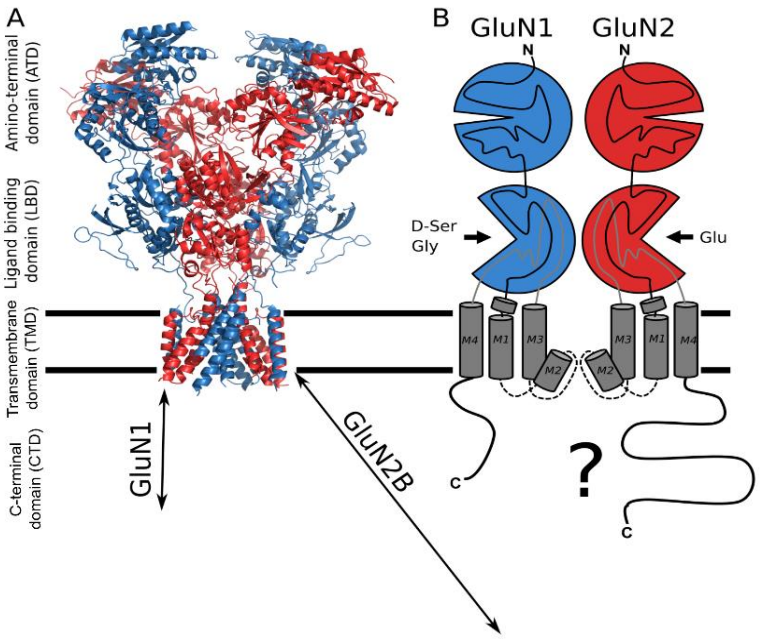

Figure 1.9 - Overview of the NMDA receptor domain structure

a) Crystal structure of the rat GluN1/GluN2B (pdb: 4PE5) ((Karakas & Furukawa, 2014) shows the overall heterotetrameric structure of the NMDA receptor without the CTDs. Assuming that the CTD has a compaction typical of intrinsically disordered proteins, the GluN2A/B CTDs are expected to have a radius of gyration of about the dimension the extracellular domains, which suggests that CTD spans a range more than twice a large.

b) Sketch of the topology of the conserved fold of ionotropic glutamate receptors. M2 does not span the membrane but forms a re-entrant channel-lining segment. The LBD includes the loop between M3 and M4, providing tight coupling between the LBD and the transmembrane domain.

Adapted from (Warnet et al., 2021).

The length of the CTD varies dramatically between paralogues, from ~ 50 residues for the shortest isoform of GluN1 up to 660 residues for the GluN2B CTD. The lack of a 3D stable structure suggests that CTDs belong to the class of intrinsically disordered regions, which are characterized by establishing transient interactions with multiple targets (Warnet et al., 2021, Kjaergaard & Kragelund, 2017). In fact, several binding partners are known to interact with the CTDs of NMDAR subunits, as illustrated in **Figure 1.10**.

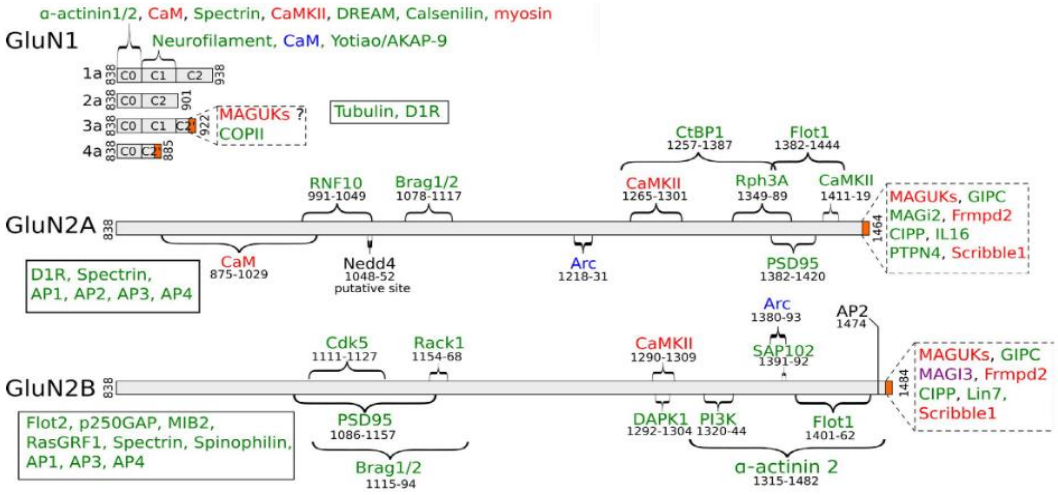

Figure 1.10 - Protein interactions mapped biochemically to the GluN1, GluN2A and GluN2B C-terminal domain. Adapted from (Warnet et al., 2021)

D) Does subunit composition influence NMDAR synaptic function?

In higher brain structures (hippocampus and cortex), GluN2A and GluN2B are the predominant regulatory subunits (Monyer et al., 1994). In each NMDA receptor, the respective GluN2 subunits can be identical or different, giving rise to diheteromeric and tri-heteromeric receptors (Al-Hallaq et al., 2007, Rauner & Köhr, 2011).

The GluN2 subtype dictates NMDAR properties thus influencing their mediated responses. Despite the 70% amino acid sequence homology (C. C. Wang et al., 2011), GluN2B and GluN2A confer specific properties to NMDARs, as reviewed in (Yashiro & Philpot, 2008). When compared to GluN2A, GluN2B-NMDA receptors exhibit:

- Lower open probability and peak currents (Erreger et al., 2005) .

- Slower rising and decaying times, thus staying open for a longer time (Vicini et al., 1998) (**Figure 1.11 a**).

- More charge (approximately 2-fold) for a single synaptic event (Erreger et al., 2005) and more Ca^{2+} per unit of current (Sobczyk et al., 2005).

- Higher affinity for CAMKII binding, which is essential for LTP (Mayadevi et al., 2002).

- Higher mobility, diffusing in the dendritic shaft, spine neck and head, whereas GluN2A–NMDAR are mostly confined in the postsynaptic density (PSD) located at the spine head (Groc et al., 2006) (**Figure 1.11 b**).

- Higher affinity for the antagonist Ifenprodil (>400-fold selectivity for GluN2B-NMDAR compared to GluN2A-NMDARs (Williams, 1993) and its derivatives (such as Ro 25-6981) (Karakas et al., 2011). In contrast, TCN-201 (3-chloro-4-fluoro-N-[(4-[(2-(phenylcarbonyl)hydrazino)carbonyl]phenyl)methyl]benzenesulfonamide) and zinc (Zn^{2+}) act as antagonists with higher selectivity for GluN2A when compared to GluN2B-NMDARs (Hansen et al., 2012, Rachline et al., 2005).

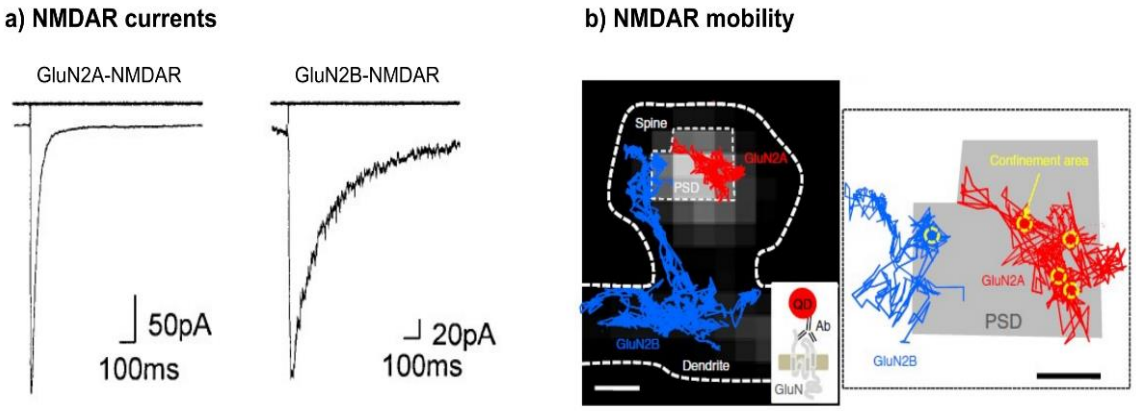

Figure 1.11 – GluN2A and GluN2B-NMDARs exhibit different properties, including deactivation kinetics and mobility.

a) NMDA channel currents obtained by Patch-Clamp after 1-ms applications of L-glutamate (1 mM) to human embryonic kidney 293 cells (HEK-293) transfected with distinct NMDA receptor subunits. Adapted from (Vicini et al., 1998).

b) On the left: Representative trajectories (50 s duration) of a surface GluN2A- (red trace) and GluN2B– (blue trace) NMDAR in the spine of a hippocampal neuron. The surface GluN2 subunit were imaged over time using single Quantum Dot (QD) tracking approach (inset, lower right). Each of the trajectories represents the diffusion of a single particle-receptor complex. The GluN2A–NMDAR is confined in the postsynaptic density (PSD), located at the spine head. The GluN2B–NMDAR diffuses in the dendritic shaft, spine neck and head, in which it is transiently retained. Scale bar=200 nm. On the right: Enlarged view of the PSD area and the surface GluN2A– and GluN2B–NMDAR trajectories. Note the presence of high confinement areas (yellow circle) in PSD part of trajectories, particularly evident for the GluN2A–NMDAR. Scale bar=100 nm. Adapted from (Bard & Groc, 2011).

Therefore, the synaptic GluN2B/GluN2A ratio determines the consequences of NMDAR activation, including total calcium influx and downstream signaling. Both GluN2B and GluN2A-NMDARs contribute to synaptic plasticity, learning and memory. However, given their different properties, the GluN2B/GluN2A ratio might influence the threshold for LTP/LTD induction. Accordingly, in GluN2B-rich synapses a modest response is expected to elevate Ca^{2+} and activate CaMKII to a level sufficient to induce LTP, lowering the threshold for LTP induction (Yashiro & Philpot, 2008), as illustrated in **Figure 1.12**.

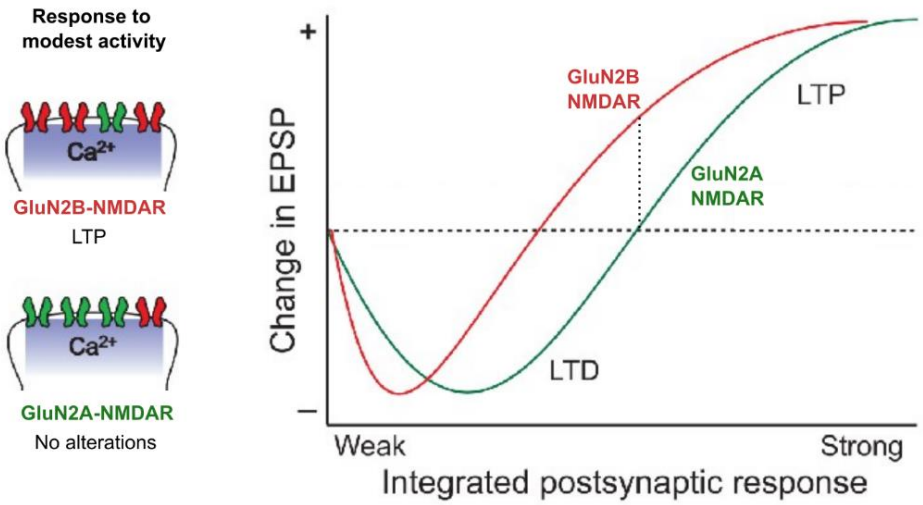

Figure 1.12 - Hypothetical model of synaptic plasticity regulation by NMDAR subunits

On the left: A model to explain why the LTD/LTP induction threshold may differ between synapses which predominantly have GluN2B-NMDARs (upper) or GluN2B-NMDAR (lower image). In these two synapses, the same frequencies of stimulation will produce different outcomes in synaptic plasticity. In GluN2B-NMDAR rich synapses, large amounts of Ca^{2+} can enter the spine through NMDARs in response to synaptic stimulation and/or the calcium is more likely to activate CaMKII. Therefore, modest synaptic activity is more likely to stimulate LTP.

On the right: The graph represents the level of the integrated postsynaptic response in the x-axis (which is related to the frequency of synaptic activation), while the y-axis represents the lasting change in synaptic strength. In GluN2B-NMDAR rich synapses, the LTD-LTP crossover point (θm) shifts to the left, favoring LTP over LTD. Adapted from (Yashiro & Philpot, 2008).

This GluN2B/GluN2A ratio is not static, changing in response to neuronal activity and sensory experience during postnatal development, (Bellone & Nicoll, 2007, Quinlan et al., 1999, Philpot et al., 2001, Yashiro et al., 2005), but also in adult synapses (Baez et al., 2013, Carta et al., 2018). Thus, depending on the physiological context, synapses adapt their GluN2-NMDAR signaling to modulate their integrative capacity.

E) Does the GluN2B/A ratio change with age?

While the GluN1 subunit is ubiquitously expressed in the brain at all ages, GluN2 subunit composition varies across brain regions and throughout time, influencing the GluN2B/A ratio (illustrated in **Figure 1.13**).

Major changes in the expression patterns of these GluN2 subunits occur during the first postnatal weeks in rodents. The GluN2A subunit gradually increases after birth,

becoming abundantly expressed in the brain. In contrast, GluN2B expression is observed at high levels during embryonic development and following birth, peaks around the first postnatal weeks (postnatal days (P) 7–10), being also expressed during adulthood (Williams et al., 1993, Monyer et al., 1994). Therefore, during early postnatal development in rodents, NMDARs change their subunit composition from primarily containing GluN2B subunits to predominantly containing GluN2A subunits (GluN2B→GluN2A switch) as illustrated in **Figure 1.13a** (X. B. Liu et al., 2004). This subunit exchange is observed throughout the brain and also occurs in humans (**Figure 1.13b**) (Law et al., 2003, Jantzie et al., 2015).

Much less is known about the impact of aging on the GluN2B/A ratio, with most studies reporting a decline in mRNA/protein levels of NMDAR subunits, which seems to be more pronounced for GluN2B, as reviewed in (Kumar, 2015).

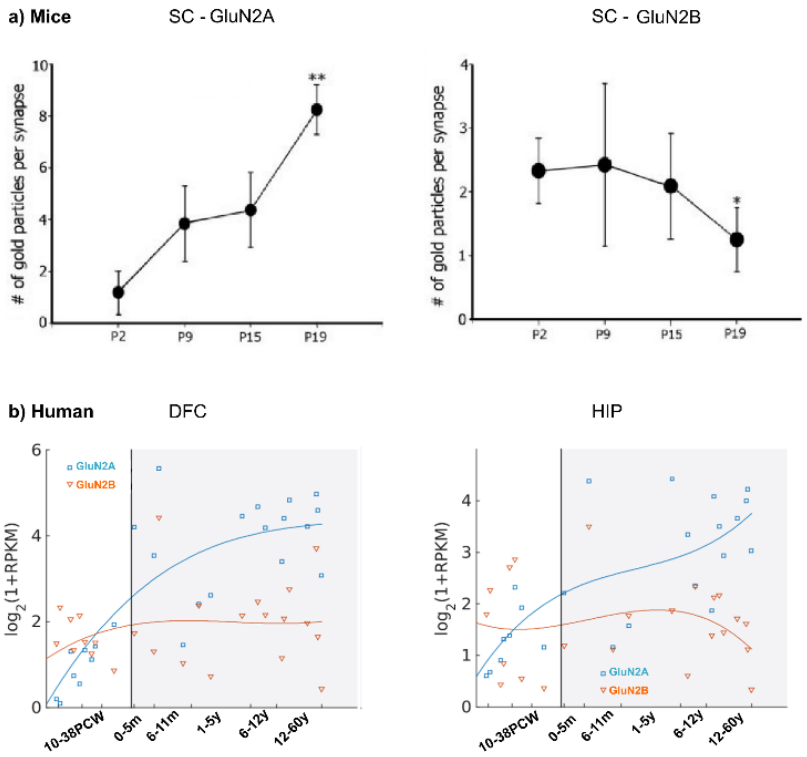

Figure 1.13 – Temporal expression/synaptic levels of GluN2A and GluN2B in mice and humans

a) Resuls obtained from GluN2A and GluN2B detection by postembedding immunogold electron microscopy in layer IV of somatosensory cortex (SC) during postnatal development (P2-P19). Adapted from (X. B. Liu et al., 2004). P – postnatal day.

b) RNA-seq results in human dorsolateral prefrontal cortex (DFC) and hippocampus (HIP) for GluN2B and GluN2A. Adapted from (Bar-Shira et al., 2015). PCW – postconceptional weeks; m – months; y – years.

The fact that GluN2B-NMDARs play a crucial role in early development is supported by the results obtained in knockout (KO) models. Accordingly, the complete loss of GluN1 or GluN2B subunits in mice is neonatally lethal, possibly due to impairments in essential functions for autonomous neonatal life, such as breathing and feeding (Kutsuwada et al., 1996, Forrest et al., 1994). In contrast, GluN2A-NMDARs knockout mice are viable, which is consistent with the reduced expression levels during development (Sakimura et al., 1995).

Importantly, the genetic replacement of GluN2B with GluN2A also results in high rates of perinatal lethality and suppressed feeding, although NMDAR currents are maintained. These experiments indicate that GluN2B-containing NMDARs activate unique processes during development that cannot be rescued by replacement with GluN2A (Gray et al., 2011).

When the GluN1 or GluN2B deletions are restricted to the CA1 pyramidal cells of the hippocampus or to the forebrain, respectively, starting only at the third postnatal week, the mutant mice are viable, but exhibit deficits in NMDAR synaptic currents, long-term potentiation and spatial memory (Tsien et al., 1996, von Engelhardt et al., 2008), similarly to GluN2A complete KO mice (Ito et al., 1997, Sakimura et al., 1995).

Overall, the results obtained in these models suggest that both GluN2B and GluN2A subunits play a crucial role for synaptic plasticity and cognitive functions, with GluN2B being particularly relevant during development.

Table 1.1 - Summary of the main results observed in knockout mouse models for NMDAR subunits.

Subunits	**Complete KO**	**Conditional KO** **(After third postnatal week)**
GluN1	**Neonatally lethal** ↓Swallowing and breathing (Forrest et al., 1994)	Restricted to CA1 (Cre T29–1) **Viable** ↓NMDAR currents, ↓LTP (field, HFS), ↓Spatial memory (21–48 days old) (Tsien et al., 1996)
GluN2B	**Neonatally lethal** Absence of suckling behavior = lack of nutrition (Kutsuwada et al., 1996)	Restricted to forebrain (CamCre4 mice) **Viable** ↓NMDAR currents, ↓LTP (cellular, LFS, CA1), ↓Spatial memory (5 months old)

		(von Engelhardt et al., 2008)
GluN2A	**Viable** ↓NMDAR currents, ↓LTP (field, HFS) in CA3-CA1, ↓Spatial memory (9-10 weeks old) (Sakimura et al., 1995)	-

Abbreviations: LTP – Long-term potentiation; HFS – high frequency stimulation; LFS – low frequency stimulation.

F) Are there age-dependent alterations in NMDAR functions and properties?

Fi) Development

The phase when NMDARs switch from GluN2B to GluN2A

During postnatal development in rodents, there is a peak in synapse formation (Blue & Parnavelas, 1983, Li et al., 2010, Steward & Falk, 1991). In the newly formed synapses, which are considered 'immature', glutamatergic synaptic transmission is mainly mediated by GluN2B-NMDARs, as shown by electrophysiology recordings in rodent hippocampal slices (Durand & Konnerth, 1996, Hsia et al., 1998, Bellone & Nicoll, 2007).

These receptors are important for the synaptic maturation process, by assuring that it occurs only when there is strong or correlated neuronal activity. When the synaptic activity is under basal levels, the synapses are kept in an 'immature' stage. In contrast, then the synaptic activity reaches a certain threshold, this results in enough Ca^{2+} entry through GluN2B-NMDARs, triggering synaptic maturation (Durand & Konnerth, 1996, Gray et al., 2011, Adesnik et al., 2008).

The predominance of GluN2B-NMDARs might be important at this stage since they integrate stimuli received in longer periods (slower kinetics) (Carmignoto & Vicini, 1992), carry more Ca^{2+} per unit of current (Sobczyk et al., 2005) and are more mobile than GluN2A-NMDARs (Groc et al., 2006). Moreover, they are thought to reduce the threshold for LTP-like responses, which act as the trigger for synaptic maturation (Yashiro & Philpot, 2008).

Accordingly, an acute and bidirectional change in GluN2 subunit composition can be induced by synaptic activity in the rodent hippocampus. Accordingly, the induction of LTP in young hippocampal slices (postnatal days 2-9) results in a very rapid switch in synaptic composition (from GluN2B to GluN2A), whereas a subsequent depotentiation reverses this activity-dependent switch. Interestingly, this protocol fails to induce any change (by LTP or depotentiation) in older hippocampal slices (P16-21), indicating that this mechanism only occurs during early postnatal development (Bellone & Nicoll, 2007).

In the cortex, this process is known to be regulated by sensory experience (Carmignoto & Vicini, 1992, Philpot et al., 2001, Quinlan et al., 1999, Quinlan et al., 2004) which triggers strong neuronal activity and induces an LTP-like response responsible for the GluN2B-GluN2A switch (Gray et al., 2011). In contrast, when animals are subjected to sensory deprivation conditions, the developmental switch does not occur (Philpot et al., 2001).

The fact that this process is highly conversed and occurs during a crucial period for synapse maturation, circuit refinement and acquisition of learning abilities indicates that it might be extremely relevant for high brain functions (Dumas, 2005). While the GluN2B predominance might be crucial during early development to allow proper synaptic formation and maturation, the shift to GluN2A might be important to reduce the synaptic response time and increase the threshold for LTP in mature synapses, leading to a better fine-tuning of synaptic plasticity mechanisms (Kirkwood et al., 1996, Barth & Malenka, 2001, Yashiro & Philpot, 2008).

When synapses undergo maturation, they suffer pronounced alterations in the PSD composition, as illustrated in **Figure 1.14**. Besides the GluN2B→GluN2A switch, the maturation process also leads to the incorporation of AMPARs at the synapse and an alteration in the main PSD scaffolding proteins (Cizeron et al., 2020). Immature synapses mainly contain GluN2B-NMDARs interacting with the scaffolding protein SAP-102 (Synapse-associated protein 102) (Zheng et al., 2010), whereas GluN2A-NMDARs mainly interact with PSD-95 (Postsynaptic density protein) in mature synapses. (Sans et al., 2000, Elias et al., 2008).

Although the molecular mechanisms that result in the developmental GluN2 subunit switch remain uncertain, they are known to involve the upregulation of GluN2A and the SAP102- PSD-95 shift (Sans et al., 2000, Elias et al., 2008).

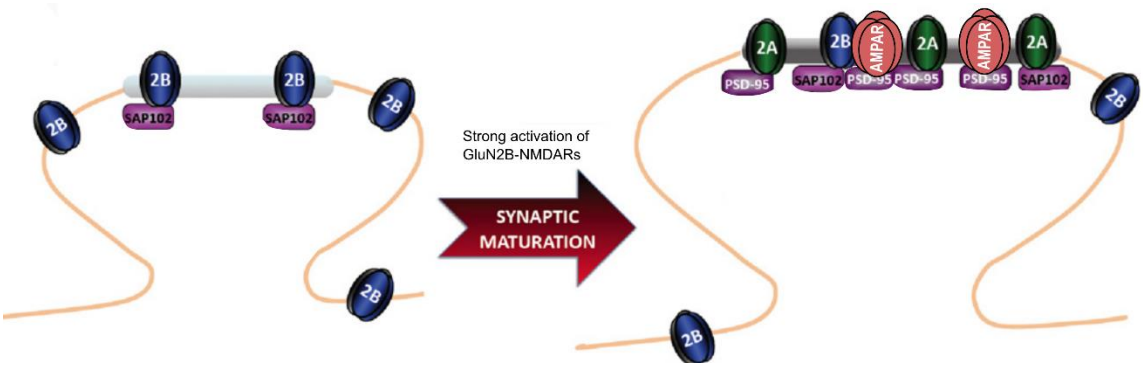

Figure 1.14 – Synaptic maturation leads to alterations in NMDAR subunit composition and postsynaptic scaffolding proteins.

Synapse maturation results in a switch in the predominant synaptic GluN2 subunit from GluN2B to GluN2A. Synaptic maturation also results in alterations in the levels of several scaffolding (SAP102 vs. PSD-95) and an increase in synaptic AMPA receptors (Sanz-Clemente et al., 2013).

Several studies have shown that NMDARs are indeed important to achieve proper synaptic maturation, although with complex and conflicting results depending on the model, timing of intervention and parameters used to study synaptic maturation, as summarized in **Table 1.2**. Overall, the results suggest that the manipulation of NMDAR levels and activity in stages of synaptic maturation is sufficient to dysregulate AMPAR currents and clusters (having either a positive or negative result), implying that NMDARs determine in which synapses AMPARs should be incorporated.

In one hand, in the absence of NMDARs, AMPAR incorporation could occur through a less selective NMDAR-independent mechanism, thus causing an increase in AMPAR currents (C. C. Wang et al., 2011, Hall et al., 2007, J. S. Ferreira et al., 2015, Gray et al., 2011, Ultanir et al., 2007, Adesnik et al., 2008, Gambrill & Barria, 2011).

On the other hand, when NMDARs are present but their activity is blocked, the NMDAR-dependent mechanism of AMPAR incorporation does not work efficiently, possibly explaining the decrease in AMPAR transmission (Liao et al., 1999, Zhu & Malinow, 2002). Thus, the results obtained so far point towards a model in which GluN2B-NMDAR activity is important to regulate synaptic maturation, as shown in **Figure 1.15**.

The fact that GluN2B deletion and knockdown cause a decline in spine density indicates that this receptor subtype is indeed essential for synapse formation and maturation. Importantly, inducing GluN2A overexpression in early developmental stages also causes a reduction in spine density, showing the importance of GluN2B-NMDAR properties at this life phase (Gambrill & Barria, 2011).

Table 1.2 – Summary of the main findings observed in rodent models when interfering with NMDAR levels/activity in immature synapses.

Strategy	Model	Effect	Ref
GluN2B→2A mice (genetic replacement)	Mouse cortical primary neurons DIV15	↑ Amplitude of AMPAR mEPSCs	(C. C. Wang et al., 2011)
GluN2A overexpression (transfection of rat organotypic hippocampal slices)	Rat organotypic hippocampal slices (CA1), P6–7 Overexpression at 4-5dic, analysis at 7-8dic	↓ Frequency of mEPSCs = Amplitude mEPSCs ↓ Spine density	(Gambrill & Barria, 2011)
GluN2B KO mice (global)	Mouse cortical primary neurons DIV 8-11	↑ Amplitude of AMPAR-mEPSCs	(Hall et al., 2007)
	Mouse hippocampal primary neurons DIV 14-15	↑ AMPAR synaptic levels	(J. S. Ferreira et al., 2015)
GluN2B conditional KO mice (GluN2Bfl/fl + Cre expression)	Mouse acute hippocampal slices (CA1), P17 (Cre expression by AAV injection at P0)	↑ Amplitude of AMPAR-EPSCs ↓ Spine density	(Gray et al., 2011)
Nex-Cre GluN1 KO mice (pyramidal neurons in the cortex and hippocampus)	Mouse slices of somatosensory cortex (Layer 2/3 pyramidal neurons) P10–P21	↑ Amplitude and frequency of mEPSCs ↓ Spine density (only after P15)	(Ultanir et al., 2007)
GluN1 conditional KO (GluN1fl/fl mice + Cre expression)	Mouse organotypic hippocampal slices, P5–P9, CA1 (CRE expression by transfection at 14-20 dic)	↑ Amplitude of AMPAR EPSCs	(Adesnik et al., 2008)
	Mouse acute hippocampal slices, P12–P19, CA1 (Cre expression by in utero electroporation)	↑ Amplitude of AMPAR EPSCs	
GluN2B KD (rat slices/ neuronal cultures)	Rat organotypic hippocampal slices, P6–7, CA1 Transfection with siRNA at 7–8 dic	↓ Frequency of mEPSCs ↓ Spine density	(Gambrill & Barria, 2011)
	Rat cortical primary neurons Transfection with siRNA at DIV 5-6, analysis at DIV 12-13 DIV	↑ Amplitude of AMPAR-mEPSCs	(Hall et al., 2007)
NMDAR chronic blocking (rat primary neurons / organotypic slices)	Rat cortical primary neurons DIV 5 to DIV12-13 AP5 (100 µM) or Ifenprodil (3 µM)	= Amplitude of AMPAR mEPSCs	(Hall et al., 2007)
	Rat hippocampal primary neurons 15-21DIV AP5 (100 µM)	↓ AMPAR clusters	(Liao et al., 1999)
	Rat organotypic hippocampal slices P0, 15 dic, CA1 CPP (100 µM) AP5 (50 µM)	↑ Frequency of mEPSCs, = Amplitude of mEPSCs = AMPAR/NMDAR ratio = Spine density	(Lüthi et al., 2001)

	Rat organotypic hippocampal slices P6, 12 dic, CA1 AP5 (200 µM)	↓ AMPAR/NNMDAR ratio (Only for treatment of 1-3 days)	(Zhu & Malinow, 2002)
NMDAR acute blocking (Rat organotypic hippocampal slices)	Rat organotypic hippocampal slices P3, P6, P9 and P12, CA1 AP5 (200 µM, 24h)	↓ AMPAR/NNMDAR ratio (Only for P3 and P6)	(Zhu & Malinow, 2002)

Abbreviations: KO – knockout; KD – knockdown; fl - floxed allele; Cre – Cre-recombinase; DIV – days in vitro; dic – days in culture; P – postnatal days; mEPSCs – miniature Excitatory Postsynaptic Currents; AP5 - (2R)-amino-5-phosphonovaleric acid (NMDAR inhibitor); CPP - 3-(2-Carboxypiperazin-4-yl)propyl-1-phosphonic acid (NMDAR inhibitor)

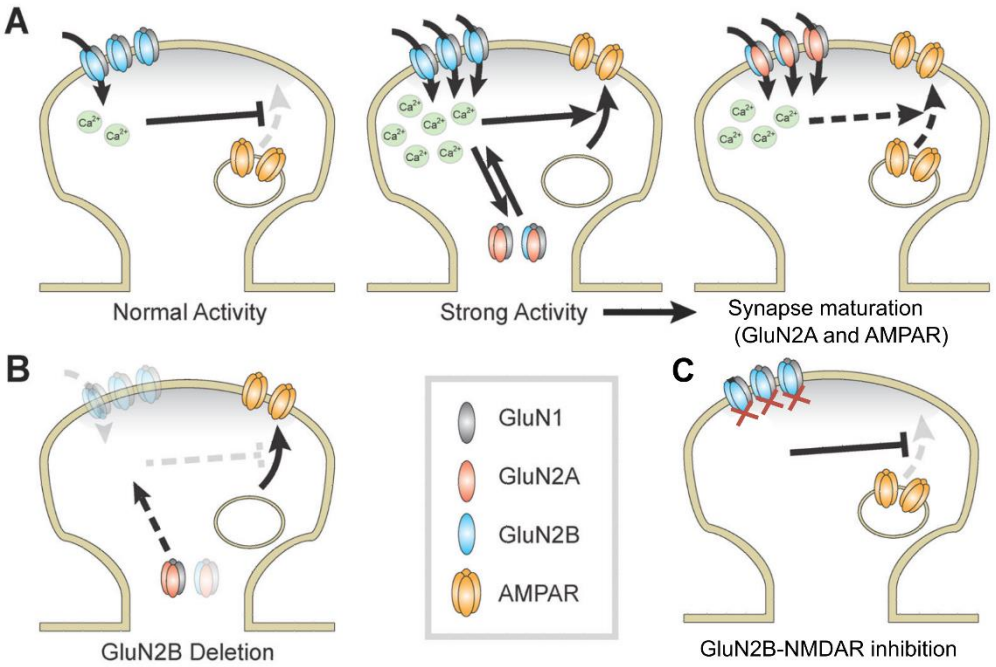

Figure 1.15 – Hypothetical model of GluN2-NMDAR contribution to synaptic maturation

a) Modest activity in immature synapses occurs predominantly through GluN2B-NMDARs and prevents the constitutive trafficking of AMPARs to the PSD. This mechanism ensures that synapses only become mature after strong or correlated activity, when enough calcium enters to override the inhibitory pathway (possibly via an LTP-like mechanism). This strong activity triggers AMPAR insertion in the PSD and the subunit switch from predominantly GluN2B-NMDARs to predominantly GluN2A-NMDARs.

b) When GluN2B subunits are deleted during early postnatal development, the inhibitory 'silencing' signal is absent, and AMPARs constitutively traffic to the PSD.

c) When GluN2B-NMDARs are inhibited, there is no strong synaptic activity, thus the AMPAR insertion and NMDAR subunit switch do not occur.

Adapted from (Gray et al., 2011).

Fii) Aging

The phase when NMDARs might contribute to synaptic dysfunction

Several studies indicate that aging is associated with alterations in NMDAR levels and properties, but the underlying mechanisms are still not known. The fact that aging is a highly heterogeneous process both in humans and other species make this analysis extremely challenging, sometimes leading to contradictory results. Studies in rodents suggest that animals can be classified as impaired and unimpaired considering their behavioral performance in learning/memory tasks, which allows a better correlation with alterations at the synaptic level (Fischer et al., 1989, Temido-Ferreira et al., 2020).

Most studies so far have reported a decline in mRNA/protein levels of NMDAR subunits upon aging in the cortex and hippocampus, with contradictory results depending on the species, brain region/subregion and subunit (P. Liu et al., 2008, Adams et al., 2001). This decrease is particularly consistent for GluN2B protein levels, being described in wild-type mice (3-4 vs. 26-30 months old) (Magnusson et al., 2002, Zhao et al., 2009), in F344 rats (4 vs. 24 months) (Clayton & Browning, 2001) and non-human primates (6–8 vs. 24–26 years (Bai et al., 2004). A recent study in humans also showed a negative correlation between age (≈20-60 years) and the total GluN2B levels in the temporal cortex (Pegasiou et al., 2020). Additionally, the cortex and hippocampus are characterized by a decrease in NMDAR binding by its agonist ([^{3}H]glutamate) or antagonists ([3H]CPP, [3H]MK801) upon aging, both in wild-type mice (3 vs. 28-30 months) (Magnusson & Cotman, 1993, Magnusson, 1995, Magnusson, 2000), F344 rats (5 vs. 24 months) (Wenk et al., 1991) and non-human primates (4-9 vs. 29-34 years) (Wenk et al., 1991). Similarly, humans also exhibit a decline in binding of [3H]MK801 to the NMDA receptor upon aging (24 weeks gestation to 100 years old) in the frontal cortex (Piggott et al., 1992). The main findings regarding NMDAR subunit levels and binding in aged wild-type mice are summarized in **Table 1.3**.

Table 1.3 – Summary of the main findings observed in aged wild-type mice regarding NMDAR subunit levels and binding.

Parameter	Model	Results	Ref
NMDAR subunit levels	C57Bl/6 mice 3 vs. 30-month-old mice.	Cortex: ↓GluN2B, ↓GluN1, =GluN2A (membrane fractions) Hippocampus: ↓GluN1, = GluN2B, = GluN2A (membrane fractions)	(Magnusson et al., 2002)
	C57BL/6JNIA mice 4 vs. 26 months old	Cortex: ↓GluN2B, = GluN1 (not in whole lysates, only in synaptosomes) Hippocampus: ↓GluN2B, = GluN1 (whole lysates + synaptosomes)	(Zhao et al., 2009)
NMDAR binding	C57Bl/6 mice 3 vs. 30 months	↓NMDA-displaceable [3H]glutamate and [^{3}H]CPP binding (cortex and hippocampus)	(Magnusson, 2000)
	C57B1 and BALB/c mice 3 vs. 30 months	↓NMDA displaceable [^{3}H]-glutamate binding (cortex and hippocampus)	(Magnusson & Cotman, 1993)
	C57B1/6 mice 3 vs. 28-30 months	↓NMDA displaceable [^{3}H]-glutamate and [^{3}H]CPP binding (cortex and hippocampus)	(Magnusson, 1995)

Abbreviations: CPP- [(±)-2-carboxypiperazin-4-yl] propyl-1-phosphonic acid; [^{3}H] - radioactive isotope of hydrogen (Tritium)

Additionally, several studies reported alterations in NMDAR function, as shown by a decrease in the amplitude of field NMDAR-mediated excitatory post-synaptic potentials (NMDAR-fEPSPs) in the CA1 region of the hippocampus in wild-type mice (3–5 vs. 23–27-months) (Billard & Rouaud, 2007) and F344 rats (Eckles-Smith et al., 2000, Bodhinathan et al., 2010, Kumar & Foster, 2013).

Similar outcomes were reported when measuring evoked NMDAR-mediated excitatory post-synaptic potentials (NMDAR-EPSCs) in individual CA1 pyramidal cells, which showed a lower amplitude in aged F344 rats (4–6 months vs. 24-26 months) (Kumar et al., 2019). Moreover, the duration of NMDAR-fEPSPs tends to increase in aged Sprague-Dawley rats (3–4-vs. 25–33-months) (Jouvenceau et al., 1998), but it is still not clear if this occurs due to alterations in NMDAR subunit composition.

Emerging evidence shows that NMDARs function differently in aged or adult synapses, namely considering the incongruent results regarding GluN2B-NMDAR impact on memory performance. Some studies suggest that increasing GluN2B levels could alleviate the age-associated memory impairments in mice. Accordingly, forebrain-

specific GluN2B transgenic mice exhibit increased LTP, accompanied by a better recognition, contextual and cued fear memory and spatial learning compared to wild-type mice with the same age (15–18-months) (Brim et al., 2013). Additionally, viral-induced overexpression of GluN2B in the hippocampus/cortex of aged wild-type mice (22-26 months) resulted in increased NMDAR EPSPs and improved spatial memory (Cao et al., 2007). However, there is also evidence that aged mice (26 months old) with higher GluN2B and GluN1 expression exhibit poorer memory (Zhao et al., 2009), which might indicate that NMDARs have different properties upon aging. Accordingly, two independent studies have shown that the association between GluN2B and PSD-95 increases in aged synapses, based on results from GluN2B co-immunoprecipitation in synaptosomes from the frontal cortex of wild-type aged mice (3 vs. 26 months) (Zamzow et al., 2013) and proximity ligation assays in dorsal CA1 of aged (3–4 vs. 20–23 months) (al Abed et al., 2020).

Considering the potential role of NMDARs in age-associated memory impairments, NMDAR antagonists have emerged as potential compounds to counteract these alterations. However, antagonists such as memantine have shown both prejudicial (Creeley et al., 2006, Pinho et al., 2017) and beneficial effects in rodents (Pietá Dias et al., 2007, Zoladz et al., 2006, Beracochea et al., 2008), depending on the age, type of administration, dose and memory task involved in the study, as summarized in **Table 1.4**.

Overall, the results propose that memantine could be beneficial in age-impaired animals or in situations of excessive NMDAR activation (Zajaczkowski et al., 1997). This is consistent with the proposed mode action for memantine, by acting as a non-competitive NMDAR antagonist that blocks pathological tonic NMDAR activation while preserving their physiological transient synaptic activation (Parsons et al., 2007, Danysz & Parsons, 2003, Lipton, 2006, X. Song et al., 2018). Considering that memantine is an approved therapeutic drug for moderate to severe Alzheimer's disease (AD) (Reisberg et al., 2003), it is possible that blocking NMDAR pathological activity might also be beneficial for AD patients.

Table 1.4 – Summary of the effects obtained upon memantine administration in wild-type rodents and human AD patients.

Model	Memantine Treatment	Synaptic plasticity	Learning/memory	Ref
Adult Sprague Dawley rats 6 -8 months	i.p (2.5, 5, 10, mg/kg) Single injection, before behavioral tests	-	↓ Memory retention 2.5, 5, and 10 mg/kg Hole-board test	(Creeley et al., 2006)
Adult Wistar rats, 2-4 months	i.p. (1, 5 or 10 mg/kg/day) for 15-20 days	No effect	No effect Morris Water Maze	(Pinho et al., 2017)
Adult Sprague-Dawley rats	i.p. (2.5, 3.75, 5, or 7.5 mg/kg) Single injection, before behavioral tests	-	↑ Memory retention (5 or 7.5 mg/kg) Radial-arm water maze (24h retention trial)	(Zoladz et al., 2006)
Aged Wistar rats 24 months	i.p. (20 mg/kg/day) for 21 days Last injection 1w before behavioral tests	-	↑ Memory retention Novel object recognition task 1 week after the last injection	(Pietá Dias et al., 2007)
Aged Wistar rats 17–25 months	i.p. (1, 5 or 10 mg/kg/day) for 15-20 days	↓ LTP magnitude (increased in aged comparing to adults (2-4 months)) 10 and 5 mg/Kg/day	↓ Place learning (Impaired in aged comparing to adults (2-4 months)) 10 mg/kg/day Morris water maze	(Pinho et al., 2017)
Aged C57Bl/6 mice 18-20 months	Oral gavage (3 or 0.3 mg/kg/day) for 7 days	-	↑ Spatial memory 3mg/kg Contextual serial discrimination (Impaired in aged mice when comparing to adults (4 to 5 months))	(Beracochea et al., 2008)
Human AD patients (moderate-to-severe)	Oral (20 mg/day) for 28 weeks	-	↑Performance in CIBIC-Plus, ADCS-ADLsev and Severe Impairment Battery	(Reisberg et al., 2003)

Abbreviations: ip – Intraperitoneal; w - week; CIBIC-Plus - Clinician's Interview-Based Impression of Change Plus Caregiver Input; ADCS-ADLsev - Alzheimer's Disease Cooperative Study Activities of Daily Living Inventory modified for severe dementia; AD – Alzheimer's Disease

Taken together, this data indicates that NMDARs in aged synapses have different but still unknown properties, potentially contributing to synaptic dysfunction in later life stages. In fact, aging is associated with calcium dyshomeostasis (Hajieva et al., 2009), (Oh et al., 2013) alterations in synaptic plasticity (Burke & Barnes, 2006), namely a shift from LTD to LTP (Temido-Ferreira et al., 2020), and memory deficits (Tombaugh et al., 2002) in wild-type rodents. Similar mechanisms might occur in human aging, which is also characterized by alterations in in cortical plasticity (Freitas et al., 2011), as well as impairments in cognition (Singh-Manoux et al., 2012) and spatial memory (Newman & Kaszniak, 2000).

Considering the impact of the GluN2B/A ratio in Ca^{2+} influx and in defining a threshold for LTP, alterations in the subunit composition could eventually explain these age-associated properties, but this hypothesis has not been explored so far.

The main findings related to NMDAR function in aged synapses in wild-type rodents, namely in CA3-CA1 synapses, are summarized in **Figure 1.16**.

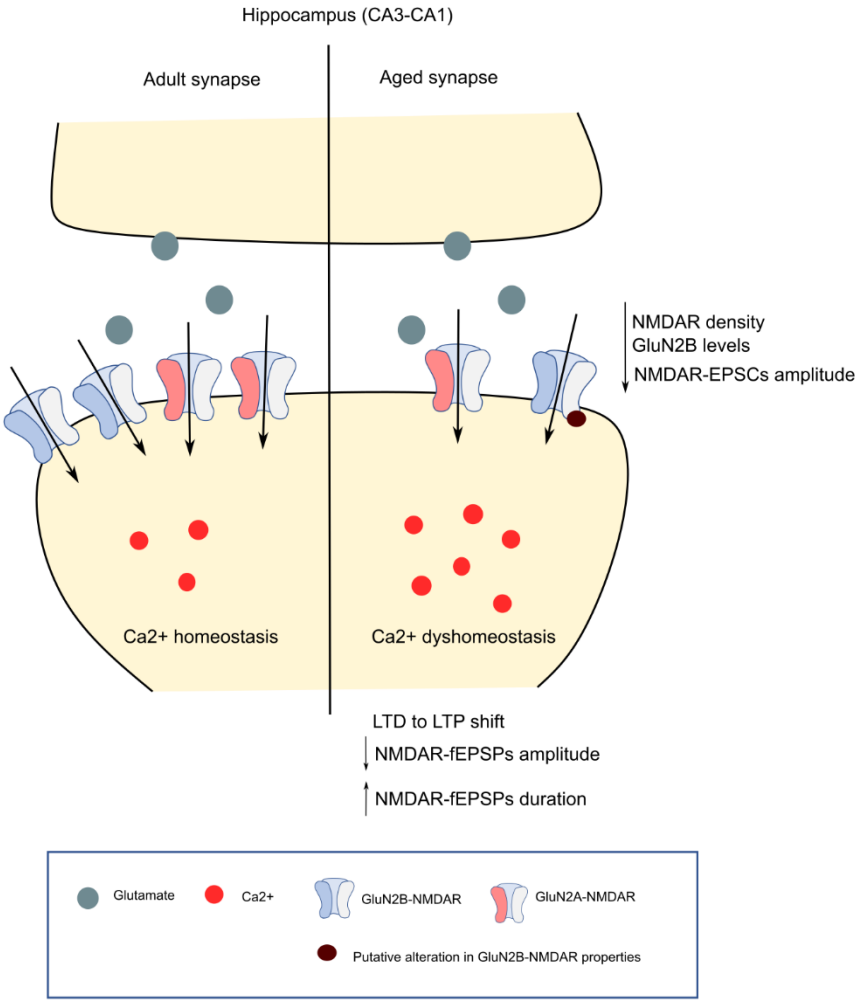

Figure 1.16 – Summary of age-associated alterations in NMDAR levels/function in aged synapses in wild-type rodents, namely in CA3-CA1 synapses. Adapted from (Temido-Ferreira et al., 2019).

G) Which factors regulate NMDAR synaptic content?

The age-dependent properties of NMDARs might correlate with alterations in the GluN2B/A ratio and the respective contribution at the synapse. The NMDAR synaptic content is regulated by multiple mechanisms, including biogenesis, insertion into the plasma membrane, stabilization at synaptic sites, trafficking in/out of the synapses by lateral diffusion, endocytosis, recycling and degradation, as reviewed in (Vieira et al., 2020, Bard & Groc, 2011) and illustrated in **Figure 1.17**.

Tetrameric NMDARs are assembled in the endoplasmic reticulum (ER) (Hawkins et al., 2004) and undergo maturation in the Golgi, being subsequently transported in vesicles to the synapse (Setou et al., 2000). Alternatively, NMDARs can bypass this classical route by being transported to Golgi outposts close to the synapse (Jeyifous et al., 2009). The incorporation of NMDARs at the membrane takes place mainly at extrasynaptic sites along the somatodendritic compartment (Gu & Huganir, 2016), with the receptors then relocating to the synaptic membrane via lateral diffusion (Ladepeche, Dupuis, & Groc, 2014, Tovar & Westbrook, 2002, Groc et al., 2006). Anchoring in the postsynaptic density is achieved by interactions between the CTD of NMDAR subunits and scaffolding proteins, most notably from the PSD-95 family of membrane-associated guanylate kinases (MAGUKs) family (Steigerwald et al., 2000, Barda et al., 2010) as well as interactions with transmembrane proteins (reviewed in (Petit-Pedrol & Groc, 2021)). NMDAR lateral mobility allows the receptors to exit the postsynaptic density and move to the extrasynaptic regions, where they can undergo endocytosis (Blanpied et al., 2002, Lavezzari et al., 2004). Then, this pool of internalized receptors can either be recycled to the cell surface or targeted to lysosomes for degradation (Scott et al., 2004).

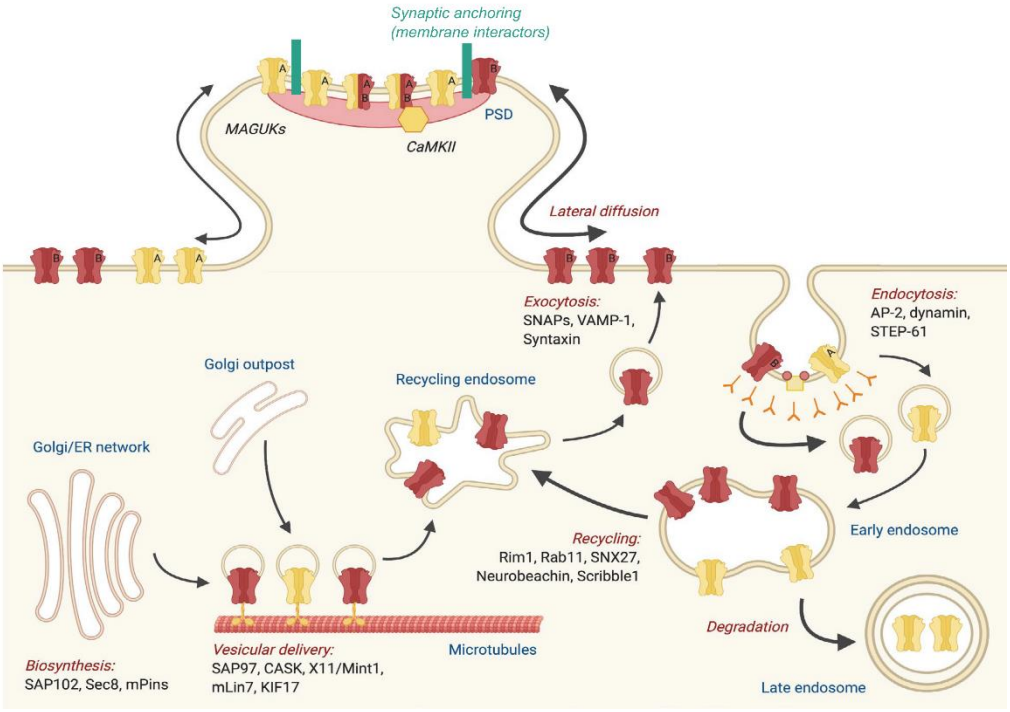

Figure 1.17 - NMDAR synaptic content is regulated by multiple mechanisms, including biogenesis, insertion into the plasma membrane, stabilization at synaptic sites, trafficking in/out of the synapses by lateral diffusion, endocytosis, recycling and degradation. Adapted from (Vieira et al., 2020, Groc & Choquet, 2020).

Overall, the half-life of NMDARs is expected to last between 2 and 34 h (Huh & Wenthold, 1999) and the average synaptic residency time is within the minute range (Barda et al., 2010, Groc et al., 2006, Tovar & Westbrook, 2002), showing that these processes are highly dynamic. Accordingly, approximately 30–40% of surface NMDAR are mobile and, at a given time point, approximately 30% of these surface receptors (mostly GluN2B–NMDARs) exchange between the synaptic and extra synaptic areas (Barda et al., 2010, Groc et al., 2006, Tovar & Westbrook, 2002).

There is a wide variety of posttranslational modifications (PTMs) that can control NMDAR trafficking, synaptic levels and properties (glycosylation, phosphorylation, palmitoylation, ubiquitination and sumoylation). In particular, several phosphorylation sites on NMDAR subunit CTDs have shown to regulate NMDARs, as reviewed in (Lussier et al., 2015). Some phosphorylated resides interfere with NMDAR interaction with scaffolding proteins and endocytosis, while others affect the gating and Ca^{2+} permeability without altering the surface levels of NMDARs, as exemplified in **Figure 1.18**.

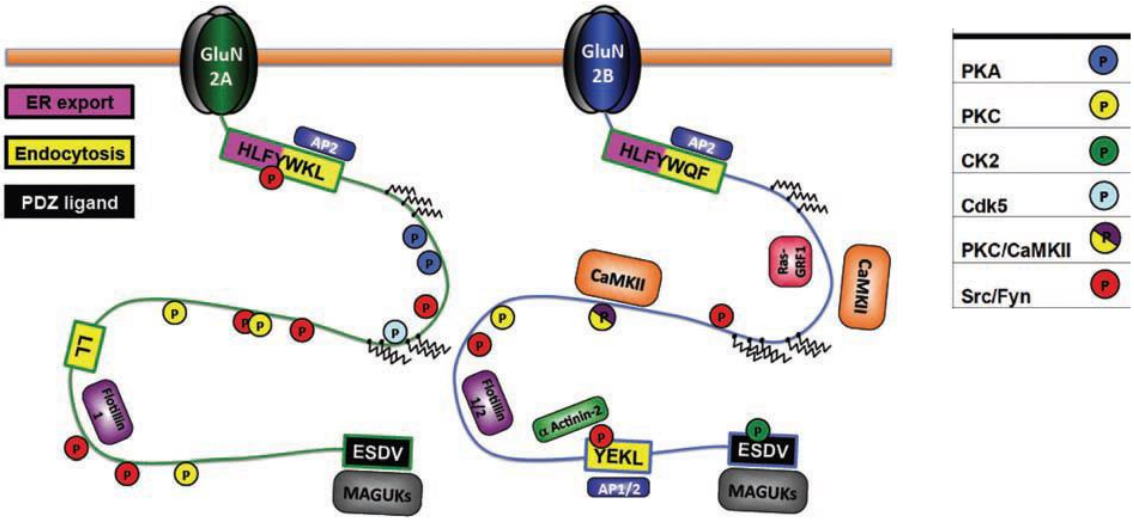

Phospho site (kinase)	Impact on NMDARs	Reference
Y1472 GluN2B (Fyn)	↓ Endocytosis ↑ Synaptic levels	(Nakazawa et al., 2001, Prybylowski et al., 2005)
S1480 GluN2B (CK2)	↓ Binding to MAGUK proteins ↓Synaptic levels	(Hee et al., 2004, Chiu et al., 2019)
S1166 GluN2B (PKA)	↑NMDAR Ca^{2+} permeability ↑GluN2B-NMDAR currents = Surface levels	(Aman et al., 2014, Skeberdis et al., 2006, Murphy et al., 2014)
S1048 GluN2A (DYRK1A)	↓ Endocytosis ↑ Synaptic levels ↑GluN2A-NMDAR currents	(Grau et al., 2014)

Figure 1.18 - Examples of phosphorylation sites on the C-terminal of NMDAR subunits and their impact in NMDAR function

Adapted from (Sanz-Clemente et al., 2013)

The main scaffold proteins that anchor and stabilize surface NMDARs at glutamatergic synapses are the PSD-95 family of MAGUKs (e.g. PSD-95, SAP-102) (X. Chen et al., 2015). PSD-95 exhibits low levels in young neurons (rat hippocampus, postnatal day 2), which increase with age (from P10 to 6 months). In contrast, the number of SAP102-positive synapses is higher during early postnatal development (rat hippocampus, postnatal day 2), then decreasing with age (6 months). The fact that SAP102 is highly mobile in spines (80%, in primary neuronal cultures), compared with PSD-95 (36%) might indicate that NMDAR properties/trafficking might also differ depending on their associated MAGUK (Sans et al., 2000, Zheng et al., 2010).

Besides the PSD-95 family, other proteins have shown to interact and contribute to NMDAR synaptic retention (e.g. Ephrin B, Reelin and matrix metalloprotease 9, (Dalva

et al., 2000, Groc et al., 2007, Michaluk et al., 2009). The amyloid precursor protein has been identified as a potential regulator of NMDAR, but the underlying mechanisms are still not known.

1.2.2 APP as a putative regulator of NMDARs

The amyloid precursor protein (APP) has emerged as a strong candidate for the regulation of NMDARs, considering the following observations (summarized in **Table 1.5**):

- **APP interacts with NMDARs** – observed upon exogenous expression in cell lines, but also endogenously in neuronal cultures and brain tissue from adult mice, by co-immunoprecipitation (Cousins et al., 2009, Hoe et al., 2009).

- **APP regulates NMDAR surface levels** - GluN2B-NMDAR surface levels increase due to APP overexpression and decrease after APP knockdown in primary neuronal cultures with exogenous NMDAR expression (Hoe et al., 2009).

- **APP knockdown** during embryonic development in mice leads to a **decline in GluN2B-NMDAR synaptic contribution** in CA1 pyramidal neurons during postnatal stages (P7-9) (Pousinha et al., 2017).

- The **APP intracellular domain (AICD) increases the GluN2B-NMDAR synaptic contribution** in CA1 pyramidal neurons of adult rats (P32–40). These results were observed upon AICD viral delivery (2 weeks) or *ex vivo* incubation (for 2h) (Pousinha et al., 2017).

Altogether, these studies suggest that APP interacts and regulates NMDARs, but the underlying mechanisms and functional relevance of this regulation remain to be elucidated. Two independent studies showed an interaction between APP and NMDAR subunits by co-immunoprecipitation and concluded that APP overexpression results in increased surface levels of GluN2B-containing NMDARs (Cousins et al., 2009, Hoe et al., 2009).

However, there are some conflicting results in terms of the selectivity of this effect for GluN2B/GluN2A receptors, as well as the proposed mechanism of action. According to Hoe et al., APP regulates GluN2B-containing NMDARs specifically, whose surface levels increase due to APP overexpression and decrease after APP knockdown, whereas no effect was reported for GluN2A. The authors suggest that APP acts by decreasing GluN2B-NMDAR internalization (Hoe et al., 2009). On the other hand, Cousins et al. have observed enhanced surface expression of both NMDAR subtypes after APP overexpression. The authors suggest that APP interacts with the GluN1 subunit in the endoplasmic reticulum, pointing towards a role in receptor trafficking (Cousins et al.,

2009). Some of these confounding results might be explained by differences in the experimental models. The work by Cousins et al. involves heterologous protein expression in cell lines, thus it is possible that this accumulation and association of APP with NMDAR subunits at the ER might occur as an artifact of the high concentration of these proteins in the cell. On the other hand, Hoe et al. have used neuronal cultures and recorded NMDAR currents mediated by endogenous receptors, whereas the analysis of surface NMDAR levels was performed upon transfection with NMDAR subunits. It is possible that the specificity of the APP response for the GluN2B receptors only occurs in a neuronal context and depending on the maturation state, since these cells have unique mechanisms to regulate NMDARs at the synapse.

When investigating the APP-NMDAR interaction in brain tissue, both studies reported an association between GluN1 and APP and no apparent specificity for GluN2B receptors. However, the discrimination between the exact subunit interacting with APP is technically challenging, since GluN1/GluN2A/GluN2B might exist in the same protein complexes (Rauner & Köhr, 2011), being all detected following APP immunoprecipitation.

In conclusion, APP has been proposed to associate with NMDARs and regulate their surface levels. Several answers remain to be answered, such as the selectivity of this effect for GluN2B receptors, the mechanism involved and the domains of APP/NMDAR subunits responsible for this association.

According to previous results obtained by our group (Pousinha et al., 2017), the APP intracellular domain might be the mediator of some of these responses. Accordingly, Pousinha et al. have demonstrated a critical physiological role for a particular APP fragment (APP intracellular domain (AICD)) in controlling GluN2B-NMDARs at CA1 excitatory synapses. This study was performed in wild-type mice/rats at different stages: i) first week of life, when synapses are still immature and contain predominantly GluN2B subunits; ii) adult stages, characterized by mature synapses where GluN2A is the most abundant subunit.

To study the role of APP in early developmental stages, the authors depleted APP in neuronal precursor cells of the hippocampus by *in utero* electroporation of a short-hairpin RNA (shRNA) against APP (shAPP). When analyzing NMDAR EPSCs during the first week of postnatal development, Pousinha et al. observed a reduction in GluN2B-NMDAR synaptic contribution due to APP depletion. This effect was rescued by incubating the hippocampal slices with an AICD peptide (for 2h).

Moreover, this study explored the impact of elevated AICD levels in adult stages, by incubating adult hippocampal slices with the same peptide. This treatment resulted in an

increased GluN2B-NMDAR synaptic contribution, which was dependent on AICD nuclear localization and transcriptional alterations.

Therefore, the emerging model indicates that APP alters synaptic GluN2B-NMDAR contribution, towards a GluN2B-rich profile, potentially through its intracellular domain.

Altogether, these studies suggest that the regulation of synaptic NMDARs by APP might occur through several putative mechanisms (illustrated in **Figure 1.19**), possibly contributing to age-related alterations in NMDAR properties.

Table 1.5: Summary of the main findings related to APP regulation of NMDAR in cell lines, neuronal cultures and wild-type rodents.

Parameter	Model	Results	Ref
APP-NMDAR interaction	Rat primary hippocampal neurons (DIV14) Mouse brain (adult)	APP interacts with GluN1 (Co-IP)	(Hoe et al., 2009)
	HEK293 cells transfected with NMDAR subunits (with and without exogenous APP expression) Rat brain (adult)	APP interacts with GluN1/GluN2A/GluN2B (Co-IP)	(Cousins et al., 2009)
Impact of APP silencing on NMDARs	CGCs DIV5 Transfected with APP siRNA, analysis 2–3 days after transfection	↓ NMDAR currents	(Hoe et al., 2009)
	Hippocampal neurons (DIV10-12) Transfected with APP siRNA, analysis 2–3 days after transfection	= NMDAR currents	(Hoe et al., 2009)
	Hippocampal neurons (DIV10-12) Transfected with APP siRNA and NMDAR subunits, analysis 8–14 days after transfection	↓GluN1 and GluN2B surface levels (No effect on GluN2A) ↑GluN2B endocytosis	(Hoe et al., 2009)
	CD1 mice, In vivo electroporation with APP shRNA, analysis at P7–9, CA1 Rescue by AICD incubation in hippocampal slices (2h, 100nM)	↓GluN2B-NMDAR contribution	(Pousinha et al., 2017)
Impact of APP overexpression on NMDARs	CGCs DIV5 Transfected with APP, analysis 2–3 days after transfection	↑ NMDAR currents ↑ GluN2B NMDAR contribution	(Hoe et al., 2009)
	Hippocampal neurons (DIV14) Transfected with APP, analysis 2–3 days after transfection	↑ NMDAR currents	(Hoe et al., 2009)
	Hippocampal neurons (DIV10-12) Transfected with APP and NMDAR subunits, analysis 8–14 days after transfection	↑ GluN1 and GluN2B surface levels (No effect on GluN2A) ↓GluN2B endocytosis	(Hoe et al., 2009)
	HEK293 cells transfected with NMDAR subunits (with vs. without exogenous APP expression)	↑GluN2B and GluN2A-NMDAR surface levels = Total levels of NMDAR subunits	(Cousins et al., 2009)

Impact of AICD increased levels on NMDARs	Sprague Dawley adult rats AAV-AICD injection in the hippocampus at P21-22, analysis at P32–40	↑ NMDAR currents ↑GluN2B-NMDAR contribution	(Pousinha et al., 2017)
	Sprague Dawley adult rats, P32–40 AICD delivery ex vivo (100nM), incubation of hippocampal slices for 2h	↑GluN2B-NMDAR contribution	(Pousinha et al., 2017)

Abbreviations: HEK293 - Human embryonic kidney 293 cells, CGCs - Cerebellar granule cells, DIV – days in vitro, P- postnatal day; Co-IP - co-immunoprecipitation; AAV – adenoassociated virus.

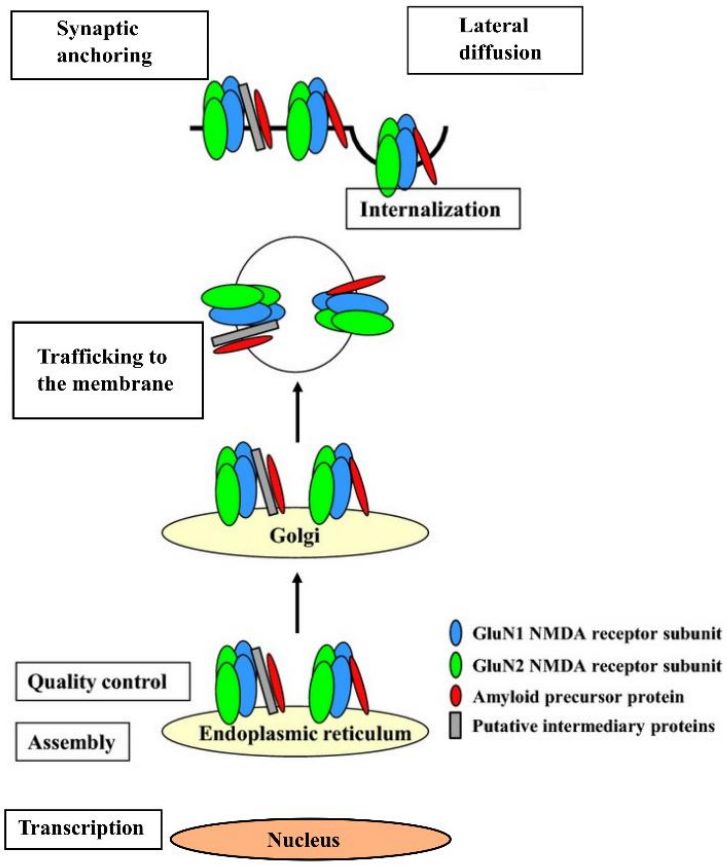

Figure 1.19- Schematic representation of the putative mechanism by which APP might regulate NMDARs. Adapted from (Cousins et al., 2015).

A) Integrating APP domains with its functions

APP is a transmembrane single-pass glycoprotein, being considered as a receptor-like modulatory protein (as reviewed in (Reinhard et al., 2005)). It is expressed in a variety of tissues, but most abundantly in the brain (NCBI, n.d.) . It is mostly known for being involved in Alzheimer's Disease pathology, since its cleavage generates the amyloid-

beta (Aβ) peptide, which accumulates in the brains of AD patients and has neurotoxic effects (Hardy & Higgins, 1992). Although the physiological function of APP is not completely understood, it has been described as regulator of several neuronal processes including synaptogenesis, synaptic plasticity (reviewed in (U. C. Müller & Zheng, 2012)) and calcium signalling (Paschou et al., 2023).

APP is ubiquitously expressed in the brain and exhibits three major isoforms in mammals (APP695, APP751, APP770) as illustrated in **Figure 1.20a**, with APP695 being the most predominantly expressed in neurons (Tanaka et al., 1989).

Being a transmembrane single-pass glycoprotein, APP is composed of the following domains (reviewed in (Dawkins & Small, 2014)) and illustrated in **Figure 1.20b**:

- N-terminal domain (NTD) – large extracellular domain containing two domains (E1 and E2) important for dimerization, ligand/metal binding and cell adhesion.
- Transmembrane domain (TMD) – a single transmembrane span that contributes to dimerization. Includes the Aβ domain, which has been linked to Alzheimer's Disease pathology.
- C-terminal domain (CTD) - known to interact with several adaptors/ signal transduction proteins (in particular the YENPTY motif). It is important for APP transport, endocytosis and the regulation of signaling pathways.

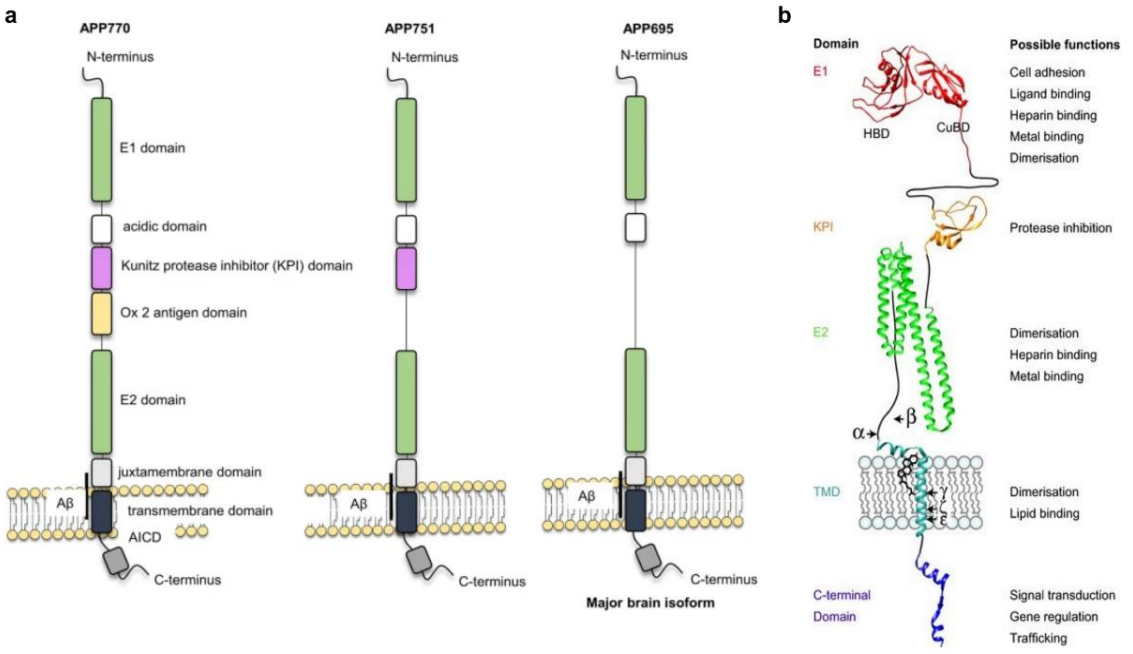

Figure 1.20 - The amyloid precursor protein isoforms and domains.

a) Schematic representation of the three common isoforms of APP—695, 751 and 770—highlighting individual domains present in each protein. Adapted from (Delport & Hewer, 2022).
b) Hypothetical 3-dimensional structure of APPbased on the following protein data bank files: E1 domain (3KTM), Kunitz protease inhibitor (KPI) domain (1ZJD), E2 domain (3UMK), transmembrane domain (TMD) (2LLM) and intracellular domain (3DXC). Adapted from (Dawkins & Small, 2014).

B) APP binding partners modulate its function

Since APP exhibits no enzymatic activity, it has been described as a receptor-like modulatory protein. Accordingly, both extra- and intracellular domains of APP are involved in its biological functions, suggesting that APP links extracellular cues (e.g. ligand or substratum binding) to intracellular signaling pathways (via scaffolding proteins, Ca^{2+} regulation, interactions with the cytoskeleton and/or protein kinases) (reviewed in (Reinhard et al., 2005)). APP regulatory role is possibly mediated by its interaction with extracellular and intracellular binding partners, with more than 200 having already been identified (U. C. Müller et al., 2017), as illustrated in **Figure 1.21a**. One of the described APP interactors is the NMDAR, although the putative binding site and the functional relevance of this interaction are still largely unknown.

In particular, the intracellular domain has been described as a signaling hub with several interaction partners such as adaptor proteins involved in multiple neuronal mechanisms (e.g. Fe65, DAB1 (disabled homologue 1), GRB2 (growth factor receptor-bound protein 2), X11/Mint, Gαo/s) (U. C. Müller et al., 2017), as shown in **Figure 1.21a, b**.

Fe65 has emerged as an APP important interactor, especially considering the similar phenotypes observed in mouse knockout models for the Fe65 and APP family members (Guénette et al., 2006, Strecker et al., 2016, B. Wang et al., 2004). Importantly, Fe65 is an adapter protein that binds to the APP intracellular (A^{666} to M^{693}, including the ^{682}YENPTY^{687} motif (APP695 numbering)) (**Figure 1.21a, b**) through its phosphotyrosine binding domain 2 (PTB2) (Radzimanowski et al., 2008) and regulates APP trafficking and processing (Sabo et al., 1999), as well as APP-mediated transcriptional effects (Konietzko et al., 2019, Probst et al., 2021).

Additionally, the APP intracellular domain interacts with heterotrimeric G Proteins, namely the Gαo (Nishimoto et al., 1993) and Gαs subunits (Deyts et al., 2012), leading to their activation. The cytoplasmic APP sequence H^{657} to L^{676}, which includes the ^{672}RHLSK^{676} motif (APP695 isoform numbering) (**Figure 1.21a, b**) has been identified as the putative binding site (Nishimoto et al., 1993, Deyts et al., 2012). Following activation, the Gs and Go class of G-proteins mediate stimulation or inhibition of adenylate cyclase activity, respectively (Eason et al., 1992). Thus, it has been suggested that APP signaling

might preferentially activate Gαo- or Gαs- associated responses in a context-dependent manner (e.g. different ligands, neuronal activity, etc.) (Copenhaver & Kögel, 2017).

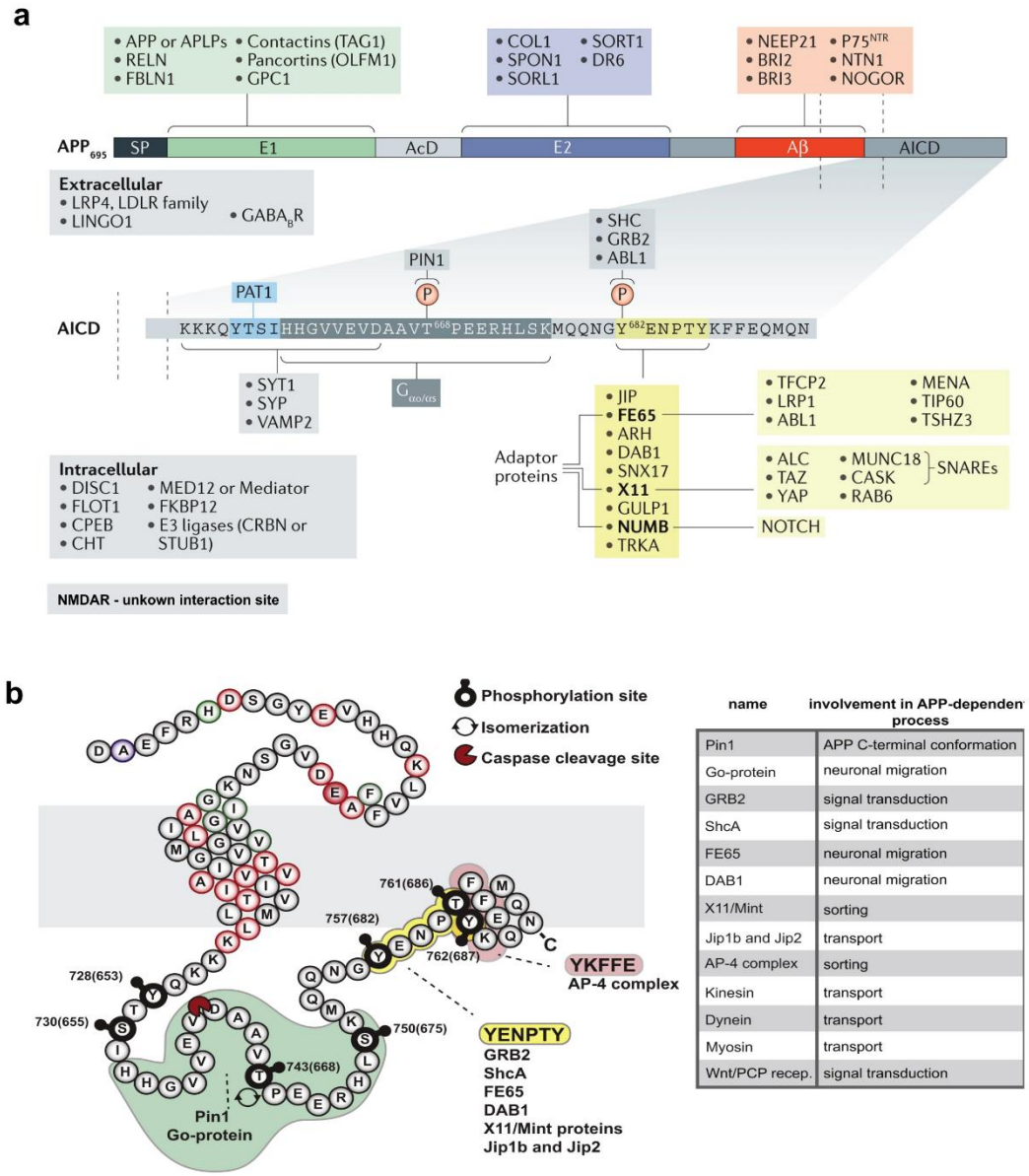

Figure 1.21 – Schematic representation of APP interaction partners

a) Representation of some of the APP identified interaction partners. APP interacts with several proteins through its extracellular portion (top) and its intracellular domain (bottom). Known interactors with mapped APP-binding motifs are shown in the same colour as their interacting APP domains. Extracellular and intracellular interactors with non-mapped interaction sites are listed underneath (in grey). Adapted from (U. C. Müller et al., 2017).

b) The illustrated the intracellular domain of APP and its binding partners. The domain involved in Go/Gs binding is shown in green, while the YENPTY and YKFFE domains are illustrated in yellow and red

are, respectively, being required for binding to other interaction proteins. The amino acid residues numbering corresponds to the APP770 (and APP695 isoform). Adapted from (van der Kant & Goldstein, 2015).

Moreover, APP signaling is modulated by its ability to establish cis- and trans-dimers with itself and other proteins of the same family mainly through the E1 and E2 domains (Hoefgen et al., 2014), as illustrated in **Figure 1.22**. In particular, APP trans-dimers have shown cellular adhesion properties (Soba et al., 2005). In contrast, APP processing by secretases has the opposite effect, possibly by destabilizing APP trans-dimers (Stahl et al., 2014). Therefore, APP function might be modulated by the balance between dimerization and processing.

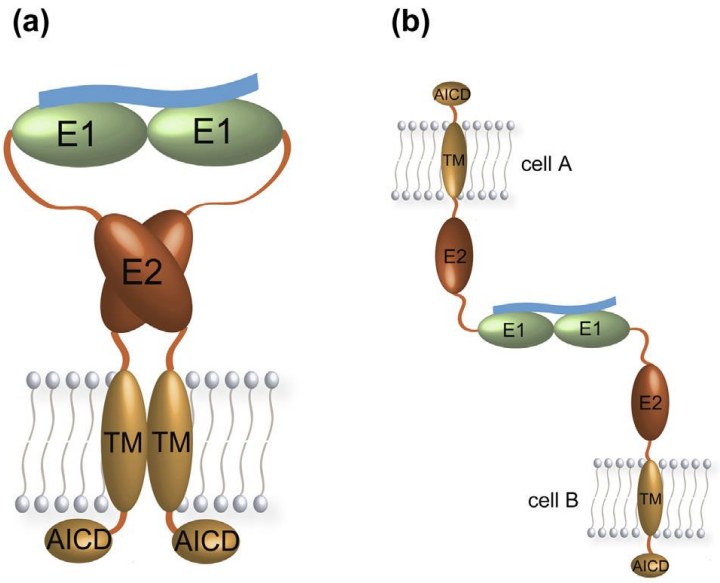

Figure 1.22 - Model of APP cis and trans dimerization.

a) If both APP molecules are located at the same membrane, they form cis-dimers, which can influence APP signaling.

b) If two APP molecules are located at different cell membranes they can form trans-dimers, contributing to cell adhesion. Adapted from (Hoefgen et al., 2014).

C) APP is located at synaptic terminals

APP distribution is ubiquitous throughout the brain and shows high expression levels in the hippocampus and cerebral cortex both in rodents (Apelt et al., 1997, Löffler & Huber, 1992, Lorent et al., 1995, Allen Institute for Brain Science (2004), n.d.) and humans (Goedert, 1987, Higgins et al., 1988, Solà et al., 1993). Although generally considered a neuronal protein (Guo et al., 2012, del Turco et al., 2016), there are some reports detecting APP in glial cells (Reichard et al., 2003, Trapp & Hauer, 1994). Importantly,

APP is detected in rodent synaptosomes throughout life (Kirazov et al., 2001), being located both in the pre- and post-synaptic terminals in adult rodents and aged postmortem brain tissue (Laßek et al., 2013, Lundgren et al., 2020), Ferrer-Raventós et al., 2023) and in rodent primary neuronal cultures (Hoe et al., 2009, Kedia et al., 2020).

APP expression in rodents is known to start during embryonic development (embryonic day 7.5 in mice) (Ott & Bullock, 2001) increasing after birth and showing a peak at the second postnatal week (Trapp & Hauer, 1994, Kirazov et al., 2001). Less is known about the temporal expression of APP in the human brain, having been detected during pre/postnatal development and adulthood (Haytural et al., 2019, Reichard et al., 2003), and showing a tendency for a decrease in synaptosomal levels in aged subjects (20 years vs. 80 years, cortex) (Pliássova et al., 2016). Additionally, previous studies reported an increased activity of secretases involved in APP proteolytic processing (β- and γ-secretase) in the mouse aged brain (Fukumoto et al., 2004, Placanica et al., 2009), accompanied by an increased accumulation of APP-derived fragments in the mouse aged brain and in mouse aged primary neuronal cultures (Burrinha et al., 2021).

Overall, the subcellular distribution of APP suggests that it could play important roles at the synapse. Moreover, the peak of protein levels observed during early postnatal development indicates that APP might be particularly relevant during the formation and maturation of synaptic connections. On the other hand, alterations in APP levels/ processing upon aging could potentially interfere with its physiological functions.

D) APP trafficking and processing

APP trafficking and processing might modulate its neuronal functions, namely by regulating the levels of surface APP and its derived fragments, as illustrated in **Figure 1.23**. Upon synthesis in the ER, APP is transported through the Golgi apparatus to the Trans-Golgi network (TGN), undergoing posttranslational modifications (e.g. glycosylation, phosphorylation), as reviewed in (Haass et al., 2012). In neurons, this is followed by APP transport to axons and dendrites (Simons et al., 1995, Back et al., 2007, Delbove et al., 2018). While anterograde transport of APP in axons has been well characterized, being mediated by kinesin-1 (Kamal et al., 2000), much less information is known about the transport of APP within the dendrites (as reviewed in (Muresan & Ladescu Muresan, 2015)) (**Figure 1.24 a**).

APP is then trafficked to the cell surface, with APP plasma membrane fraction accounting for less than 20% of the total protein levels in basal conditions (de Coninck et al., 2018). A recent study in mouse primary neuronal cultures showed that APP undergoes lateral

diffusion on the synaptic membrane and is transiently immobilized in nanodomains, which are abundant at the post-synapse, as illustrated in **Figures 1.24 b, c** (Kedia et al., 2020). When present at the cell surface, APP might be processed by α-secretase and γ-secretase (**Figure 1.23**) (Delbove et al., 2018), (reviewed in (Wilquet & Strooper, 2004)). On the other hand, when the uncleaved APP at the plasma membrane is internalized to early endosomes, it can be sorted into different pathways, including being recycled back to the TGN or to the plasma membrane. Alternatively, it can be processed by β- and γ-secretase at the endosomal membrane or undergo degradation in late endosomes/lysosomes (**Figure 1.23**) (as reviewed in (Burrinha & Cláudia, 2022)).
Overall, APP displays a fast turnover, with a half-life ranging from approximately 1 hour to approximately 4 hours (considering studies *in vitro* and *in vivo*), as reviewed in (Hunter & Brayne, 2012), suggesting it could play a dynamic function at the synapse.

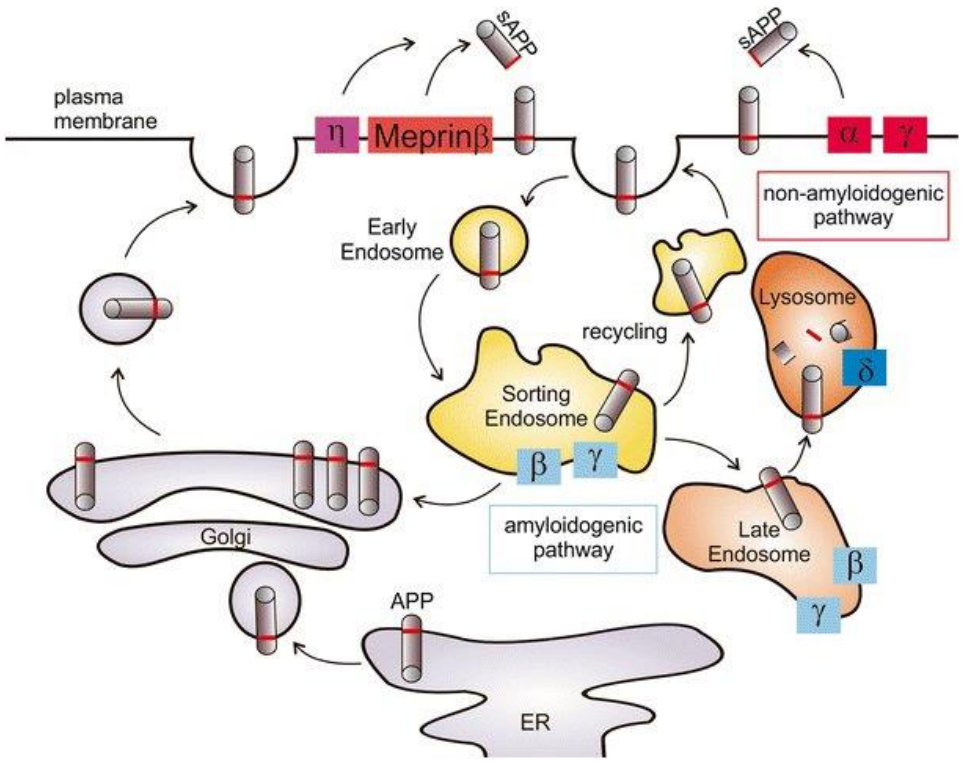

Figure 1.23 – APP trafficking and processing. Adapted from (Eggert et al., 2018).

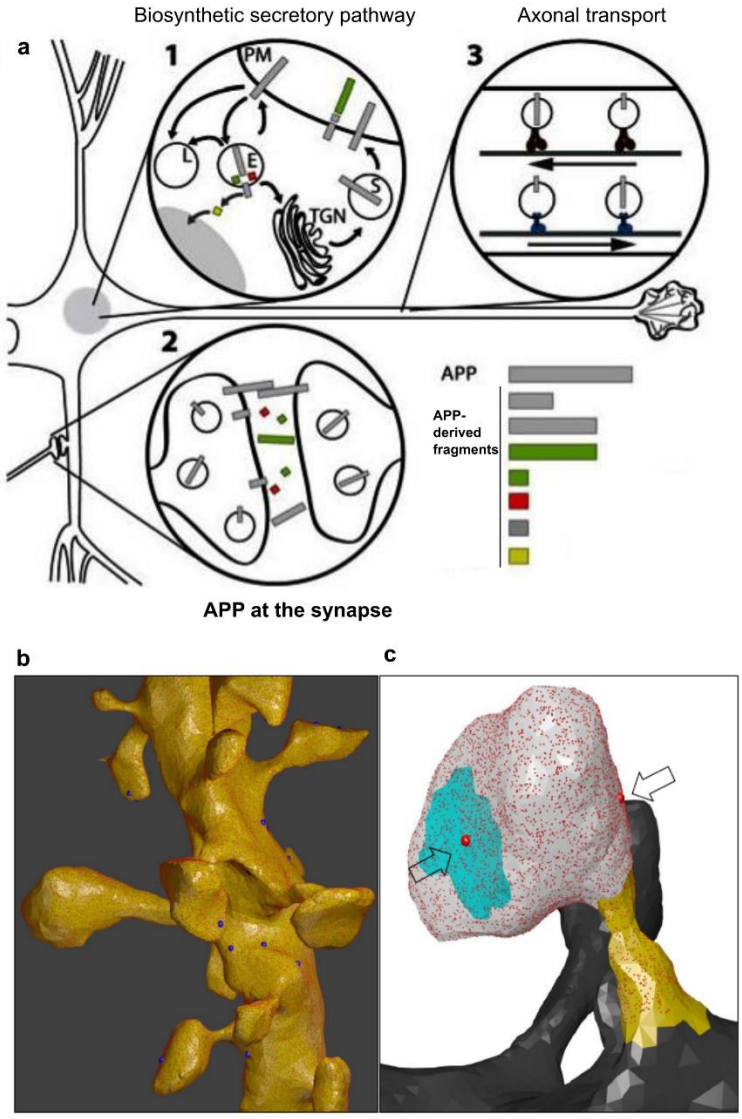

Figure 1.24 – APP is located at the synapse.

a) Schematic depiction of the intracellular trafficking and synaptic location of APP. 1 Major trafficking steps of APP at the biosynthetic secretory pathway. TGN Trans-Golgi network, PM plasma membrane, E endosome, L lysosome. 2 Anterograde and retrograde axonal transports of APP. 3 Localization of APP and secretion of APP fragments at the synaptic compartment. Adapted from (Brunholz et al., 2012).

b) *In silico* reconstruction of APP nanoscale distribution in a CA1 dendrite. APP distribution data was obtained by super resolution microscopy in mouse primary neuronal cultures (DIV21) and applied to a dendritic shaft model of pyramidal neurons from the CA1–CA3 region of the adult rat hippocampus. Yellow represents the geometrical reconstruction of dendritic shaft. Red puncta represent monomeric APP and blue clusters indicate nanodomains of APP. Adapted from (Kedia et al., 2020).

c) *In silico* reconstruction of APP distribution in functional zones of excitatory synapses in a CA1 dendrite. APP distribution data was obtained by super resolution microscopy in mouse primary neuronal cultures (DIV21) and applied to a dendritic shaft model of pyramidal neurons from the CA1–CA3 region of the adult rat hippocampus. Yellow, white and cyan regions indicate extrasynaptic, perisynaptic (endocytic zone) and postsynaptic density, respectively. Red puncta represent APP monomers and red clusters represent APP

nanodomains. Arrows indicate APP nanodomains in post and perisynaptic regions Adapted from (Kedia et al., 2020).

E) Why is it challenging to study APP physiological roles at the synapse?

It is particularly difficult to decipher the APP synaptic function given the functional redundancy with members of the same protein family, but also considering the multiple APP fragments generated by secretase cleavage, which play distinct neuronal functions (U. C. Müller & Zheng, 2012). Finally, the fact that APP is involved in the pathogenesis of Alzheimer's Disease (Hardy & Higgins, 1992), has led to multiple studies in the context of disease, while little is known about the physiological role APP.

Ei) APP family members – overlapping functions

In mammals, APP is a member of the APP family of proteins, which also includes APP-like protein 1 and 2 (APLP1 and APLP2) (Wasco et al., 1993). All family members share a similar structure, in which the C-terminal domain, in particular the YENPTY motif, is highly conserved (**Figure 1.25 a, b)**, whereas the N terminus is more divergent (Shariati & de Strooper, 2013). APLP2 is expressed in multiple organs and tissues, whereas APLP1 is mainly expressed in the brain, resembling APP695 (Lorent et al., 1995) (**Figure 1.25a**). Although processing by secretases is a common feature of APP and APP-like proteins (Eggert et al., 2004), APP is the only family member with an Aβ peptide domain, as represented in **Figure 1.25 a**.

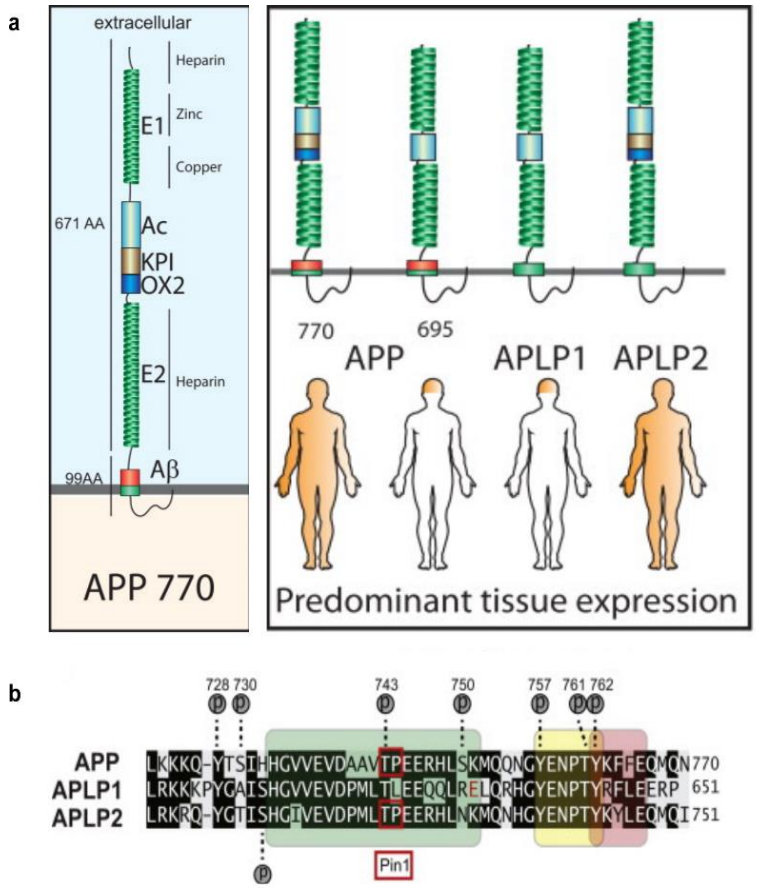

Figure 1.25 – Tissue expression, protein domains and homology in the C-terminal sequence for the APP family members.

a) Domain organization and tissue expression of APP (770 and 695), APLP1 and APLP2.

b) Alignment of the intracellular C-terminal domain of APP, APLP1, and APLP2 showing high sequence homology between the members of this family.

Adapted from (van der Kant & Goldstein, 2015)

Importantly, models lacking only one of the family members are viable and show subtle phenotypes (Dawson et al., 1999, Heber et al., 2000, von Koch et al., 1997). In contrast, APP/APLP2 and APLP1/APLP2 knockout mice as well as triple knockouts for APP/APLP1/APLP2 die shortly after birth (Heber et al., 2000, von Koch et al., 1997), as described in **Table 1.6**. Overall, these findings indicate that APP family members might have overlapping functions and compensate for each other. Alternatively, they might possess unrelated nonredundant functions, with the net effect leading to lethality in double/triple knockout mice. This aspect should be taken into consideration when studying APP physiological roles, since APLPs might compensate for the lack of APP.

Table 1.6 – Reported viability for single, double and triple knockout (KO) mice for APP family proteins.

Model		Viability	Reference
Single KO	APP	Viable	(Dawson et al., 1999)
	APLP1	Viable	(Heber et al., 2000)
	APLP2	Viable	(von Koch et al., 1997)
Double KO	APP/APLP1	Viable	(Heber et al., 2000)
	APP/APLP2	Early postnatal lethality	(von Koch et al., 1997, Heber et al., 2000)
	APLP1/APLP2	Early postnatal lethality	(Heber et al., 2000)
Triple KO	APP/APLP1/APLP2	Early postnatal lethality	(Heber et al., 2000)

Eii) APP processing – multiple fragments

The canonical model of APP proteolysis involves processing by one of the following pathways: i) the non-amyloidogenic, which preferentially occurs at the cell surface; and ii) the amyloidogenic, which leads to Aβ production and occurs in early endosomes, as reviewed in (Haass et al., 2012) (**Figure 1.26**).

Non-amyloidogenic processing starts with APP cleavage by α-secretase (Sisodia, 1992), mainly ADAM10 (disintegrin and metalloproteinase domain-containing protein 10) (P. H. Kuhn et al., 2010). This cleavage step releases the soluble ectodomain of APP (sAPPα) and gives rise to a membrane-tethered intracellular C-terminal fragment, denominated CTFα or C83. The subsequent intramembrane cut by γ-secretase (a multi-subunit protease complex containing presenilin) liberates a peptide called p3 and the APP intracellular domain (AICD) (Kojro & Fahrenholz, 2005), as illustrated in **Figure 1.26**.

On the other hand, the amyloidogenic processing mainly occurs in early endosomes (Koo & Squazzo, 1994) , where APP and β-secretase converge (Das et al., 2013). This pathway involves an initial APP cleavage by β-secretase (β-site APP-cleaving enzyme 1: BACE1), leading to the extracellular release of a soluble APP peptide (sAPP-β) and the retention of the corresponding C-terminal fragments CTF-β (C99) or CTF- β' (C89). Then, CTFβ is subjected to γ-secretase cleavage, yielding Aβ and AICD (Wilquet & Strooper, 2004), as represented in **Figure 1.26**.

Despite having the same amino acid sequence, AICDs from each pathway show distinct stability and function. When produced through the amyloidogenic pathway, AICD is thought to form a protein complex with Fe65, being transported to the nucleus and

showing transcriptional roles (Belyaev et al., 2010), whereas the same peptide is rapidly degraded in the cytosol by insulin-degrading enzyme when originated from non-amyloidogenic processing (Edbauer et al., 2002).

Besides negatively regulating the APP cellular adhesion properties, APP processing gives rise to multiple proteolytic products which have physiological/pathological roles in neurons (as reviewed in (U. C. Müller et al., 2017)). Besides the conventional amyloidogenic / non-amyloidogenic processing, alternative APP-cleavage pathways have been recently discovered (e.g. δ-, η- and meprin pathways, as reviewed in (Andrew et al., 2016). Therefore, it is extremely difficult to discriminate between signaling by APP full-length or its derived fragments.

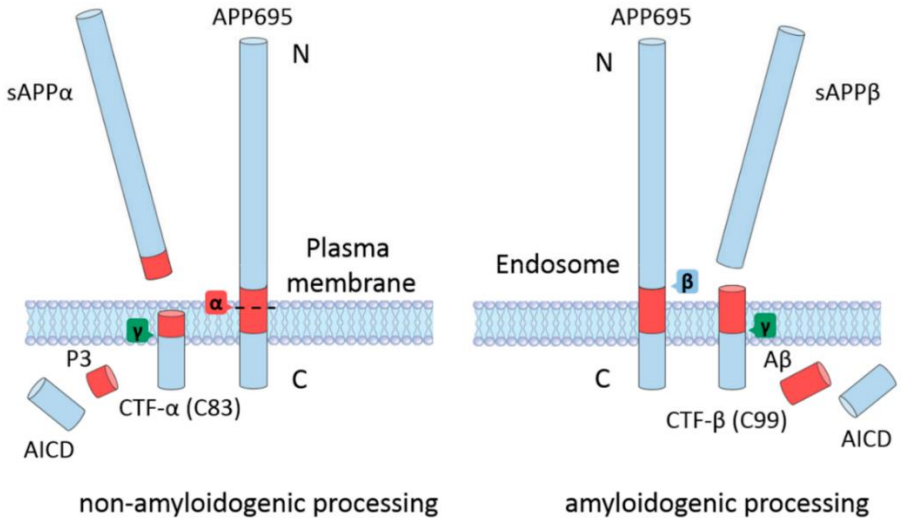

Figure 1.26 –The proteolytic cleavage of APP by the non-amyloidogenic and amyloidogenic processing pathways. Adapted from (T. Zhang et al., 2020).

Eiii) APP is involved in Alzheimer's Disease

APP is involved in the pathogenesis of Alzheimer's Disease (Hardy & Higgins, 1992), explaining why most studies so far have been performed in the context of disease, while far less is known about APP physiological role.

Accordingly, AD (in both sporadic and familial forms) is characterized by the accumulation of Aβ (generated from APP amyloidogenic processing), which has been associated with synaptic and memory impairments, as reviewed in (Hampel et al., 2021). Interestingly, additional studies showed that AD patients also exhibit an accumulation in APP full-length and other APP-derived fragments, including increased levels of CTFβ in synapses (Ferrer-Raventós et al., 2023), elevated AICD levels (Ghosal et al., 2009) and APP full-length accumulation around amyloid plaques (Jordà-Siquier et al., 2022). This

data indicates that both APP full-length and its derived amyloidogenic fragments might be involved and/or affected in AD.

Importantly, familial AD (fAD) patients (<1% total cases) carry autosomal dominant mutations in the presenilin proteins (PSEN1, PSEN2 - part of γ-secretase) or in APP, as reviewed in (Tcw & Goate, 2017). Most APP pathogenic mutations cluster around the γ-secretase cleavage site (**Figure 1.27**) and result in increased production of longer forms of Aβ, which tend to be less soluble and more toxic (Shen & Kelleher, 2007). Additionally, the pathogenic Swedish mutation (Mullan et al., 1992) and the protective Iceland mutation (Jonsson et al., 2012) occur in sequences adjacent to the β-secretase cleavage site (**Figure 1.27**), having opposite effects in Aβ levels (Citron et al., 1992), (Jonsson et al., 2012).

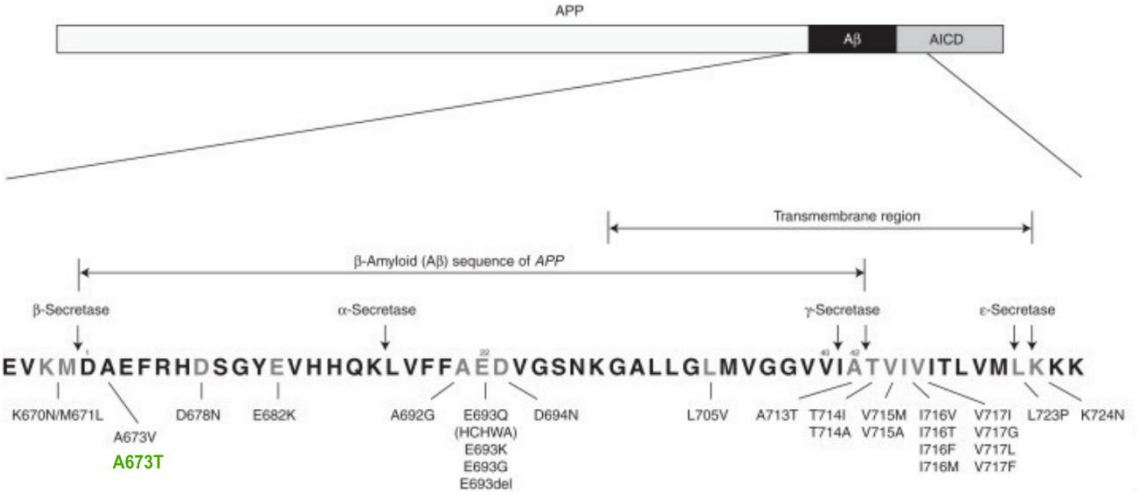

Figure 1.27 – Schematic illustration of APP sequence (top) and the location of pathogenic substitutions in APP linked to familial AD, as well as the A673T protective mutation (in green). Adapted from (Tcw & Goate, 2017).

Considering the neurotoxic effects of Aβ accumulation (Mucke & Selkoe, 2012), the modulation of APP processing has emerged as a potential therapeutical approach in AD. However, clinical trials involving β- and γ-secretase inhibitors have shown no positive effects in cognitive performance and were associated with serious side effects (Doody et al., 2013), (Egan et al., 2018), possibly because they interfered with other γ-and β-secretase substrates with crucial biological functions.

Accordingly, BACE1 (β-secretase) is involved in important brain processes including myelination, neuronal migration, cell adhesion, dendrite/spine development and synaptic

plasticity and has substrates such as NRG1 (Neuregulin 1), Sez6 (Seizure-related gene 6), CHL1 (Close homologue of L1) and Contactin-2, as reviewed in (Munro et al., 2016). Moreover, PSEN1 (γ-secretase) is associated with neurite outgrowth and cell adhesion, having notch and ephrins as substrates (reviewed in (Haapasalo & Kovacs, 2011)).

Finally, ADAM10 (α- secretase) has been implicated in neuronal differentiation and migration, cell adhesion, neurite outgrowth, synaptic functions, acting on substrates such as Notch, Cadherins, Ephrins and NLGN1 (Neuroligin-1) (P.-H. Kuhn et al., 2016).

The fact that conditional forebrain postnatal KO models for BACE1, PSEN1 and ADAM10 show memory and/or synaptic deficits (Ou-Yang et al., 2018, Yu et al., 2001, Prox et al., 2013) indicates that all secretases have important physiological functions in the brain. Thus, caution might be taken when pharmacologically modulating APP processing since other substrates might act as confounding factors.

Considering the contribution of APP and its processing pathways to Alzheimer's Disease pathology, the elucidation of APP physiological function in neurons might be extremely useful to better understand the disease.

F) Which mouse models have been used to study APP physiological functions?

Several knockout and knock-in (KI) mouse models have been developed to study the physiological role of APP in the brain.

Firstly, a single APP knockout mouse model was developed, which only exhibited a subtle phenotype, with LTP, learning and memory impairments starting at 10 months of age (Dawson et al., 1999, Tyan et al., 2012). These findings led to the hypothesis that other APP family members could compensate for the lack of APP.

Thus, double (DKO) and triple (TKO) knockout mouse models have been generated to study the APP family members, avoiding compensatory responses. However, since these animals die shortly after birth (Heber et al., 2000, von Koch et al., 1997, Herms et al., 2004) (**Table 1.6**), the development of conditional knockouts specific to the forebrain has emerged as a suitable alternative.

When the triple KO is induced in the forebrain during embryonic development (E11.5) (NexCre cTKO), mice show gross brain morphology alterations related to developmental deficits (agenesis of the corpus callosum and disrupted hippocampal lamination) (Steubler et al., 2021). This clearly shows the crucial role of the APP family proteins for neuronal positioning/migration, which is further supported by the dysregulation of

neuronal migration observed in the rat cortex after *in utero* knockdown of APP (Young-Pearse et al., 2007). However, given these gross brain malformations, it is not possible to dissect the APP physiological role in synapse formation/maturation processes and synaptic plasticity in postnatal/adult stages using this model, since they might occur as consequences of impaired brain development.

In contrast, when the triple KO is induced only after the second postnatal week (Camk2a Cre cTKO), APP is still present at normal levels during embryonic and early postnatal development. Therefore, the deficits in NMDAR responses, LTP, learning and memory observed in this model at 3 months of age possibly correlate with APP function in mature synapses (S. H. Lee et al., 2020). This model is suitable to study APP roles in adult/mature synapses but does not allow to take conclusions about the impact of APP in synapse formation/maturation during the first two weeks of life.

An alternative model is the conditional APP depletion during embryonic development at the forebrain on a constitutive global APLP2KO background. These mice (NexCre cDKO) allow to study APP in all steps of synapse formation, maturation and maintenance. They are viable and exhibit no brain morphology alterations, indicating that APLP1 might compensate for the lack of APP and APLP2 during embryonic development. However, they exhibit LTP and learning/ memory impairments at young adult stages (4-6 months), suggesting that APLP1 compensation is not sufficient at this stage (Hick et al., 2015). However, we cannot determine if these impairments are due to alterations in synapse formation/maturation during early postnatal development or if they arise only upon adulthood.

The main findings obtained in these knockout mouse models regarding brain development, synaptic function/plasticity and learning/memory are summarized in **Table 1.7**. Overall, these studies show that the phenotype depends on the developmental stage is which the knockout is induced, as illustrated in **Figure 1.28**.

Table 1.7 – Summary of the main findings observed in viable mouse models of APP single KO and APP family members conditional KO.

Mouse Model	Description	Timing of KO	Region of KO	Phenotype	References
APP KO	Complete knockout of APP	Embryonic development	Full brain	↓LTP ↓Learning and memory (only after 10 months)	(Dawson et al., 1999, Tyan et al., 2012)
NexCre cDKO	Conditional **double** KO (Conditional APP KO + Global APLP2 KO)	Embryonic development	Forebrain (excitatory)	↓LTP ↓Learning and memory (4-6 months)	(Hick et al., 2015)
NexCre cTKO	Conditional **triple** KO (APP, APLP1, APLP2)	Embryonic development	Forebrain (excitatory)	**Altered brain morphology** ↓ Dendritic length and spine density of pyramidal cells ↓Basal synaptic transmission ↓LTP ↓Learning and memory (4-7 months)	(Steubler et al., 2021)
Camk2a Cre cTKO	Conditional **triple** KO (APP, APLP1, APLP2)	Postnatal day 18	Forebrain	↓NMDAR response ↓LTP ↓Learning and memory (3 months)	(S. H. Lee et al., 2020)

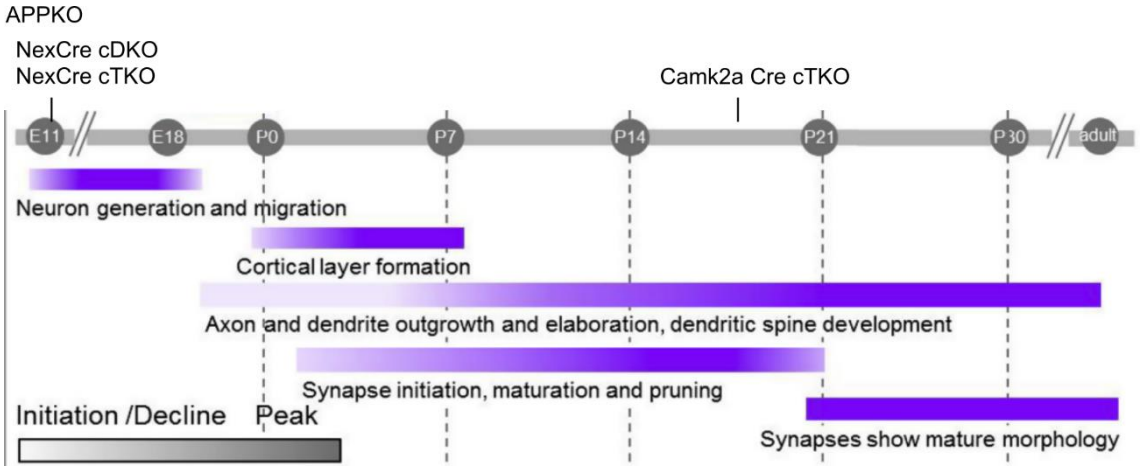

Figure 1.28 - Schematic representation of the cortical development and synaptogenesis in rodents, as well as the developmental stage in which the knockout of APP/APP family members is induced in following mouse models: APP KO, NexCre cDKO, NexCre cTKO and Camk2a Cre cTKO. Adapted from: (Allen, 2020)

Moreover, knock-in models have been originated to decipher the role of different APP domains or derived fragments, including the sAPPα-KI mice (which only produce the sAPPα) and the APPΔCT15-KI mice (which express APP lacking the last 15 amino acids, which include the YENPTY motif (Ring et al., 2007), as illustrated in **Figure 1.29**. Interestingly, both single knock-in lines are viable and show a wild type-like phenotype (2-15 months), possible due to a functional compensation by APP family members.

When the same models were bred to an APLP2-KO background, generating double mutants (DM), they exhibited partial viability. In both cases, mice displayed LTP and learning/memory impairments in young adult stages (Klevanski et al., 2015, Weyer et al., 2011), showing the functional relevance of the APP intracellular domain.

Moreover, Matrone et al. have created a knock-in model with a mutation in the highly conserved ^{682}YENPTY^{687} motif. The mutation occurs at the tyrosine residue 682, which is replaced by a glycine (Y682G), giving rise to the APP YG/YG mouse model. These mice are characterized by an age-dependent decline in cognitive functions (after 7 months of age), similarly to what occurs in the APP KO model (Matrone et al., 2012). When crossing this mouse line with APLP2 KO mice, Barbagallo et al. have reported postnatal lethality and neuromuscular defects, as observed in APP/APLP2 double KOs (Barbagallo et al., 2010).

The main findings obtained in these knockout mouse models regarding brain development, synaptic function/plasticity and learning/memory are summarized in **Table 1.8**.

Altogether, these studies suggest that APP family members have important physiological roles in neurons, at least partly mediated by the APP intracellular domain. However, the mechanisms behind APP roles in brain development, synaptic plasticity, learning and memory are not fully understood.

Table 1.8 – Summary of the main findings observed in mouse APP knockin models.

Model	Single Mutant (age)	Double Mutant (in APLP2KO) (age)	References
sAPPα -KI mice (only sAPPα)	Viable Wild-type like (2-15months)	Partially viable ↓LTP ↓Learning and memory (3-13months)	(Ring et al., 2007, Weyer et al., 2011)
APPdCT15 KI mice (APP lacking the last 15 a.a.)	Viable Wild-type like (2-15months)	Partially viable ↓LTP ↓Learning and memory (5-12months)	(Ring et al., 2007, Klevanski et al., 2015)
APP YG/YG mice (tyrosine 682 is replaced by a glycine (Y682G))	Viable ↓Learning and memory (only after 7 months)	Early postnatal lethality	(Matrone et al., 2012, Barbagallo et al., 2010)

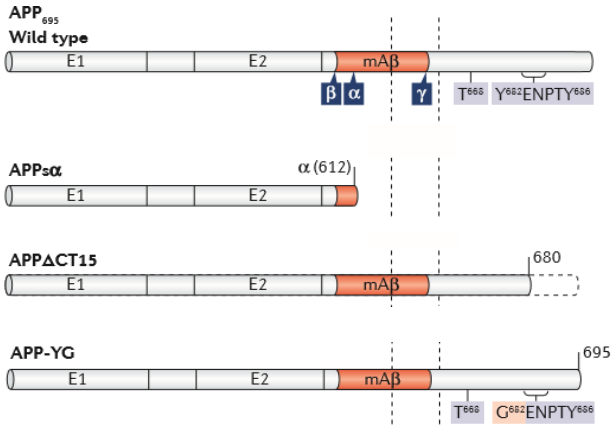

Figure 1.29 – Schematic representation of APP and APP variants expressed in knock-in mice. Adapted from (U. C. Müller et al., 2017).

G) APP regulates synaptic adhesion and synaptogenesis

APP has been described as a synaptic adhesion molecule, considering its synaptic localization, its ability to promote cell-cell interactions and the fact that APP loss results in altered synapse formation, as illustrated in **Figure 1.30a** (reviewed in (Sosa et al., 2017)).

Accordingly, several studies indicate that APP family members promote cell adhesion, by forming trans-dimers in intercellular contact sites. Soba et al. have used Drosophila Schneider (S2) cells and analyzed co-clustering after mixing two cell pools that express

proteins of the APP family. The authors have shown that these proteins promote cell adhesion, by stabilizing cell–cell interactions through trans-dimerization via the E1 domain. Moreover, in this study, the depletion of APP family members was sufficient to cause a reduction in intercellular adhesion in mouse embryonic fibroblasts (MEFs) (Soba et al., 2005).

The main question was whether this intercellular interaction would also occur between pre and postsynaptic terminals, where APP family members are located. Using mouse brain samples, Soba et al. showed that APP family members form dimers at the synapse (Soba et al., 2005).

This data suggested that APP could work as a synaptic adhesion molecule, possibly contributing to synaptogenesis. This hypothesis was tested in the neuromuscular synapse, using APP conditional knockout mouse models for motor neurons or in the muscle. The authors showed that both pre- and postsynaptic APP are required for the proper apposition of pre-synaptic proteins and post-synaptic receptors, leading to neuromuscular synapse development (Z. Wang et al., 2009). This possibly explains the neuromuscular junction deficits observed in APP/APLP2 double knockout mice (P. Wang et al., 2005).

This led to the hypothesis that APP could act in a similar way in central synapses. Wang et al. showed that APP promotes synaptogenesis *in vitro*, by using a co-culture system in which primary neurons were cultured together with HEK293 cells overexpressing APP. The authors observed an increase in synaptogenesis in neuronal axons contacting with HEK cells, which required APP expression in both contact sites. In fact, this synaptogenic effect was inhibited when HEK293 cells overexpressing APP were co-culture with APP-depleted primary neurons. Importantly, only the full-length protein and not the extra/intracellular domains alone were able to rescue synaptogenesis in this condition (Z. Wang et al., 2009).

These results suggest that the full-length protein would be the one responsible for synaptic adhesion and synaptogenesis, whereas APP processing could potentially interfere with these processes. Accordingly, APP cleavage deficient forms have shown to induce an increase in cell aggregation (tested in S2 cells) and synaptogenesis (tested in a co-culture with APP-HEK cells and primary neurons) (Stahl et al., 2014). Therefore, the current model suggests that APP-trans dimerization induces synaptogenesis and cell

adhesion, whereas APP processing reduces dimerization, having an inhibitory role in both processes, as illustrated in **Figure 1.30b**.

By acting as a synaptic adhesion molecule, APP might be able to recruit important components to pre and postsynaptic terminals, assuring their proper apposition (**Figure 1.30a**). In fact, APP-depletion in rat primary neuronal cultures results in a lower puncta density of pre-synaptic (Bassoon) and postsynaptic (PSD-95) markers (K. J. Lee et al., 2010), which is similar to the recently reported results in APP-depleted human induced neurons (Zhou et al., 2022). To better understand the synaptogenic function of APP, future studies will be important to identify the list of pre- and post-synaptic components that are regulated by APP, as well as to unravel how APP controls their recruitment and/or stabilization at synaptic sites.

By inducing the clustering of synaptic proteins in newly formed synapses, APP could contribute to the consequent activation of signaling pathways, leading to dendritic spine formation and synapse maturation, as described for other synaptic adhesion molecules, as illustrated in **Figure 1.30a** (Dalva et al., 2007).

Accordingly, loss/gain of function experiments implicate APP in the regulation of spine density. APP KO hippocampal neuronal cultures have shown a reduction in spine density compared with wild-type neurons (Tyan et al., 2012), similarly to the effect observed upon APP knockdown in neuronal cultures (K. J. Lee et al., 2010).

This defect is also observed in CA1 neurons from APP KO mice only upon aging (Tyan et al., 2012) and in young adult NexCre-cDKO mice (11-13 weeks) (Hick et al., 2015). Interestingly, Zou et al. have proposed a role for APP in the regulation of spine dynamics, since both spine formation and elimination are reduced in the somatosensory cortex of APP KO mice (5-7 months old) (Zou et al., 2016). On the other hand, APP overexpression has resulted in increased spine densities in hippocampal neuronal cultures, being dependent on both the extracellular and intracellular domains of APP (K. J. Lee et al., 2010). The results obtained regarding spine/synapse density upon manipulation of APP levels in neuronal cultures and mouse models are summarized in **Tables 1.9 and 1.10**.

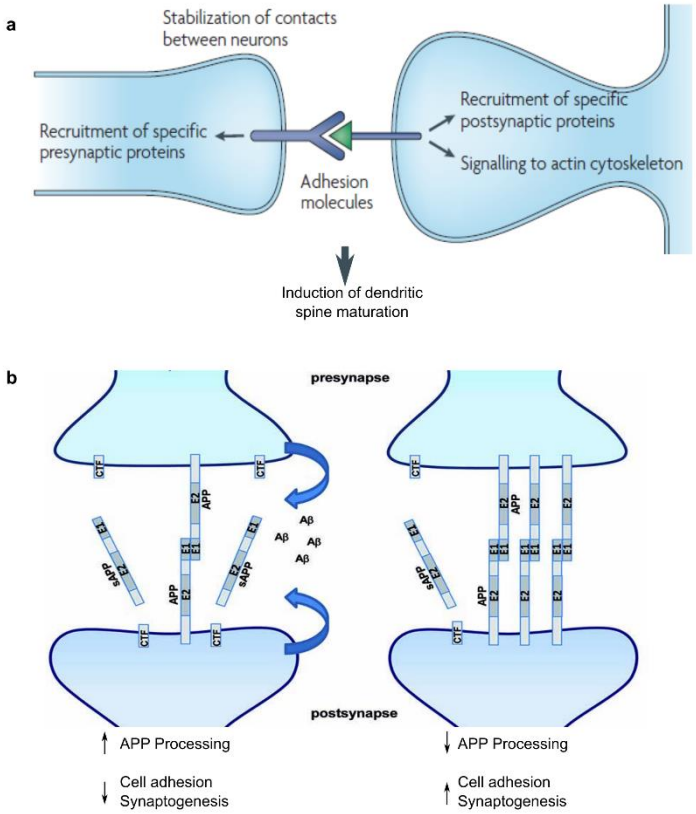

Figure 1.30 – APP is a synaptic adhesion molecule which contributes to synaptogenesis.

a) Functions of synaptic adhesion molecules during synaptogenesis. Adapted from (Dalva et al., 2007).

b) APP processing alters the levels of APP available for trans-dimerization at the synapse, thereby influencing its ability to promote cell adhesion and synaptogenesis. Adapted from (Stahl et al., 2014).

H) APP regulates glutamatergic transmission, synaptic plasticity and memory

In mature synapses, synaptic adhesion molecules interact and modulate pre- and post-synaptic components (**Figure 1.31**) (reviewed in (Dalva et al., 2007)). Accordingly, APP interacts and regulates synaptic vesicle proteins at the presynaptic active zone in the mouse brain (del Prete et al., 2014, Laßek et al., 2014) and facilitates glutamate release in mouse hippocampal slices (Fanutza et al., 2015). Moreover, APP exhibits postsynaptic functions, having been described as a regulator of glutamate ionotropic receptors. Previous studies suggest that APP/APP-derived fragments regulate the levels of AMPAR subunits (Paschou et al., 2023, Martinsson et al., 2019), the synaptic levels and currents of kainate receptores (Barthet et al., 2022) and the surface levels and currents of NMDARs (Hoe et al., 2009, Cousins et al., 2009, Pousinha et al., 2017).

Consistent with this hypothesis, Hoe et al. have observed a reduction in NMDAR subunits located at the dendritic surface following APP silencing, accompanied by a decrease in NMDA-evoked current densities in cerebellar granule cells. In contrast, APP overexpression has been associated with an increase in NMDAR-mediated currents and surface levels in the same model (Hoe et al., 2009). Moreover, Camk2a Cre cTKO mice exhibit a decrease in NMDAR currents while the AMPAR component is maintained (S. H. Lee et al., 2020). Finally, APP depletion during embryonic development has proved to reduce GluN2B-NMDAR currents in infant mice (Pousinha et al., 2017).

The impact of APP on NMDARs might result in alterations in synaptic plasticity mechanisms. Accordingly, APP KO mice exhibit impairments in LTP and learning skills upon aging (observed at 10 months, but not at 4 months) (Dawson et al., 1999) and NexCre-cDKO mice show pronounced deficits in LTP, learning and memory performance in young adult stages (2-6 months) (Hick et al., 2015).

Concurrently, transgenic mouse models of APP overexpression exhibit progressive learning and memory impairments. Accordingly, two independent studies have reported deficits in behavioral tests upon aging (8-12 months), whereas earlier time points (5-6 months) were characterized by a normal performance (Moran et al., 1995),

Altoghether, these studies show the importance of maintaining APP under physiological levels to obtain normal synaptic plasticity mechanisms, learning and memory skills. The exact mechanisms by which APP regulates these processes are still unknown but might potentially involve NMDAR regulation. Another open question in the field is whether these effects are mediated by APP-full length and/or its derived fragments. The APP intracellular domain has emerged as an important domain for these functions, considering the impairments in LTP and hippocampus-dependent behavior observed in APPsα-KI mice and APPdCT15-KI / APLP2 KO mice (Weyer et al., 2011, Klevanski et al., 2015).

The results obtained regarding glutamatergic transmission, synaptic plasticity and/or learning/memory upon manipulation of APP levels in neuronal cultures and mouse models are summarized in **Tables 1.9 and 1.10**.

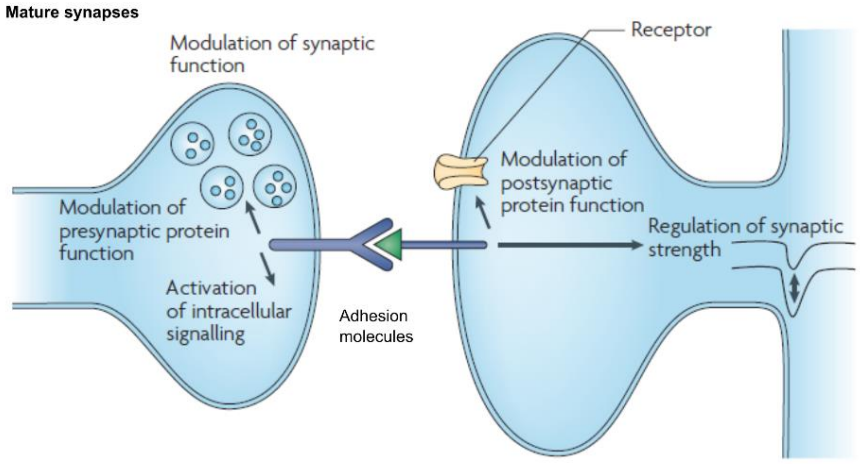

Figure 1.31 – Synaptic adhesion molecules modulate the function of pre- and post-synaptic proteins in mature synapses, having an impact in synaptic plasticity mechanisms.

Adapted from (Dalva et al., 2007).

Table 1.9 – Summary of the main findings observed in APP knockout (KO) and knockdown (KD) models *in vitro* (rodent neuronal cultures and human induced neurons) and *in vivo* (rodents).

	Model	Spine/synapse density	Glutamatergic transmission	Synaptic plasticity	Learning/ memory
In vitro	APP KO rodent primary neurons	↓ **Spine density** Hippocampal neurons, DIV 16-21 (Tyan et al., 2012)	-	-	-
	APP KO Human iNs	↓ **Synapse density** Human iNs, DIV 35-40 (Zhou et al., 2022)	↓ **mEPSCs frequency** ↓ **Amplitude of evoked EPSCs** Human iNs, DIV 35-40 (Zhou et al., 2022)	-	-
	APP KD rodent primary neurons	↓ **Synapse density** Hippocampal neurons, DIV 21-24 (K. J. Lee et al., 2010)	↓ **NMDAR currents** CGCs, DIV 7-8 NMDA-evoked current densities (Hoe et al., 2009)	-	-

In vivo	APP KO mice	↓ **Spine density** -Mice, 12 months Cortex (layers II/III) and Hippocampus (CA1) (K. J. Lee et al., 2010) -Mice, 12-15months, CA1 (Tyan et al., 2012) **= Spine density** -Mice, 4 months, CA1 (Tyan et al., 2012) -Mice, 5-7 months Somatosensory cortex (Layer V) (Zou et al., 2016) ↑ **Spine density** Mice, 4-6 months, Cortex (Bittner et al., 2009) ↓ **Spine formation and elimination** Mice, 5-7 months Somatosensory cortex (Layer V) (Zou et al., 2016)	-	↓ **LTP** -Mice, 8–12 months, 20–24 months CA1 (Seabrook et al., 1999) -Mice, 8–12 months, 20–24 months CA1 (Dawson et al., 1999) -Mice, 12-15months CA1 (Tyan et al., 2012) -Mice, 9–12months CA1 (Ring et al., 2007) **= LTP** Mice, 4 months, CA1 (Tyan et al., 2012)	↓ **Learning and memory** -Mice,10 months Conditioned avoidance test, Watermaze test (Dawson et al., 1999, Ring et al., 2007) **= Learning and memory** -Mice, 4 months Conditioned avoidance test, Watermaze test (Dawson et al., 1999, Ring et al., 2007)
	APP KD in mice	-	↓ **GluN2B-NMDAR contribution** -Mice, P7–9, *In utero* electroporation with shAPP Evoked NMDAR-EPSCs, CA1 (Pousinha et al., 2017)	-	-
	NexCre cDKO mice	↓ **Spine density and size** Mice, 11-13 weeks, CA1 (Hick et al., 2015)	**= NMDAR and AMPAR currents** -Mice, 4-6 months, Spontaneous synaptic mEPSCs (AMPAR and NMDAR), CA1 (Hick et al., 2015)	↓ **LTP** -Mice, 4-6 months, CA1 (Hick et al., 2015)	↓ **Learning and memory** -Mice, 2-5 months Morris water maze, radial maze (Hick et al., 2015)
	Camk2a Cre cTKO mice	-	↓ **NMDAR currents =AMPAR currents** -Mice, 3 months Evoked NMDAR-EPSCs, CA1 (S. H. Lee et al., 2020)	↓ **LTP** -Mice, 3 months, CA1 (S. H. Lee et al., 2020)	↓ **Learning and memory** -Mice, 3 months Morris water maze test (S. H. Lee et al., 2020)
	APPdCT 15 KI/ APLP2 KO mice	-	-	↓ **LTP** Mice, 9-12-months CA1 (Klevanski et al., 2015)	↓ **Learning and memory** -Mice, 5.5–7months T-maze, radial maze (Klevanski et al., 2015)
	sAPPsα - KI / APLP2 KO mice	**= Spine density** Mice, 3-5 months, CA1 (Weyer et al., 2011)	-	↓ **LTP** Mice, 3-5 months; 10-13 months, CA1 (Weyer et al., 2011)	↓ **Learning and memory** -Mice, 3-5 months T maze, radial maze (Weyer et al., 2011)
	APP YG/YG	↓ **Spine density** Mice (2 and 7months), CA1 (Matrone et al., 2012)	-	-	↓ **Learning and memory** -Mice, 7 months Active avoidance, NOR, RAWM tests

					(Matrone et al., 2012) **= Learning and memory** -Mice, 4 months Active avoidance, NOR, RAWM tests (Matrone et al., 2012)

Abbreviations: DIV – days in vitro, CGCs - Cerebellar granule cells, iNs – induced neurons, NOR - novel object recognition, RAWM - radial-arm water maze,

Table 1.10 – Summary of the main findings observed in APP overexpression models in rodents (in vitro and and in vivo models).

	Model	**Spine density**	**Glutamatergic transmission**	**Learning/memory**
In vitro	APP overexpression in primary neurons	↑ **Spine density** Hippocampal neurons DIV 21-24 (K. J. Lee et al., 2010)	↑ **NMDAR currents** CGCs, DIV 7-8 Hippocampal neurons, DIV 11–13 NMDA-evoked current densities (Hoe et al., 2009)	-
In vivo	Transgenic mice expressing human APP in neurons	-	-	↓ **Learning and memory** -Mice, 12 months (Moran et al., 1995) -Mice, 8 months (Simón et al., 2009) **= Learning and memory** -Mice, 6 months (Moran et al., 1995) -Mice, 5 months (Simón et al., 2009) Y maze, water maze, object recognition

Abbreviations: DIV – days in vitro, CGCs - Cerebellar granule cells, iNs – induced neurons, NOR - novel object recognition, RAWM - radial-arm water maze,

Overall, these findings show that APP is able to modulate neuronal activity. Interestingly, neuronal activity is also able to modulate APP. Accordingly, electrical and chemical stimulation in rodent hippocampal slices (Farber et al., 1995, Kamenetz et al., 2003), as well as NMDAR activation in primary neuronal cultures (Hoey et al., 2009) results in increased secretion of APP-derived fragments, which might in turn also affect synaptic

transmission. The complex interplay between APP, its cleavage products and synaptic transmission is not fully understood. However, it has been suggested that the function of APP trans-dimers might dominate under conditions of low neuronal activity or in early steps of synaptogenesis, whereas activity-dependent increase of APP processing might lead to a domination of APP cleavage products function (Stahl et al., 2014).

I) Which are the physiological/pathological roles of APP-derived fragments?

Not only APP full-length protein, but also its derived fragments are known to play important synaptic roles, as summarized in **Table 1.11**. However, discriminating the effects of each APP fragments is extremely challenging. Most studies so far were based on the overexpression of these fragments, thereby not recapitulating what happens in physiological conditions. When considering the fragments generated by the conventional APP processing pathways (amyloidogenic and non-amyloidogenic), important effects have been attributed to sAPP α, CTFβ, Aβ and AICD (reviewed in (U. C. Müller et al., 2017)). Additionally, fragments originated from η-secretase cleavage have also shown important synaptic roles (Willem et al., 2015, Mensch et al., 2021).

The acute application of sAPPα has been linked to neuroprotective actions (Corrigan et al., 2014, Smith-Swintosky et al., 1994, Hefter et al., 2016), being able to increase spine density (Weyer et al., 2014), NMDAR activation (Taylor et al., 2008, Moreno et al., 2015) and LTP at the CA1 region of the hippocampus (A. Ishida et al., 1997, Moreno et al., 2015, Xiong et al., 2017), together with an improved spatial memory in rodents (Xiong et al., 2017).

In contrast, CTFβ overexpression leads to a reduction in NMDAR currents (Hoe et al., 2009), LTP magnitude (Nalbantoglu et al., 1997) and memory performance (Nalbantoglu et al., 1997, D. K. Song et al., 1998, Berger-Sweeney et al., 1999), as well as an impaired lysosomal-autophagic function in rodent models (Lauritzen et al., 2012). Importantly, this fragment has shown to accumulate at the synapses of Alzheimer's Disease patients (Ferrer-Raventós et al., 2023).

Interestingly, dose-dependent responses have been observed upon Aβ incubation/injection. When present in picomolar concentrations (close to physiological conditions, (Cirrito et al., 2003)), Aβ causes an increase in LTP and memory functions (Puzzo et al., 2008). In contrast, higher doses have a negative effect in spine density (Smith et al., 2009), NMDAR currents (Hoe et al., 2009), LTP (Puzzo et al., 2008) and

memory tasks in rodent models (Gulisano et al., 2018), possibly recapitulating the responses triggered by the accumulation of Aβ oligomers/plaques in AD patients/mouse models.

Finally, the viral expression/ *ex vivo* delivery of AICD results in increased NMDAR activation in adult rats, favoring the GluN2B-NMDAR contribution, together with an impairment in LTP and spatial memory (Pousinha et al., 2017, Pousinha et al., 2019). Moreover, AICD has been described as a transcription regulator, although the relevance of this response in physiological conditions is still controversial.

In conclusion, different APP fragments (illustrated in **Figure 1.32**) might have distinct dose-dependent roles in glutamatergic neurotransmission, synaptic plasticity and memory, as summarized in **Table 1.11**. Therefore, maintaining normal levels of APP and its derived fragments seems to be crucial to normal synaptic function.

Table 1.11 – Summary of the main functions of APP fragments derived from amyloidogenic/non-amyloidogenic pathways regarding spine density, glutamatergic transmission, synaptic plasticity and learning/memory reported in rodent models.

APP fragment	Spine density	Glutamatergic transmission	Synaptic plasticity	Learning/memory	Other roles
sAPPα	↑ **Spine density** Rescue of deficits in APP KO organotypic hippocampal cultures (Weyer et al., 2014)	↑**NMDAR currents** Rats (1.5-2 months) sAPPα (0.03 nM), HFS-evoked summated NMDAR-EPSC peak amplitude, dentate gyrus (Taylor et al., 2008) Rats (6 months, 24–27 months old sAPPα (0.1 nM), hippocampal slices Increased I_{SE} (fEPSP slope/PFV slope ratio of NMDA synaptic potentials, CA1 (Moreno et al., 2015)	↑ **LTP** Rats (1.5-2 months) Infusion of sAPPα *in vivo* (11 nM), dentate gyrus (Taylor et al., 2008) Rats (2-3 months) sAPPα (100 nM), CA1 (A. Ishida et al., 1997) Rats (24–27 months) sAPPα (0.1 nM), CA1 (Moreno et al., 2015) Rats (24 months) sAPPα (10 nM), CA1 Rescue of deficits upon aging (Xiong et al., 2017) Mice (APP/APLP2 cKO, 4-6 months) sAPPα (10 nM), CA1 (Hick et al., 2015)	↑ **Learning and memory** Rats (24 months) Intra-hippocampal injection sAPPα (300 nM) Novel object location, not watermaze test (Xiong et al., 2017)	**Neuroprotective** (traumatic brain injury, ischemia, hypoxia) (Corrigan et al., 2014, Smith-Swintosky et al., 1994, Hefter et al., 2016)
CTFβ	**-**	↓ **NMDAR currents** CGCs (DIV 7-8) Transfection (Hoe et al., 2009)	↓ **LTP** Mice (8 months), transgenic CA1 (Nalbantoglu et al., 1997)	↓ **Learning and memory** Mice (8 months), transgenic Morris water maze (Nalbantoglu et al., 1997)	**Lysosomal-autophagic pathology** Mice (2 months), viral delivery of C99 at P0, (Lauritzen et al., 2012)

				Mice(4-10 months), transgenic, Morris water maze (Berger-Sweeney et al., 1999) Mice, Injection of CTFβ, Passive avoidance performance (D. K. Song et al., 1998)	
Aβ	↓ **Spine density** Mice (4-months) Hippocampal slices, incubated with Aβ (100 nM) (Smith et al., 2009)	↓**NMDAR currents** CGCs (DIV 7-8) incubation Aβ (2μM) (Hoe et al., 2009)	↑ **LTP** Mice (3-4 months) Aβ (200 pM), CA1 ↓ **LTP** Mice (3-4 months) Aβ (above 20 nM), CA1 (Puzzo et al., 2008)	↑ **Learning and memory** Mice (3-4 months) Injections of Aβ (200 pM), Morris water maze (Puzzo et al., 2008) ↓ **Learning and memory** Mice (3—6 months) Injections of Aβ (200 nM), Morris water maze (Gulisano et al., 2018)	Major APP fragment associated with AD pathogenesis; gives rise to Aβ oligomers and plaques (Hardy & Higgins, 1992)
AICD	**-**	↑**NMDAR currents** Rats (4-6 weeks, Viral injection CA1 (Pousinha et al., 2017) ↑ **GluN2B-NMDAR contribution** Rats (1-2 months) Delivery ex vivo (100 nM), CA1 (Pousinha et al., 2017)	↓ **LTP** Rats (1-2months) Delivery ex vivo (100 nM), CA1 (Pousinha et al., 2017)	↓ **Learning and memory** Rats (1-2months) Viral injection Spatial object recognition task (Pousinha et al., 2019)	**Transcriptional regulation** (Cao & Sudhof, 2001)

Abbreviations: I_{SE} - index of synaptic efficacy, PFVs - Presynaptic fiber volleys, HFS – high frequency stimulation

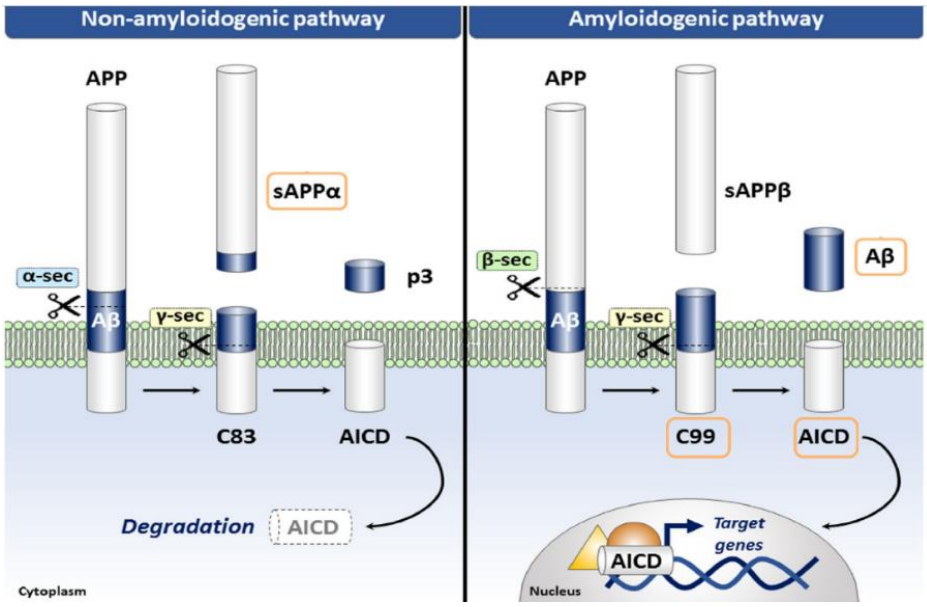

Figure 1.32 – Schematic representation of the APP-derived fragments, indicating in orange the ones that have been shown to influence NMDAR transmission. Adapted from (Coronel et al., 2019).

J) Is AICD a transcription regulator?

AICD has been proposed to translocate to the nucleus (Cupers et al., 2001, Y. Gao & Pimplikar, 2001) and regulate transcription of target genes (Cao & Sudhof, 2001). The most accepted model is that AICD is stabilized by interacting with Fe65, then forming a transcriptionally active complex in the nucleus in combination with Tat-interactive protein 60 (Tip60), which is a histone acetyltransferase (Cao & Sudhof, 2001, Y. Gao & Pimplikar, 2001). The Fe65 PTB2 domain is essential for Fe65-AICD binding, whereas the Fe65 PTB1 domain mediates its interaction with Tip60 (Feilen et al., 2017).

A series of target genes have been reported for AICD, being involved in several cellular functions, as reviewed in (T. Müller et al., 2008):

- APP processing/degradation: neprilysin (MME, Aβ degradation) (Belyaev et al., 2009), APP, BACE (von Rotz et al., 2004).

- Cell survival/apoptosis: Stathmin1 (STMN) (T. Müller et al., 2013), KAI1 (von Rotz et al., 2004), Epidermal growth factor receptor (EGFR) (Y. W. Zhang et al., 2007).

- Metabolism: Glycogen synthase kinase 3β (GSK3β) (Kim et al., 2003), Low-density lipoprotein receptor-related protein 1 (LRP1) (Q. Liu et al., 2007).

- Actin dynamics: Transgelin (TAGLN), Tropomyosin 1 (TPM1), α2-Actin (ACTA2) (T. Müller et al., 2007).

- Synaptic transmission: GluN2B (Pousinha et al., 2017).

The great majority of the studies have been performed *in vitro*, using cell lines overexpressing AICD/APP. Therefore, contradictory results have been reported depending on the cell line and system used to induce expression (von Rotz et al., 2004, T. Müller et al., 2007¸Belyaev et al., 2009, Pardossi-Piquard et al., 2005, A. C. Chen & Selkoe, 2007), The fact that some studies induce the co-expression of AICD together with Fe65/Tip60 is another confounding factor, making it challenging to differentiate AICD role by itself (Pardossi-Piquard et al., 2005, T. Müller et al., 2007, T. Müller et al., 2013). Moreover, the overexpression system is considered an artificial system, questioning the physiological relevance of AICD nuclear effects. For some targets, the contradictory or negative results obtained in APP/APLP2 single/double knockout models (A. C. Chen & Selkoe, 2007, Hébert et al., 2006) suggest that APP/AICD might induce transcriptional alterations only when overexpressed.

Interestingly, two studies by Zhang et al. and Liu et al. have shown evidence for AICD transcriptional regulation of EGFR and LRP1 under physiological conditions. By chromatin immunoprecipitation, the authors have reported an interaction between the promoter regions of these genes and endogenous AICD in wild-type mouse brains. Moreover, both studies report transcriptional alterations upon APP depletion, that can be rescued by reintroducing only the AICD peptide (Y. W. Zhang et al., 2007, Q. Liu et al., 2007).

In summary, the impact of AICD nuclear signaling in neurons under physiological conditions, its mechanism of action and the complete list of target genes in this cell type remain to be elucidated. Studying the role of endogenous AICD has proven to be technically challenging giving the short half-life of this peptide (≈5 min) (Cupers et al., 2001), being normally detected in low levels in the rodent brain and primary neuronal cultures.

1.3 Hypothesis and aims

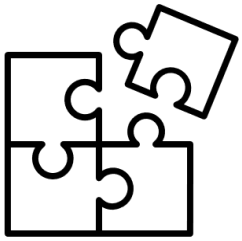

NMDARs are glutamatergic ionotropic receptors essential for synaptic maturation during development and synaptic plasticity in adult stages, whose properties are known to change depending on the life stage (Pérez-Otaño & Ehlers, 2004).

In particular, the subunit composition of synaptic NMDARs (GluN2B vs. GluN2A) has important implications in NMDAR function. GluN2B-NMDARs, which predominate during development, favor slower kinetics, more Ca^{2+} charge transfer, higher mobility and a lower threshold for LTP (Yashiro & Philpot, 2008).

GluN2B-NMDARs play important roles in immature synapses, possibly facilitating the LTP-like mechanism required for the synaptic maturation process, which involves a GluN2B to GluN2A shift (Bellone & Nicoll, 2007). Thus, GluN2A-NMDARs are the predominant subtype in adult stages, allowing for a better fine-tuning of which synapses should undergo potentiation (Williams et al., 1993). Much less is known about what happens in aging, with previous studies showing that NMDAR properties suffer alterations, exhibiting slower responses and lower current amplitudes and being less associated with good memory performance (Kumar, 2015). However, it is still not known if this relates to alterations in the GluN2B/A relative contribution.

These alterations in NMDAR properties might be caused by different regulation mechanisms. APP, which is mainly known to be involved in Alzheimer's Disease (Hardy & Higgins, 1992), has emerged as a putative regulator of NMDARs. Although the physiological role of APP is not fully understood, it is known to regulate synaptogenesis and synaptic plasticity and might have different effects when acting through the full-length protein or its derived fragments (U. C. Müller & Zheng, 2012). Additionally, APP has shown to interact and regulate NMDAR surface levels and currents (Hoe et al., 2009, Cousins et al., 2009, Pousinha et al., 2017), but the functional relevance of this interaction at different life stages, as well as the underlying mechanisms of regulation have not been explored so far.

We hypothesize that APP is important to stabilize NMDARs at the synapse, thus being particularly relevant during development, when new synapses are formed. On the other hand, APP could mainly work as a modulator of NMDAR activity in adult stages, when most synapses are in the mature state. Finally, we hypothesize that this process becomes dysregulated upon aging, possibly causing NMDAR aberrant function and synaptic plasticity impairments.

Therefore, our main hypothesis is that:

APP regulates NMDARs in an age-dependent manner.

Thus, we defined two main aims for this work:

1) Study how APP regulates NMDARs in immature and mature synapses.
2) Investigate how APP regulates NMDARs in aged synapses.

2 Methods

2.1 Models

In order to elucidate how APP regulates NMDARs in immature, mature and aged synapses, we used the following models:

A) Hippocampi from wild-type C57Bl/6 mice at different ages: infants (7-10 days), adults (10-16 weeks) and aged (18 – 20 months)

We used infant mice (7-10 days) because they mainly have immature synapses, thereby being considered as a suitable model to study synapse formation and maturation. These processes occur during the second postnatal week in mice and at around 3.5 years in humans (**Figure 2.1**) (Pressler & Auvin, 2013).

As our model of mature synapses, we used adult mice with 10-16 weeks, which is equivalent to 25 years in humans (**Figure 2.1**) (Flurkey et al., 2007). This was considered our reference group for comparisons with either infant or aged mice.

Finally, aged mice with 18 – 20 months (which is equivalent to 65 years in humans) were used as a model of aged synapses (**Figure 2.1**) (Flurkey et al., 2007), considering the synaptic plasticity and memory impairments reported at this stage (Radulescu et al., 2021).

We collected the **hippocampus** of wild-type mice at these different ages because this brain region is involved in spatial and episodic memory (Burgess et al., 2002). Additionally, the hippocampus is particularly vulnerable to the aging process (Burke & Barnes, 2006, Temido-Ferreira et al., 2019) and it is one of the most affected regions in Alzheimer's Disease (Scheff et al., 2006). Therefore, it is a suitable brain region to study molecular mechanisms involved in age-associated deficits in synaptic plasticity.

B) Human cortical post-mortem tissue from subjects with different ages (18-89 years old)

We used human post-mortem brain tissue from subjects with different ages to understand if the findings obtained in mice could also apply to humans.

In this case, we used **pre-frontal cortical** tissue because this brain region is important for working memory and executive function (Lara & Wallis, 2015), being vulnerable to the aging process (Burke & Barnes, 2006) and highly affected in Alzheimer's Disease (Salat et al., 2001). Therefore, it is a suitable alternative to hippocampal tissue, which is

extremely rare in human biobanks, allowing to study molecular mechanisms involved in synaptic plasticity.

Figure 2.1– Representation of the ages selected for this study in mice, as well as the corresponding ages in humans (Pressler & Auvin, 2013, Flurkey et al., 2007).

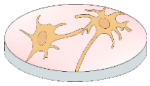

C) Rat hippocampal primary neuronal cultural cultures

We used this *in vitro* model to better elucidate APP regulation of NMDARs in immature synapses. Accordingly, rat primary neuronal cultures recapitulate the synapse development process (Grabrucker et al., 2009) and the NMDAR developmental switch (Corbel et al., 2015), while providing appropriate imaging resolution to detect NMDARs at the post-synapse (J. S. Ferreira et al., 2017).

2.2 Protocols

A) Human and mouse samples

Human samples

The use of human samples was conducted in accordance with the Helsinki Declaration as well as national ethical guidelines. Protocols were approved by the Local Ethics Committee and the National Data Protection Committee. Samples of post-mortem brain tissue from the prefrontal cortex of subjects with different ages (81-89 years old) were obtained from the National Institute of Legal Medicine and Forensic Sciences, Coimbra, Portugal, the Neuro-CEB Biological Resource Center (BRC), France and the Newcastle Brain Tissue Resource, United Kingdom. The gender and postmortem delay period for each sample are depicted in **Table 2.1**.

Table 2.1 – Gender and postmortem delay period for the human samples used in this study.

Age	Gender	Postmortem delay period
18	F	81h
21	M	≥30h
22	M	≥30h
28	M	12h
31	M	36h
32	M	48h
38	M	24h
38	M	24h
40	F	36h
41	M	24h
41	M	24h
52	F	29h
60	M	≥30h
65	M	≥30h
69	M	6h
72	M	29h
73	M	22h
78	M	23h
80	F	25h
81	F	75h
89	F	12h

Abbreviations: M- Male, F – Female, h- hours

Mouse samples

Animal procedures were performed at the Rodent Facility of Instituto de Medicina Molecular, that is a licensed establishment (license number 017918/2021) in compliance with the European Directive 2010/63/EU, transposed to Portuguese legislation in DL 133/2013. All animal research projects carried out at iMM are reviewed by the Animal Welfare Body (ORBEA-iMM) to ensure that the use of animals is carried out in accordance with the applicable legislation and following the 3R's principle. Environmental conditions were kept constant: food and water ad libitum, 22-24 ºC, 45-65% relative humidity, 14h light/10 dark cycles, 3 to 4 mice per cage.

Experiments performed at IPMC were done according to policies on the care and use of laboratory animals of European Communities Council Directive (2010/63) and the protocols were approved by the French Research Ministry following evaluation by a specialized ethics committee (protocol number 00973.02) All efforts were made to minimize animal suffering and reduce the number of animals used. The animals were housed three per cage under controlled laboratory conditions with food and water ad libitum, a 12 hr dark light cycle and a temperature of 22 ±2°C.

Male and female wild-type (gender balanced) C57BL/6 mice at different ages were used: infant (7-10 days), adult (10 – 16 weeks) and aged (18 – 20 months). A C7BL/6-129SvJ female mouse bearing three mutations (3xTg-AD) associated with familial AD (amyloid precursor protein [APPswe], presenilin-1 [PSEN1] and microtubule-associated protein tau [MAPT]) (Mutant Mouse Research and Resource Center at The Jackson Laboratory) was used as reference.

BACE1 Inhibitor treatment

LY2811376 ((4S)-4-[2,4-difluoro-5-(5-pyrimidinyl)phenyl]-5,6-dihydro-4-methyl-4H-1,3-thiazin-2-amine) was obtained from Medchem Express (Sweden) and prepared in 10% DMSO, 40% PEG300, 5% Tween-80, 45% saline. C57BL/6 aged mice (18 – 20 months) received LY2811376 at 100 mg/kg body weight by oral gavage as described in (Filser et al., 2015). Animals treated with LY2811376 (n=3) or vehicle (n=2) were sacrificed ≈12h after treatment.

B) Patch Clamp electrophysiology

Newborn mice were anesthetized through hypothermia, whereas adult and aged mice were anesthetized [ketamine (150 mg/kg)/xylazine (10 mg/kg)]. All groups were

transcardially perfused with artificial cerebrospinal fluid (aCSF) for slice preparation containing (in mM): 119 NaCl, 2.5 KCl, 1.25 NaH2PO4, 26 NaHCO3, 1.3 MgSO4, 2.5 CaCl2 and 11 D-glucose, oxygenated with 95% O2 and 5% CO2, pH 7.4. Acute transverse hippocampal slices (250 µm) were prepared on a vibratome (Microm HM600V, Thermo Scientific, France) in ice-cold dissecting solution containing (in mM): 234 sucrose, 2.5 KCl, 0.5 CaCl2, 10 MgCl2, 26 NaHCO3, 1.25 NaH2PO4 and 11 D-glucose, oxygenated with 95% O2 and 5% CO2, pH 7.4. Slices were incubated for 60 min at 37°C, in an artificial CSF (aCSF) solution, oxygenated with 95% O2 and 5% CO2, pH 7.4. Slices were used after recovering for another 30 min at room temperature. To measure pharmacologically isolated NMDAR EPSCs, slices were perfused with the oxygenated aCSF at 31 ± 1°C in the continuous presence of 50 mM picrotoxin (Sigma-Aldrich, dissolved in DMSO) to block GABAergic transmission and DNQX (10 µM) to block AMPA receptors.

Recording pipettes (5-6 MΩ) for voltage-clamp experiments were filled with a cesium gluconate solution containing the following: 117.5 mM Cs-gluconate, 15.5 mM CsCl, 10 mM TEACl, 8 mM NaCl, 10 HEPES, 0.25 mM EGTA, 4 mM MgATP and 0.3 NaGTP (pH 7.3; osmolarity 290-300 mOsm). Slices were visualized on an upright microscope with IR-DIC illumination (Scientifica, Ltd). Whole-cell recordings were performed using a Multiclamp 700B (Molecular Devices) amplifier, under the control of pClamp10 software (RRID:SCR_011323) (Molecular Devices). The Schaffer collateral pathway was stimulated at 0.10 Hz using electrodes (glass pipettes filled with aCSF) placed in the stratum radiatum.

After a tight seal (>1 GW) on the cell body of the selected CA1 pyramidal neuron was obtained, whole-cell patch clamp configuration was established, and cells were left to stabilize for 2–3 min before recordings began. Pharmacologically isolated NMDAR EPSCs were recorded from cells voltage clamped at +40 mV. Holding current and series resistance were continuously monitored throughout the experiment, and if either of these two parameters varied by more than 20%, the experiment was discarded. Electrical stimulation was adjusted to elicit EPSCs of approximately 150 pA amplitude in the different studied groups.

The following parameters have been measured by Patch-Clamp:

- **NMDAR EPSCs deactivation kinetics**

Decay time was fitted with a double exponential function, using Clampfit software, to calculate both slow and fast decay time constants, τfast and τslow, respectively. The

weighted time constant (τweighted) was calculated using the relative contribution from each of these components, applying the formula: τw = [(af. τf) + (as. τs)]/(af + as), where af and as are the relative amplitudes of the two exponential components, and τf and τs are the corresponding time constants.

- **GluN2B-NMDAR contribution**

NMDAR EPSCs were measured immediately before (5 min) and 25-20 min after ifenprodil (5μM) perfusion to selectively block GluN2B-NMDARs.

- **APP C-terminal antibody impact on NMDAR currents**

The APP C-terminal antibody Y188 (ab32136, Abcam, raised against human APP (aa 675- C-terminus, APP695 numbering)) was added to the intracellular solution to a final concentration of 0.4μg/mL (2.57nM). In the control condition, the same antibody was heat-inactivated by incubation at 98ºC for 10min. The percentage of reduction in NMDAR EPSCs due to the APP C-terminal antibody incubation was calculated comparing the baseline amplitude (15-20min) with the final amplitude (55-60 min) and normalized with the control condition for each age.

- **PTB2 peptide effect on GluN2B-NMDAR synaptic contribution**

Expression and purification of His-tagged fusion proteins (PTB1-p (Fe65 G366 - R506, 6xHis-tag, 16.7KDa) and PTB2-p (Fe65 K536 - Q666, 6xHis-tag, 15.1KDa) in Escherichia coli were performed by Svenja König and Stefan Kins (University of Kaiserslautern).

Hippocampal slices were incubated with either the PTB2-p or the respective control (PTB1-p) at a final concentration of 5nM for 3h, followed by Patch-Clamp electrophysiology recordings.

For more details about the Patch Clamp methodology used in this study, please see ***Section 2.4A.***

C) Protein analysis

Total lysates

For the preparation of total protein lysates, hippocampi from C57BL/6 wild-type mice were dissected and snap-frozen in liquid nitrogen. Mouse and human frozen tissue samples were resuspended in A-EDTA buffer (10 mM HEPES-KOH pH 7.9, 10 mM KCl, 1.5 mM $MgCl_2$, 0.1 mM EDTA, 0.3% NP-40 with protease and phosphatase inhibitors)

and homogenized using a Glass/Teflon Potter Elvehjem homogenizer, as described in (Pousinha et al., 2017). Protein quantification was performed using BioRad DC Protein assay kit. Lysates were diluted in water and 5x sample buffer (Final concentration: 50mM Tris HCl pH 6.8, 2% SDS, 6% glycerol, 0.1% bromophenol blue, 121mM DTT) and denatured at 95°C for 10 min before being used for Western Blot analysis.

Fractionation into PSD-enriched fractions

Mouse and human frozen tissue were subjected to the fractionation protocol adapted from (Frandemiche et al., 2014), all centrifugation steps were performed at 4°C and all solutions contained protease/phosphatase inhibitors.

Samples were first homogenized using a Glass/Teflon Potter Elvehjem homogenizer in Buffer I (0.32M sucrose and 10mM HEPES, pH 7.4) and then centrifugated (1.000 g for 10min) to remove nuclei and cell debris. This centrifugation step was repeated 3 times, until the supernatant was completely clear.

Then, the supernatant was subjected to a centrifugation at 12.000 g for 20min. The pellet was recovered to obtain a crude membrane fraction, which was resuspended in Buffer II (4mM HEPES and 1 mM EDTA, pH 7.4) and centrifuged twice at 12.000 g for 20 min.

The pellet was then resuspended in 25µL of Buffer III (20 mM HEPES, 100mM NaCl, 0,5% Triton X100, pH= 7.2) and incubated 1h at 4°C with mild agitation. By centrifuging the samples at 12.000 g for 20 min it was possible to pellet the synaptosome membrane fraction, whereas the supernatant was collected as the non-postsynaptic density membrane fraction (non-PSD) or Triton-soluble fraction.

Finally, the pellet was solubilized in 25µL Buffer IV (20 mM HEPES, 0.15 mM NaCl, 1% TritonX-100, 1% sodium deoxycholate, 1% SDS, pH 7.5) for 1 h at 4°C and centrifuged at 10.000 g for 15 min. The supernatant contained the PSD or Triton-insoluble fraction.

The integrity of non-PSD was verified by immunoblotting for synaptophysin, which was enriched in the non-PSD fraction, and the integrity of the PSD fraction was confirmed by the immunoblotting of PSD-95 enriched in this compartment, as shown in **Section 2.4B.**

Synaptosomes preparation

The protocol for synaptosome preparation was adapted from (Lopes et al., 1999), all centrifugation steps were performed at 4°C and all solutions contained protease/phosphatase inhibitors.

Hippocampi from C57BL/6 wild-type mice were dissected, resuspended in a 0.32 M sucrose solution containing 50mM Tris, 2 mM EDTA, pH=7.6 and homogenized using a Glass/Teflon Potter Elvehjem homogenizer. The suspension was centrifuged at 3.000 g during 10 min to remove nuclei and cell debris.

The supernatant was collected and centrifuged at 14.000 g for 12 min to obtain the crude membrane fraction.

The pellet was resuspended in 1.8 ml of a 45% vol/vol Percoll solution made up in a Krebs-Ringer solution (140mM NaCl, 1mM EDTA, 10mM HEPES, 5mM KCl, pH= 7.4). After centrifugation at 21.100g for 2 min, the top layer was collected (synaptosome fraction) and washed twice in Krebs-Ringer solution (centrifugation at 21.100g, 2 min).

When synaptosome fractions were used for co-immunoprecipitation experiments, they were subsequently resuspended in the respective Co-IP buffer (50mM Tris HCl pH 7.5; 150 mM NaCl; 2 mM EDTA; 1% Triton with protease and phosphatase inhibitors).

Co-immunoprecipitation

For immunoprecipitation in total lysates, frozen tissue (from mice or humans) was resuspended in immunoprecipitation buffer (50mM Tris HCl pH 7.5; 150mM NaCl; 2mM EDTA; 1% Triton with protease and phosphatase inhibitors) and homogenized using a Glass/Teflon Potter Elvehjem homogenizer. Following a centrifugation at 1.000g, 10 min 4°C to remove nuclei and cell debris, the supernatant was collected.

Protein quantification of total lysates and mouse synaptosome fractions was performed using the BioRad DC Protein assay kit.

The immunoprecipitation protocol was adapted from (Tomé et al., 2021). For each sample, 50µL of Dynabeads were washed 3 times with washing buffer (0.1% BSA; 2mM EDTA in phosphate-buffered saline (PBS)). Dynabeads were then resuspended in 500uL washing buffer and the appropriate volume of antibody: APP C-terminal Y188 (3µg, ab32136, Abcam), PSD-95 (3µg, ab18258, Abcam) or Normal rabbit IgG (3µg, 12-370, Merck Millipore) and incubated overnight at 4°C under rotation.

Following 3 washing steps with washing buffer, dynabeads were resuspended in 350uL washing buffer and incubated with 500µg of protein lysate diluted in Immunoprecipitation buffer (500µL) for 2h at 4°C under rotation. Following 5 washing steps with Immunoprecipitation buffer, dynabeads were gently resuspended in 60µL of pre-heated 2x sample buffer (140mM Tris HCl pH 6.8, 4% SDS, 13.6% glycerol, 272mM DTT, 0.004% Blue bromophenol) in RIPA (50mM Tris, 1mM EDTA, 150mM NaCl, 0.1% SDS,

1%Tergitol-type NP-40, pH 8.0). Finally, samples were incubated for 10 min at 95°C, the supernatant was collected and used for Western Blot analysis.

Western blotting (NMDAR subunits)

Following protein quantification using BioRad DC Protein assay kit, samples were diluted in water and 5x sample buffer (Final concentration: 50mM Tris HCl pH 6.8, 2% SDS, 6% glycerol, 0.1% bromophenol blue, 121mM DTT) and denatured at 95°C for 10 min. The immunoprecipitated samples were directly loaded in the gel.

Gel electrophoresis was performed as described previously (D. G. Ferreira et al., 2017), in Tris-glycine buffer with 10% SDS using 10-12% and 4% acrylamide resolving and stacking gels, respectively. Proteins were electro-transferred to 0.45µm Polyvinylidene fluoride (PVDF) membranes in Tris-glycine buffer with 20% methanol at 350mA for 90 min.

After transfer, all membranes were blocked with 3% BSA in TBS-T (20 mM Tris,150 mM NaCl, 0.1% Tween-20) at room temperature (RT) for 1h and incubated with primary antibodies (diluted in 3% BSA TBS-T) overnight at 4°C. The following antibodies were used: GluN2A (1:200, sc-136004, Santa Cruz), GluN2B (1:1000, D15B3, Cell Signalling), GluN1 (1 :500, 556308 BD Pharmigen), Phospho-GluN2B Y1472 (1:1000, #4208, Cell Signalling) PSD95 (1:1000, D27E11, Cell signalling), Synaptophysin (1:200, S5768, Merck Millipore), β-actin (1 :1000, sc-47778, Santa Cruz), GAPDH (1:1000, AM4300, Invitrogen). After three washing steps of 10min with TBS-T, membranes were incubated with horseradish peroxidase (HRP)—conjugated anti-mouse or anti-rabbit secondary antibodies for 1 h at RT: Goat Anti-Mouse IgG HRP (1:4000, 10004302, Cayman Chemicals) or Goat Anti-Rabbit IgG HRP (1:10.000, 1706515, Bio-Rad). After three washing steps of 10min with TBS-T, chemiluminescent detection was performed with enhanced chemiluminescence (ECL) western blotting detection reagent (GE Healthcare).

Western blotting (APP and APP fragments)

Following protein quantification using BioRad DC Protein assay kit, lysates were diluted in water and 5x sample buffer, following denaturation at 95°C for 10 min. as described previously.

For APP, APP-CTFs and AICD analysis, optimal conditions for low molecular mass proteins separation were used, as described in (Willem et al., 2015). Proteins were

separated using precast gradient Tricine Protein Gels (10–20%, 1 mm, Novex) in Tris-tricine buffer (1M Tris, 1M Tricine, 1% SDS). Samples were electro-transferred at 400mA for 1h to 0.2µm Nitrocellulose membranes using a Tris Glycine buffer (25 mM Tris, 190 mM glycine) with 20% ethanol. Proteins transferred to nitrocellulose membranes were additionally denatured by boiling the membrane in PBS for 5 min, acting as an antigen retrieval step to detect AICD, as described in (Pimplikar & Suryanarayana, 2011).

After transfer, we followed the same protocol as before, using the following antibodies: APP C-terminal Y188 (1:1000, ab32136, Abcam), β-actin (1 :1000, sc-47778, Santa Cruz), GAPDH (1:1000, AM4300, Invitrogen).

For more details about the methodology used in this study for the detection and identification of APP-derived fragments, please see ***Section 2.4C****.*

Chemiluminescent detection and Western Blot quantification

Chemiluminescent detection was performed with enhanced chemiluminescence (ECL) western blotting detection reagent (GE Healthcare). For AICD detection, longer exposure times were applied (150 times longer than for APP full-length). Optical density was determined with Image-J, according to the software instructions (T. Ferreira. & Rasband, 2012). When analyzing total lysates, results were normalized with β-actin (in mice) or GAPDH (in humans). When analysing PSD-enriched fractions, the levels of the proteins of interest (GluN2B, GluN2A and APP) were normalized to PSD-95 as in (Holehonnur et al., 2016), to account for the possible variability in protein loading, PSD fractionation efficiency and number of synapses at each age. With this type of normalization, our output corresponds to the protein levels per PSD-95, therefore reflecting the synaptic composition rather than the absolute values.

D) APP knockdown in primary neuronal cultures

Primary neuronal cultures

Hippocampal neurons were cultured from 18-day Sprague-Dawley rat embryos, adapting the protocol from (Temido-Ferreira et al., 2019, Faria-Pereira et al., 2022, Afonso et al., 2019). Briefly, embryos were collected in Hank's Balanced Salt Solution (HBSS, Corning) and rapidly decapitated. After removing the meninges, hippocampi were dissociated in HBSS with 0.25% trypsin at 37°C for 15 min, resuspending every 3min. The tissue was

then washed with HBSS containing 30% fetal bovine serum (FBS) to stop trypsin activity, followed by three washing steps with HBSS.

Cells were resuspended in neuronal plating medium (MEM (Minimum Essential Medium) supplemented with 10% horse serum, 0.6% glucose, and 100 U/mL Pen-Strep), gently dissociated and filtered through a 70µm strainer. Finally, cells were plated on poly-D-lysine-coated glass coverslips (0.1mg/mL PDL in 0.1M borate buffer, pH 8.5) in 24-multi well plates at a final density of 70.000 cells/coverslip, in neuronal plating media and maintained at 37°C in a 5% CO_2-humidified incubator.

After 4 hours, the plating medium was replaced for neuronal culture medium: Neurobasal Medium (Gibco–Life Technologies) supplemented with B-27 supplement, 25µM Glutamic acid, 0.5mM Glutamine, and 20 U/ml penicillin/streptomycin. Cultures were maintained in the humidified incubator for 2 weeks, feeding the cells once per week with neuronal culture medium by replacing half of the medium per well. This protocol is associated with an enrichment in neuronal cells (NeuN-positive cells ≈80%) and a low number of glial cells (GFAP-positive cells ≈6%) at DIVs 11-14 (Faria-Pereira et al., 2022).

Plasmid generation

Primary neuronal cultures were transfected with AAV-shRNA–mCherry plasmids, with a shRNA against APP (shAPP) or a shRNA control sequence (shCTR).

The control plasmid was kindly provided by Dirk Grimm (University of Heidelberg) and corresponds to AAV-U6-shCTR-CMV-mCherry plasmid, where shCTR is a non-silencing sequence: GTAACGACGCGACGACGTAA, with no identified targets in the rat genome, confirmed by NCBI Basic Local Alignment Search Tool (BLAST).

For the generation of the shRNA-APP construct, we used the following sequence: GCACTAACTTGCACGACTATG (Young-Pearse et al., 2007), which is complementary to the mRNA NCBI reference sequences for rat and mouse APP (confirmed by NCBI Basic Local Alignment Search Tool (BLAST)). This construct, which was provided by Tracy Young-Pearse (Harvard Medical School) in the pENTR-U6 vector, was then subcloned into an adeno-associated virus backbone (AAV-U6-shRNA empty-CMV-mCherry plasmid), kindly provided by Dirk Grimm.

Briefly, the shRNA insert was generated by PCR amplification using primers with AscI and XhoI restriction sites (Forward Primer: AscI-U6 5'-GCGGCGCGCCAGGAAGAGGGCCTATTTCCCATG-3'; Reverse Primer: XhoI-PolyA-Active 5'-GCAAGTTAGTGCTTTTTTCTAGACCCTCGAGCG-3'). Subsequently, the PCR product and the AAV-U6-shRNAempty-CMV-mCherry plasmid were digested with

AscI and XhoI restriction enzymes. Following gel purification, the shRNA construct was ligated into the AAV plasmid and the ligation product was transformed into Top10 chemically competent cells. Both plasmids were purified using the EndoFree Plasmid Maxi Kit (Qiagen) and verified by DNA sequencing (Primer 5'-GGGCCTATTTCCCATGATTCC- 3').

Neuronal transfection

Primary neuronal cultures were transiently transfected at 7-8 days *in vitro* (DIV) using the calcium phosphate transfection protocol adapted from (Silva et al., 2019, Jiang et al., 2004, Dudek et al., 1998).

For each well, 1.5 µg plasmid DNA was diluted in 17.5µL TE buffer (10 mM Tris, 1 mM EDTA, pH 7.3). $CaCl_2$ solution (2.5M in 10mM HEPES, pH 7.2) was added dropwise to the diluted DNA (final concentration = 250 mM $CaCl_2$) and gently mixed.

This mix was then added dropwise to an equivalent volume of HEPES-buffered saline transfection solution (in mM: 274 NaCl, 10 KCl, 1.4 Na_2HPO4, 11 dextrose, 42 HEPES, pH 7.2), gently mixed and incubated at RT for 30 min, vortexing every 5 min.

During this period, neurons were treated with 2 mM kynurenic acid (glutamate receptor antagonist) in conditioned neuronal culture medium (in a new multi-well plate), to reduce excitotoxicity. The precipitates were then added dropwise to pre-conditioned neurons, followed by an incubation of 2-3h at 37°C in a 5% CO_2-humidified incubator. The calcium phosphate-DNA precipitates facilitate DNA binding to the surface and entering by endocytosis.

Finally, DNA precipitates in excess were dissolved by incubating the neurons in an acidified neuronal culture medium (in mM: 2 kynurenic acid, ~5 HCl final concentration) for 15-20 min at 37ºC to dissolve the precipitates in excess and reduce neurotoxicity. Coverslips were transferred to the original plates with conditioned neuronal culture media maintained in the humidified incubator.

Immunocytochemistry

The immunostaining protocol was adapted from (J. S. Ferreira et al., 2017). Briefly, neurons were fixed at DIV 14-15 (7 days after transfection) in 4% sucrose and 4% paraformaldehyde (PFA) in PBS for 20 min at RT.

Neurons were then washed 3 times with PBS and permeabilized with PBS + 0.25% (v/v) Triton X-100 at RT (for 10min in the case of intracellular epitopes and 5 min for extracellular targets). Following 3 washing steps in PBS, cells were incubated in 10% BSA in PBS for 1 h at RT to block nonspecific staining. Incubation with primary antibodies was performed overnight at 4°C in a humidified chamber, with antibodies diluted in 3% BSA in PBS: APP Y188 (1:100, ab32136, Abcam), GluN2B (1:100, AGC-003, Alomone), GluN2A (1:100, AGC-002, Alomone), PSD-95 (1:50, ADI-VAM-PS002-E, Enzo).

Following 4 washing steps in PBS, cells were incubated with the appropriate secondary antibody diluted in 3% BSA PBS (1:500) for 1h at RT: Donkey anti-Rabbit IgG Alexa Fluor 488, Donkey anti-Mouse IgG Alexa Fluor 488 or Donkey anti-Rabbit Alexa Fluor 647 (Thermo Fisher). Finally, cells were incubated with Hoechst 33258 (12 ug/mL in PBS, Life Technologies) for 5min to stain the nuclei, washed 3 times with PBS and mounted in Fluoromount aqueous mounting medium (Sigma).

Microscopy imaging and analysis

All images were acquired in a Zeiss LSM 880 laser scanning confocal microscope using a Plan-Apochromat 63x/1.4 oil immersion objective.

For the analysis of APP immunofluorescence in transfected neurons, Hoechst fluorescence was detected using 405 nm for excitation (Diode laser with 30 mW nominal output – 2% transmission) and a 415-475 nm detection window, with PMT gain set to 610 and offset to -1. Alexa Fluor 488 fluorescence was detected using the 488 nm laser line of an Ar laser for excitation (25 mW nominal output – 1% transmission) and a 498-557 nm detection window, with GaAsP detector gain set to 500 and offset to 1. mCherry fluorescence was detected using 594 nm for excitation (HeNe laser with 2 mW nominal output – 5% transmission) and a 600-735 nm detection window, with PMT gain set to 700 and offset to 1. The pinhole size was set to 1.67 AU for Hoechst, 1.37 AU for Alexa Fluor 488 and 1.1 AU for mCherry. Z-stacks of the three channels were acquired with Zoom set to 1 (134.95x134.95 µm area with 1024x1024 pixel frame size - 0.13 µm pixel size) with a 0.49 µm slice interval, a line average of 2 and 1.03 µs pixel dwell time (unidirectional scan). The APP (Alexa Fluor 488) relative fluorescence intensity was manually quantified using ImageJ, after maximum intensity projection. For each condition, 7 transfected neurons were analyzed by defining regions of interest (ROI) which corresponded to the cell bodies using the mCherry channel. The average intensity of Alexa Fluor 488 was then determined for each ROI. All values were normalized to the average intensity in transfected neurons from the control condition (%).

For the analysis of GluN2B, GluN2A and PSD-95 in dendrites of transfected neurons, Alexa Fluor 488 fluorescence was detected using the 488 nm laser line of an Ar laser for excitation (25 mW nominal output – 3% transmission) and a BP 495-550 + LP 570 nm filter set for detection in the Airyscan unit, with gain set to 790 and offset to 0. mCherry fluorescence was detected using 561 nm for excitation (DPSS laser with 20 mW nominal output – 7.5% transmission) and a BP 495-550 + LP 570 nm filter set in conjunction with a SP 615 nm secondary beam splitter for detection, with gain set to 850 and offset to 0 in the Airyscan unit. Alexa Fluor 647 fluorescence was detected using 633 nm for excitation (HeNe laser with 5 mW nominal output – 14.5% transmission) and a BP 570-620 + LP 645 nm filter set in conjunction with a LP 660 nm secondary beam splitter for detection with gain set to 760 and offset to 0 in the Airyscan unit. The pinhole size was set to 2.66 AU for Alexa Fluor 647, 2.16 AU for mCherry and 2.49 AU for Alexa Fluor 488. Z-stacks of the three channels were acquired with Zoom set to 3.8 (35.51x35.51 µm area with 836x836 pixel frame size - 0.04 µm pixel size) with a 0.18 µm slice interval, a line average of 2 and 2.53 µs pixel dwell time (unidirectional scan). All data sets were subjected to Airyscan processing in ZEN using the same parameters.

The analysis of GluN2B, GluN2A and PSD-95 in transfected neurons was performed using an in-house developed macro for ImageJ developed by Clara Barreto and José Henriques. For each condition, 13 dendrites from transfected neurons were analyzed. Following maximum intensity projection and manual selection of the dendritic area using the mCherry channel, images were segmented with user-defined intensity thresholds for GluN2B/A (Alexa Fluor 647) and PSD-95 (Alexa Fluor 488), which were maintained constant for all conditions. The mean fluorescence intensity and the percentage of dendritic area with positive signal (above threshold) were quantified for each channel in the segmented images. GluN2B/A and PSD-95 clusters were detected by particle analysis, which also allowed us to quantify average cluster sizes in each case. The colocalization area was determined by identifying the pixels where both GluN2B or GluN2A and PSD95 intensity values were above the respective threshold. The relative GluN2B/A synaptic content was then determined as the ratio between the area occupied by colocalized pixels and the total area with GluN2B/A staining. The fluorescence density was calculated as the mean fluorescence intensity multiplied by the percentage of dendritic area with positive signal for each channel. All quantifications were normalized to the average values of transfected dendrites from the control condition (%).

E) Statistical Analysis

All statistical analyses were performed with GraphPad Prism software. Results are referred in the text as mean ± Standard Error of the Mean (SEM), which is also represented in the graphs, together with dot plots with individual values. Statistical analyses were performed after evaluating normality using the Shapiro–Wilk test. When comparing two groups, the statistical comparison included Unpaired t test (in case of normal distribution) or Mann-Whitney test (in case the distribution was not normal). When comparing more than two groups, the statistical comparison included One-way ANOVA followed by Tukey's multiple comparison tests (in case of normal distribution). When the graphs represent relative levels, the values are expressed in relation to the reference group. When comparing infant or aged mice with adult, the values are expressed in relation to the adult group. Significance was determined according to the following criteria: $p>0.05$= not significant, $*p<0.05$, $**p<0.01$ $***p<0.001$ and $****p< 0.0001$.

2.3 Supplementary Protocols

*(Relative to the Supplementary Results, **Section 3.4**)*

A) Prediction of aminoacid disorder in the structure of APP and NMDAR subunits

The computer prediction of aminoacid disorder in the structure of mouse and human APP and NMDAR subunits (GluN1, GluN2A and GluN2B) was performed using the prDOS algorithm, considering a probability threshold of 0.5 to determine the disordered segments (http://prdos.hgc.jp) (T. Ishida & Kinoshita, 2007).

B) AICD incubation in mouse primary neuronal cultures

Primary neuronal cultures

Hippocampal neurons were cultured from 18-day C57Bl/6 mouse embryos, as previously described (Temido-Ferreira et al., 2020). Briefly, embryos were collected in Hank's Balanced Salt Solution and rapidly decapitated. Meninges were removed, and the hippocampi were dissociated and incubated for 15 min in HBSS with 0.025% trypsin. Cells were washed once with HBSS with 30% FBS, centrifuged three times, re-suspended in Neurobasal Medium (Gibco–Life Technologies, USA) supplemented with 2% B-27 supplement, 25 µM Glutamate, 0.5mM glutamine, and 2 U/ml penicillin/streptomycin, gently dissociated and filtered through a 70 µm strainer. Cells were plated on poly-D-lysine-coated plates and grown for 14 days at 37 °C in a 5% CO_2-humidified atmosphere in the previously described supplemented Neurobasal medium. At 15 DIV, neurons were treated with TAT-AICD-NLS or TAT-SCR-NLS (100 nM) for 2 h.

TAT peptides

The peptides TAT-AICD-NLS and TAT-SCR-NLS were synthesized by PSL GmbH (Heidelberg, Germany) and have been validated by (Pousinha et al., 2017). TAT-AICD-NLS contained the TAT sequence (YGRKKRRQRRR), conferring cell permeability, fused to the N-terminal of AICD: MLKKKQYTSIHHGVVEVDAAVTPEERHLSKMQQNGYENPTYKFFEQMQN. The SV40 nuclear localization signal (NLS; PKKKRKV) was added to the AICD C-terminal for nuclear translocation. The TAT-SCR-NLS contained the same TAT and NLS sequences at each end of a scrambled version of the AICD sequence:

VQGITQKMYHNQEGKFLNQKVNVKTHMQFEHETLVDSMKAYYRVEEPSPA. The purity of peptides was above 90%–95%.

Quantitative PCR

Total RNA was extracted and purified using the RNeasy Plus Mini Kit (QIAGEN, Germany). RNA quality was assessed by NanoDrop 2000 (Thermo Scientific, USA) analysis (A260/A280≈2; 260/235 >1.8). Total RNA was reverse-transcribed using random primers and SuperScript First-Strand Synthesis System for RT-PCR (Invitrogen, USA). Real-time quantitative polymerase chain reaction (RT-qPCR) analysis was performed on a Corbett Rotor-gene 6000 apparatus (QIAGEN, Germany) using Power SYBR Green PCR Master Mix (Applied Biosystems, UK), 0.2 mM of each primer and 0.4 ng/µL of cDNA. The thermal cycler conditions were 10 min at 95ºC, 40 cycles of a two-step PCR, 95ºC for 15 s followed by 56ºC for 25 s with a final thermal ramp from 72 to 95ºC. The primers presented high amplification efficiency (>80%) and the R^2 values of standard curves was approximately 0.99.

Reference genes were PPIA (cyclophilin A) and Rpl13A (ribosomal protein L13A) and amplifications were carried out in triplicates and according to the MIQE guidelines (Bustin et al., 2009). The relative expression of target genes was determined by the comparative CT method (Schmittgen & Livak, 2008).

Primer design

The primers used in RT-qPCR were designed using Primer-Blast (http://www.ncbi.nlm.nih.gov/tools/primer-blast/). The following standard design parameters from Primer-Blast were used: 1) Tm between 57 and 63°C (60°C as the optimum value), with a maximum difference between the primers of 3°C, 2) primer size varied between 15 and 25 nucleotides (20nt as the optimum value), and 3) GC content between 30 and 80%. The “Max Self Complementarity value” was set at 8 and “3’ complementary value” at 3. The PCR product size was limited between 80 and 120 base pairs (bp).

To avoid possible genomic DNA amplification, the option “Primer must span an exon-exon junction” was whenever possible selected. Concerning “Primer Pair Specificity Checking Parameters”, the database used was “Ref Seq RNA” from the organism Mus musculus. The options ‘Enable search for primer pairs specific to the intended PCR template’ and “Allow primer to amplify mRNA splice variants” were selected.

The best sequences of pairs of RT-qPCR primers were subsequently analyzed for genomic DNA amplification and secondary structures.

We used the OligoAnalyzer tool (IDT, USA) (http://eu.idtdna.com/analyzer/Applications/OligoAnalyzer) to confirm that the secondary structures have a ΔG value between 0 and -9 kcal/mol and the melting temperature of folded sequence is 5 to 10 °C lower than the annealing temperature. This software was used to study the possible formation of hairpins, self and hetero-dimers.
Additionally, we used the Oligocalc tool (http://www.basic.northwestern.edu/biotools/OligoCalc.html) to check potential hairpin and self-complementary formation. The selected primers were produced by Invitrogen, UK (HPLC purified) and the respective sequences are listed in **Table 2.2.**

Table 2.2: Sequence of primers used for Quantitative PCR in this study.

Primer	Target gene	Forward Primer	Reverse primer
CypA	PPIA peptidylprolyl isomerase A (cyclophilin A)	TATCTGCACTGCCAAGACTGAGTG	CTTCTTGCTGGTCTTGCCATTCC
Rpl13a	Ribosomal protein L13A	GGATCCCTCCACCCTATGACA	CTGGTACTTCCACCCGACCTC
LRP1	Low density lipoprotein receptor-related protein 1	AGTGTGCCAATGGGGAATGT	CGTGAGTTGCAGTAGGAGGG
GSK3B	Glycogen synthase kinase 3 beta	GAGAACCACCTCCTTTGCGG	TGCTGCCATCTTTATCTCTGCTA
Grin2b	Glutamate ionotropic receptor NMDA type subunit 2B	AAACCAAGAGAGTCGACGAGC	TTTTGGGAACGAGCTTTGCTG

Immunocytochemistry

Primary neurons were used for immunocytochemistry experiments as previously described (D. G. Ferreira et al., 2017). Briefly, neurons were fixed with 4% paraformaldehyde for 10 min at RT, followed by a permeabilization step with 0.05% Triton X-100 (Sigma–Aldrich) for 10 min at RT. After blocking in 10% FBS for 30 min, the cells were incubated with the primary antibody (APP Y188 (1:100, ab32136, Abcam), diluted in PBS 0.05% Tween 20, 4% FBS) overnight at 4 °C. After washing with PBS, cells were incubated with the secondary antibody for 1 h at RT. Finally, cells were stained with Hoechst 33258 (12 µg/mL in PBS) for 5 min and mounted in Fluoromount Aqueous Mounting Medium (Sigma). Images were acquire using a Zeiss Axiovert 200M widefield fluorescence microscope.

Subcellular Fractionation and Western Blot

We performed a subcellular fractionation to separate the nuclear and cytosolic/membrane fractions, as previously described (Fonseca-Gomes et al., 2019).

All centrifugation steps were performed at 4°C and all solutions contained protease/phosphatase inhibitors. Briefly, cells were washed twice with PBS and detached from the plate surface using a PBS-EGTA solution. Cells were centrifuged at 800g for 5 min and the pellet was collected and resuspended in harvest buffer containing 10 mM HEPES (pH 7.9), 50 mM NaCl, 0.5 M sucrose, 0.1 mM EDTA, Triton X-100 (0.5%), 1 mM DTT. The homogenate was incubated on ice for 5 minutes and then centrifuged at 1200g for 10 min to collect the nuclear fraction (pellet) and the cytoplasmic and membrane proteins fraction (supernatant). The latter was cleaned up through a re-centrifugation at 16000g, for 15 min. The fraction enriched in nuclear proteins was resuspended in Buffer A, composed by 10mM HEPES (pH7.9), 10mM KCl, 0.1 mM EDTA, 0.1 mM EGTA, 1 mM DTT and centrifuged at 1200g for 10 min. The pellet obtained was resuspended in Buffer C (10 mM HEPES (pH 7.9), 500 mM NaCl, 0.1 mM EDTA, 0.1 mM EGTA, 0.1% NP-40, 1 mM DTT and mixed vigorously for 15 minutes at 4°C. After a new centrifugation at 16000g for 10 min, the supernatant (nuclear fraction) was collected. The fractions obtained in this protocol: cytoplasmic/membrane proteins (Cyto + Memb) and nuclear proteins (Nucleus) were analyzed by western blotting, which was performed as described in **section 2.2C** (Western blotting (APP and APP fragments). We used the following primary antibodies: APP Y188 (1:1000, ab32136, Abcam), Lamin A/C (1:1000, #2032, Cell Signalling) and anti-α-tubulin (1:1000, sc-8035, Santa Cruz).

C) AAV-shAPP production and validation

Recombinant adeno-associated virus (rAAV) vectors encoding a shRNA against APP were produced as previously described (Hauck et al., 2003). Briefly, AAV-293 cells (RRID:CVCL_6871) (Agilent Technologies) were co-transfected with the AAV-shAPP–mCherry plasmid (described in the **section 2.2D**) and three helper plasmids (pH21, pRV1 and pFD6) using the calcium phosphate method. 65 hours post-transfection, the cells were harvested and rAAVs were purified using 1 ml HiTrap heparin columns (Sigma-Aldrich), followed by concentration using Amicon Ultra centrifugal filter devices (Millipore). Titer quantification was performed by vector genome quantification through qPCR quantification of free Inverted terminal repeats (ITR2).

In vivo AAV injections

C57BL/6JRj adult mice (8 weeks) were injected with the AAV-shAPP–mCherry in both dorsal hippocampi. Stereotaxic injections were performed using a stereotaxic frame

(Kopf Instruments) under general anesthesia with xylazine and ketamine (10 mg/kg and 150 mg/kg, respectively). 500nl of AAV-shAPP–mCherry were injected in each hippocampus with an injection rate set at 100nl/min. Coordinates for dorsal hippocampus were adjusted from Paxinos and Watson (AP: -2,2, ML ± 1,5, DV -1,4). Injected mice were sacrificed three weeks post-injection.

Immunohistochemistry

Brains were removed from anesthetized mice subjected to intracardiac perfusion of PBS followed by 4% PFA in PBS and used for immunohistochemistry as previously described (Pousinha et al., 2017). After being post-fixed in 4% PFA overnight, mouse brains were washed in PBS and sectioned (40 µm) using a vibratome. Sections were incubated in blocking buffer (10% goat serum; 0.1% Triton X-100; 0.5% BSA in PBS) for 30 min at RT. Sections were then incubated with the primary antibody APP C-terminal Y188 (1:500, ab32136, Abcam) for 24h at 4°C in PBS with 1% goat serum, 0.1% Triton X-100% and 0.5% BSA. After two washes in PBS, sections were incubated with an anti-rabbit Alexa488 conjugated secondary antibody for 2 h at RT. After three washes in 0.1M Phosphate buffer, sections were mounted on glass slides using Mowiol. Images were acquired using a confocal microscope TCS SP5 (Leica Microsystems, France). The APP knockdown efficiency was calculated by quantifying APP mean fluorescence intensity in mCherry positive (transduced) or negative (non-transduced) cells using ImageJ.

2.4 Supporting information

A) Patch-Clamp electrophysiology

Using Patch-Clamp electrophysiology, we can measure the synaptic currents mediated by NMDARs (ion flux) upon electrical stimulation. In this work, we recorded pharmacologically isolated NMDAR excitatory postsynaptic currents (NMDAR EPSCs) in single CA1 glutamatergic neurons of mice hippocampal slices.

We used the whole-cell configuration, which means that the electrode was left in place on the cell and suction was applied to rupture the membrane patch, thus providing access from the interior of the pipette to the intracellular space of the cell (Segev et al., 2016), as illustrated in **Figure 2.2**.

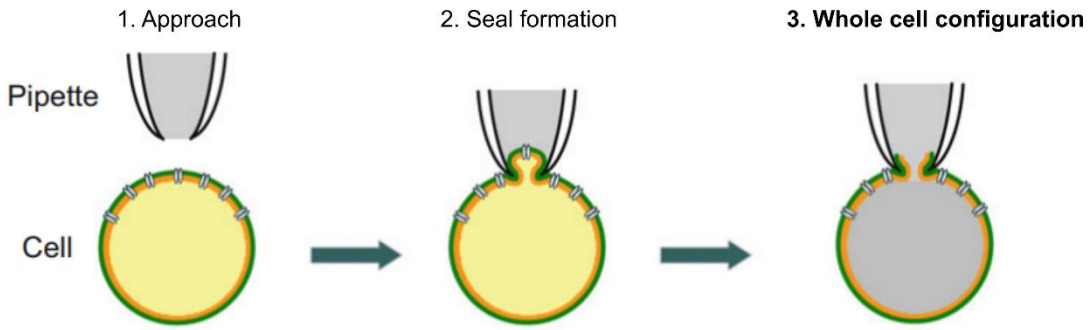

Figure 2.2 - Diagram depicting the basic procedural steps to establish the whole-cell configuration for Patch-clamp recordings. Adapted from (Segev et al., 2016), (C.-Y. Chen, 2017).

Our recordings were performed in the hippocampus, by stimulating the Schaffer collateral pathway established between the presynaptic CA3 and the postsynaptic CA1 neurons (**Figure 2.3**). We selected this pathway because it is important for learning and memory functions (Gruart et al., 2006, Bahar et al., 2011), and it is known to be affected by aging (reviewed in (Temido-Ferreira et al., 2019)).

Given the voltage-dependent properties of NMDARs flow (Nowak et al., 1984), recordings were performed in neurons voltage-clamped at +40mV, i.e. the membrane voltage is kept constant, allowing to measure ionic currents (voltage clamp configuration). To specifically detect NMDAR currents, we pharmacologically inhibited AMPARs and GABA transmission.

Importantly, our recordings consist of synaptic NMDAR currents only, since the afferent stimulation was maintained at a low frequency (<0.1 Hz), avoiding the activation of extrasynaptic NMDARs (Papouin et al., 2012).

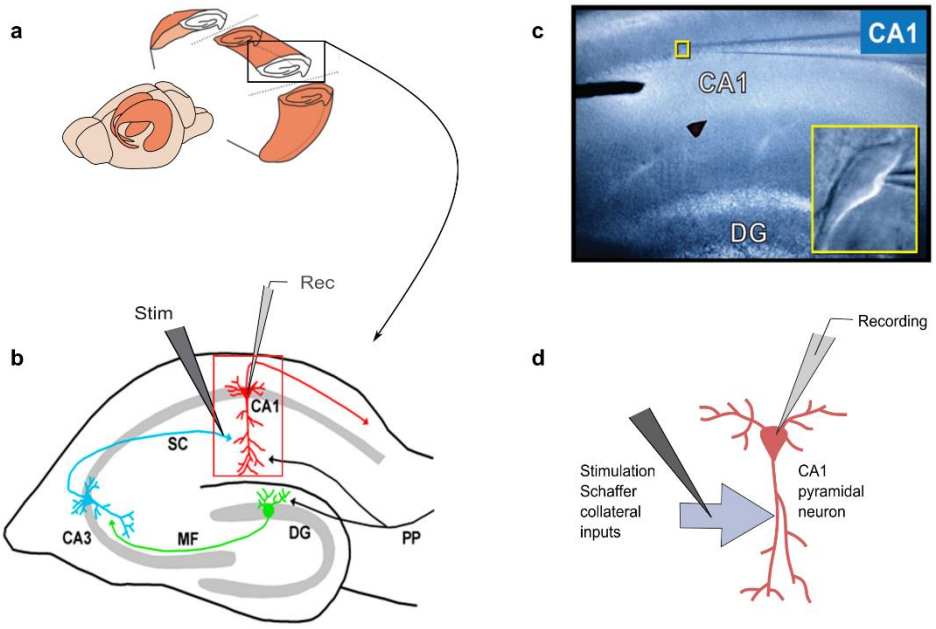

Figure 2.3 – Representation of the Patch-Clamp electrophysiology configuration used in this work to measure NMDAR EPSCs in CA1 pyramidal neurons.

a) Schematic representation of the mouse hippocampus (shown in orange) and the preparation of transverse hippocampal slices. Adapted from (Temido-Ferreira et al., 2019, Sun et al., 2018).

b) Representation of the hippocampal circuitry, including the CA3-CA1 pathway: CA3 pyramidal cells (light blue) excite CA1 pyramidal cells (red) via the Schaffer collateral (SC) pathway. Adapted from (Cammalleri et al., 2019).

c) Microscopy images of recording (Rec) and stimulation (Stim) electrodes in the hippocampal slice. Inset image corresponds to the expanded view of the tip of the recording electrode (yellow box) showing the individual pyramidal neuron for intracellular recordings. Adapted from (Plasticity lab, n.d.).

d) Schematic representation of a CA1 pyramidal neuron, showing the positions for the recording and stimulation electrodes.

By measuring NMDAR EPSCs, we can analyze different properties, such as the deactivation kinetics (which relies on subunit composition) and the relative contribution of GluN2B-NMDARs.

NMDAR EPSCs deactivation kinetics – this parameter is known to be higher in GluN2B-NMDARs when compared to the GluN2A subtype. The kinetic analysis involves decomposing the current into a slow and fast component, by using a mathematical

algorithm, and determining the amplitude and time constant for each, as illustrated in **Figure 2.4**. The weighted time constant is calculated based on the relative contribution of slow and fast components.

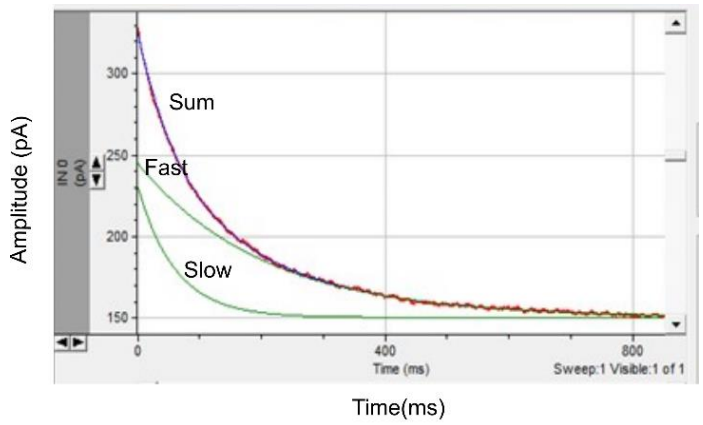

Figure 2.4 – Example of NMDAR-EPSCs trace and its decomposition into a slow and fast component**.**

GluN2B-NMDAR contribution – we can determine the contribution of GluN2B-NMDARs to total synaptic NMDAR currents by performing recordings before and after applying a GluN2B-NMDAR specific inhibitor. Ifenprodil is a noncompetitive inhibitor with a >400-fold selectivity for GluN2B-NMDARs compared to GluN2A-NMDARs (Williams, 1993). It acts by decreasing the GluN2B-NMDAR open probability and by biasing the receptor towards low open probability gating modes (Amico-Ruvio et al., 2012).

B) Fractionation into PSD-enriched fractions

We prepared PSD-enriched fractions from mouse and human brain samples, following the protocol described in **Section 2.2C**. For both cases, we confirmed that the non-PSD fraction contained high levels of synaptophysin (pre-synaptic marker), whereas the PSD fraction was enriched in PSD-95 (postsynaptic marker). We detected APP both in non-PSD and PSD fractions, whereas NMDAR subunits were more abundant in PSD fractions, as shown in **Figure 2.5.**

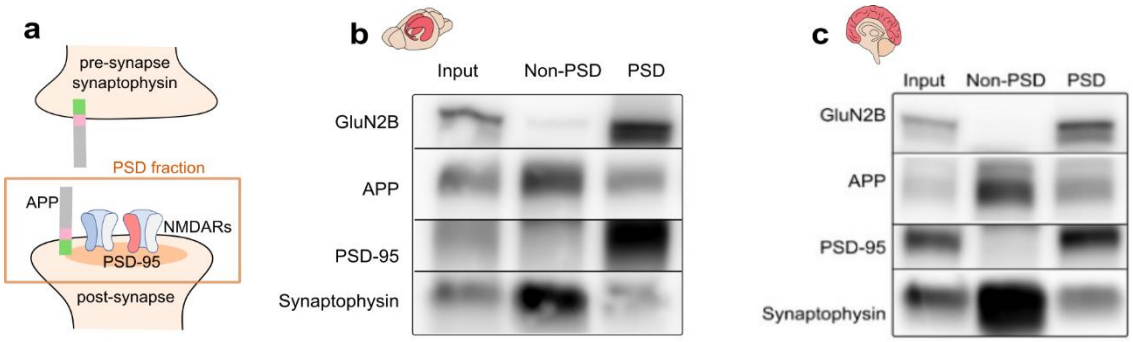

Figure 2.5 - Fractionation of mouse (hippocampal) and human (prefrontal cortical) tissue into PSD-enriched fractions.

a) Schematic representation of non-PSD and PSD-fractions and the respective proteins detected in this study.

b) Representative western blot of hippocampal PSD-enriched fractions from adult wild-type C57BL/6 mice (10 – 16 weeks). Membranes were immunoblotted with antibodies for GluN2B, APP, PSD-95 and synaptophysin.

c) Representative western blot of PSD-enriched fractions from postmortem pre-frontal cortex tissue of an adult human subject (22 years old). Membranes were immunoblotted with antibodies for GluN2B, APP, PSD-95 and synaptophysin.

C) Western Blotting (APP and APP-derived fragments)

Detecting and identifying APP-derived fragments is technically challenging, since the different CTFs (10-14 KDa) and the AICD (6 KDa) are small fragments with molecular weights that are difficult to discriminate by Western Blot (Cui et al., 2011). Moreover, AICD exhibits low levels and is rapidly degraded, only being detectable under optimal conditions (Cupers et al., 2001).

Therefore, we performed several tests using hippocampal tissue from C57Bl/6 wild-type mice to determine the best conditions for detection and discrimination of these fragments by Western Blot, using an antibody against the APP C-terminal.

We used a tricine gel system with a low pH in the gel buffer and tricine instead of glycine in the running buffer. As a result, the smaller proteins and peptides migrate separately from the free dodecyl sulfate (DS) ions from SDS (present in the samples and running buffers), contrary to what happens in the traditional tris-glycine protein gel system. Consequently, this allows the detection of sharper bands and at a higher resolution at low molecular weights.

Given its low levels and instability (Edbauer et al., 2002), detecting AICD in wild-type mice/human samples by Western Blot is technically challenging. Thus, we performed an antigen retrieval step as described in (Pimplikar & Suryanarayana, 2011) to improve AICD detection. Although it is not entirely clear why incubating the membranes in boiling PBS increases the detectability of AICD, it has been proposed that this step leads to the complete denaturation of AICD, which then refolds as the buffer returns to RT. It is also possible that boiling PBS removes residual SDS and allows better protein folding (Pimplikar & Suryanarayana, 2011).

Detection of CTFs and AICD

After loading different quantities of protein in the gel (30, 50 or 75µg), we concluded that 50µg would be the ideal dose, since it allows the detection of AICD (which is not possible when loading only 30µg of protein in the gel) but avoids artifacts due to protein overloading (as observed for 75µg of protein) **(Figure 2.6 a, b)**. Using 50µg of protein, we tested different exposure times upon chemiluminescence exposure, concluding that, on average, ≈2s is ideal to detect APP, ≈14s for CTFs and >5min for AICD **(Figure 2.6 c)**.

Discrimination of APP CTFs

APP is known to generate three species of CTFs (C99, C89, and C83). Both C99 and C89 are products of cleavage by β-secretase (CTFβ and CTFβ'), whereas C83 is a product of cleavage by α-secretase (CTFα). These fragments are phosphorylated at Thr668 and detected as phosphopeptides (pC99, pC89, and pC83) (Suzuki & Nakaya, 2008). Thus, using Western blot analysis, typical CTFs species usually appear as five bands: pC99, C99, pC89, a mixture of C89 plus pC83, and C83. We were able to identify the different CTFs by comparing samples with (+) or without (-) treatment with phosphatase inhibitors. A 3xTg-AD mouse (6 months) was used as control, showing an enrichment in C99 and C99-p fragments (**Figure 2.6 d**). Using this band correspondence, we were able to calculate an approximation of the CTFβ/α ratio in mice wild-type samples.

Table 2.3 – Predicted molecular weights for APP, APP C-terminal fragments and AICD in mice. Adapted from (Kimura et al., 2016), (Chang et al., 2003).

APP fragments	**Size (KDa)**
Full-length	100-140
CTFβ (C99)	14
CTFβ' (C89)	12
CTFα (C83)	10
AICD	6

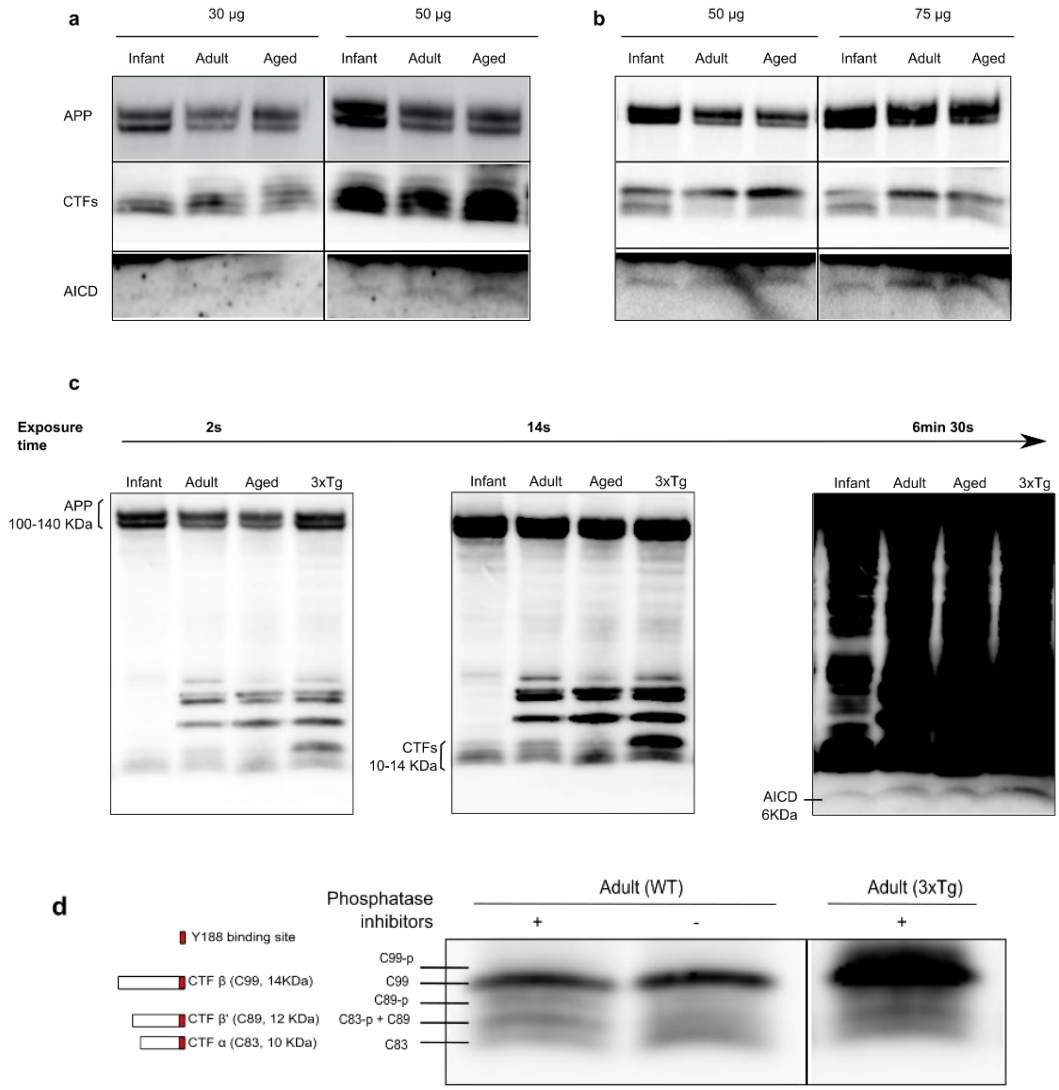

Figure 2.6 - Detection and identification of APP C-terminal fragments and AICD

Western blot analysis of hippocampal samples from C57BL/6 wild-type mice with different ages: infant (7-10 days), adult (10 – 16 weeks) and aged (18 – 20 months). Membranes were immunoblotted with an antibody for the APP C-terminal to detect APP, APP C-terminal fragments (CTFs) and the APP Intracellular Domain (AICD).

a) Representative western blot from hippocampal samples of mice with different ages (50 µg or 30 µg).

b) Representative western blot from hippocampal samples of mice with different ages (50 µg or 75 µg).

c) Representative western blot from hippocampal samples of mice with different ages (50 µg), using different exposure times to detect APP, CTFs and AICD.

d) Representative western blot from hippocampal samples (50µg) of wild-type mice with different ages and an adult 3xTg-AD mouse (6 months). The samples were prepared with (+) or without (-) phosphatase inhibitors. The various species of CTFs are schematically represented: CTFβ (C99), CTFβ' (C89) and CTFα (C83) and the Y188 antibody binding is schematically represented in red.

3 Results

Author contributions

All the experimental work was performed by Joana Rajão-Saraiva, at Instituto de Medicina Molecular João Lobo Antunes (iMM), Lisbon, Portugal and at University Côte d' Azur, Centre National de la Recherche Scientifique (CNRS) UMR 7275, Institut de Pharmacologie Moléculaire et Cellulaire (IPMC), Valbonne, France, except where otherwise stated. Hélène Marie (IPMC) has assisted in designing and cloning the shAPP plasmids and producing the viral vectors. Paula A. Pousinha (IPMC) performed the whole-cell patch-clamp recordings and viral injections. Aurore Ribera and Sébastien Moreno (IPMC) performed the *in vivo* pharmacological treatment in aged mice. Francisco J. Enguita (iMM) performed the prediction of aminoacid disorder in the structure of APP and NMDAR subunits. Bendiab Sofiane (IPMC) quantified the AAV-shAPP silencing in adult mice. Stefan Kins (Division of Human Biology and Human Genetics, University of Kaiserslautern, Kaiserslautern, Germany) provided the PTB1-p and PTB2-p peptides, expressed and purified by Svenja König. Mariana Temido-Ferreira and Joana E. Coelho (iMM) assisted with the preparation of primary neuronal cultures.

3.1 Does APP regulate NMDARs in immature and mature synapses?

We investigated whether APP acts as a regulator of NMDARs in synapses that are still immature (abundant during early postnatal development) and in mature synapses, which are the predominant type in adult stages. We addressed this question by using *in vitro* and *in vivo* physiological models of immature/mature synapses, in which we disrupted APP function using knockdown approaches or by interfering with the APP-NMDAR interaction.

A) APP interacts with the predominant NMDAR subtypes in immature and mature synapses

Our hypothesis is that APP interaction with NMDARs could be important to regulate their synaptic levels and/or function (Cousins et al., 2009, Hoe et al., 2009, Pousinha et al., 2017). To assess if this occurs both in immature and mature synapses, we used the hippocampi of C57BL/6 wild-type infant (7-10 days) and adult mice (10 – 16 weeks) as our models of immature and mature synapses, respectively.

We started by assessing whether APP-NMDAR interaction occurs at both ages. For that purpose, we immunoprecipitated APP in hippocampal samples using an antibody against the APP C-terminal domain, followed by detection of NMDAR subunits in immunocipitated (IP) samples. In the hippocampus, NMDARs contain GluN1 obligatory subnits and GluN2A and/or GluN2B regulatory subunits (Monyer et al., 1994). To identify the NMDAR subtypes that interact with APP at each age, we calculated the GluN2B/GluN2A ratio in IP samples. We found that this interaction mainly occurs with GluN2B subunits during postnatal development and both with GluN2A and GluN2B in adult animals (**Figure 3.1 a, b**). Additionally, we showed that this interaction occurs in synaptic fractions, possibly regulating the synaptic pool of NMDARs at each stage (**Figure 3.1 c**).

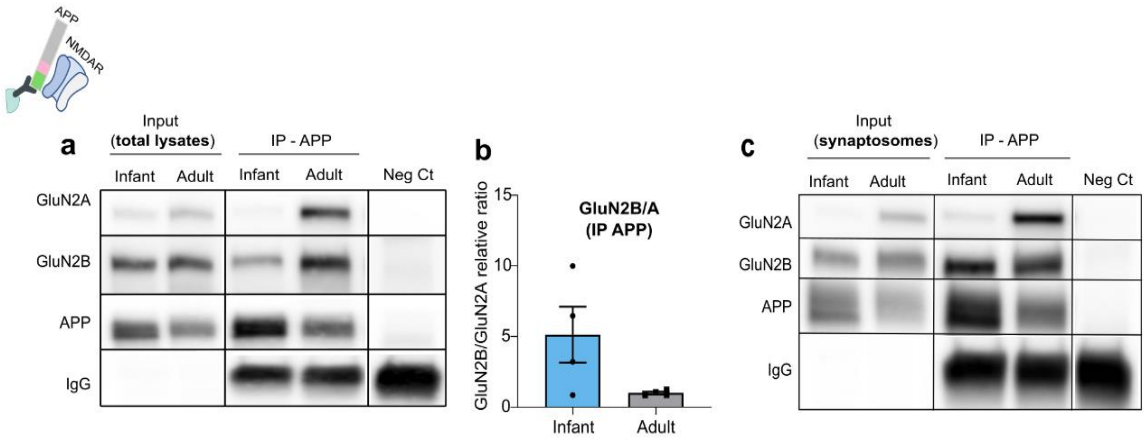

Figure 3.1 – APP interacts with NMDARs in immature and mature synapses.

a) Representative western blot of hippocampal lysates of infant (7-10 days) and adult (10 – 16 weeks) wild-type C57BL/6 mice immunoprecipitated for APP. Membranes were immunoblotted with antibodies for GluN2A, GluN2B and APP. The schematic representation shows NMDARs being co-immunoprecipitated with APP, using an antibody against the APP C-terminal.

b) Results from blots as shown in a) from APP immunoprecipitated (IP) samples. The GluN2B/A relative ratio in IP samples is represented as the mean ± SEM relative to the adult group (Unpaired t-test, n=4).

c) Representative western blot of synaptosome fractions from the hippocampi of infant and adult wild-type C57BL/6 mice immunoprecipitated for APP. Membranes were immunoblotted with antibodies for GluN2A, GluN2B and APP.

We then assessed whether the NMDAR subunits that co-immunoprecipitate with APP reflect the NMDAR population that is expressed at each stage. When analyzing total hippocampal lysates, we found that NMDARs are expressed in lower levels in infant mice than in adults, as shown by the decrease in the obligatory GluN1 subunit levels (more than 50%) (**Figure 3.2 a, e**), as well as in GluN2A and GluN2B levels (**Figure 3.2 a, b, c**). We also found a reduction in PSD-95 protein levels, which is consistent with the immature profile of the synapses at this stage (**Figure 3.2 a, f**). To determine the predominant NMDAR subtype at each age, we calculated the GluN2B/GluN2A ratio and found an 8-fold increase in infant mice when compared to adults (**Figure 3.2 a, d**), confirming that GluN2B-NMDARs are the predominant subtype in infant mice.

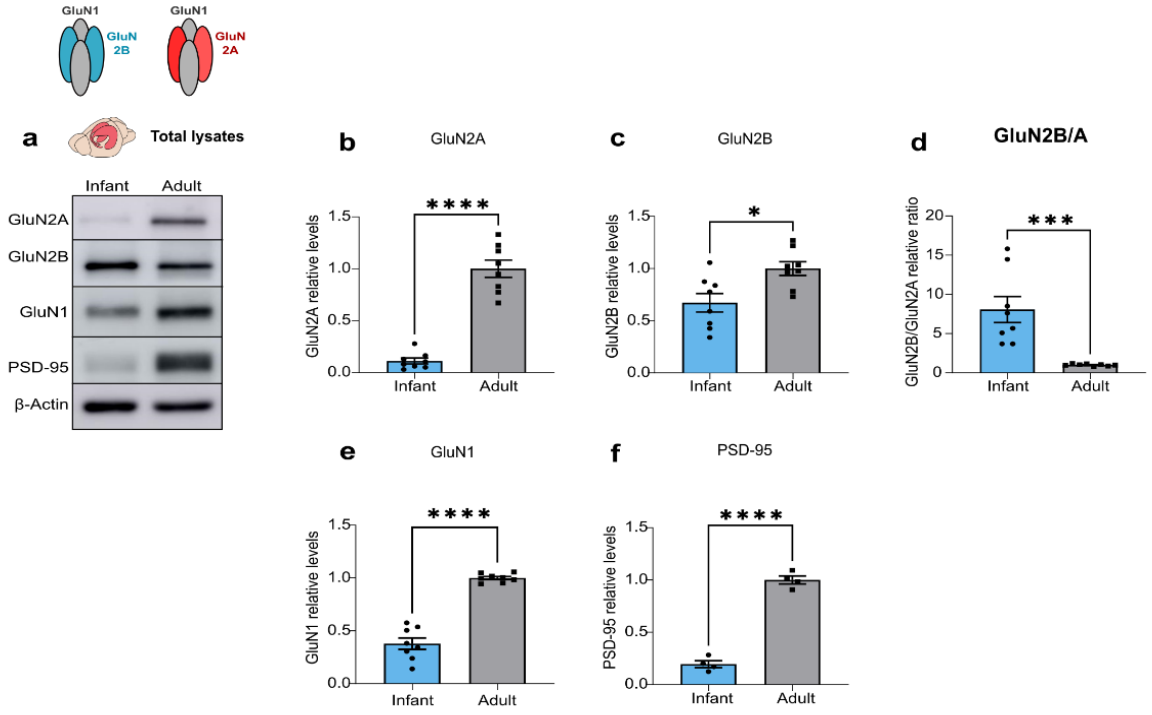

Figure 3.2 – The GluN2B/GluN2A subunit ratio in total lysates is higher in infant mice.

a) Representative western of hippocampal lysates from infant (7-10 days) and adult (10 – 16 weeks) wild-type C57BL/6 mice. Membranes were immunoblotted with antibodies for GluN2A, GluN2B, GluN1, PSD-95 and β-actin.

b, c, e, f) Results from blots as shown in **a)** from hippocampal lysates were normalized with β-actin and are expressed as the mean ± SEM relative to the adult group (Unpaired t-test, *p<0.05, ****p<0.0001); b, c, e) n=8; f) n=4.

d) Results from blots as shown in a) from hippocampal lysates show the GluN2B/GluN2A ratio and are expressed as the mean ± SEM relative to the adult group (Unpaired t-test, ***p<0.001, n=8).

We then confirmed if this peak in GluN2B/GluN2A ratio also occurs in fractions enriched in the postsynaptic density (PSD). We observed an increase in GluN2B postsynaptic levels in infants (**Figure 3.3. a, c**), whereas no significant alterations were found for GluN2A and GluN1 (normalized with PSD-95) (**Figure 3.3. a, b, e**). Altogether, this results in a 4-fold increase in the GluN2B/GluN2A ratio in infant mice, when compared to adults (**Figure 3.3. a, d**). These findings show that the GluN2B-NMDARs are the predominant subtype in immature synapses, whereas both GluN2A and GluN2B are abundant in mature synapses. This is consistent with the fact that APP mainly interacts with GluN2B in infant mice, but also interacts with GluN2A in adults.

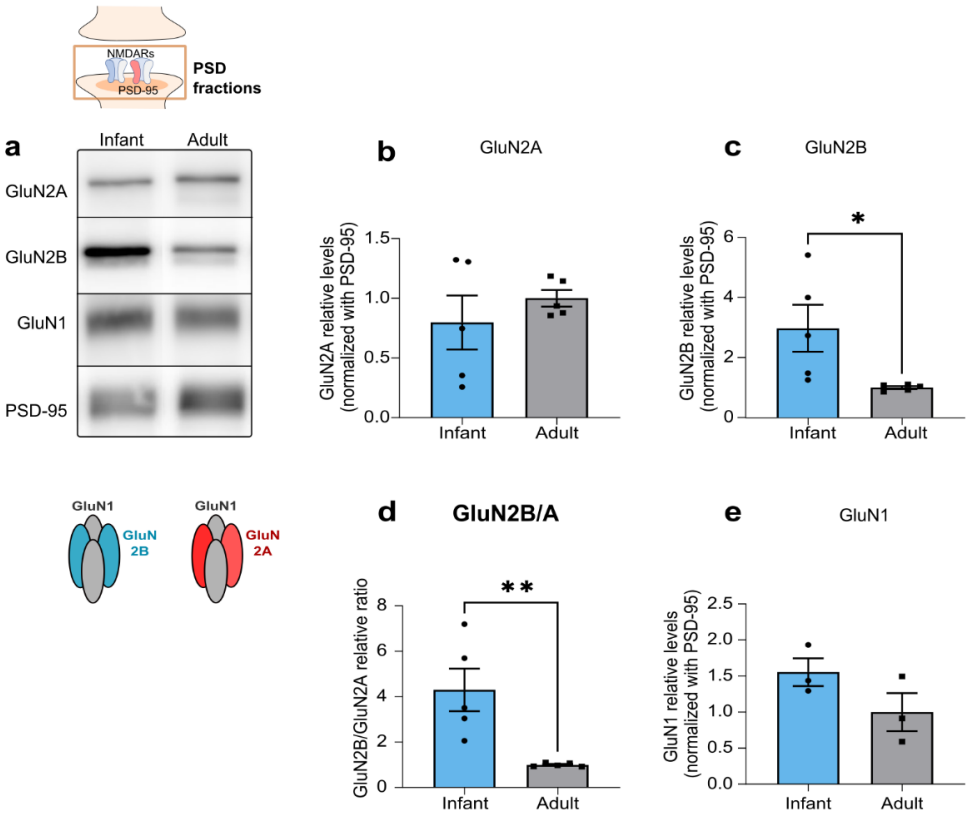

Figure 3.3 – The GluN2B/GluN2A subunit ratio is higher in immature synapses.

a) Representative western blot of hippocampal lysates subjected to biochemical fractionation to obtain PSD-enriched fractions from (7-10 days) and adult (10 – 16 weeks) wild-type C57BL/6 mice. Membranes were immunoblotted with antibodies for GluN2A, GluN2B, GluN1 and PSD-95. The schematic diagram shows the isolation of PSD-enriched fractions to specifically study the NMDARs present at the post-synapse.

b, c, e) Results from western blots of PSD-enriched fractions as shown in a) were normalized with PSD-95 and are expressed as the mean ± SEM relative to the adult group (Unpaired t-test, *p<0.05); b, c) n=5; e) n=3.

d) Results western blots of PSD-enriched fractions as shown in a) show the relative GluN2B/GluN2A in PSD-enriched fractions and are expressed as the mean ± SEM relative to the adult group (Unpaired t-test, **p<0.01, n=5).

To assess if this peak of GluN2B/GluN2A protein ratio correlates with a peak in GluN2B-NMDAR relative contribution to total synaptic currents, we performed Patch-Clamp recordings in CA1 pyramidal cells in the hippocampus, by electrically stimulating the Schaffer collaterals (**Figure 3.4 a**). We measured the total NMDAR excitatory postsynaptic currents (EPSCs) and then determined the effect of the selective GluN2B inhibitor, ifenprodil (5μM). We found that the GluN2B-NMDAR contribution is higher in infants (50,88% ± 5,58) when compared to adults (14,20% ± 4,32), as depicted in **Figure 3.4 b-d**.

Since subunit composition determines NMDAR kinetics (Vicini et al., 1998), we also determined the NMDAR EPSCs decay time at each age. Therefore, we calculated the respective slow/fast components and, based on their relative contribution, determined the weighted time constant (τweighted). We found that this value was higher in infant mice (156,2 ms ± 4,20), compared to the reference group of adults (126,3 ms ± 9,11), indicating that NMDAR-mediated currents exhibit slower deactivation kinetics during postnatal development (**Figure 3.4 e, f**).

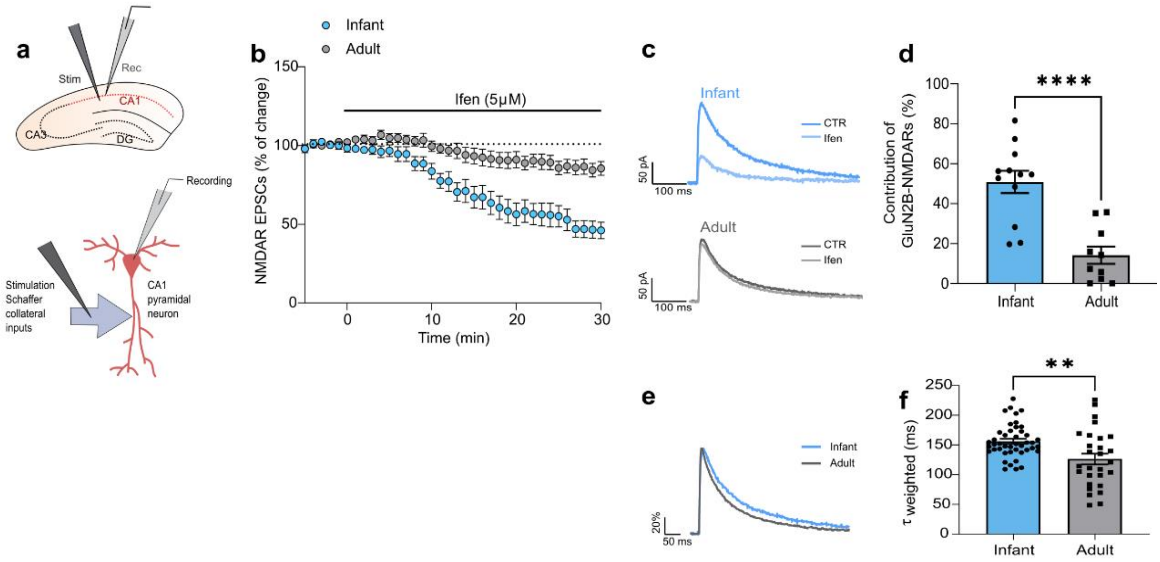

Figure 3.4 – NMDAR synaptic currents show an increase in GluN2B-NMDAR contribution and slower deactivation kinetics in immature synapses.

a) Schematic diagram showing the locations of stimulating and recording electrodes in the hippocampus and in a CA1 pyramidal neuron for whole cell patch-clamp experiments.

b) Time course of ifenprodil (5µM) effect on pharmacologically isolated NMDAR EPSC amplitude in CA1 pyramidal neurons, measured by whole-cell patch clamp in infant (7-10 days) and adult (10 – 16 weeks) C57BL/6 wild-type mice. Results are expressed as the mean ± SEM (n=10-12).

c) Traces show NMDAR EPSCs recorded before (CTR) and after 30 min of Ifenprodil 5 µM perfusion (Ifen).

d) GluN2B contribution was calculated as the percentage of change in NMDAR EPSC amplitude after 30 min of ifenprodil perfusion. Results are expressed as the mean ± SEM (Unpaired t-test, ****p<0,0001, n=10-12).

e) Comparison of representative whole-cell patch-clamp recordings of pharmacologically isolated NMDAR EPSCs, normalized to the peak amplitude (in %), from infant and adult mice.

f) The weighted time constant (τweighted) was calculated using the relative contribution of both slow/fast components of NMDAR EPSCs and reflects the overall deactivation kinetics. Results are expressed as the mean ± SEM (Unpaired t-test, **p<0.01, n=28-44).

Altogether, this data indicates that APP interacts with the predominant subtype of synaptic NMDARs at each stage, thereby mainly interacting with GluN2B-NMDARs in immature synapses and with both GluN2B and GluN2A-NMDARs in mature synapses.

B) APP is highly abundant in immature synapses, where it regulates NMDAR currents through the intracellular domain

We hypothesized that the ability of APP to work as a NMDAR regulator would depend on the levels of APP and/or the extent by which it is processed. Accordingly, both the full-length protein and its derived fragments have been described as potential regulators of NMDARs (Hoe et al., 2009, Pousinha et al., 2017).

Thus, we measured the levels of APP full-length (APP), APP C-terminal fragments (CTFs), and APP intracellular domain (AICD) in hippocampal lysates of infant and adult mice (**Figure 3.5 a**). We found no differences in the overall levels and processing of APP into C-terminal fragments when comparing both ages (**Figure 3.5 a-c**). However, the levels of AICD in relation to APP showed to be significantly lower in infants when compared to adult mice (**Figure 3.5 a, d**).

Since APP interacts with NMDARs in synaptic fractions, we hypothesize that the levels of APP at the post synapse could influence its ability to regulate NMDARs. We were able to detect APP in PSD fractions of both ages and found a 5-fold increase in infants when compared to adults (**Figure 3.5 e, f**).

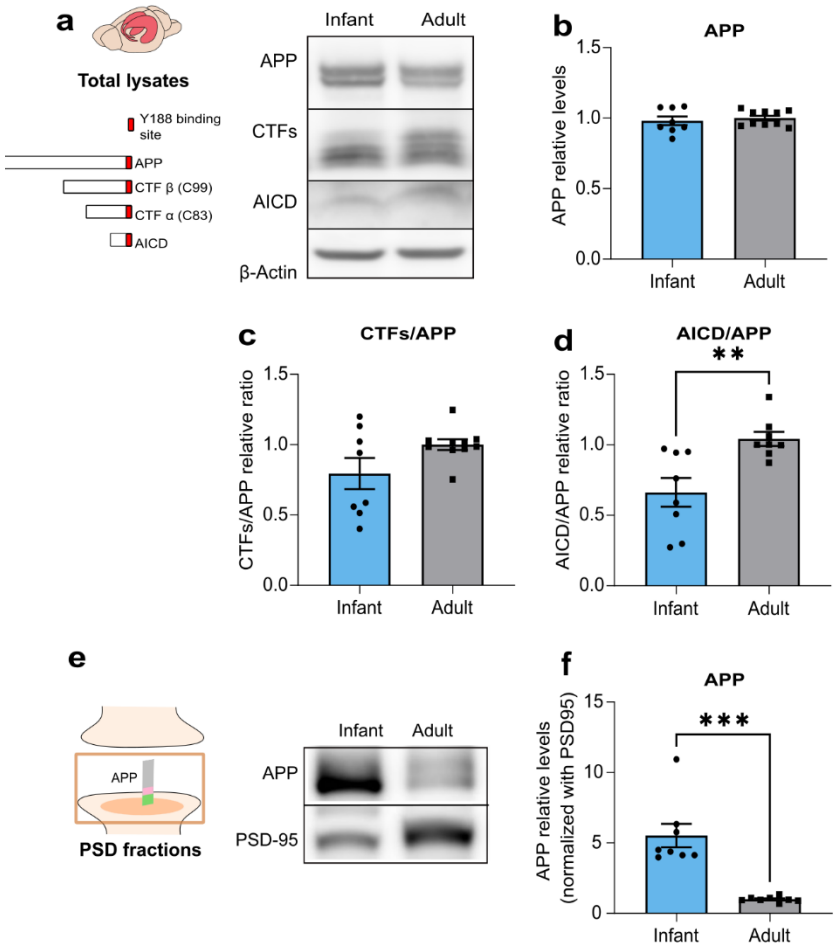

Figure 3.5 - APP is highly abundant in immature synapses

a) Representative western blot of hippocampal lysates from in infant (7-10 days) and adult (10 – 16 weeks) C57BL/6 wild-type mice. Membranes were immunoblotted with antibodies for β-actin as the loading control and for the APP C-terminal (Y188, to detect APP full-length (APP), APP C-terminal fragments (CTFs β and α) and the APP Intracellular Domain (AICD). The Y188 antibody binding site is schematically represented in red (on the left).

b) Results from blots shown in a) from mouse hippocampal lysates were normalized with β-actin and are expressed as the mean ± SEM relative to the adult group (Unpaired t-test, n=8-10).

c) Results from blots shown in a) from mouse hippocampal lysates represent the ratio between CTFs and APP. Results are expressed as the mean ± SEM relative to the adult group (Mann Whitney test, n=8-10).

d) Results from blots shown in a) from mouse hippocampal lysates represent the ratio between AICD and APP. Results are expressed as the mean ± SEM relative to the adult group (**p<0.01, Unpaired t-test, n=8-10).

e) Representative western blot of hippocampal PSD-enriched fractions from infant and adult wild-type C57BL/6 mice. Membranes were immunoblotted with antibodies for APP and PSD-95.

f) APP levels were normalized with PSD-95 and are expressed as the mean ± SEM relative to the adult group (Mann Whitney test, ***p<0.001, n=8).

We then investigated if the APP-NMDAR interaction could regulate NMDAR-mediated currents. Since a previous study by our group showed that the APP intracellular domain is able to regulate the GluN2B-NMDAR contribution (Pousinha et al., 2017), we identified this domain as the putative binding site to NMDARs. We found that the intracellular domains of APP and NMDAR subunits do not show a stable 3D structure, thus it was not possible to obtain a reliable prediction of the APP-NMDAR interaction at the structural level (**Supplementary Figure 3.1**).

Therefore, we used an antibody against the APP C-terminal (APPCt Ab, clone Y188) to interfere with the putative binding domain and potentially disrupt the APP-NMDAR interaction. For that purpose, we performed Patch-Clamp electrophysiology experiments introducing the antibody (final concentration 2.5nM) in the recording pipette to allow access to the intracellular space (**Figure 3.6 a**). When recording NMDAR EPSCs in these conditions, we observed a reduction of approximately 20% in NMDAR EPSCs in infant mice, compared to the control condition (heat inactivated APPCt antibody) (as illustrated in **Figure 3.6 b-d)**. In contrast, in adult mice we found no alterations in NMDAR-mediated currents when interfering with the APP C-terminal (**Figure 3.6 d**).

To test if this response in infant mice is caused by a reduction in GluN2B-NMDAR currents, we perfused hippocampal slices with a GluN2B-NMDAR selective antagonist, ifenprodil (5µM), for 30 min at the end of the experimental protocol (60-90 min) (**Figure 3.6 e, f**). As shown, the contribution of GluN2B-NMDARs was less pronounced in neurons treated with the APPCt antibody, when compared to the control condition (approximately 20% vs. 47%) (**Figure 3.6 f-h**). This data indicates that, in infant mice, interfering with the APP intracellular domain results in a decrease in NMDAR currents, predominantly of the GluN2B subtype.

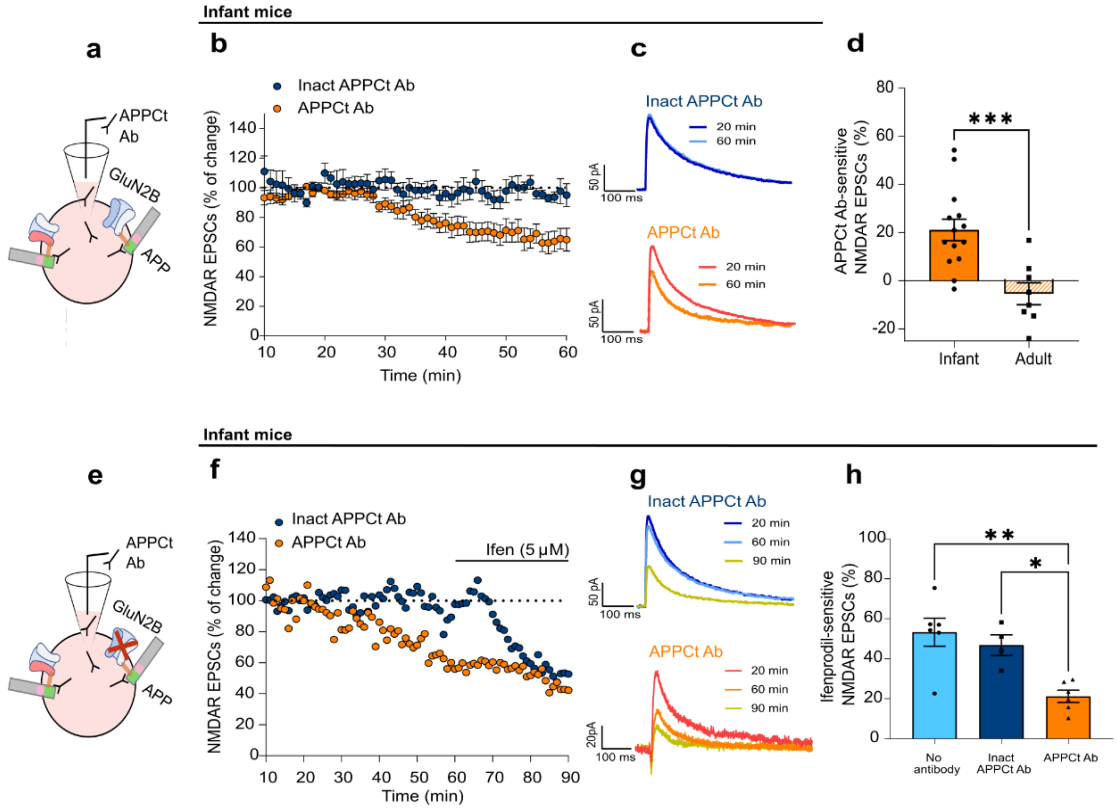

Figure 3.6 - The APP intracellular domain regulates NMDAR currents in immature synapses

a) Schematic diagram showing the strategy used to interfere with the APP C-terminal domain: the antibody was added to the intracellular solution in the patch pipette to diffuse into the intracellular space.

b) Time course of NMDAR EPSC amplitude measured by whole-cell patch clamp in CA1 pyramidal neurons of infant (7-10 days) C57BL/6 wild-type mice during 60 min of incubation with an antibody against the APP C-terminal (APPCt Ab). In the control condition, the antibody was heat inactivated (Inact APPCt Ab). Results are expressed as the mean ± SEM (n=6-10).

c) Traces show NMDAR EPSCs recorded at 20min (baseline) and 60min by patch clamp in CA1 pyramidal neurons of infant mice. The APP Ct antibody was inside the patch pipette during the whole course of the experiment (60min).

d) The percentage of NMDAR EPSCs sensitive to APPCt Ab was determined for infant (7-10 days) and adult (10 – 16 weeks) C57BL/6 wild-type mice. The effect was calculated comparing the baseline amplitude (15-20 min) with the final amplitude (60 min) and normalized with the control condition (Inact APPCt Ab) for each age. Results are expressed as the mean ± SEM (Unpaired t-test, ***p<0.001, n=8-15)

e) Schematic diagram showing the strategy used to determine the percentage ifenprodil-sensitive NMDAR EPSCs in neurons treated with the APP Ct Ab.

f) Time course of NMDAR EPSC amplitude measured by whole-cell patch clamp in CA1 pyramidal neurons of infant C57BL/6 wild-type mice during 90 min of incubation with the APPCt antibody and perfusion with ifenprodil (5µM) at 60-90 min. In the control condition, the antibody was heat inactivated (Inact APPCt Ab) (n=1).

g) Traces show NMDAR EPSCs recorded at 20min (baseline), 60min and 90min by patch clamp in CA1 pyramidal neurons of infant mice. The APPCt antibody was inside the patch pipette during the whole course of the experiment (90min), whereas Ifenprodil perfusion occurred from 60 to 90min.

h) The percentage of ifenprodil-sensitive NMDAR EPSCs in infant mice was calculated comparing the amplitude at 60 min with the final amplitude (90 min). The effect of ifenprodil on NMDAR EPSCs was calculated in neurons without antibody incubation (No antibody, used as reference), incubated with the APPCt antibody (APPCt Ab) or the heat-inactivated antibody (Inact APPCt Ab) for 90 min. Results are expressed as the mean ± SEM (One-way ANOVA followed by Tukey's multiple comparisons test, **p<0.01, *p<0.05, n= 4-6).

C) APP modulates the NMDAR synaptic content in immature synapses

The reported impact of APP on NMDAR transmission suggested a role for APP in regulating NMDARs, being particularly relevant in immature synapses.

To assess the outcomes of APP depletion in immature synapses, we transfected primary neuronal cultures (7 days *in vitro* (DIV)) with a plasmid encoding a short-hairpin RNA (shRNA) sequence against APP (shAPP) or the respective control (shRNA with no silencing effect, shCTR) (**Figure 3.7 a**). The APP knockdown was efficient, leading to a reduction of approximately 80% in APP immunoreactivity, when compared to the control condition, evaluated 7 days post-transfection (14 DIV) (**Figure 3.7 b, c**).

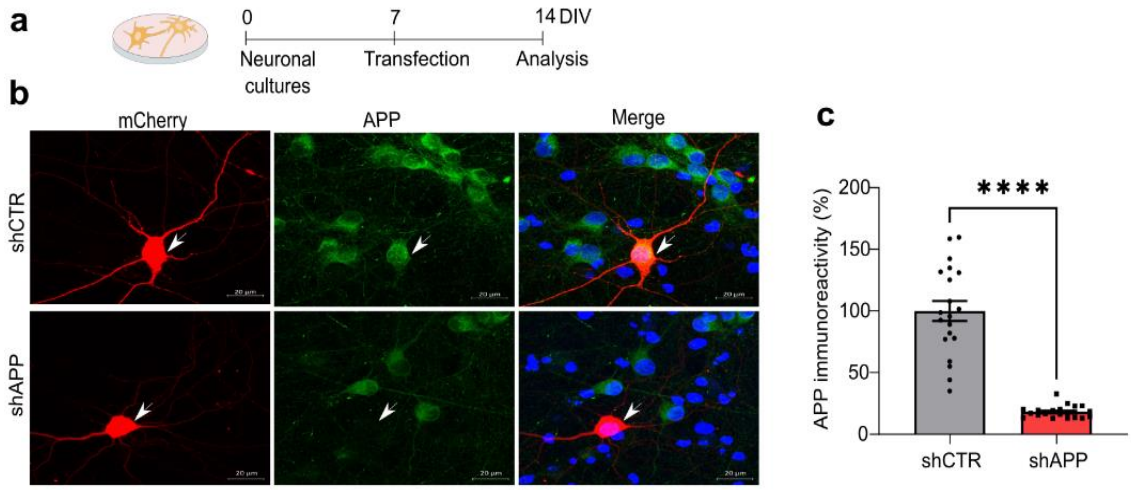

Figure 3.7 – Transfection of primary neuronal cultures with shAPP leads to an efficient reduction in APP levels.

a) Schematic representation of shRNA transfection in rat hippocampal primary neuronal cultures (7 days *in vitro* (DIV)) and consequent analysis (DIV14).

b) Representative immunocytochemistry analysis of APP immunofluorescence in primary neuronal cultures at DIV14 transfected with shAPP or the respective control (shCTR) at DIV7. mCherry (reporter plasmid) is

shown in red, APP is labelled in green and cell nuclei are stained with Hoechst in blue. Transfected neurons are indicated by arrows. Scale bars represent 20 µm.

c) APP immunoreactivity (%) in transfected neurons is expressed as the mean ± SEM, using the control condition as reference (Mann-Whitney test, ****p<0.0001, n=20-21 cells, 3 independent cultures).

When analyzing the impact of APP depletion in NMDAR subunits, we found no significant differences in GluN2B positive area, average particle size, mean fluorescence intensity and fluorescence density, indicating that the total levels/area and clustering remained unaltered (**Figure 3.8, a-d**) However, APP knockdown resulted in a 20% reduction in the percentage of GluN2B clusters that co-localize with PSD-95 (post-synaptic marker) (**Figure 3.8 a, e**).

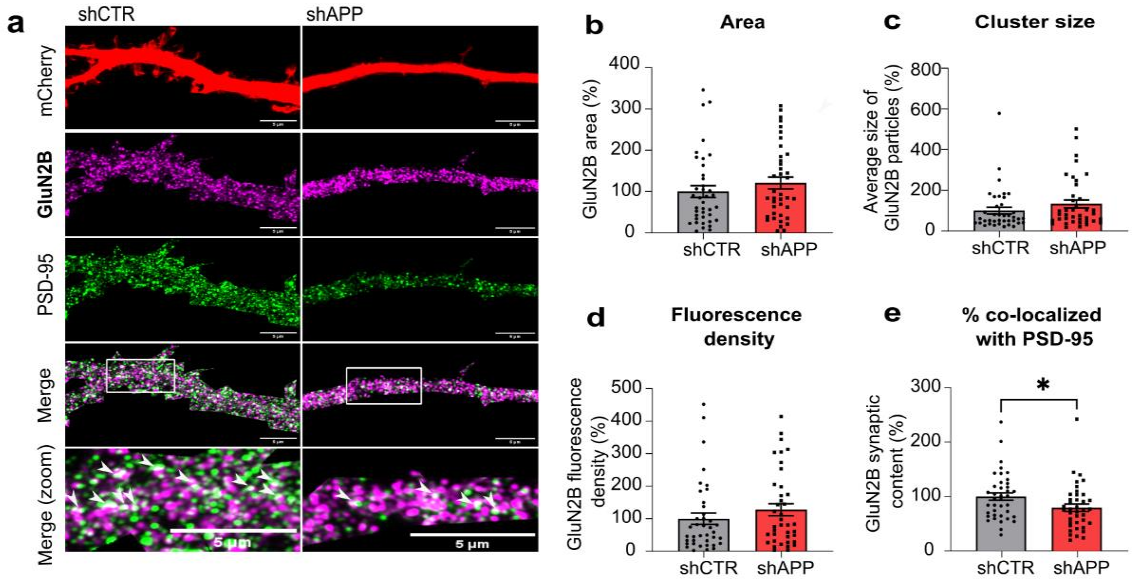

Figure 3.8 – APP knockdown causes a reduction in GluN2B synaptic content

a) Representative immunocytochemistry analysis of rat primary neuronal cultures (DIV14) transfected with shAPP or the respective control (shCTR) at DIV7. mCherry (reporter plasmid), labelled in red, was used to identify dendrites of transfected neurons. GluN2B is shown in magenta and PSD-95 is labelled in green. Higher magnification images are shown at the bottom, with arrows indicating GluN2B/PSD95 co-localization (white). Scale bars represent 5 µm.

b-e) Results of immunocytochemistry experiments as illustrated in a) to analyze GluN2B area, average cluster size, fluorescence density and synaptic content (based on GluN2B–PSD95 co-localization) in dendrites of transfected neurons. Results are expressed as the mean ± SEM relative to the control condition (%). For each case, the statistical analysis was performed by Mann-Whitney test, *p<0.05, n= 39, 3 independent cultures.

Similar results were obtained for GluN2A, since we found no significant alterations in GluN2A positive area, cluster size and fluorescence density (**Figure 3.9 a-d**).

Additionally, we observed a 56% reduction in the percentage of GluN2A clusters that co-localize with PSD-95 (**Figure 3.9 a, e**).

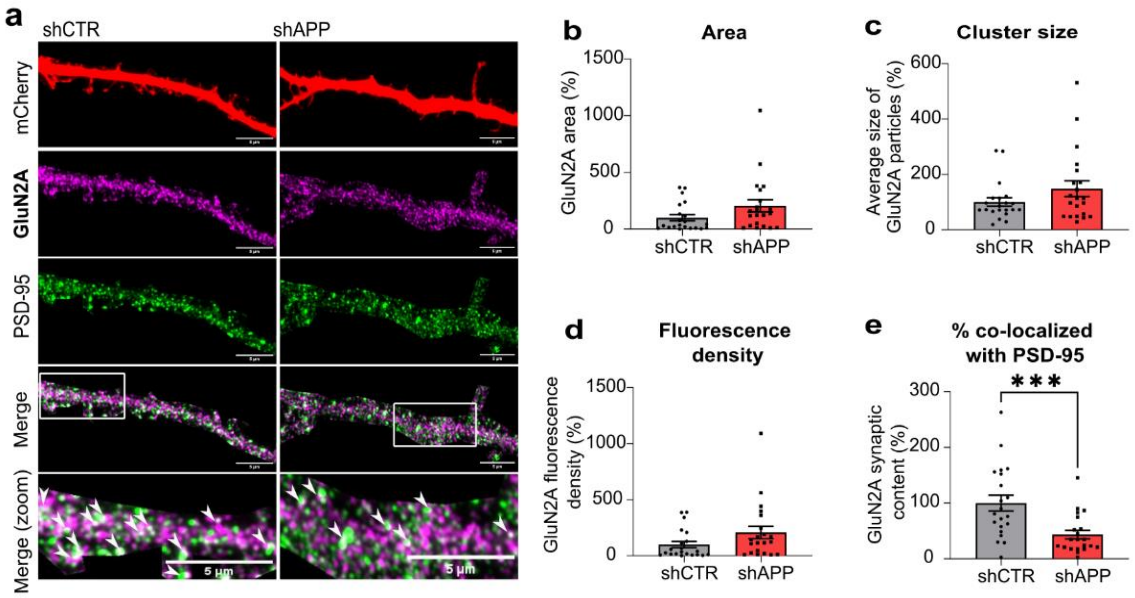

Figure 3.9 - APP knockdown causes a reduction in GluN2A synaptic content

a) Representative immunocytochemistry analysis of rat primary neuronal cultures (DIV14) transfected with shAPP or the respective control (shCTR) at DIV7. mCherry (reporter plasmid), labelled in red, was used to identify dendrites of transfected neurons. GluN2A is shown in magenta and PSD-95 is labelled in green. Higher magnification images are shown at the bottom, with arrows indicating GluN2A/PSD95 co-localization (white). Scale bars represent 5 µm.

b-e) Results of immunocytochemistry experiments as illustrated in a) to analyze GluN2A area, average cluster size, fluorescence density and synaptic content (based on GluN2A–PSD95 co-localization) in dendrites of transfected neurons. Results are expressed as the mean ± SEM relative to the control condition (%). For each case, the statistical analysis was performed by Mann-Whitney test, ***p<0.001, n= 21, 3 independent cultures.

Moreover, we found a reduction in PSD-95 dendritic area and average particle size (less than 20%), whereas the fluorescence density was not altered (**Figure 3.10 a-c**). These results suggest that APP depletion affects PSD-95 distribution and clustering but not the total protein levels.

Figure 3.10 - APP knockdown causes a reduction in PSD-95 area and cluster size

a-c) Results of immunocytochemistry experiments as illustrated in **Figure 3.8a** to analyze PSD-95 area, average cluster size and fluorescence density in dendrites of transfected neurons. Results are expressed as the mean ± SEM relative to the control condition (%). For each case, the statistical analysis was performed by Mann-Whitney test, *p<0.05, **p<0.01, n=39 dendrites, 3 independent cultures.

The results obtained in APP-depleted neurons suggest that APP plays an important role in immature synapses, namely by controlling the synaptic content of NMDARs. We propose that the APP interaction with NMDARs is important to recruit/anchor them in newly formed synapses. This is consistent with the peak of APP levels at the post-synapse during early postnatal development, when APP interacts mainly with GluN2B-NMDARs, which are the predominant NMDAR subtype. This interaction, likely mediated by the APP C-terminal, proved to be essential to maintain normal NMDAR transmission in infant mice. The fact that this effect was not observed in adult mice indicates that the APP-NMDAR regulation mechanisms are age-dependent.

3.2 Does APP regulate NMDARs in aged synapses?

Since aging is associated with synaptic impairments which are associated with NMDARs (Kumar et al., 2019), mainly with the GluN2B subtype (Zhao et al., 2009), we hypothesized that the APP-NMDAR regulation mechanisms might suffer alterations at later life stages. Using physiological models of aging, we identified the properties that are altered in APP/NMDARs in aged synapses and found strategies to counteract these alterations. Since the adult mice group was used as reference, the results presented below for adults correspond to the same results described in **Section 3.1**.

A) APP interaction with NMDARs is maintained upon aging

To study NMDAR regulation by APP in aged synapses, we used aged C57BL/6 wild-type mice (18 – 20 months) and compared them to adult mice (10 – 16 weeks).

We observed that the APP-NMDAR interaction is maintained upon aging, since both GluN2A and GluN2B co-immunoprecipitated with APP in total lysates and in synaptosomal fractions (**Figure 3.11 a, c**). Moreover, the GluN2B/A ratio in immunoprecipitated samples showed no statistical differences in adult and aged mice (**Figure 3.11 a, b**). We then assessed if interfering with the APP C-terminal during a short period (60 min) would be enough to alter NMDAR-mediated currents. For that purpose, we recorded NMDAR EPSCs while introducing an APP C-terminal antibody (APPCt Ab, clone Y188, 2.5nM) in the recording pipette to allow diffusion to the intracellular space. We observed no alterations in NMDAR-mediated currents using this approach in aged mice, similarly to what happens in adults (**Figure 3.11 d**).

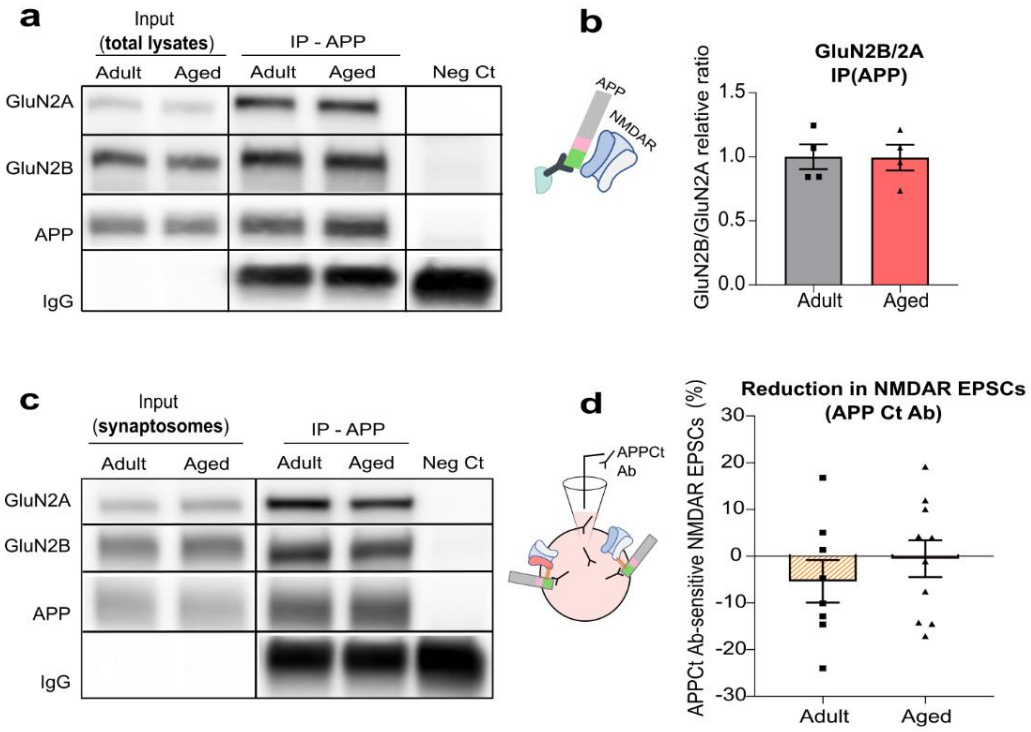

Figure 3.11 – APP interaction with synaptic NMDARs is maintained upon aging.

a) Representative western blot of hippocampal lysates of adult (10 – 16 weeks) and aged (18 – 20 months) C57BL/6 wild-type mice immunoprecipitated for APP. Membranes were immunoblotted with antibodies for GluN2A, GluN2B and APP.

b) Results from blots as shown in a) from APP immunoprecipitated (IP) samples. The GluN2B/A relative ratio in IP samples is represented as the mean ± SEM relative to the adult group (Unpaired t-test, n=4). The schematic representation shows NMDARs being co-immunoprecipitated with APP, using an antibody against the APP C-terminal.

c) Representative western blot of synaptosome fractions from the hippocampi of adult and aged wild-type C57BL/6 mice immunoprecipitated for APP. Membranes were immunoblotted with antibodies for GluN2A, GluN2B and APP.

d) The percentage of NMDAR EPSCs sensitive to APPCt Ab was determined for adult and aged C57BL/6 wild-type mice. The effect was calculated comparing the baseline amplitude (15-20 min) with the final amplitude (60 min) and normalized with the control condition (Inact APPCt Ab) for each age. Results are expressed as the mean ± SEM (n=8-14). The schematic diagram shows the strategy used to interfere with the APP C-terminal domain: the antibody was added to the intracellular solution in the patch pipette to diffuse into the intracellular space.

We then assessed if the NMDAR subunits that co-immunoprecipitate with APP correspond to the NMDAR subtypes that are expressed in adult and aged synapses. We found no significant alterations between both groups in the levels of the obligatory GluN1 subunit (**Figure 3.12 a, e**), in contrast with the regulatory subunits. Accordingly, the GluN2B levels significantly decreased (**Figure 3.12 a, c**), whereas the GluN2A showed a tendency for a decline in aged mice (**Figure 3.12 a, b**). When calculating the

GluN2B/GluN2A ratio, we found no significant alterations between adult and aged mice, indicating that the balance between both NMDAR subtypes is maintained. Additionally, the total levels of PSD-95 were not altered upon aging (**Figure 3.12 a, f**).

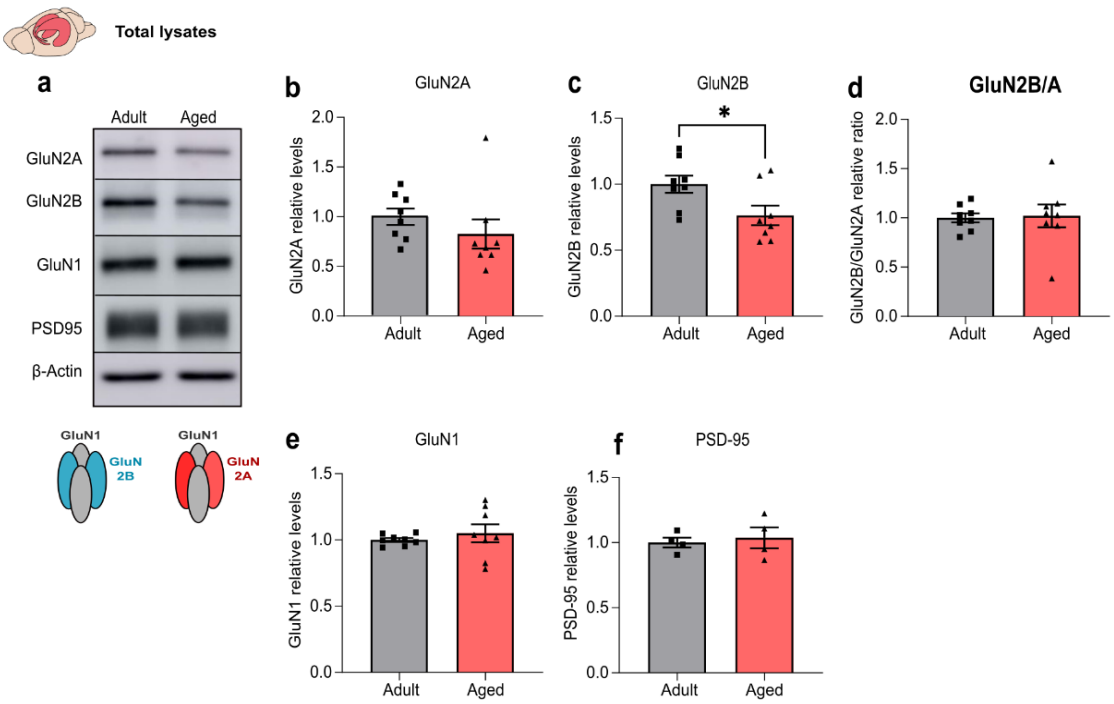

Figure 3.12 – The ratio between GluN2B/GluN2A total levels is maintained upon aging.

a) Representative western of hippocampal lysates from adult (10 – 16 weeks) and aged (18 – 20 months) C57BL/6 wild-type mice. Membranes were immunoblotted with antibodies for GluN2A, GluN2B, GluN1 and β-actin.

b, c, e, f) Results from blots as shown in a) from hippocampal lysates show GluN2A, GluN2B, GluN1 and PSD-95 levels normalized with β-actin. Results are expressed as the mean ± SEM relative to the adult group; b) Mann Whitney test, n=8; c) Unpaired t-test, *p<0.05, n=8; e) Unpaired t-test, n=8; f) Unpaired t-test, n=4.

d) Results from blots as shown in a) from hippocampal lysates show the GluN2B/ GluN2A ratio. Results are expressed as the mean ± SEM relative to the adult group. Unpaired t-test, n=8.

We then confirmed that the GluN2B/GluN2A ratio was also maintained upon aging in PSD-enriched fractions. Accordingly, we found no alterations in the postsynaptic levels of each subunit (GluN2A, GluN2B and GluN1, normalized to PSD-95 content) (**Figure 3.13 a-e**).

Altogether, our results show that the ratio between GluN2B and GluN2A subunit levels is maintained upon aging, both in total lysates, postsynaptic fractions and APP immunoprecipitated samples. Additionally, we found no alterations in the APP-NMDAR

interaction between adult and aged mice. Interfering with the APP C-terminal during a short period (60 min) did not cause alterations in the total NMDAR synaptic currents, indicating that other APP-NMDAR regulatory mechanisms might occur in mature synapses (both adult and aged).

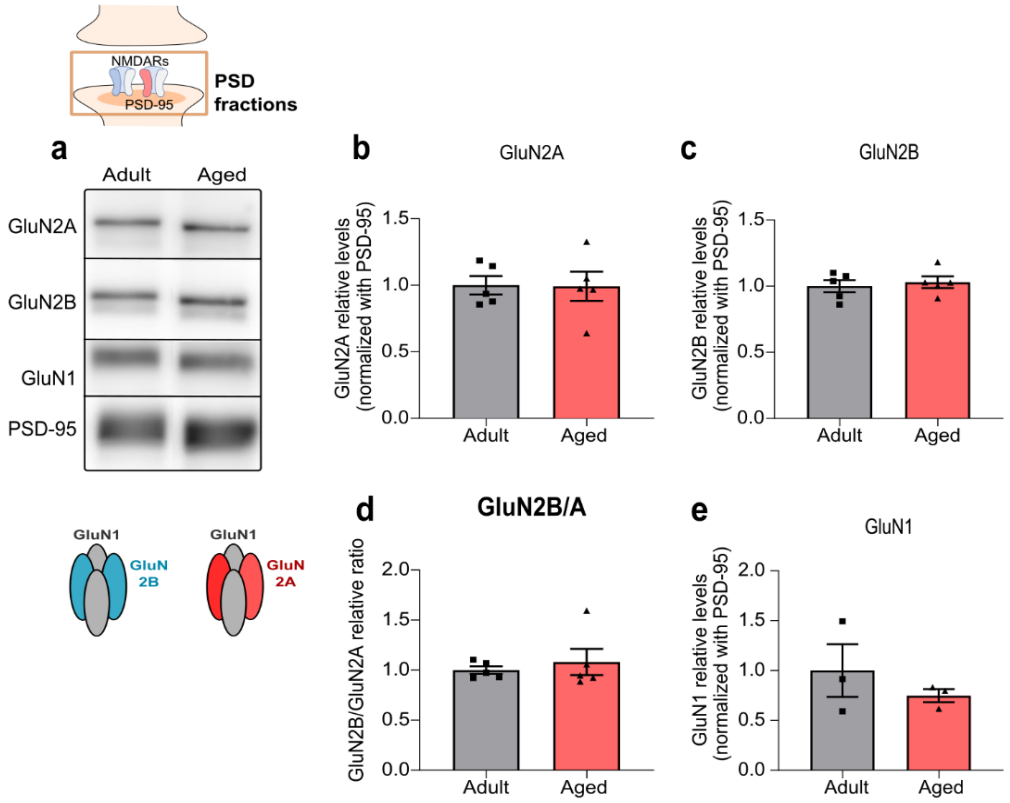

Figure 3.13 – The ratio between GluN2B/GluN2A postsynaptic levels is maintained upon aging.

a) Representative western blot of hippocampal lysates subjected to biochemical fractionation to obtain PSD-enriched fractions from adult (10 – 16 weeks) and aged (18 – 20 months) wild-type C57BL/6 mice. Membranes were immunoblotted with antibodies for GluN2A, GluN2B, GluN1 and PSD-95.

b, c, e) Results from blots as shown in a) from PSD-enriched fractions show GluN2A, GluN2B and GluN1 levels normalized with PSD-95 and are expressed as the mean ± SEM relative to the adult group, Unpaired t-test; b, c) n=5; e) n =3.

d) Results from blots as shown in a) from PSD-enriched fractions show the GluN2B/ GluN2A ratio and are expressed as the mean ± SEM relative to the adult group (Mann Whitney test, n=5).

B) Aged mice exhibit an increase in the relative contribution of GluN2B-NMDAR synaptic currents

Our results indicate that the subunit composition of the NMDARs is similar in adult and aged mice. We thus investigated if there are functional alterations in these receptors, by recording pharmacologically isolated NMDAR excitatory post-synaptic currents (NMDAR EPSCs) in CA1 pyramidal cells in the hippocampus upon electrical stimulation of the Schaffer collaterals (**Figure 3.14 a**).

We found that the relative contribution of GluN2B-NMDAR currents is higher in aged mice (33,11% ± 6,72), when compared to adults (14,20% ± 4,32), as depicted in **Figure 3.14 b-d**. This is accompanied by an increase in τweighted in aged mice (177,0 ms ± 12,66), compared to the reference group of adults (126,3 ms ± 9,11) (**Figure 3.14 e, f**). These results indicate that the NMDAR-mediated currents in aged synapses have a larger contribution of the GluN2B subtype and have slower deactivation kinetics.

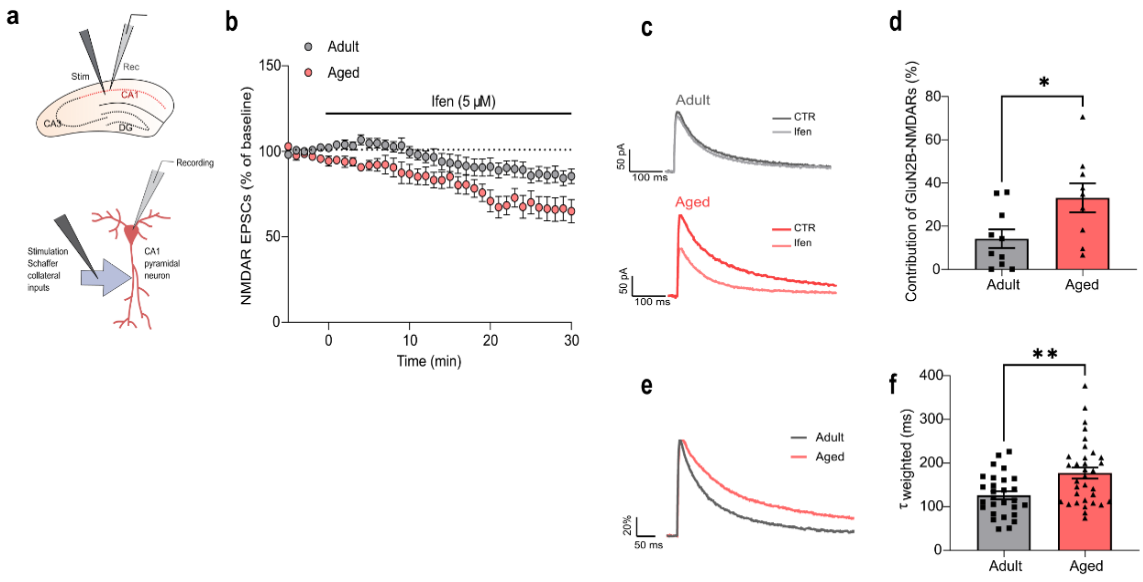

Figure 3.14 - Aged mice exhibit an increase in the relative contribution of GluN2B-NMDAR synaptic currents

a) Schematic diagram showing the locations of stimulating and recording electrodes in the hippocampus and in a CA1 pyramidal neuron for whole cell patch-clamp experiments.

b) Time course of ifenprodil (5μM) effect on pharmacologically isolated NMDAR EPSC amplitude in CA1 pyramidal neurons, measured by whole-cell patch clamp in adult (10 – 16 weeks) and aged (18 – 20 months) C57BL/6 wild-type mice. Results are expressed as the mean ± SEM, n=9-12.

c) Traces show NMDAR EPSCs recorded before (CTR) and after 30 min of Ifenprodil 5 μM perfusion (Ifen).

d) GluN2B contribution was calculated as the percentage of change in NMDAR EPSC amplitude after 30 min of ifenprodil perfusion. Results are expressed as the mean ± SEM (n=9-12). Unpaired t-test *p<0.05, n=9-12.

e) Comparison of representative whole-cell patch-clamp recordings of pharmacologically isolated NMDAR EPSCs, normalized to the peak amplitude (in %) from adult and aged mice, illustrating differences in deactivation kinetics.

f) The weighted time constant ($\tau_{weighted}$) was calculated using the relative contribution of both slow/fast components of NMDAR EPSCs and reflects the overall deactivation kinetics. Results are expressed as the mean ± SEM (Mann-Whitney test, **p<0.01, n=28-33).

Since this increase in GluN2B-NMDAR currents contribution did not correlate with alterations in GluN2B/GluN2A protein levels, we hypothesize that other properties such as stabilization by PSD-95 or the phosphorylation status of GluN2B might be altered upon aging.

Considering that NMDAR synaptic stabilization can be modulated by post-translational modifications of NMDAR subunits (Sanz-Clemente et al., 2013), we assessed whether the GluN2B phosphorylation status was altered upon aging as a possible explanation for the increased GluN2B-NMDAR contribution measured by electrophysiology. We determined the levels of phosphorylated GluN2B (pGluN2B) at the tyrosine 1472 residue (Y1472) since it is known to enhance GluN2B-PSD95 binding (Nakazawa et al., 2001, Prybylowski et al., 2005). However, we found no age-related alterations in the pGluN2B/GluN2B ratio (**Figure 3.15 a, b**). Additionally, by immunoprecipitating PSD-95 and quantifying the levels of co-immunoprecipitated NMDAR subunits, we found that the interaction of GluN2B/GluN2A with PSD-95 was not altered in aged mice (**Figure 3.15 c-f**). suggesting that other mechanisms might be involved.

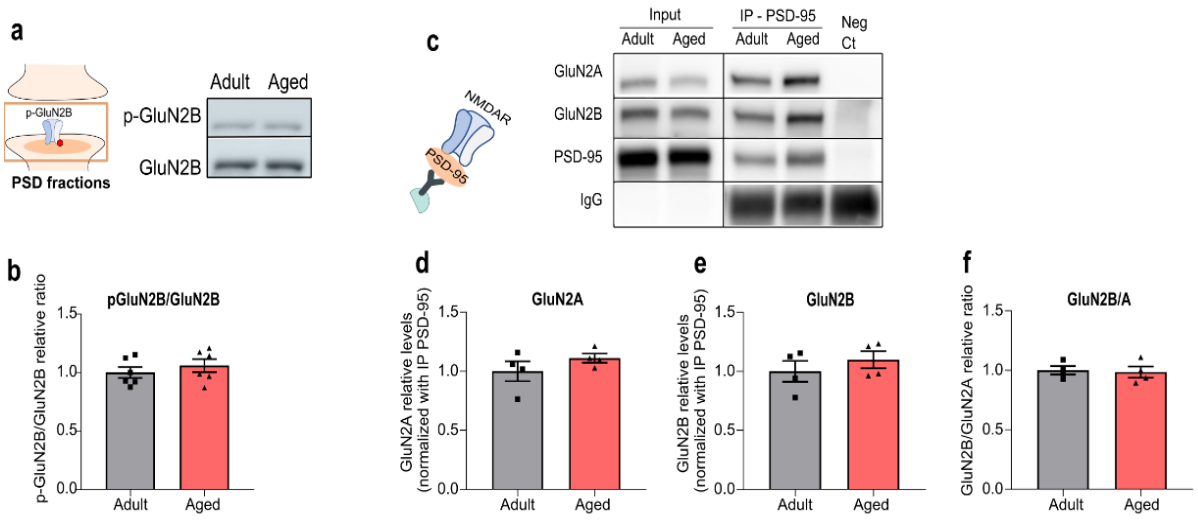

Figure 3.15 – Aged mice do not exhibit alterations in GluN2B Y1472 phosphorylation or NMDAR interaction with PSD-95

a) Representative western blot of hippocampal lysates subjected to biochemical fractionation to obtain PSD-enriched fractions from adult (10 – 16 weeks) and aged (18 – 20 months) wild-type C57BL/6 mice. Membranes were immunoblotted with antibodies for pGluN2B (p-Y1472) and GluN2B.

b) The pGluN2B/GluN2B ratio was quantified in PSD-enriched fractions as shown in a) and expressed as the mean ± SEM relative to the adult group (Unpaired t-test, n=6)

c) Representative western blot of hippocampal lysates from adult and aged C57BL/6 wild-type mice immunoprecipitated for PSD-95. Membranes were immunoblotted with antibodies for GluN2A, GluN2B and PSD-95.

d, e) Results from blots as shown in c) from PSD-95 immunoprecipitated (IP) samples show GluN2B and GluN2A normalized with IP PSD-95 and are expressed as the mean ± SEM relative to the adult group (Unpaired t-test, n=4).

f) Results from blots as shown in c) from PSD-95 immunoprecipitated (IP) samples show the GluN2B / GluN2A ratio and are expressed as the mean ± SEM relative to the adult group (Unpaired t-test, n=4).

C) APP processing contributes to the increase in GluN2B-NMDAR relative currents upon aging

The fact that aged mice exhibit an increase in GluN2B-NMDAR relative currents suggests that the properties of these receptors might be altered. Since the APP interaction with GluN2B is maintained, we hypothesize that other signaling mechanisms, possibly mediated by APP-derived fragments, might be involved. A previous study by our group showed that one of these fragments, the AICD, has the ability to increase the GluN2B-NMDAR synaptic contribution, following a 2h incubation in adult hippocampal slices (Pousinha et al., 2017). Therefore, we investigated if APP levels and processing were altered in aged mice.

We found no alterations in the total and postsynaptic APP levels when comparing adult and aged mice (**Figure 3.16 a-d**). However, we detected a 1.4-fold increase in the absolute levels of CTFs, as well as in relation to APP, in aged mice (**Figure 3.16 c, e, f**), indicating that APP processing increases upon aging. Additionally, we found no statistically significant alterations in the levels of APP intracellular domain (AICD) (**Figure 3.16 c, h, i**).

To elucidate if this increased processing was associated with a specific pathway, we performed an approximate discrimination of the CTFs derived from α-secretase cleavage (CTFα (C83), ≈10KDa) or β-secretase processing (CTFβ (C99), ≈14KDa) based on their molecular weight. Additionally, we used a transgenic mouse model (3xTg-AD, 6 months)

as reference, since this model exhibits a predominant accumulation of CTFβ over the smaller CTFα (Lauritzen et al., 2012) (**Figure 3.16 c**). Using this strategy, we found no statistically significant differences in the CTF β/α ratio upon aging (**Figure 3.16 c, g**).

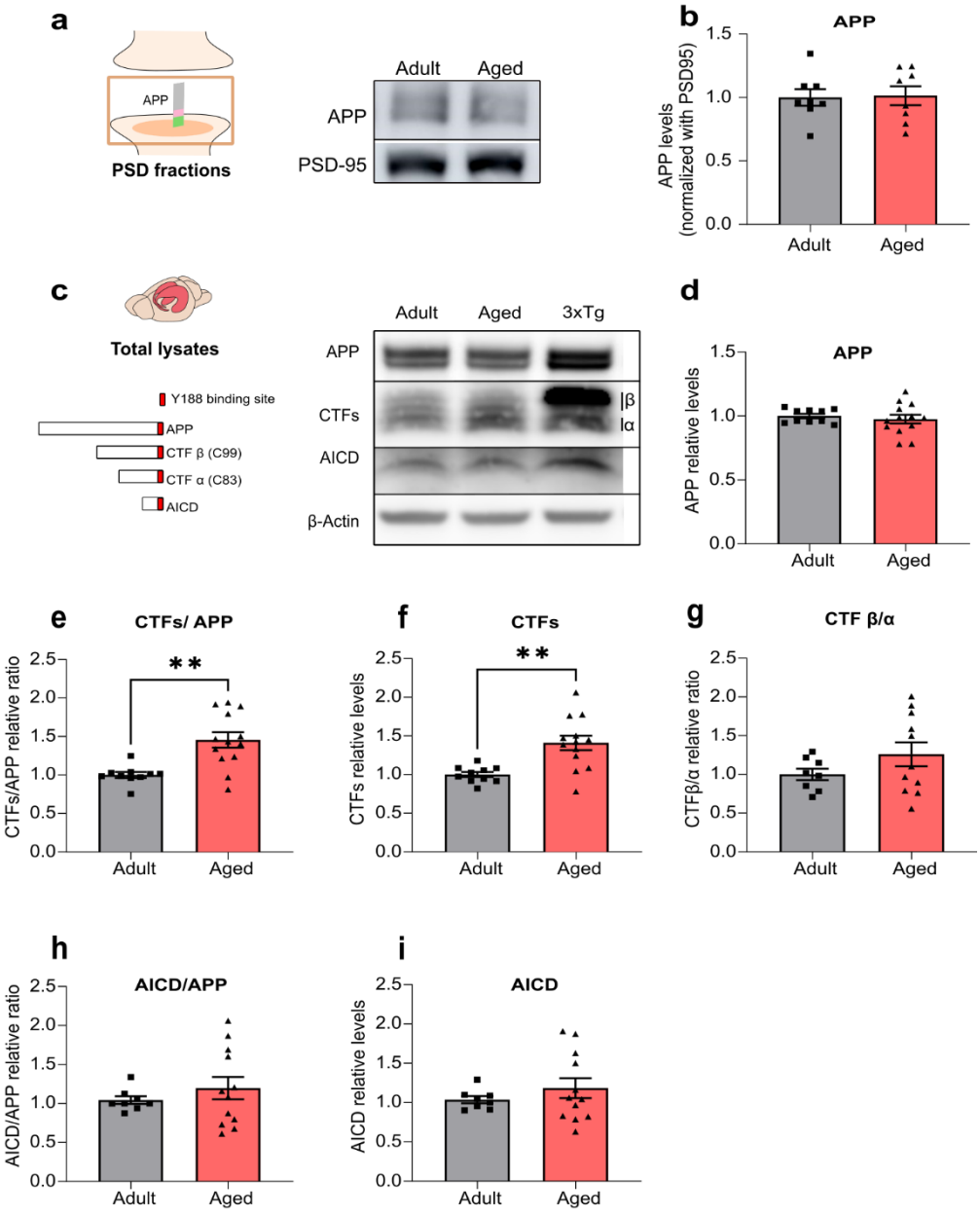

Figure 3.16 – APP processing increases upon aging

a) Representative western blot of hippocampal PSD-enriched fractions from adult (10 – 16 weeks) and aged (18 – 20 months) C57BL/6 wild-type mice. Membranes were immunoblotted with antibodies for APP and PSD-95.

b) Results from blots as shown in a) show the APP levels normalized to PSD-95 and expressed as the mean ± SEM relative to the adult group (n=8).

c) Representative western blot of hippocampal lysates from adult and aged C57BL/6 wild-type mice. Membranes were immunoblotted with antibodies for β-actin as the loading control and for the APP C-terminal

(Y188, to detect APP full-length (APP), APP C-terminal fragments (CTFs β and α) and the APP Intracellular Domain (AICD)). A female triple transgenic mouse (3xTg-AD, 6 months) was used as a positive control for APP-derived fragments. The Y188 antibody binding site is schematically represented in red (on the left).
d) Results from blots shown in c) from mouse hippocampal lysates were normalized with β-actin and are expressed as the mean ± SEM relative to the adult group (Unpaired t-test, n=10-13)
e) Results from blots shown in c) show the ratio between CTFs and APP are expressed as the mean ± SEM relative to the adult group (Mann Whitney test, **p<0.01, n=10-13).
f) Results from blots shown in c) show the levels of CTFs normalized with β-actin and are expressed as the mean ± SEM relative to the adult group (Unpaired t-test, **p<0.01, n=10-13).
g) Results from blots shown in c) show the ratio between CTFβ and CTFα and are expressed as the mean ± SEM relative to the adult group (Unpaired t-test, n=8-11).
h) Results from blots shown in c) from mouse hippocampal lysates were normalized with β-actin and are expressed as the mean ± SEM relative to the adult group (Unpaired t-test, n=8-12)
i) Results from blots shown in c) show the ratio between AICD and APP are expressed as the mean ± SEM relative to the adult group (Unpaired t-test, n=8-12).

Our results point towards a model in which signaling mediated by APP derived fragments might be increased in aged mice, potentially altering the GluN2B-NMDAR properties and increasing their relative currents. Thus, we investigated if inhibiting APP processing could normalize the GluN2B-NMDAR synaptic contribution.

We blocked the APP amyloidogenic pathway in aged mice by inhibiting the β-site APP-cleaving enzyme 1 (BACE 1), as illustrated in **Figure 3.17 a**. This treatment was performed by oral administration of the BACE1 inhibitor (BI, LY2811376 (100mg/kg)), 12h prior to patch-clamp recordings (**Figure 3.17 b**).

We determined the GluN2B-NMDAR contribution by measuring the effect of ifenprodil (5μM) on total NMDAR EPSCs. The BI-treated aged mice showed a significant decrease in GluN2B-NMDAR contribution when compared to the vehicle-treated group (20,07% ± 3,12 vs. 37,95% ± 8,44) (**Figure 3.17 c-e**), reaching similar levels to untreated adult mice (14,20% ± 4,32). These findings suggest that the age-related increase in APP processing contributes to the excessive GluN2B-NMDAR contribution observed at this stage.

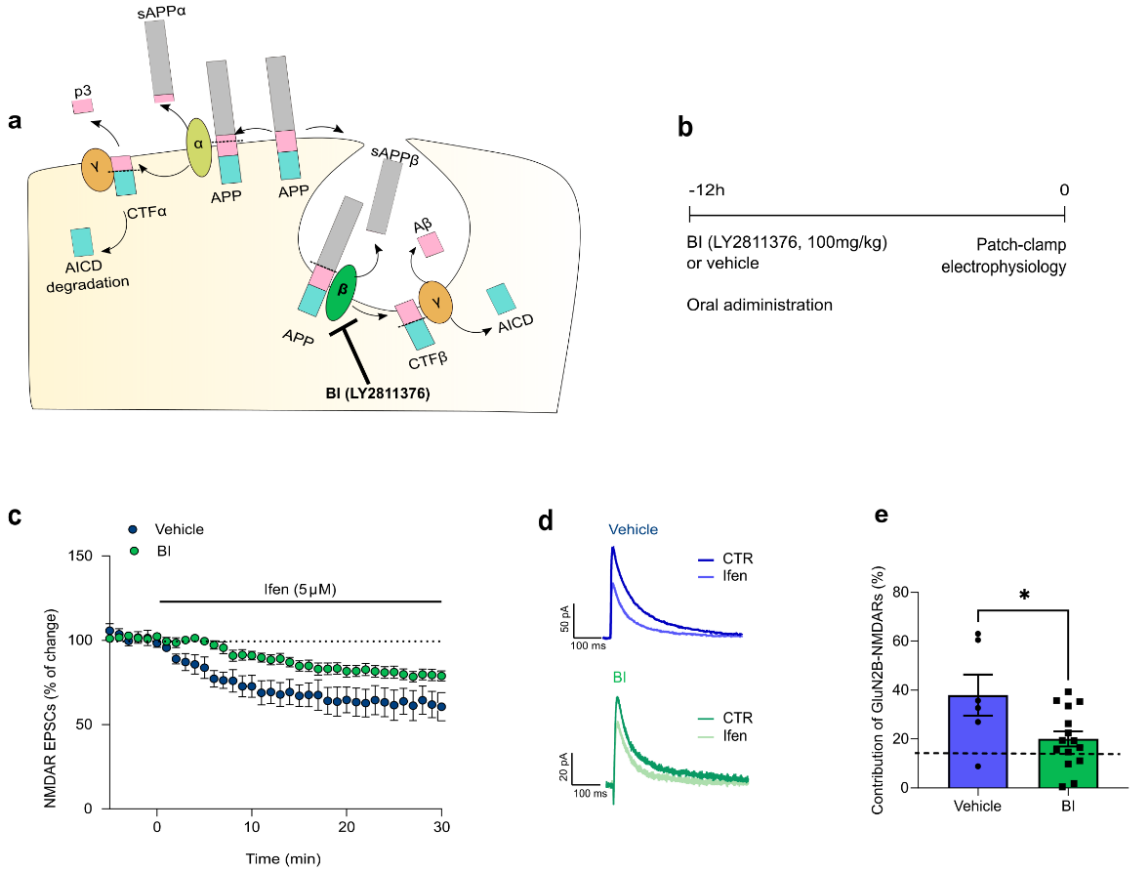

Figure 3.17- Inhibiting APP β-secretase processing normalizes the GluN2B-NMDAR contribution in aged mice

a) Schematic diagram adapted from (Grimm et al., 2013) showing the experimental approach to interfere with APP processing. The the β-site APP-cleaving enzyme 1 (BACE 1) inhibitor (BI) LY2811376 interferes with the APP amyloidogenic processing pathway.

b) Representation of the timeline for treatment of aged mice with vehicle vs. BI (LY2811376, 100mg/kg) 12h prior to patch-clamp recordings.

c) Time course of ifenprodil (5µM) effect on pharmacologically isolated NMDAR EPSC amplitude in CA1 pyramidal neurons, measured by whole-cell patch clamp in aged (18 – 20 months) C57BL/6 wild-type mice (vehicle vs. BI). Results are expressed as the mean ± SEM (n=6-15).

d) Traces show NMDAR EPSCs recorded before (CTR) and after 30 min of Ifenprodil 5 µM perfusion (Ifen).

e) GluN2B-NMDAR contribution was calculated as the percentage of change in NMDAR EPSCs after ifenprodil perfusion (for 30 min) in aged mice (vehicle vs. BI). Results are expressed as the mean ± SEM (Unpaired t-test, *p<0.05, n=6-15). The dashed line corresponds to the GluN2B-NMDAR contribution obtained in untreated adult mice (14,20%).

D) Interfering with APP intracellular signaling normalizes the GluN2B-NMDAR contribution in aged mice

We hypothesize that the increase in the levels of APP C-terminal fragments in aged mice could contribute for a higher contribution of GluN2B-NMDAR synaptic currents. Therefore, we tested the impact of an interfering peptide that is known to bind to the APP intracellular domain. Accordingly, a previous study by our group has implicated the ^{682}YENPTY^{687} sequence of APP in regulating GluN2B-NMDAR contribution (Pousinha et al., 2017). Considering that the PTB2 domain of Fe65 (an APP-binding partner) is known to bind a portion of the APP intracellular domain (including the Y^{682}ENPTY^{687} sequence) (Feilen et al., 2017), we used this domain as a putative interfering peptide (136 amino acids, 15KDa) to block APP intracellular signaling pathways (**Figure 3.18 a**). We used as our control a peptide with another domain of Fe65 (PTB1 domain, PTB1-p), which does not bind to APP (Cao & Sudhof, 2001).

When measuring NMDAR EPSCs in hippocampal slices from aged mice pre-incubated with PTB2-p for >3h (**Figure 3.18 b**), we found that the GluN2B-NMDAR relative contribution decreased when compared to the control condition (13,49 ± 4,08 vs. 39,72 ± 5,13), reaching similar levels to untreated adult mice (14,20% ± 4,32) (**Figure 3.18 c-e**).

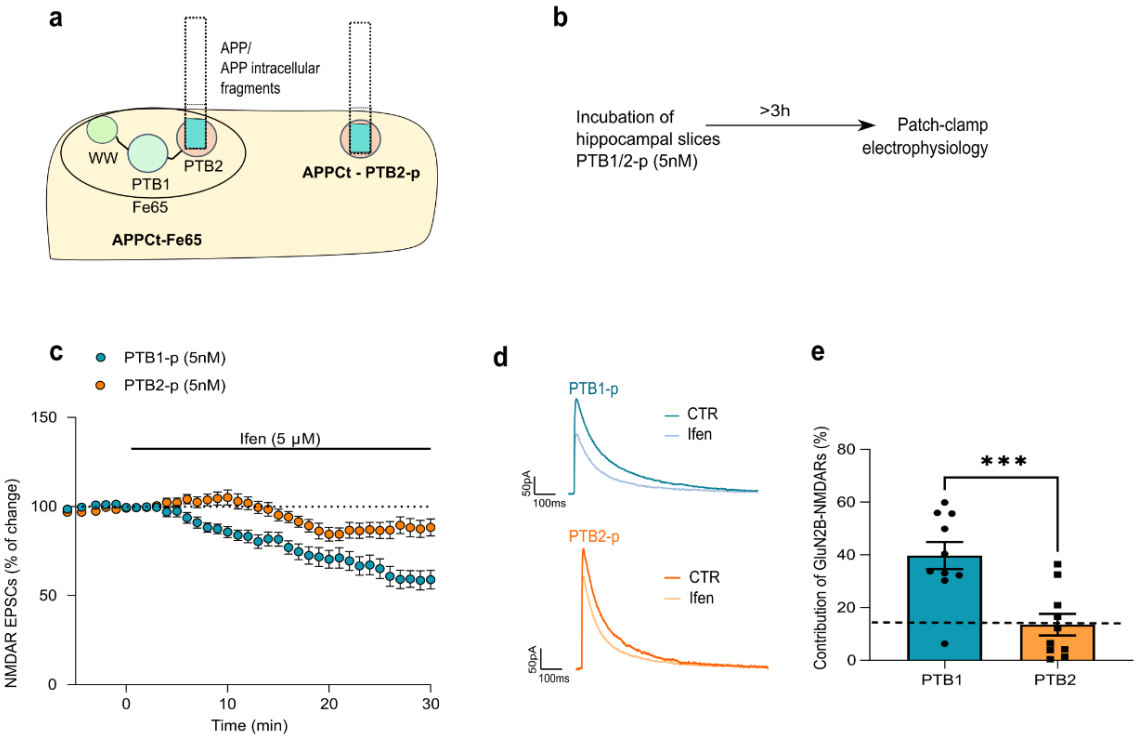

Figure 3.18 - Interfering with APP intracellular signaling normalizes the GluN2B-NMDAR contribution in aged mice

a) Schematic representation showing the Fe65 interaction with the APP C-terminal (APP Ct) domain through the PTB2 domain. The PTB2 peptide (PTB2-p) is proposed to work as an interfering peptide, by binding to the APP Ct.

b) Representation of the timeline for the incubation of hippocampal slices from aged mice with PTB1-p or PTB2-p (5nM, >3h before Patch-Clamp recordings).

c) Time course of ifenprodil (5µM) effect on pharmacologically isolated NMDAR EPSC amplitude in CA1 pyramidal neurons, measured by whole-cell patch clamp in aged (18 – 20 months) C57BL/6 wild-type mice (PTB1-p vs. PTB2-p). Results are expressed as the mean ± SEM (n=10).

d) Traces show NMDAR EPSCs recorded before (CTR) and after 30 min of Ifenprodil 5 µM perfusion (Ifen).

e) GluN2B contribution was calculated as the percentage of change in NMDAR EPSCs after ifenprodil perfusion (for 30 min) in aged mice (PTB1-p vs. PTB2-p). Results are expressed as the mean ± SEM (Unpaired t-test, ***p<0.001, n=10). The dashed line corresponds to the GluN2B-NMDAR contribution registered in untreated adult mice (14,20%).

Importantly, this effect was observed upon incubation with the PTB2-p for >3h, but not for shorter time periods (2h), as shown in **Figure 3.19**.

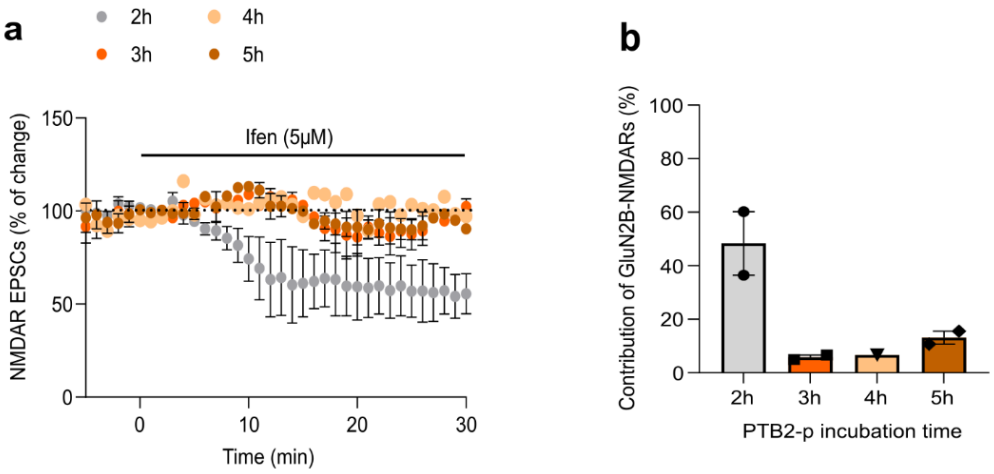

Figure 3.19 – The effect of PTB2-p on GluN2B-NMDARs depends on the incubation time

a) Time course of ifenprodil (5µM) effect on pharmacologically isolated NMDAR EPSC amplitude in CA1 pyramidal neurons, measured by whole-cell patch clamp in in aged (18 – 20 months) C57BL/6 wild-type mice (PTB2-p 5nM incubation for 2, 3, 4 or 5h prior to patch-clamp recordings, n=1-2).

b) GluN2B contribution was calculated as the percentage of change in NMDAR EPSCs after ifenprodil perfusion (for 30 min) in aged mice (PTB2-p incubation (5nM) for 2, 3, 4 or 5h prior to patch-clamp recordings, n=1-2).

Considering that both inhibition of β-APP processing and interference with APP C-terminal had a similar effect in GluN2B-NMDAR contribution in aged mice, we propose that the accumulation of APP intracellular fragments and the activation of the respective signaling pathways is the underlying mechanism for this alteration.

E) APP interacts with NMDARs in humans and tends to be more processed upon aging

To elucidate if APP interaction with NMDARs also occurs in humans, we analyzed lysates from post-mortem brain tissue (prefrontal cortex) of subjects with different ages (18 - 89 years old). We confirmed that GluN2B-NMDARs interact with APP in samples from adult (22 years) and aged (89 years) human subjects (**Figure 3.20 a**), indicating that the putative regulation mechanism described in mice might also occur in humans. When analyzing total lysates, we found no correlation between age and GluN2B or PSD-95 levels (**Figure 3.20 b-d**). Similarly, no age-related correlation was observed for the levels of GluN2B in PSD-enriched fractions (**Figure 3.20 e, f**). This data corroborates our hypothesis that there might be alterations in NMDAR functional properties, whereas their synaptic levels are maintained upon aging.

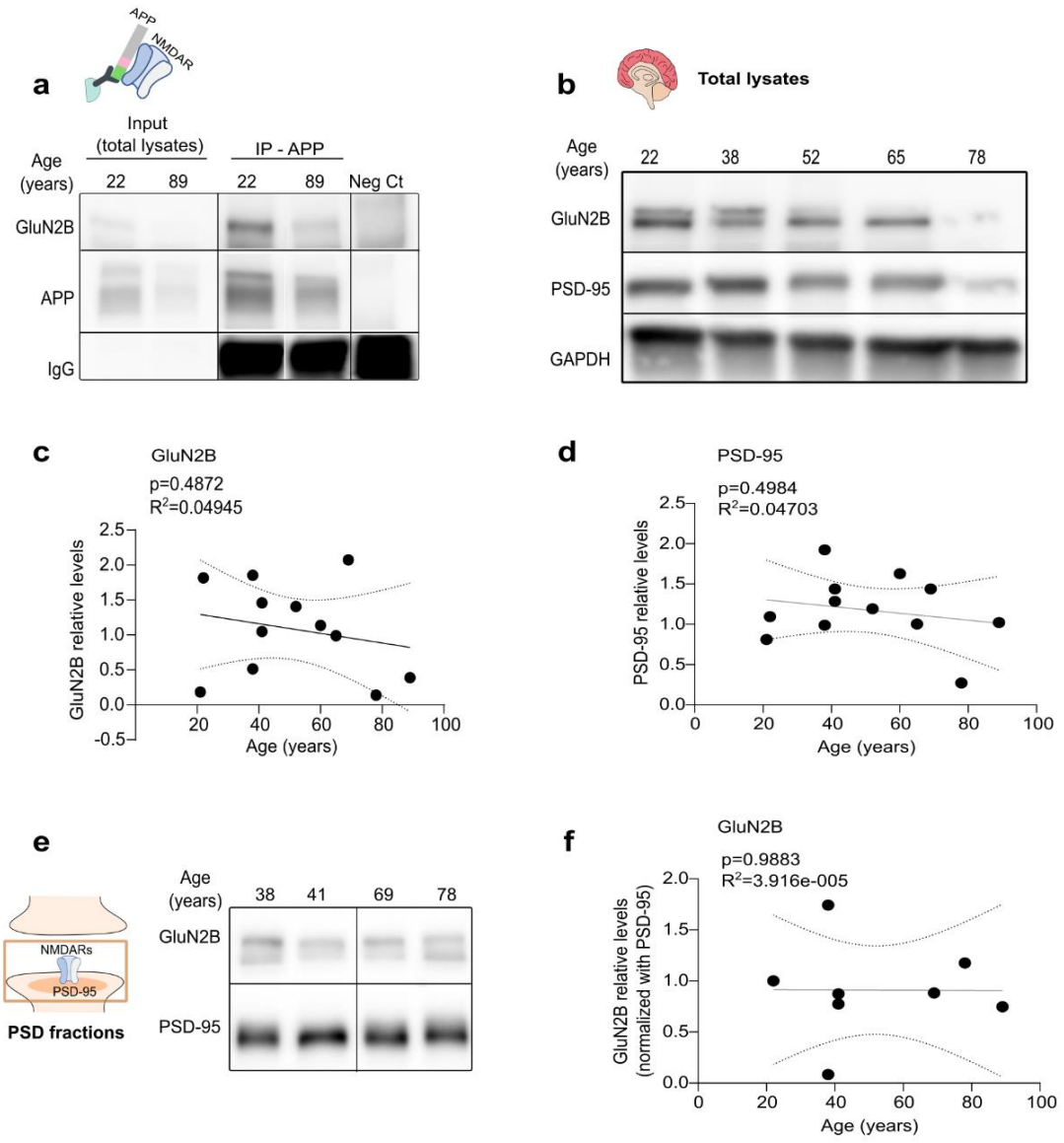

Figure 3.20 – NMDARs interact with APP in humans and show no alterations in GluN2B levels upon aging.

a) Representative Western blot of postmortem brain tissue (prefrontal cortex) from human subjects (adult = 22 and aged = 89 years old) immunoprecipitated for APP. Membranes were immunoblotted with antibodies for GluN2B and APP.

b) Representative western blot of prefrontal cortex human samples (21 to 89 years old). Membranes were immunoblotted with antibodies for GluN2B, PSD-95 and GAPDH.

c, d) Linear regression graphs calculated from blots as shown in b) show the variation in c) GluN2B and d) PSD-95 levels (normalized with GAPDH) depending on the age of human subjects (n=12). Dotted lines represent the 95% confidence intervals. The values obtained for 20–25-year-old subjects were used as reference. Statistical analysis was performed using Pearson's correlation (two-tailed p value). c) p=0.4872, R^2=0.04945; d) p=0.4984, R^2=0.04703.

e) Representative western blot of prefrontal cortex human samples (21 to 89 years old) subjected to biochemical fractionation to obtain PSD-enriched fractions. Membranes were immunoblotted with antibodies for GluN2B and PSD-95.

f) Linear regression graph calculated from blots of PSD-enriched fractions as shown in e) shows the variation in GluN2B levels (normalized with PSD-95) depending on the age of human subjects (n=8). Statistical analysis was performed using Pearson's correlation (two-tailed p value), p=0.9883, R^2=3.916e-005. Dotted lines represent the 95% confidence intervals. The values obtained for 20–25-year-old subjects were used as reference.

We then investigated if APP levels/processing are altered upon aging in humans, possibly interfering with GluN2B-NMDAR properties. We found an inverse correlation between age and APP levels (**Figure 3.21 a, b**), and a positive correlation in APP processing into CTFs and AICD (**Figure 3.21 a, c, f**). Additionally, we observed an increase in the absolute levels of AICD, whereas no correlation was obtained for total CTF levels or for the CTF β/α ratio (**Figure 3.21 d, e, g**).

These findings indicate that the mechanisms observed in mice could also occur in humans, since APP interacts with NMDARs in both species. We found no age-related alterations in GluN2B synaptic levels in humans and mice, indicating that other properties might be altered, contributing to the increase in GluN2B-NMDAR synaptic contribution observed in mice. Finally, the increase in APP processing occurs in both species and has shown to contribute to increased GluN2B-NMDAR relative currents in mice, thus suggesting that a similar mechanism might potentially occur in humans.

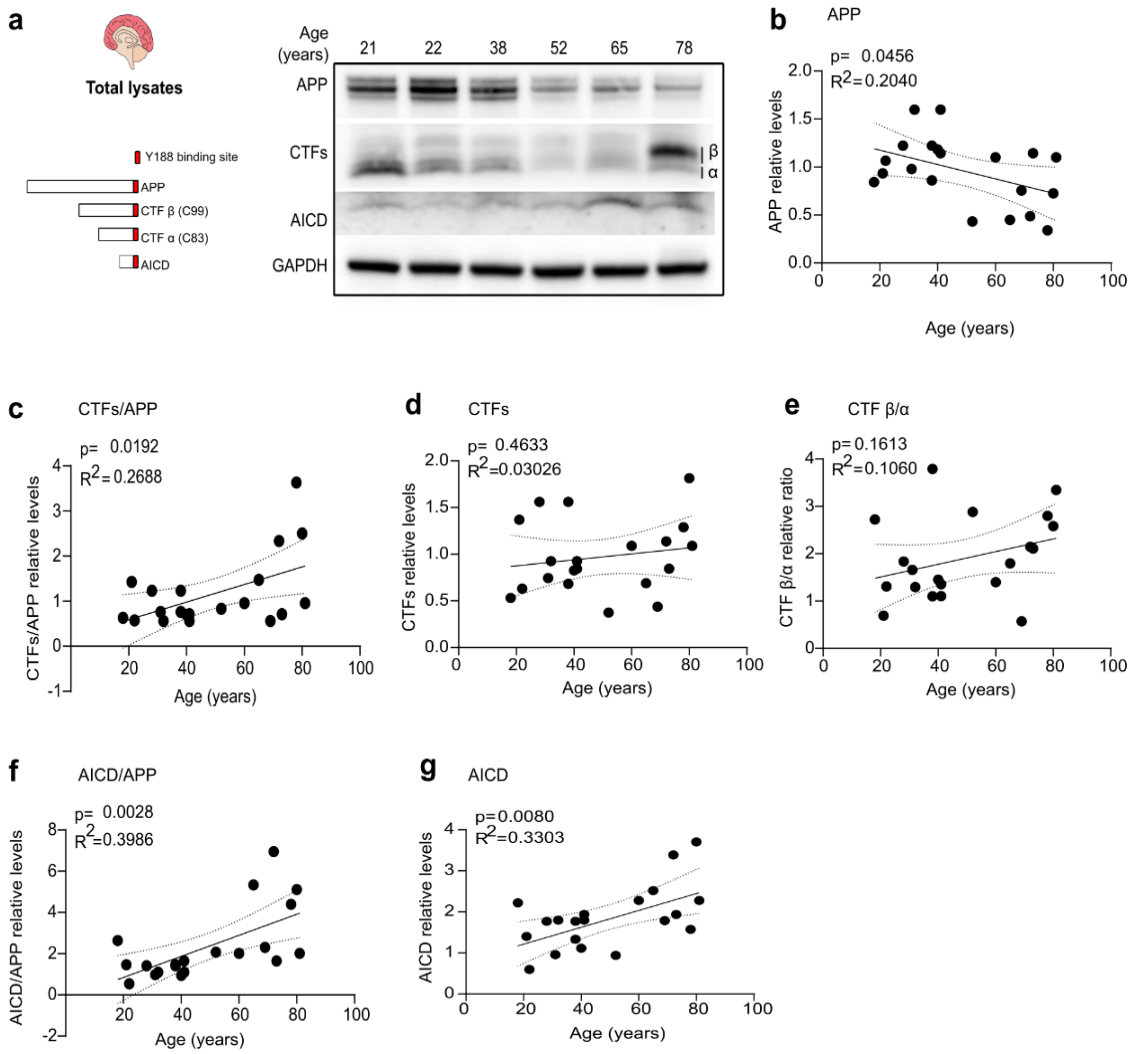

Figure 3.21 – APP processing tends to increase upon aging in humans

a) Representative Western blot of prefrontal cortex human samples (18 to 81 years old). Membranes were immunoblotted with antibodies for GAPDH as the loading control and for the APP C-terminal (Y188, to detect APP, CTFs β and α, and AICD). The Y188 antibody binding site is schematically represented in red (on the left).

b - g) Linear regression graphs calculated from blots as shown in a). Statistical analysis was performed using Pearson's correlation (two-tailed p-value), n=20 and dotted lines represent the 95% confidence intervals. The values obtained for 20–25-year-old subjects were used as reference. b) APP levels (normalized to GAPDH) depending on the age of human subjects, p = 0.0456, R^2 = 0.204; c) Ratio between APP-CTFs and APP depending on the age of human subjects, p = 0.0192, R^2 = 0.2688; d), CTFs levels (normalized to GAPDH) depending on the age of human subjects, p = 0.4633, R^2 =0.03026; e) CTF β/α ratio depending on the age of human subjects, p= 0.1613, R^2= 0.1060; f) Ratio between AICD and APP depending on the age of human subjects, p = 0.0028, R^2 = 0.3986; g) AICD levels (normalized to GAPDH) depending on the age of human subjects, p = 0.0080, R^2 = 0.3303.

Altogether, our results point towards a model in which APP increased processing upon aging in mice and humans favors APP signaling through its intracellular fragments. By activating putative signaling pathways, these fragments have shown to contribute to an increase in GluN2B-NMDAR relative currents in aged mice. Accordingly, we were able to restore the GluN2B-NMDAR contribution to adult-like levels in mice by inhibiting APP processing or interfering with APP intracellular signaling.

3.3 Summary

In this work we show that APP regulates NMDARs in an age-dependent manner, acting through different mechanisms during postnatal development, adulthood and aging.

During synaptic maturation stages, APP and GluN2B-NMDARs are highly abundant and interact at the synapse. The APP C-terminal, which likely acts as the binding site, proved to be essential to maintain normal NMDAR transmission, possibly by stabilizing the receptors at the synapse. Accordingly, APP-depleted neurons showed a reduction in the synaptic content of NMDAR subunits. Considering the role of NMDARs in synapse maturation, we can hypothesize that the APP-NMDAR regulation at this stage might be important to achieve functional and mature synapses during postnatal development.

Although this interaction is maintained in adult and aged synapses, NMDAR-mediated currents showed to be unaltered at these stages when interfering with the APP C-terminal during a short period of time (1h). Thus, we concluded that the APP-NMDAR regulatory mechanisms are different in adult/aged mice when compared to infants.

We hypothesize that alterations in the APP-NMDAR regulation mechanisms could be the underlying mechanism for age-related alterations in NMDAR properties. Accordingly, we found that aged mice exhibit an increase in GluN2B-NMDAR relative currents, which does not correlate with alterations in subunit levels. We propose that APP intracellular fragments, whose levels tend to increase in aged mice, activate signaling pathways that ultimately lead to increased GluN2B-NMDAR relative currents. Accordingly, we were able to normalize the GluN2B-NMDAR contribution in aged mice (to adult-like levels) using two distinct strategies: inhibiting APP processing or interfering with APP intracellular signaling. Finally, the fact that APP processing also tends to increase with human aging suggests that a similar mechanism might occur in mice and humans. Considering the impact of NMDARs on synaptic plasticity, this increase in GluN2B-NMDAR relative currents might potentially contribute to age-related synaptic and memory impairments.

The main findings of our work are illustrated in **Figure 3.22.**

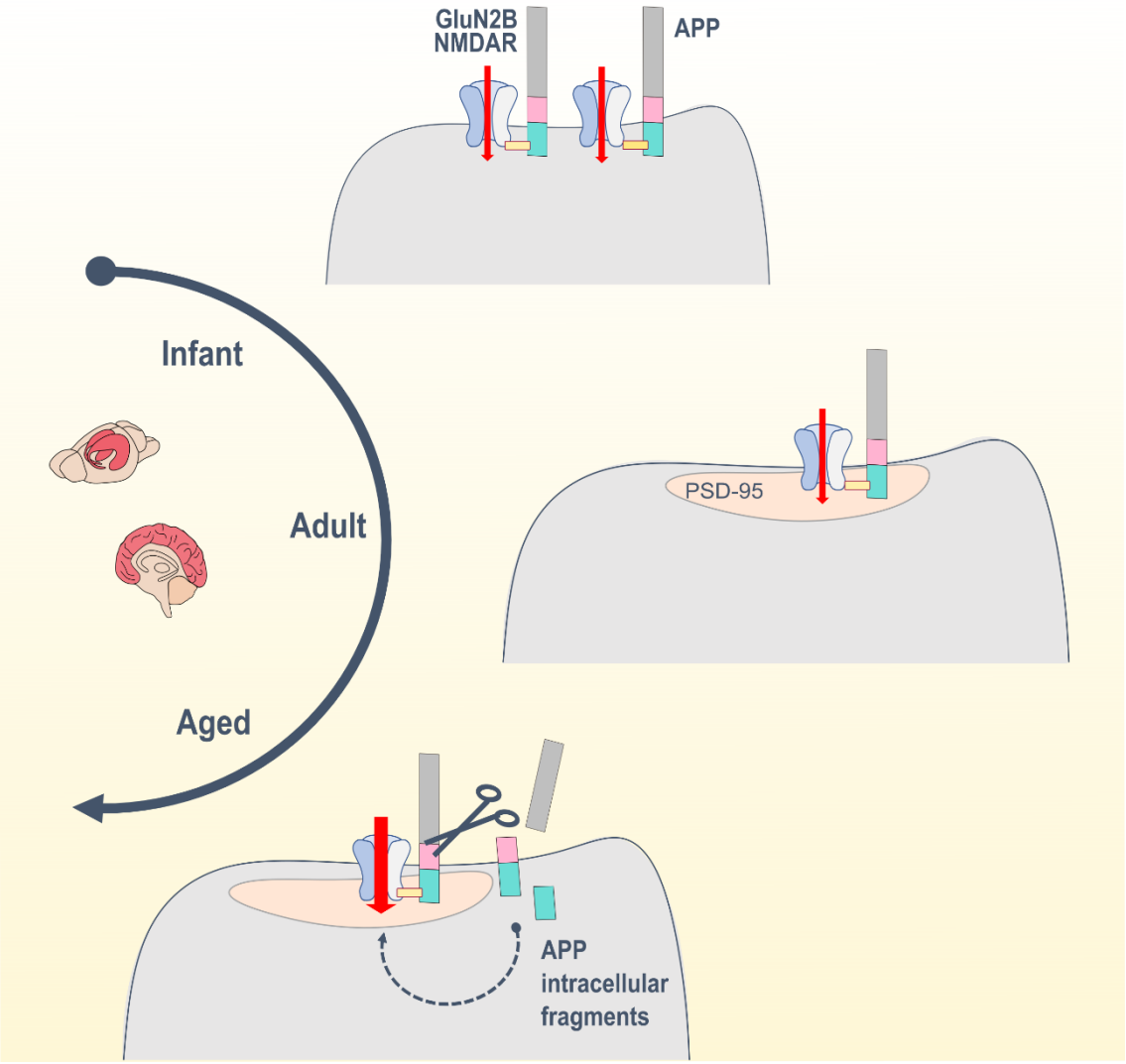

Figure 3.22 – Schematic representation of GluN2B-NMDAR regulation by APP at different life stages (development, adulthood and aging).

3.4 Supplementary Results

In this section we present results obtained during the PhD that are not part of the core of this dissertation, but are useful for the discussion and future perspectives of this work.

A) Prediction of aminoacid disorder in the structure of APP and NMDAR subunits

We hypothesize that APP interacts with NMDARs through the C-terminal, since a previous report by other group has shown that the AICD is able to increase GluN2B-NMDAR synaptic contribution (Pousinha et al., 2017). We found that the C-terminal domains in APP and NMDAR subunits do not have a defined 3D structure, explaining why it was not possible to create a structural model of interaction using docking models. We obtained a computer prediction using the prDOS algorithm, which is a server that predicts the disordered regions of a protein from its amino acid sequence. Based on this, we could identify several unstructured segments in mouse and human APP, GluN1, GluN2A and GluN2B aminoacid sequences (**Supplementary Figure 3.1 a, b**). These disordered segments might potentially work as binding sites for the APP-NMDAR interaction.

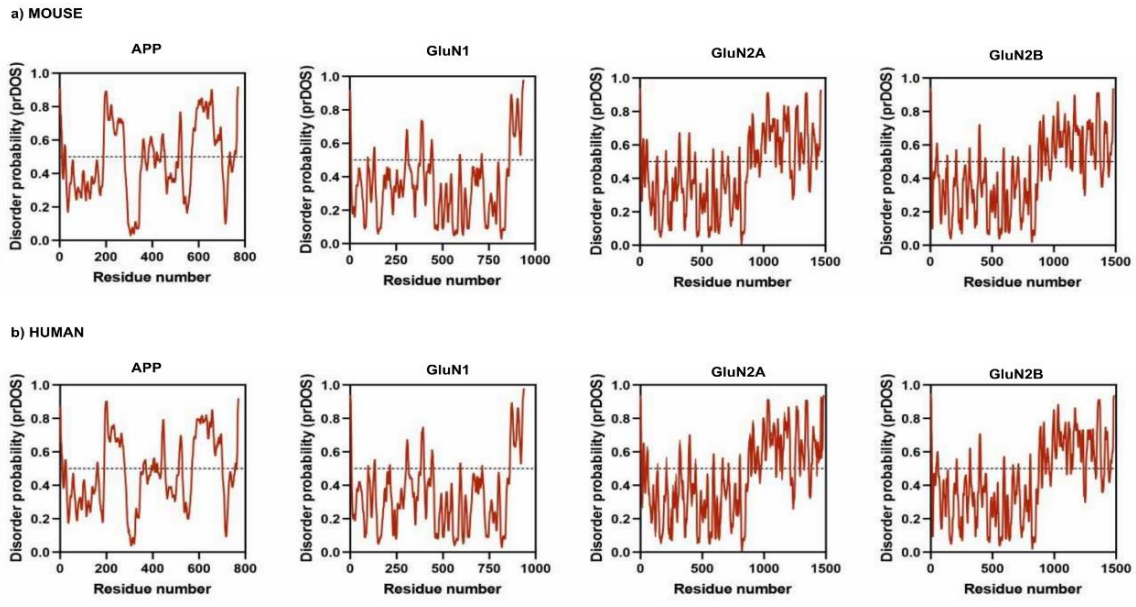

Supplementary Figure 3.1 - Computer prediction of aminoacid disorder in the structure of the **a)** mouse and **b)** human APP, GluN1B, GluN2A and GluN2B subunits by the prDOS algorithm (T. Ishida & Kinoshita, 2007)

The dashed line represents the threshold for disordered segments. The prediction determined the presence of unstructured segments in the C-terminal region of the mouse APP protein. In the case of the NMDAR protein subunits, GluN1, GluN2A and GluN2B are well structured proteins in the N-terminal domain (corresponding to the extracellular and membrane-spanning segments of the protein), whereas they show a strong disorder probability in their C-terminal domains.

B) Transcriptional effects of AICD in primary neuronal cultures

AICD is considered a transcription regulator (Cao & Sudhof, 2001), which has shown to modulate GluN2B-NMDAR levels and currents upon viral delivery in adult rats (Pousinha et al., 2017). Thus, we assessed whether AICD *ex vivo* delivery (for 2h) is able to induce an increase in GRIN2B mRNA levels in rodent primary neuronal cultures.

To study this hypothesis, we used mouse hippocampal primary neuronal cultures as our model. At 15 days *in vitro* (DIV), we incubated the neurons with an AICD peptide coupled to a cell penetrating domain (TAT) and a nuclear localization sequence (NLS) (TAT-AICD-NLS). We used a scramble sequence (TAT-SCR-NLS) as the control condition, as previously described (Pousinha et al., 2017). After incubating the neurons with the peptides for 2h at a final concentration of 100nM (**Supplementary Figure 3.2 a**), we assessed whether the AICD peptide was located in the nucleus.

For that purpose, we analyzed nuclear protein fractions and detected a strong increase in AICD levels (when compared to the control condition) (**Supplementary Figure 3.2 b**). This observation was supported by immunocytochemistry experiments, in which we detected a strong overlap between AICD and nuclear staining (**Supplementary Figure 3.2 c**).

We then evaluated the impact of this treatment on the mRNA levels of GRIN2B and other previously described AICD targets: Glycogen synthase kinase 3β (GSK3β) (Kim et al., 2003) and Low-density lipoprotein receptor-related protein 1 (LRP1) (Q. Liu et al., 2007). However, we found no significant alterations in the expression levels of these targets (**Supplementary Figure 3.2 d-f**).

Using this experimental model, dose and timing of incubation, we could not detect GRIN2B transcriptional alterations, in contrast with the results obtained in adult rats injected with viral vectors encoding for AICD. Thus, differences in the duration of treatment (acute vs. chronic increased AICD levels) or in the experimental model (primary neuronal cultures vs. adult rats) might explain these differences.

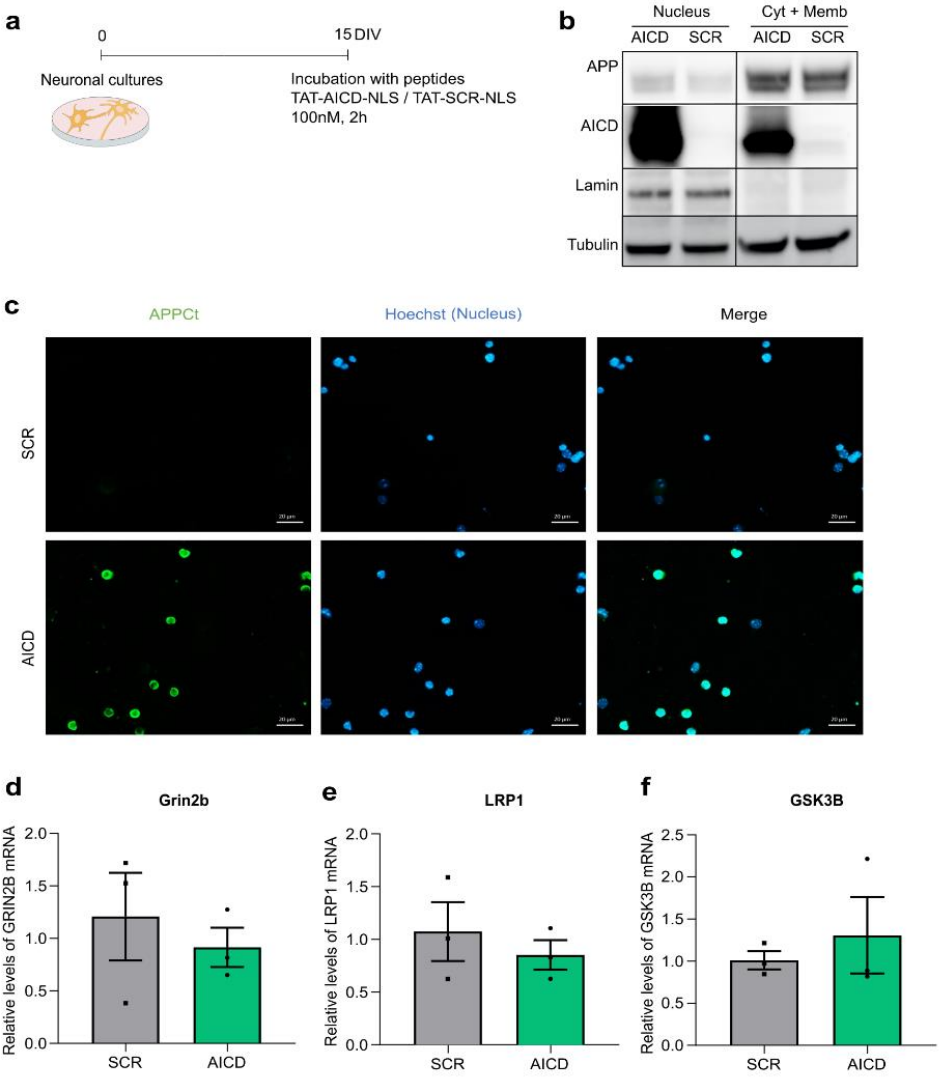

Supplementary Figure 3.2 - Transcriptional effects of AICD in primary neuronal cultures

a) Schematic representation of the incubation of mouse hippocampal primary neuronal cultures (15 days *in vitro* (DIV)) with TAT-AICD-NLS or TAT-SCR-NLS (100nM, 2h).

b) Representative Western Blot of nuclear and cytosolic/membrane protein fractions from primary neurons incubated with TAT-AICD-NLS (AICD) or TAT-SCR-NLS (SCR). Membranes were immunoblotted with antibodies for the APP C-terminal (to detect APP (APP) and the APP Intracellular Domain (AICD), for Lamin (nuclear marker) and α-tubulin.

c) Immunocytochemistry analysis of neuronal cultures treated with TAT-SCR-NLS or TAT-AICD-NLS (100nM, for 2h). AICD was detected with an antibody por the APP C-terminal (APP Ct) and is labeled in green, whereas cell nuclei (Hoechst) are stained in blue. Scale bars represent 20 µm.

d, e, f) Relative expression levels of GRIN2B, LRP1 and GSK3β mRNA were determined by quantitative real-time PCR. Results are expressed as the mean ± SEM relative to the control condition (SCR). CypA and Rpl13A were used as internal controls for normalization. Unpaired t-test, n=3.

C) Production and validation of a viral vector to knockdown APP *in vivo*

Our results indicate that APP regulates NMDARs in an age-dependent manner. Thus, APP knockdown might be a useful strategy to fully understand the APP physiological role in synapses at different ages, since it potentially overcomes compensatory mechanisms by APP family members (observed in knockout models) and might be induced at different ages. Taking this into account, we have developed a new viral vector to induce APP knockdown *in vivo,* by designing and producing an adeno-associated virus (AAV1/2) encoding for a shRNA against APP (previously validated in (Young-Pearse et al., 2007)) under the control of a U6 promoter and using mCherry as reporter (AAV-shAPP). When injecting these viral vectors in the hippocampus of adult (10 – 16 weeks) C57BL/6 wild-type mice and analyzing mCherry expression 3 weeks post-injection, we have detected an efficient viral transduction in the hippocampus (**Supplementary Figure 3.3 a**). Moreover, we measured the APP knockdown efficiency by comparing the APP mean fluorescence intensity in mCherry positive (transduced) or negative (non-transduced) cells, having found an approximately 70% reduction in APP levels in transduced cells (**Supplementary Figure 3.3 b, c**). Thus, this new viral vector proved to efficiently induce APP knockdown in adult mice and might be used in the future to study APP physiological functions at different ages.

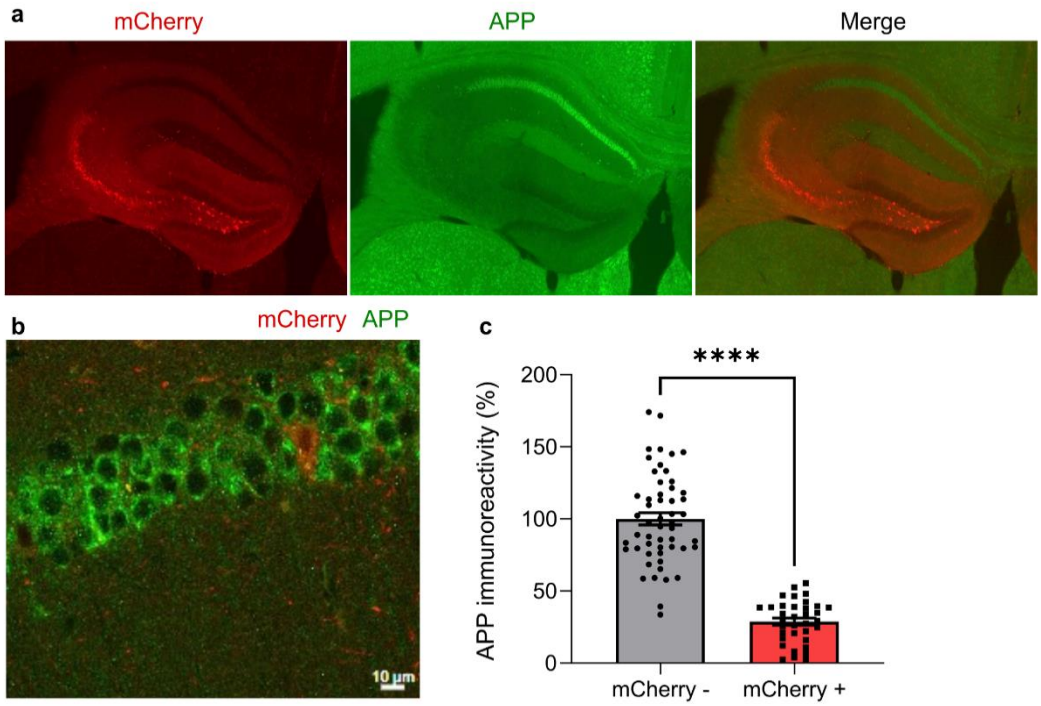

Supplementary Figure 3.3 – AAV-shAPP injection in adult mice leads to an efficient APP knockdown

a) Representative images of hippocampal slices from adult (10 – 16 weeks) C57BL/6 wild-type mice, 3 weeks after injecting AAV-shAPP in the hippocampus. mCherry (reporter) is shown in red and APP is labelled in green.

b) Representative images of hippocampal slices from adult (10 – 16 weeks) C57BL/6 wild-type mice, 3 weeks after injecting AAV-shAPP in the hippocampus. APP is labelled in green and mCherry (reporter) is shown in red, allowing to differentiate transfected from non- transfected neurons.

c) APP immunoreactivity (%) in transfected neurons (mCherry+) is expressed as the mean ± SEM, using the non-transfected neurons (mCherry -) as reference (Unpaired t test, ****$p<0.0001$, n=35-53 cells).

4 Conclusions

4.1 Discussion

Brain plasticity is what make us able to adapt, learn new skills and form memories, being essential throughout our life, but acting through different mechanisms depending on our age (Costandi, 2016). The structural plasticity processes that occur during early development are essential to form synapses, leading to the establishment of neuronal networks (Huttenlocher & Dabholkar, 1997). This is followed by the synaptic maturation stage, in which part of the newly formed synapses are selected for stabilization, leading to functional networks (Huttenlocher et al., 1982). In contrast, in adult stages, most synapses are already in the mature state, thus the synaptic plasticity mechanisms mainly involve the potentiation or depression of preexisting synapses (Citri & Malenka, 2008).

By acting as coincidence detectors of pre and postsynaptic activity, NMDARs act as important mediators of synaptic maturation during development and synaptic plasticity in adult stages (Pérez-Otaño & Ehlers, 2004). Importantly, age-related differences in NMDAR properties might occur due to alterations in the subunit composition. In the hippocampus, NMDARs contain GluN1 obligatory subnits and GluN2A and/or GluN2B regulatory subunits (Monyer et al., 1994). NMDARs with GluN2B subunits are characterized by higher Ca^{2+} entry, slower kinetics, higher mobility and a lower threshold to induce potentiation, when compared to GluN2A-NMDARs (Yashiro & Philpot, 2008). Therefore, GluN2B-rich synapses are expected to be more susceptible to potentiation (even upon modest stimulation) and more dynamic, considering the movement of receptors in and out of the synapse, being particularly relevant in newly formed synapses to promote their maturation process. In contrast, GluN2A-NMDARs are the predominant subtype in mature synapses, leading to a higher stability and assuring that potentiation only occurs upon strong stimulation (Williams et al., 1993, Yashiro & Philpot, 2008).

Thus, deciphering the multiple mechanisms that regulate NMDAR properties is essential to fully understand synaptic maturation and plasticity processes and how they change throughout life. The amyloid precursor protein has emerged as a potential NMDAR regulator, given its ability to regulate NMDARs (through the full-length protein and/or its derived fragments) (Pousinha et al., 2017, Cousins et al., 2009, Hoe et al., 2009) and its important role in NMDAR-dependent processes, such as the formation of new synapses and synaptic plasticity (U. C. Müller et al., 2017). However, the relevance and underlying mechanisms of APP-NMDAR regulation at different life stages have not been explored so far.

Since APP is known to be important during development, namely by working as a synaptogenic and synaptic adhesion molecule (Z. Wang et al., 2009), we started by investigating the role of APP-NMDAR regulation in immature synapses. One of the important steps in synaptic maturation is the recruitment of scaffolding proteins such as PSD-95 that bind and stabilize NMDARs at the synapse (Elias et al., 2008). In contrast, the mechanisms that anchor NMDARs in newly formed synapses (before maturation) are still largely unknown. Synaptic adhesion molecules are strong candidates for this function since they are abundant in new synaptic contact sites and are able recruit pre- and post-synaptic components (Dalva et al., 2007). In particular, APP has emerged as a potential stabilizer, since it accumulates at synaptic terminals (Kirazov et al., 2001), where pre- and post-synaptic APP form trans-dimers contributing to synaptic adhesion and synaptogenesis (Soba et al., 2005), namely by inducing the clustering of synaptic components (K. J. Lee et al., 2010). One of these components might be the NMDARs, which are known to interact with APP (Cousins et al., 2009, Hoe et al., 2009).

Therefore, we explored the functional relevance of APP-NMDAR interaction in immature and mature synapses using wild-type infant and adult mice as our models. Importantly, we found that APP interacts with NMDARs at the synapse, mainly with GluN2B in immature synapses and with both GluN2A and GluN2B in mature synapses (**Figure 3.1**). Additional co-immunoprecipitation experiments will be important to further characterize this interaction and confirm if it occurs through the full-length APP protein or/and through their intracellular fragments. Moreover, future studies using proximity ligation assay (Lundgren et al., 2020), electron microscopy and array tomography (Kay et al., 2013) in hippocampal samples will be valuable to confirm that NMDARs and APP are in close proximity at the synapse.

In this study, we showed that APP interacts with the NMDAR synaptic pool that is expressed at each life stage. NMDARs are mainly composed of GluN2B subunits in infant mice, as evidenced by the peak in the GluN2B/GluN2A ratio (**Figure 3.2 and 3.3 d**) as well as the high GluN2B-NMDAR contribution to NMDAR EPSCs (more than 50%) (**Figure 3.4 d**). Importantly, this data is in accordance with the previously described NMDAR developmental switch (GluN2B to GluN2A) that occurs during postnatal development (Williams et al., 1993). In contrast, adult mice are characterized by a lower GluN2B/A ratio, mainly associated with an increase in GluN2A expression. We can hypothesize that this predominance of GluN2B-NMDARs during development is important to facilitate the LTP-like response involved in synaptic maturation (Gray et al., 2011). In contrast, the shift to GluN2A in mature synapses might lead to more stable

synapses, with a lower threshold for potentiation, in adult stages (Yashiro & Philpot, 2008) .

Importantly, we now show that the peak of GluN2B-NMDAR contribution observed in infant mice is accompanied by peak in APP post-synaptic levels (**Figure 3.5 f**). This is consistent with the putative role of APP in stabilizing and recruiting synaptic components to newly formed synapses (K. J. Lee et al., 2010).

The APP function as a synaptic adhesion molecule is known to depend on both N- and C-terminal domains (Z. Wang et al., 2009). The N-terminal of APP is important to form trans-dimers at the synapse, leading to synaptic adhesion (Hoefgen et al., 2014), whereas the C-terminal could potentially work as the binding site for synaptic components (U. C. Müller et al., 2017), such as NMDARs. Thus, we investigated if interfering with the APP C-terminal could disrupt NMDAR-mediated currents in infant mice. Importantly, when we introduced an antibody against the APP C-terminal in the intracellular space via the patch pipette, we were able to induce a 20% reduction in NMDAR-mediated currents in infant mice (**Figure 3.6 d**).

Since the C-terminal domain of APP and NMDARs subunits present no stable 3D structure, it was not possible to generate a structural model of the APP-NMDAR interaction using docking methods. Accordingly, the analysis of the protein organization level revealed that APP and NMDAR subunits present intrinsically disordered segments at the C-terminal (**Supplementary Figure 3.1**). These disordered segments are usually characterized by establishing interactions with diverse partners, since the flexible segments can adapt themselves by induced folding to different targets (Wright & Dyson, 2015). In particular, the APP YENPTY motif is a strong candidate for the interaction, being highly conserved within the APP family members and across species (Shariati & de Strooper, 2013) and known to interact with several proteins (van der Kant & Goldstein, 2015). It is thus conceivable that it could act as the interacting site for NMDARs either directly or indirectly.

Many of the already characterized interactions between intrinsically disordered segments are transient and fine-tuned by post-translational modifications (Wright & Dyson, 2015). Thus, we can hypothesize that the APP-NMDAR interaction is dynamic and regulated by synaptic activity. One possible mechanism to regulate this interaction would be through the balance between APP dimerization (which promotes synaptogenesis) and processing (which limits the synaptogenic effect) (Stahl et al., 2014). We can hypothesize that under basal conditions, APP forms trans-dimers in

contact sites and stabilizes NMDARs at the synapse, whereas increased synaptic activity might trigger APP processing (Stahl et al., 2014, Kamenetz et al., 2003).

To better elucidate if APP acts by regulating the synaptic content of NMDARs, we silenced APP in primary neuronal cultures, since this model recapitulates the synapse development process (Grabrucker et al., 2009) and the NMDAR developmental switch (Corbel et al., 2015), while providing appropriate imaging resolution to study synaptic proteins (J. S. Ferreira et al., 2017). When we depleted APP using a shRNA, we found a significant reduction in GluN2B and GluN2A synaptic location (20% and 56% respectively), without interfering with their total levels or clustering (**Figures 3.8 and 3.9**). These findings suggest that APP does not affect the subunits expression levels or their ability to cluster, but it is required for their co-localization with post-synaptic markers.

It is possible that APP directly regulates PSD-95 area and average particle size (**Figure 3.10**). In that case, the decline in GluN2B/A co-localization with PSD-95 might occur as an indirect response. Alternatively, considering the key role of GluN2B-NMDARs for synaptic maturation, we can hypothesize that the impaired GluN2B synaptic location could disturb this process, causing a reduction in PSD-95 and GluN2A recruitment to newly formed synapses (Gray et al., 2011). Accordingly, NMDAR synaptic activity has been associated with PSD-95 recruitment to new synapses (de Roo et al., 2008) and this process might become impaired upon APP depletion. Although we cannot state if PSD-95 and/or GluN2B-NMDARs are the primary responsible for this effect, our results are consistent with the recently described findings in APP-depleted human neurons. Zhou et al. observed a decrease in synapse density (measured by PSD-95 clusters) and in the amplitude of evoked EPSCs upon APP deletion (Zhou et al., 2022), but the authors have not explored the relative contribution of NMDARs for this effect. Moreover, our findings might help to explain why silencing APP during embryonic development causes the loss of GluN2B-NMDAR synaptic contribution in infant mice, as previously shown by our group (Pousinha et al., 2017).

When compared to APP depletion, the short interference manipulation of the APP C-terminal using an antibody has the advantages of manipulating single neurons and avoiding prolonged structural effects on the PSD. Altogether, the results obtained with both strategies point towards a model in which APP interference/ silencing destabilizes the permanence of NMDARs at the synapse.

Our main findings regarding APP-NMDAR regulating in immature synapses are summarized in **Figure 4.1**. Moreover, the graphical abstracts in the Appendix show analogies to illustrate the putative mechanism of NMDAR stabilization by APP (**Figure 4.4**) and the possible impact in the synaptic maturation process (**Figure 4.5**).

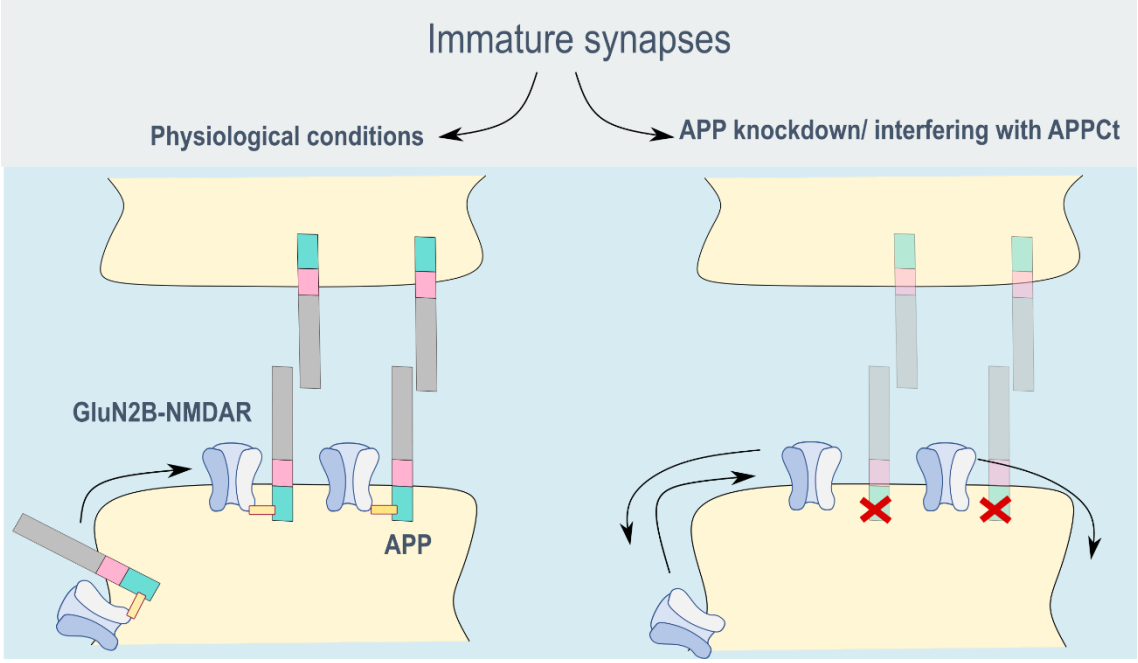

Figure 4.1 – Hypothetical model of APP-NMDAR regulation in immature synapses. APP interacts with GluN2B-NMDARs, stabilizing the receptors at the synapse and maintaining normal NMDAR transmission. When knocking-down APP or interfering with the APP C-terminal (APPCt), this stabilizing effect is lost, leading to less GluN2B-NMDARs at the synapse and a reduction in NMDAR currents.

We propose that the APP-NMDAR regulation is relevant to regulate NMDAR synaptic content during development, when synapse formation and maturation processes are highly abundant, and both APP and GluN2B levels/contribution reach their peak. In contrast, this mechanism might become less relevant after maturation, when PSD-95 is recruited to the synapse, and allows for more stable anchoring of the receptors (Elias et al., 2008).

Accordingly, we observed no alterations in NMDAR EPSCs in adult animals when interfering with the APP C-terminal domain for 1h (**Figure 3.6 d**), contrary to what happens in infants, which may allow for different interpretations. Considering the technical approach we used, it is possible that the accessibility of the APP C-terminal epitope at the post-synapse might be precluded in adult stages, considering the extensive alterations that occur in PSD structure and composition after postnatal

development (Gonzalez-Lozano et al., 2016) and the high molecular weight of the antibody (150 KDa). However, we can also hypothesize that the APP regulation of NMDARs has indeed a higher impact during development, which is consistent with the marked decline of postsynaptic APP levels observed in adult stages (5-fold decrease when compared to infant mice) (**Figure 3.5 f**). Given the increased association of PSD-95 with NMDARs in mature synapses (Petralia et al., 2005, Elias et al., 2008), we can assume that the NMDAR synaptic stabilization becomes less dependent on APP upon adulthood.

However, the fact that the Camk2a-Cre cTKO mouse model (triple conditional knock-out for APP family members in excitatory forebrain neurons starting at postnatal weeks 3-4) exhibits LTP impairments and reduced NMDAR-mediated responses in adult stages, suggests that some form of NMDAR regulation by APP family members still occurs later in life (S. H. Lee et al., 2020). Moreover, mouse models in which the APP C-terminal domain is mutated (Matrone et al., 2012) or depleted (APPdCT15 knock-in mice/ APLP2 KO) (Klevanski et al., 2015) exhibit impairments in synaptic plasticity/ memory in adult stages, which might be explained by alterations in NMDAR function, although this hypothesis has not been explored so far. Therefore, we propose that APP is still able to regulate NMDARs in mature synapses, possibly through different mechanisms. The fact that APP interference only occurred for 1h could explain the absence of effect in NMDAR currents, since the regulatory mechanisms in adults might involve signaling pathways that take more time to be induced/inhibited. Future studies using APP knockdown strategies *in vivo* could help to unravel the impact of APP in NMDARs currents at different ages (infant, adult, aged mice), while overcoming the potential compensation by APP family members (which is thought to occur in APP knockout mice) (Dawson et al., 1999). Taking this into account, we have developed an AAV vector encoding a short-hairpin RNA against APP (AAV-shAPP), which proved to efficiently silence APP in adult mice after being injected in the hippocampus (**Supplementary Figure 3.3**). Thus, this tool might be useful in the future to better elucidate the role of APP-NMDAR regulation at different ages.

Considering the previously described alterations in NMDARs at aged synapses and their contribution to synaptic impairments at this stage (Kumar, 2015), we hypothesize that the APP-NMDAR regulation might become dysregulated upon aging. However, we found no alterations in the APP interaction with GluN2B and GluN2A in mice upon aging (**Figure 3.11 a, c**), since the GluN2B/GluN2A ratio was similar in APP immunoprecipitated samples from adult and aged mice (**Figure 3.11 b**). Moreover, no alterations were found regarding the GluN2B/GluN2A ratio in PSD-fractions in aged

mice, when compared to adults (**Figure 3.13 d**). This data suggests that APP interacts with the NMDARs (both GluN2B and GluN2A subtypes) that are present at the synapse, showing no age-related alterations. However, we found that the NMDARs at aged synapses have different properties than in adulthood, staying open for a longer time and having a larger GluN2B-NMDAR contribution (33% vs 14%) (**Figure 3.14**). Since the electrophysiological recordings showed no correlation with the ratio between GluN2B/A postsynaptic levels, we hypothesize that this is not caused by an increase in GluN2B levels but rather an alteration in GluN2B-NMDAR properties (e.g. gating, Ca^{2+} permeability, deactivation kinetics). However, we can also hypothesize that the increased contribution measured in Patch-Clamp might be specific of this circuit, i.e. CA1 aged pyramidal neurons might have increased levels of GluN2B, but this is not detected when performing Western Blot analysis of whole hippocampal lysates. The analysis of protein lysates from the CA1 (obtained from laser capture microdissections (as in (Barthet et al., 2018)) might be a useful strategy to elucidate this question in the future.

Importantly, previous studies suggest that aging is associated with alterations not only in synaptic but also in extrasynaptic NMDARs (Potier et al., 2010). However, given the low frequency stimulation used in the Patch-Clamp experiments in this study (0.1 Hz), the recorded NMDAR EPSCs are known to mainly derive from synaptic NMDARs (Papouin et al., 2012). Thus, we hypothesize that the increased GluN2B-NMDAR contribution measured in this study occurs due to alterations in the properties of synaptic, rather than extrasynaptic NMDARs.

It is possible that this excessive GluN2B-NMDAR functional contribution relates to alterations in APP-NMDAR regulation mechanisms. Despite having found no differences in total/postsynaptic APP levels in aged mice when compared to adults, we found that APP processing and CTF levels were increased upon aging (**Figure 3.16**).

To elucidate if APP processing contributes to this excessive GluN2B-NMDAR contribution in aged mice, we inhibited one of the APP processing pathways using a single dose treatment of a BACE1 inhibitor, 12h before Patch-Clamp recordings. According to previous studies, this same dosage and timing of administration efficiently reduces APP β-secretase processing and does not cause significant adverse effects (Filser et al., 2015, May et al., 2011). The fact that APP endocytosis and BACE1 activity tend to increase in aged mice (Fukumoto et al., 2004, Burrinha et al., 2021) reinforces the relevance of targeting this enzyme and processing pathway. Moreover, the APP Iceland mutation, which is associated with a reduction in amyloidogenic peptides, has shown to protect against age-related cognitive decline in healthy human subjects (Jonsson et al., 2012). This data suggests that inhibiting APP β-processing might be

beneficial in aged subjects. We found that this treatment significantly reduced the relative GluN2B-NMDAR contribution from approximately 40 to 20%, reaching comparable values to untreated adult mice (14%) (**Figure 3.17**). These findings suggest that APP processing plays a role in the excessive GluN2B-NMDAR contribution upon aging. Future studies will be important to elucidate if this response is caused by a reduction in the levels of APP amyloidogenic fragments and not by alterations in other BACE1 substrates (Munro et al., 2016). To address these questions, we could use an endosomally targeted sterol-linked BACE1 inhibitor, which has shown to block cleavage of APP but not of other substrates that are processed in an endocytosis-independent manner (ben Halima et al., 2016). Moreover, it is also possible that the effects observed in this study upon BACE1 inhibition could arise from a compensatory increase in signaling by APP non-amyloidogenic fragments. If that is the case, we could test different doses/timings of administration to avoid compensatory responses.

Additionally, it remains to be elucidated if the excessive GluN2B-NMDAR contribution upon aging is caused by an overall increase in APP processing or specifically induced by the increase in amyloidogenic fragments. The fact that we found no significant differences in the CTFβ/ α ratio upon aging suggests that both processing pathways might increase upon aging (**Figure 3.16 g**). A more detailed analysis of APP processing will be important to elucidate this question, by identifying the ratio between soluble APP α and β by Western Blot (as described in (Willem et al., 2015)) and/or by characterizing the full pattern of APP fragments by mass spectrometry (as described in (Mosser et al., 2021, Brinkmalm et al., 2013)).

Since we hypothesize that APP intracellular fragments could contribute to the increase in GluN2B-NMDAR relative currents, we used an interfering peptide (PTB2-p,15 KDa) that binds to the APP intracellular domain. A >3h incubation of hippocampal slices from aged mice with PTB2-p was able to normalize the GluN2B-NMDAR contribution (**Figure 3.18**), indicating that signaling by the APP intracellular domain is involved in GluN2B-NMDAR increased contribution upon aging. It remains to be elucidated if this effect is caused by a reduction in signaling mediated by the APP full-length or its derived intracellular fragments or even by other Fe65 binding partners (Augustin & Kins, 2021). Additional studies using PTB2-p in combination with APP processing inhibitors, as well as testing other interfering peptides targeting the APP intracellular domain, would be extremely valuable to address these questions.

The fact that we detected an effect in GluN2B-NMDAR relative currents using the interfering peptide (15 KDa, >3h) (**Figure 3.18**), but no alterations in total NMDAR EPSCs when using the APP C-terminal antibody (150 KDa, 1h) (**Figure 3.11 d**) might

have different interpretations. It is conceivable that the APP C-terminal signaling pathways take more than 1h to be activated/inhibited, explaining the lack of effect of the antibody. Accordingly, the PTB2-p effect was observed upon peptide incubation for 3h, but not for 2h (**Figure 3.19**), indicating that the time might be an important factor in these experiments. Future studies exploring the PTB2-p cellular uptake mechanism and kinetics will be important to elucidate this issue. Additionally, we can hypothesize that the ability to interfere with the APP C-terminal is different for the PTB2-p or the antibody, especially considering their molecular weights (10 times larger in the case of the antibody).

Altogether, the results obtained in aged mice suggest that the APP intracellular fragments contribute to the excessive GluN2B-NMDAR synaptic contribution in aged mice. However, the specific fragments involved in this response, as well as the underlying mechanisms remain to be elucidated.

Considering that the increase in GluN2B-NMDAR functional contribution is not accompanied by an increase in GluN2B levels, we hypothesize that posttranslational mechanisms such as phosphorylation might be involved. Depending on the site, phosphorylation events might affect gating, permeability to different ions, deactivation kinetics, trafficking, endocytosis, etc. (**Figure 1.18**), (Sanz-Clemente et al., 2013). We have shown that the Y1472 phosphorylation site is not altered upon aging (**Figure 3.15 b**), indicating that other posttranslational mechanisms might be involved. In particular, the phosphorylation of GluN2B on Ser1166 by Protein Kinase A (PKA) has emerged as a good candidate, since it causes an increase in Ca^{2+} influx and current amplitude in GluN2B-containing receptors, without affecting their trafficking and surface expression (Aman et al., 2014, Skeberdis et al., 2006, Murphy et al., 2014). Interestingly, PKA also regulates GluN2A-NMDARs Ca^{2+} permeability, but does not alter their current amplitude, contrary to what happens in the GluN2B subtype (Skeberdis et al., 2006, Murphy et al., 2014). Therefore, an overactivation of PKA is expected to cause an increased contribution of GluN2B-NMDAR relative currents, similarly to our findings in aged mice.

Interestingly, a previous study by Deyts et al. has described an association between the APP intracellular domain and the heterotrimeric G-protein subunit $G\alpha_s$. This interaction is thought to stimulate adenylate cyclase (AC), leading to an increase in cyclic adenosine monophosphate (cAMP) levels and ultimately resulting in PKA activation and enhanced phosphorylation of the respective substrates. Importantly, the activation of this signaling pathway increases upon accumulation of CTFs or of a membrane-tethered form of AICD (Deyts et al., 2012). Thus, we can hypothesize that the increased processing of APP upon aging can trigger PKA-phosphorylation of GluN2B, consequently increasing

GluN2B-NMDAR relative currents (**Figure 4.2**). If that is the case, the APP-NMDAR interaction might help to maintain GluN2B-NMDARs as part of a complex, so that it is coupled to kinases/phosphatases that regulate their properties, such as PKA (Sanderson & Dell'Acqua, 2011). Interestingly, previous studies showed that the full-length APP interacts with $G\alpha_o$, whereas the CTFs interact with Gαs, leading to the hypothesis that APP processing could induce a switching in G protein signaling (Copenhaver & Kögel, 2017).

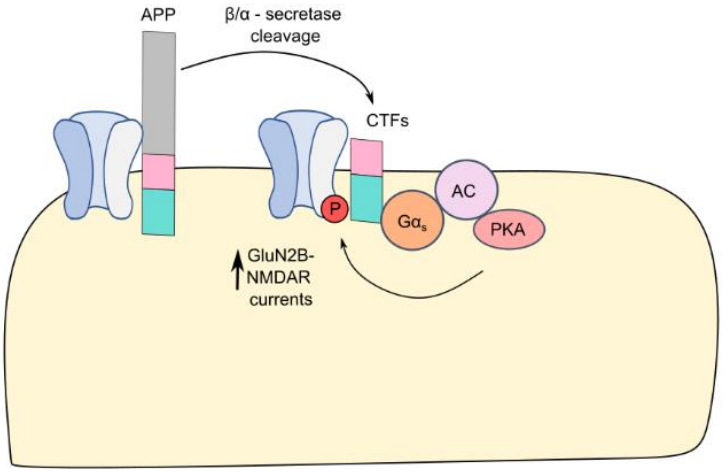

Figure 4.2 – Putative regulation mechanism, in which APP C-terminal fragments might contribute to increased PKA activation, inducing GluN2B phosphorylation. Figure adapted from (Deyts et al., 2012, Copenhaver & Kögel, 2017). AC - adenylate cyclase, PKA – Protein kinase A.

Another potential mechanism by which APP fragments could lead to excessive GluN2B-NMDAR functional contribution involves AICD transcriptional actions. Our group has previously shown that the viral-induced overexpression or exogenous delivery of this peptide (2h incubation in hippocampal slices) increases GluN2B-NMDAR synaptic contribution in adult synapses (Pousinha et al., 2017). In case there is an increase in AICD signaling upon aging, the strategies used in this work – interfering with the APP C-terminal and inhibiting BACE1 – would have an inhibitory effect on AICD signaling. In fact, the PTB2 domain of Fe65 is known to bind to AICD (Radzimanowski et al., 2008) and is essential for its transcriptional roles (Cao & Sudhof, 2001). Moreover, the biologically active form of AICD mainly derives from the amyloidogenic pathway, thus it is likely that the BACE1 inhibitor treatment would have an inhibitory effect on AICD signaling (Edbauer et al., 2002, Goodger et al., 2009). Since AICD has a transcriptional role (Cao & Sudhof, 2001), it is possible that this peptide might up/down regulate kinases/phosphatases (e.g. PKA) or other proteins that influence GluN2B-NMDAR

properties, without affecting the subunit levels. Our results using a TAT-AICD peptide incubation in primary neuronal cultures are in accordance with this hypothesis since we were not able to detect alterations in GRIN2B mRNA levels upon treatment (**Supplementary Figure 3.2**). Nevertheless, a previous study by our group has shown that AICD viral delivery in adult rats induces GluN2B upregulation (Pousinha et al., 2017), suggesting that short/prolonged AICD incubation/overexpression might cause different responses.

Thus, we can hypothesize that the PTB2-p incubation in hippocampal slices leads to the down/upregulation of AICD transcriptional targets that regulate GluN2B-NMDAR properties. However, considering the short time of PTB2-p incubation (3h), this hypothesis would only be conceivable if the target genes encode for proteins with a very fast turnover (from synthesis to degradation). Moreover, the fact that we observed a reduction in GluN2B-NMDAR contribution specifically in the case of PTB2-p, but not for PTB1-p also requires further clarification. In fact, the AICD-transcriptional action is thought to require the formation of AICD-Fe65-Tip60 complexes, in which the PTB2 domain is essential for Fe65-AICD binding and the PTB1 domain mediates the Fe65-Tip60 interaction (Feilen et al., 2017), as illustrated in **Figure 4.3**. Thus, both PTB2-p and PTB1-p were expected to interfere with AICD transcriptional action. Future studies focused on inhibiting AICD nuclear activity (as in (Branca et al., 2014)) might be important to address this question.

Taking all of this into account, our findings suggest that signaling by the APP intracellular domain contributes to increased GluN2B-NMDAR synaptic contribution in aged mice. Further studies will be important to dissect the roles of APP, CTFs and AICD and their impact in NMDARs upon aging.

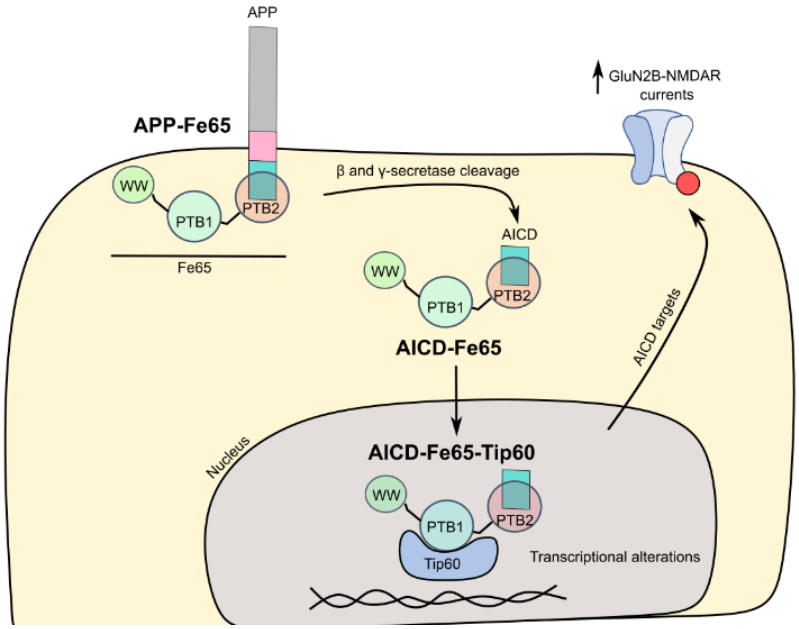

Figure 4.3 – Schematic representation of the transcriptional effects of AICD-Fe65-Tip60 complexes. Upon β and γ- secretase cleavage of APP, AICD forms complexes with Fe65 (interaction through the PTB2 domain), which translocate to the nucleus, interacting with Tip60 (interaction through the PTB1 domain). The AICD-Fe65-Tip60 complex has transcriptional effects, potentially up/down regulating kinases/phosphatase that alter GluN2B-NMDAR relative currents. Figure adapted from (Feilen et al., 2017).

Importantly, our results suggest that the mechanisms observed in mice can also occur in humans. Accordingly, we proved that the APP-NMDAR interaction occurs in brain samples from adult and aged human subjects (**Figure 3.20 a**). Similarly to mice, we observed no age-related alterations in GluN2B synaptic levels upon aging (**Figure 3.20 c**). Future studies, such as performing electrophysiological recordings in aged human brains (using nonpathological temporal cortical tissue resected during neurosurgical procedures, as in (Pegasiou et al., 2020)) will be essential to elucidate if the GluN2B relative contribution is altered in humans, similarly to what we observed in mice. Interestingly, we found an age-related decrease in human APP levels in prefrontal cortex, which was not observed in hippocampal samples from aged mice. Additional studies will be important to understand if this alteration is dependent on the species (mouse vs human) or on the brain region (hippocampus vs prefrontal cortex).

The tendency for more APP being processed (**Figure 3.21**) was observed both in humans and mice upon aging. Overall, this could disrupt the balance between signaling pathways mediated by the APP full-length and by the APP-intracellular fragments, potentially contributing to GluN2B-NMDAR excessive currents.

The age-related increase in GluN2B-NMDAR contribution, accompanied by slower NMDAR deactivation kinetics, can have great consequences at the synapse, such as favoring Ca^{2+} overload and potentially causing alterations in synaptic plasticity mechanisms (Yashiro & Philpot, 2008, Temido-Ferreira et al., 2020, Pinho et al., 2017). Thus, we can speculate that this alteration in NMDAR properties could contribute to synaptic dysregulation and memory impairments observed upon aging. To test this model, additional studies will be important to distinguish age-impaired from non-impaired mice, based on their behavioral performance in memory tests (as in (Temido-Ferreira et al., 2020)), and determine if there is a correlation with GluN2B-NMDAR relative currents.

Importantly, our results could help to clarify an apparent paradox in the field: although total NMDAR levels tend to decline in physiological aging, as reported in this study (**Figure 3.12 c**) and others (Magnusson et al., 2002, Zhao et al., 2009), NMDAR antagonists such as memantine have shown beneficial effects in aged-impaired rodents (Pietá Dias et al., 2007, Beracochea et al., 2008). We can speculate that the increased GluN2B-NMDAR contribution might start as a compensatory mechanism in response to GluN2B downregulation (Pinho et al., 2017), but might become pathological after a certain time. The fact that memantine has shown beneficial effects in age-impaired rodents and human AD patients (Reisberg et al., 2003) also support a common pathological mechanism associated with GluN2B-NMDAR excessive currents. Considering that Alzheimer's Disease is characterized by the accumulation of APP amyloidogenic fragments (Hardy & Higgins, 1992, Ghosal et al., 2009, Ferrer-Raventós et al., 2023), we can speculate that this mechanism might become exacerbated in the disease context.

4.2 Future perspectives

This work shows that APP regulates NMDARs in an age-dependent manner, opening the way to new questions: Is the APP-NMDAR regulation important for synapse maturation? Can we avoid age-associated synaptic/memory impairments by interfering with the APP-NMDAR regulation?

To address these questions, firstly we would have to validate different methods to disrupt the APP-NMDAR regulation mechanisms. One possibility would be to explore in further detail the potential of PTB2-p as an interfering peptide. Besides confirming its ability to disrupt the APP intracellular signaling and the APP-NMDAR interaction, we should also study the impact on non-specific targets and identify potential adverse effects. Additionally, the most appropriate *in vivo/in vitro* treatment protocol should be established, based on other studies using cell penetrating peptides (Plattner et al., 2014, Stanic et al., 2015). Alternatively, other interfering peptides could be selected based on peptide microarray microchips, as described previously (X. Gao et al., 2004, Plattner et al., 2014). Another possibility would be to use the YG/YG mouse model, since these mice exhibit a point mutation in the putative APP binding site (^{682}YENPTY^{687} motif), thus we could test whether the NMDAR-APP interaction and APP intracellular signaling are impaired in this model (Barbagallo et al., 2010).

Assuming these models proved to be suitable, we could use them to explore the impact of APP-NMDAR regulation in the synaptic maturation process. The results obtained in immature synapses suggest that APP could stabilize NMDARs in newly formed synapses, potentially contributing for the maturation process. Using primary neuronal cultures, we could follow this process (from 7 to 21DIV), by identifying APP, GluN2B, GluN2A and PSD-positive spines using super-resolution imaging (Hruska et al., 2022). If our hypothesis is correct, nascent synapses will be APP and GluN2B-positive, whereas GluN2A/PSD-95 would be recruited only upon maturation. This process would become impaired in conditions in which the APP-NMDAR interaction is perturbed, such as upon PTB2-p treatment or in neuronal cultures from YG/YG mice (Barbagallo et al., 2010). To investigate if this occurs due to a decrease in NMDAR anchoring at the synapse, we could follow the trajectory of these receptors using quantum-dot tracking, as described in (Groc et al., 2006). If our hypothesis is correct, inhibiting the APP-NMDAR interaction would reduce NMDAR synaptic stabilization, leading to lower retention times at the synapse.

To investigate the impact of APP-NMDAR regulation in synaptic maturation *in vivo*, we could use a commonly used method to study GluN2B to GluN2A switch in response to

activity. This mechanism has been very well characterized in the visual cortex, being prevented by rearing animals in the dark (Carmignoto & Vicini, 1992) and rapidly induced when exposing animals to light (Philpot et al., 2001). We could use this experimental paradigm to test if APP-NMDAR interaction is essential for synaptic maturation and the GluN2B-GluN2A shift in the visual cortex. By treating infant mice with PTB2-p or using infant YG/YG mice, we could compare the extent of synaptic maturation by calculating the GluN2B/A synaptic ratio before and after light exposure. At the same time, we could correlate these alterations with spine maturation by two-photon microscopy imaging (as in (Isshiki et al., 2014)).

Considering the results obtained in aged mice, it would be interesting to elucidate if the increased GluN2B relative currents correlate with an increase in phosphorylation (namely by PKA at the Ser1166) (Murphy et al., 2014). We could start by measuring the levels of phosphorylated GluN2B on residue Ser1166 in aged mice and aged primary neuronal cultures (as in (Burrinha et al., 2021)). If we detect an increase in phosphorylation, we could test the impact of PKA inhibitors validated in previous studies (Murphy et al., 2014), in an attempt to normalize GluN2B phosphorylation levels. Additionally, other phosphorylation sites might be explored using phosphoenrichment-coupled mass spectrometry analysis, as described previously (Gómez de Salazar et al., 2018).

Moreover, it would be important to assess whether APP processing regulates GluN2B-NMDAR phosphorylation state and mediated currents. Using aged primary neuronal cultures (as in (Burrinha et al., 2021)), we could manipulate APP processing and evaluate the impact on GluN2B phosphorylation and relative contribution to NMDAR EPSCs. Different conditions could be tested, such as expressing cleavage deficient forms of APP (as described in (Stahl et al., 2014)) and inhibiting β/α- secretase. To better elucidate the role of β-secretase cleavage, we could also measure the same parameters in neuronal cultures when expressing APP with mutations that favor the β-secretase cleavage (e.g. Swedish mutation, described in cases of familiar AD, (Mullan et al., 1992)). In contrast, the protective Icelandic mutation, which leads to a reduction in β-secretase APP processing (Jonsson et al., 2012), is expected to cause the opposite effect.

Finally, it would be important to investigate whether the increased GluN2B-NMDAR relative currents are associated with synaptic plasticity deficits (such as the LTD to LTP shift) and memory impairments in aged mice, which have been previously studied in our group (Temido-Ferreira et al., 2020). This would be essential to understand if GluN2B-

NMDAR excessive currents have a positive or negative impact during physiological aging.

In case they show a positive correlation with age-related synaptic and memory impairments, we could explore in further detail potential strategies for the normalization of GluN2B-NMDAR contribution. Since BACE1 inhibition is associated with adverse effects (Wessels et al., 2020), inhibiting the excessive GluN2B-NMDAR currents using memantine would be a preferential strategy. Another possibility would be to block the APP intracellular signaling using an interfering peptide such as the PTB2-p. Thus, it would be interesting to investigate the impact of treating aged mice with PTB2-p *in vivo*, both in terms of GluN2B-NMDAR relative currents, synaptic plasticity mechanisms and memory performance.

Finally, we could investigate if this age-related alteration in GluN2B-NMDAR relative currents also occurs in humans. For that purpose, we could measure NMDAR EPSCs by Patch-Clamp electrophysiology (as in (Pegasiou et al., 2020)) using human brain slices from subjects with different ages. Additionally, our group is currently generating induced human neurons (iNs) by direct conversion of fibroblasts. This might be a suitable model to measure NMDAR EPSCs in future studies, specially considering that iNs retain important aging-related signatures (Mertens et al., 2015).

4.3 Graphical Abstracts

In the context of this work, I have prepared two graphical abstracts with analogies to illustrate the putative mechanism of NMDAR stabilization by APP **(Figure 4.4)** and the possible impact in the synaptic maturation process **(Figure 4.5).**

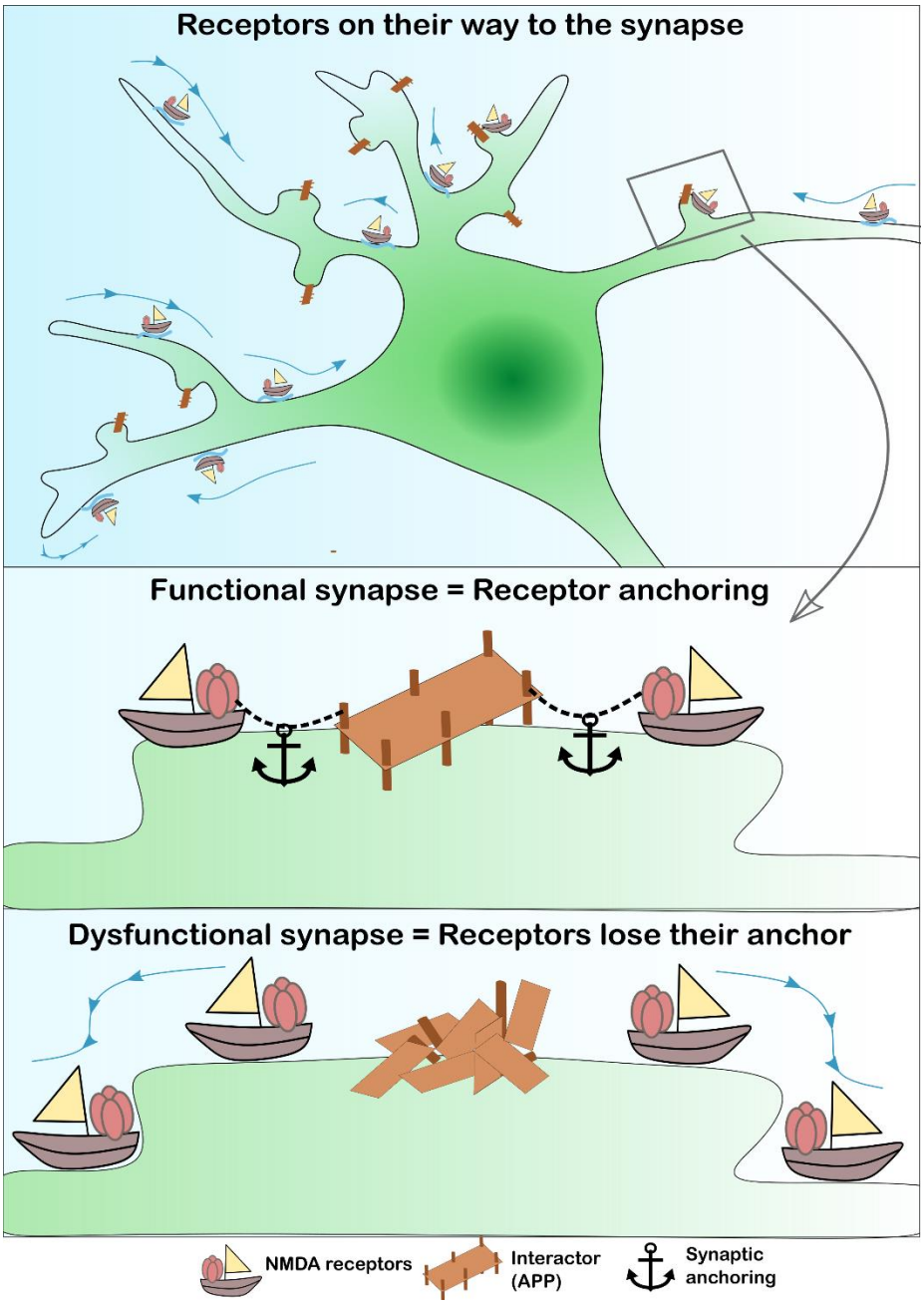

Figure 4.4 – Hypothetical model of NMDAR synaptic anchoring by APP

NMDA receptors (here represented as boats) are mobile, moving in and out of the synapses. Thus, the retention of NMDARs at the synapse depends on their interaction with other proteins. The amyloid precursor protein (APP) (here represented as a dock) is able to interact with NMDARs, potentially anchoring them at

the synapse. Thus, in conditions of APP silencing or when the APP-NMDAR interaction is disturbed, the receptors might lose their anchor, causing a decrease in NMDAR synaptic levels.

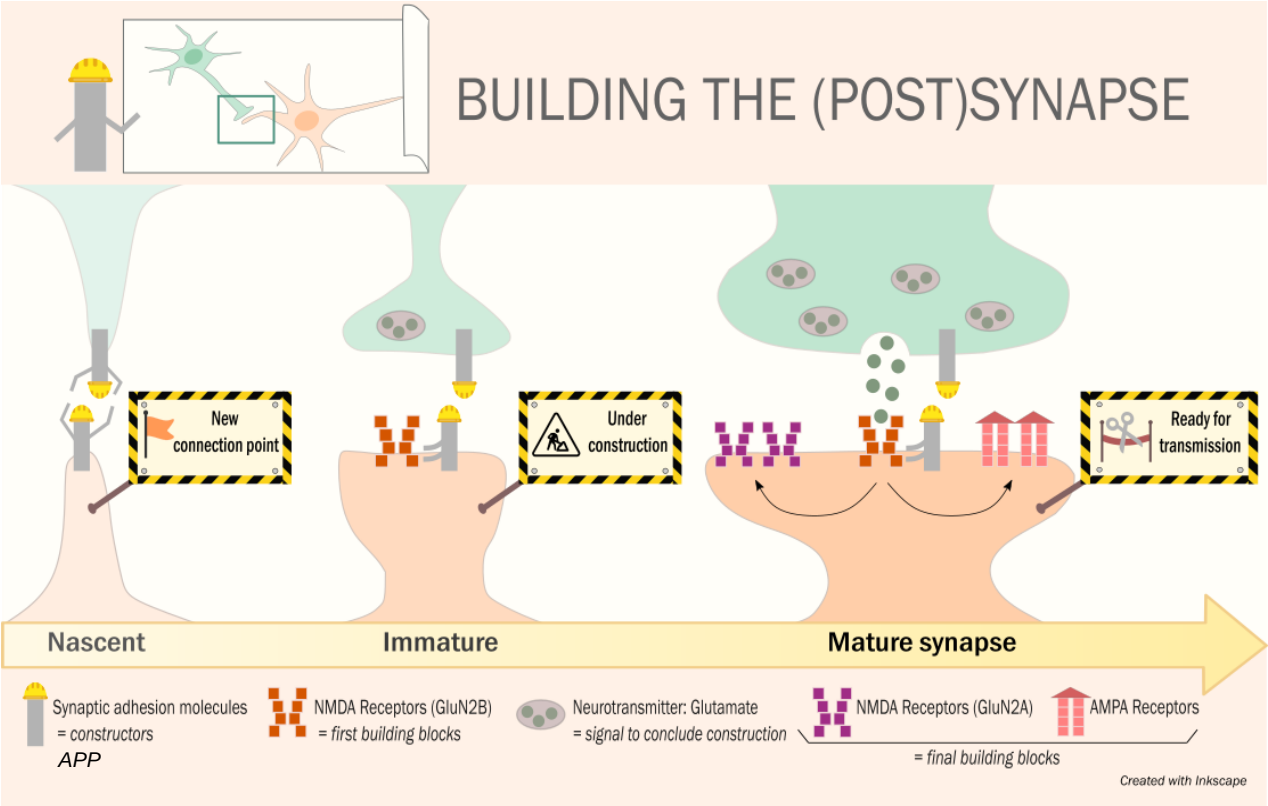

Figure 4.5 - Hypothetical model of APP-GluN2B NMDAR regulation in immature synapses and its potential impact in the synaptic maturation process

The formation and maturation of glutamatergic synapses occurs as a gradual construction process, in which synaptic adhesion molecules (SAMs), such as APP, but also NMDA receptors (NMDARs) play key roles. When there is an initial contact between an axon and a dendrite, SAMs interact with each other and stabilize the new synaptic site. Then, they act as ‘constructors’, by recruiting pre and postsynaptic components. One of the early events at the post-synapse is the insertion of ‘immature’ glutamate receptors: NMDARs with GluN2B subunits, which are considered to be the ‘first building blocks’. By interacting with SAMs, GluN2B-NMDARs are stabilized at the synapse. Therefore, when there is an increase in glutamate release, GluN2B-NMDARs are activated, transmitting a signal to 'conclude construction'. Consequently, ‘mature’ glutamate receptors (GluN2A-NMDARs and AMPA receptors) are recruited to the post-synapse and act as the ‘final building blocks’ necessary for functional synaptic transmission.

5 References

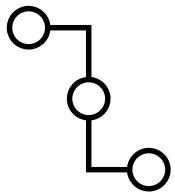

Adams, M. M., Morrison, J. H., & Gore, A. C. (2001). N-methyl-d-aspartate receptor mRNA levels change during reproductive senescence in the hippocampus of female rats. *Experimental Neurology*, *170*(1). https://doi.org/10.1006/exnr.2001.7687

Adesnik, H., Li, G., During, M. J., Pleasure, S. J., & Nicoll, R. A. (2008). NMDA receptors inhibit synapse unsilencing during brain development. *Proceedings of the National Academy of Sciences of the United States of America*, *105*(14). https://doi.org/10.1073/pnas.0800946105

Afonso, P., de Luca, P., Carvalho, R. S., Cortes, L., Pinheiro, P., Oliveiros, B., Almeida, R. D., Mele, M., & Duarte, C. B. (2019). BDNF increases synaptic NMDA receptor abundance by enhancing the local translation of Pyk2 in cultured hippocampal neurons. *Science Signaling*, *12*(586). https://doi.org/10.1126/scisignal.aav3577

al Abed, A. S., Sellami, A., Potier, M., Ducourneau, E. G., Gerbeaud-Lassau, P., Brayda-Bruno, L., Lamothe, V., Sans, N., Desmedt, A., Vanhoutte, P., Bennetau-Pelissero, C., Trifilieff, P., & Marighetto, A. (2020). Age-related impairment of declarative memory: linking memorization of temporal associations to GluN2B redistribution in dorsal CA1. *Aging Cell*, *19*(10). https://doi.org/10.1111/acel.13243

Al-Hallaq, R. A., Conrads, T. P., Veenstra, T. D., & Wenthold, R. J. (2007). NMDA di-heteromeric receptor populations and associated proteins in rat hippocampus. *Journal of Neuroscience*, *27*(31). https://doi.org/10.1523/JNEUROSCI.2155-07.2007

Allen Institute for Brain Science (2004). (n.d.). *Allen Mouse Brain Atlas, mouse.brain-map.org* . Retrieved February 2023.

Allen, N. J. (2020). Astrocyte-neuron interactions in synaptic development. In *Patterning and Cell Type Specification in the Developing CNS and PNS: Comprehensive Developmental Neuroscience, Second Edition*. https://doi.org/10.1016/B978-0-12-814405-3.00033-3

Aman, T. K., Maki, B. A., Ruffino, T. J., Kasperek, E. M., & Popescu, G. K. (2014). Separate intramolecular targets for protein kinase A control N-Methyl-D-aspartate receptor gating and Ca2+ permeability. *Journal of Biological Chemistry*, *289*(27). https://doi.org/10.1074/jbc.M113.537282

Amico-Ruvio, S. A., Paganelli, M. A., Myers, J. M., & Popescu, G. K. (2012). Ifenprodil effects on GluN2B-containing glutamate receptors. *Molecular Pharmacology*, *82*(6). https://doi.org/10.1124/mol.112.078998

Andrew, R. J., Kellett, K. A. B., Thinakaran, G., & Hooper, N. M. (2016). A Greek tragedy: The growing complexity of Alzheimer amyloid precursor protein proteolysis. In *Journal of Biological Chemistry* (Vol. 291, Issue 37). https://doi.org/10.1074/jbc.R116.746032

Apelt, J., Schliebs, R., Beck, M., Roßner, S., & Bigl, V. (1997). Expression of amyloid precursor protein mRNA isoforms in rat brain is differentially regulated during postnatal maturation and by cholinergic activity.

International Journal of Developmental Neuroscience, *15*(1). https://doi.org/10.1016/S0736-5748(96)00073-1

Augustin, V., & Kins, S. (2021). Fe65: A scaffolding protein of actin regulators. *Cells*, *10*(7). https://doi.org/10.3390/cells10071599

Back, S., Haas, P., Tschäpe, J. A., Gruebl, T., Kirsch, J., Müller, U., Beyreuther, K., & Kins, S. (2007). β-amyloid precursor protein can be transported independent of any sorting signal to the axonal and dendritic compartment. *Journal of Neuroscience Research*, *85*(12). https://doi.org/10.1002/jnr.21239

Baez, M. V., Oberholzer, M. V., Cercato, M. C., Snitcofsky, M., Aguirre, A. I., & Jerusalinsky, D. A. (2013). NMDA Receptor Subunits in the Adult Rat Hippocampus Undergo Similar Changes after 5 Minutes in an Open Field and after LTP Induction. *PLoS ONE*, *8*(2). https://doi.org/10.1371/journal.pone.0055244

Bahar, A. S., Shirvalkar, P. R., & Shapiro, M. L. (2011). Memory-guided learning: CA1 and CA3 neuronal ensembles differentially encode the commonalities and differences between situations. *Journal of Neuroscience*, *31*(34). https://doi.org/10.1523/JNEUROSCI.1671-11.2011

Bai, L., Hof, P. R., Standaert, D. G., Xing, Y., Nelson, S. E., Young, A. B., & Magnusson, K. R. (2004). Changes in the expression of the NR2B subunit during aging in macaque monkeys. *Neurobiology of Aging*, *25*(2). https://doi.org/10.1016/S0197-4580(03)00091-5

Barbagallo, A. P. M., Weldon, R., Tamayev, R., Zhou, D., Giliberto, L., Foreman, O., & D'Adamio, L. (2010). Tyr682 in the intracellular domain of APP regulates amyloidogenic APP processing in vivo. *PLoS ONE*, *5*(11). https://doi.org/10.1371/journal.pone.0015503

Bard, L., & Groc, L. (2011). Glutamate receptor dynamics and protein interaction: Lessons from the NMDA receptor. In *Molecular and Cellular Neuroscience* (Vol. 48, Issue 4). https://doi.org/10.1016/j.mcn.2011.05.009

Barda, L., Sainlos, M., Bouchet, D., Cousins, S., Mikasova, L., Breillat, C., Stephenson, F. A., Imperiali, B., Choquet, D., & Groc, L. (2010). Dynamic and specific interaction between synaptic NR2-NMDA receptor and PDZ proteins. *Proceedings of the National Academy of Sciences of the United States of America*, *107*(45). https://doi.org/10.1073/pnas.1002690107

Bar-Shira, O., Maor, R., & Chechik, G. (2015). Gene Expression Switching of Receptor Subunits in Human Brain Development. *PLoS Computational Biology*, *11*(12). https://doi.org/10.1371/journal.pcbi.1004559

Barth, A. L., & Malenka, R. C. (2001). NMDAR EPSC kinetics do not regulate the critical period for LTP at thalamocortical synapses. *Nature Neuroscience*, *4*(3). https://doi.org/10.1038/85070

Barthet, G., Jordà-Siquier, T., Rumi-Masante, J., Bernadou, F., Müller, U., & Mulle, C. (2018). Presenilin-mediated cleavage of APP regulates synaptotagmin-7 and presynaptic plasticity. *Nature Communications*, *9*(1). https://doi.org/10.1038/s41467-018-06813-x

Barthet, G., Moreira-de-Sá, A., Zhang, P., Deforges, S., Castanheira, J., Gorlewicz, A., & Mulle, C. (2022). Presenilin and APP Regulate Synaptic

Kainate Receptors. *The Journal of Neuroscience*, *42*(49), 9253. https://doi.org/10.1523/JNEUROSCI.0297-22.2022

Bellone, C., & Nicoll, R. A. (2007). Rapid Bidirectional Switching of Synaptic NMDA Receptors. *Neuron*, *55*(5). https://doi.org/10.1016/j.neuron.2007.07.035

Belyaev, N. D., Kellett, K. A. B., Beckett, C., Makova, N. Z., Revett, T. J., Nalivaeva, N. N., Hooper, N. M., & Turner, A. J. (2010). The transcriptionally active amyloid precursor protein (APP) intracellular domain is preferentially produced from the 695 isoform of APP in a β-secretase-dependent pathway. *Journal of Biological Chemistry*, *285*(53). https://doi.org/10.1074/jbc.M110.141390

Belyaev, N. D., Nalivaeva, N. N., Makova, N. Z., & Turner, A. J. (2009). Neprilysin gene expression requires binding of the amyloid precursor protein intracellular domain to its promoter: Implications for Alzheimer disease. *EMBO Reports*, *10*(1). https://doi.org/10.1038/embor.2008.222

ben Halima, S., Mishra, S., Raja, K. M. P., Willem, M., Baici, A., Simons, K., Brüstle, O., Koch, P., Haass, C., Caflisch, A., & Rajendran, L. (2016). Specific Inhibition of β-Secretase Processing of the Alzheimer Disease Amyloid Precursor Protein. *Cell Reports*, *14*(9). https://doi.org/10.1016/j.celrep.2016.01.076

Beracochea, D., Boucard, A., Trocme-Thibierge, C., & Morain, P. (2008). Improvement of contextual memory by S 24795 in aged mice: Comparison with memantine. *Psychopharmacology*, *196*(4). https://doi.org/10.1007/s00213-007-0987-5

Berardi, N., Pizzorusso, T., & Maffei, L. (2000). Critical periods during sensory development. In *Current Opinion in Neurobiology* (Vol. 10, Issue 1). https://doi.org/10.1016/S0959-4388(99)00047-1

Berger-Sweeney, J., McPhie, D. L., Arters, J. A., Greenan, J., Oster-Granite, M. lou, & Neve, R. L. (1999). Impairments in learning and memory accompanied by neurodegeneration in mice transgenic for the carboxyl-terminus of the amyloid precursor protein. *Molecular Brain Research*, *66*(1–2). https://doi.org/10.1016/S0169-328X(99)00014-5

Billard, J. M., & Rouaud, E. (2007). Deficit of NMDA receptor activation in CA1 hippocampal area of aged rats is rescued by D-cycloserine. *European Journal of Neuroscience*, *25*(8). https://doi.org/10.1111/j.1460-9568.2007.05488.x

Bittner, T., Fuhrmann, M., Burgold, S., Jung, C. K. E., Volbracht, C., Steiner, H., Mitteregger, G., Kretzschmar, H. A., Haass, C., & Herms, J. (2009). γ-secretase inhibition reduces spine density in vivo via an amyloid precursor protein-dependent pathway. *Journal of Neuroscience*, *29*(33). https://doi.org/10.1523/JNEUROSCI.2288-09.2009

Blanpied, T. A., Scott, D. B., & Ehlers, M. D. (2002). Dynamics and regulation of clathrin coats at specialized endocytic zones of dendrites and spines. *Neuron*, *36*(3). https://doi.org/10.1016/S0896-6273(02)00979-0

Blue, M. E., & Parnavelas, J. G. (1983). The formation and maturation of synapses in the visual cortex of the rat. II. Quantitative analysis. *Journal of Neurocytology*, *12*(4). https://doi.org/10.1007/BF01181531

Bodhinathan, K., Kumar, A., & Foster, T. C. (2010). Intracellular redox state alters NMDA receptor response during aging through Ca2+/calmodulin-dependent protein kinase II. *Journal of Neuroscience*, *30*(5). https://doi.org/10.1523/JNEUROSCI.5485-09.2010

Branca, C., Sarnico, I., Ruotolo, R., Lanzillotta, A., Viscomi, A. R., Benarese, M., Porrini, V., Lorenzini, L., Calzà, L., Imbimbo, B. pietro, Ottonello, S., & Pizzi, M. (2014). Pharmacological targeting of the β-amyloid precursor protein intracellular domain. *Scientific Reports*, *4*. https://doi.org/10.1038/srep04618

Brim, B. L., Haskell, R., Awedikian, R., Ellinwood, N. M., Jin, L., Kumar, A., Foster, T. C., & Magnusson, K. R. (2013). Memory in aged mice is rescued by enhanced expression of the GluN2B subunit of the NMDA receptor. *Behavioural Brain Research*, *238*(1). https://doi.org/10.1016/j.bbr.2012.10.026

Brinkmalm, G., Brinkmalm, A., Bourgeois, P., Persson, R., Hansson, O., Portelius, E., Mercken, M., Andreasson, U., Parent, S., Lipari, F., Öhrfelt, A., Bjerke, M., Minthon, L., Zetterberg, H., Blennow, K., & Nutu, M. (2013). Soluble amyloid precursor protein α and β in CSF in Alzheimer's disease. *Brain Research*, *1513*. https://doi.org/10.1016/j.brainres.2013.03.019

Brunholz, S., Sisodia, S., Lorenzo, A., Deyts, C., Kins, S., & Morfini, G. (2012). Axonal transport of APP and the spatial regulation of APP cleavage and function in neuronal cells. In *Experimental Brain Research* (Vol. 217, Issues 3–4). https://doi.org/10.1007/s00221-011-2870-1

Burgess, N., Maguire, E. A., & O'Keefe, J. (2002). The human hippocampus and spatial and episodic memory. In *Neuron* (Vol. 35, Issue 4). https://doi.org/10.1016/S0896-6273(02)00830-9

Burke, S. N., & Barnes, C. A. (2006). Neural plasticity in the ageing brain. In *Nature Reviews Neuroscience* (Vol. 7, Issue 1). https://doi.org/10.1038/nrn1809

Burnashev, N. (1998). Calcium permeability of ligand-gated channels. In *Cell Calcium* (Vol. 24, Issues 5–6). https://doi.org/10.1016/S0143-4160(98)90056-2

Burrinha, T., & Cláudia, G. A. (2022). Aging impact on amyloid precursor protein neuronal trafficking. In *Current Opinion in Neurobiology* (Vol. 73). Elsevier Ltd. https://doi.org/10.1016/j.conb.2022.102524

Burrinha, T., Martinsson, I., Gomes, R., Terrasso, A. P., Gouras, G. K., & Almeida, C. G. (2021). Upregulation of APP endocytosis by neuronal aging drives amyloid-dependent synapse loss. *Journal of Cell Science*, *134*(9). https://doi.org/10.1242/jcs.255752

Bustin, S. A., Benes, V., Garson, J. A., Hellemans, J., Huggett, J., Kubista, M., Mueller, R., Nolan, T., Pfaffl, M. W., Shipley, G. L., Vandesompele, J., & Wittwer, C. T. (2009). The MIQE guidelines: Minimum information for

publication of quantitative real-time PCR experiments. *Clinical Chemistry*, *55*(4). https://doi.org/10.1373/clinchem.2008.112797

Cammalleri, M., Bagnoli, P., & Bigiani, A. (2019). Molecular and Cellular Mechanisms Underlying Somatostatin-Based Signaling in Two Model Neural Networks, the Retina and the Hippocampus. In *International journal of molecular sciences* (Vol. 20, Issue 10). https://doi.org/10.3390/ijms20102506

Cao, X., Cui, Z., Feng, R., Tang, Y. P., Qin, Z., Mei, B., & Tsien, J. Z. (2007). Maintenance of superior learning and memory function in NR2B transgenic mice during ageing. *European Journal of Neuroscience*, *25*(6). https://doi.org/10.1111/j.1460-9568.2007.05431.x

Cao, X., & Sudhof, T. C. (2001). A transcriptionally [correction of transcriptively] active complex of APP with Fe65 and histone acetyltransferase Tip60. *Science*, *293*(5527).

Carmignoto, G., & Vicini, S. (1992). Activity-dependent decrease in NMDA receptor responses during development of the visual cortex. *Science*, *258*(5084). https://doi.org/10.1126/science.1279803

Carta, M., Srikumar, B. N., Gorlewicz, A., Rebola, N., & Mulle, C. (2018). Activity-dependent control of NMDA receptor subunit composition at hippocampal mossy fibre synapses. *Journal of Physiology*, *596*(4). https://doi.org/10.1113/JP275226

Chang, Y., Tesco, G., Jeong, W. J., Lindsley, L., Eckman, E. A., Eckman, C. B., Tanzi, R. E., & Guénette, S. Y. (2003). Generation of the β-Amyloid Peptide and the Amyloid Precursor Protein C-terminal Fragment γ Are Potentiated by FE65L1. *Journal of Biological Chemistry*, *278*(51). https://doi.org/10.1074/jbc.M309561200

Chen, A. C., & Selkoe, D. J. (2007). Response to: Pardossi-Piquard et al., “Presenilin-Dependent Transcriptional Control of the Aβ-Degrading Enzyme Neprilysin by Intracellular Domains of βAPP and APLP.” Neuron 46, 541-554. In *Neuron* (Vol. 53, Issue 4). https://doi.org/10.1016/j.neuron.2007.01.023

Chen, C.-Y. (2017). Patch Clamp Technique and Applications. In *Modern Tools of Biophysics*. https://doi.org/10.1007/978-1-4939-6713-1_3

Chen, X., Levy, J. M., Hou, A., Winters, C., Azzam, R., Sousa, A. A., Leapman, R. D., Nicoll, R. A., & Reese, T. S. (2015). PSD-95 family MAGUKs are essential for anchoring AMPA and NMDA receptor complexes at the postsynaptic density. *Proceedings of the National Academy of Sciences of the United States of America*, *112*(50). https://doi.org/10.1073/pnas.1517045112

Chiu, A. M., Wang, J., Fiske, M. P., Hubalkova, P., Barse, L., Gray, J. A., & Sanz-Clemente, A. (2019). NMDAR-Activated PP1 Dephosphorylates GluN2B to Modulate NMDAR Synaptic Content. *Cell Reports*, *28*(2). https://doi.org/10.1016/j.celrep.2019.06.030

Cirrito, J. R., May, P. C., O’Dell, M. A., Taylor, J. W., Parsadanian, M., Cramer, J. W., Audia, J. E., Nissen, J. S., Bales, K. R., Paul, S. M., DeMattos, R. B., & Holtzman, D. M. (2003). In vivo assessment of brain interstitial fluid with microdialysis reveals plaque-associated changes in amyloid-β metabolism

and half-life. *Journal of Neuroscience*, *23*(26). https://doi.org/10.1523/jneurosci.23-26-08844.2003

Citri, A., & Malenka, R. C. (2008). Synaptic plasticity: Multiple forms, functions, and mechanisms. In *Neuropsychopharmacology* (Vol. 33, Issue 1). https://doi.org/10.1038/sj.npp.1301559

Citron, M., Oltersdorf, T., Haass, C., McConlogue, L., Hung, A. Y., Seubert, P., Vigo-Pelfrey, C., Lieberburg, I., & Selkoe, D. J. (1992). Mutation of the β-amyloid precursor protein in familial Alzheimer's disease increases β-protein production. *Nature*, *360*(6405). https://doi.org/10.1038/360672a0

Cizeron, M., Qiu, Z., Koniaris, B., Gokhale, R., Komiyama, N. H., Fransén, E., & Grant, S. G. N. (2020). A brainwide atlas of synapses across the mouse life span. *Science*, *369*(6501). https://doi.org/10.1126/science.aba3163

Clayton, D. A., & Browning, M. D. (2001). Deficits in the expression of the NR2B subunit in the hippocampus of aged Fisher 344 rats. *Neurobiology of Aging*, *22*(1). https://doi.org/10.1016/S0197-4580(00)00196-2

Cooke, S. F., & Bliss, T. V. P. (2006). Plasticity in the human central nervous system. In *Brain* (Vol. 129, Issue 7). https://doi.org/10.1093/brain/awl082

Copenhaver, P. F., & Kögel, D. (2017). Role of APP interactions with heterotrimeric G proteins: Physiological functions and pathological consequences. *Frontiers in Molecular Neuroscience*, *10*. https://doi.org/10.3389/fnmol.2017.00003

Corbel, C., Hernandez, I., Wu, B., & Kosik, K. S. (2015). Developmental attenuation of N-methyl-D-aspartate receptor subunit expression by microRNAs. *Neural Development*, *10*(1). https://doi.org/10.1186/s13064-015-0047-5

Coronel, R., Palmer, C., Bernabeu-Zornoza, A., Monteagudo, M., Rosca, A., Zambrano, A., & Liste, I. (2019). Physiological effects of amyloid precursor protein and its derivatives on neural stem cell biology and signaling pathways involved. In *Neural Regeneration Research* (Vol. 14, Issue 10). https://doi.org/10.4103/1673-5374.257511

Corrigan, F., Thornton, E., Roisman, L. C., Leonard, A. v., Vink, R., Blumbergs, P. C., van den Heuvel, C., & Cappai, R. (2014). The neuroprotective activity of the amyloid precursor protein against traumatic brain injury is mediated via the heparin binding site in residues 96-110. *Journal of Neurochemistry*, *128*(1). https://doi.org/10.1111/jnc.12391

Costandi, M. (2016). *Neuroplasticity*. The MIT Press.

Cousins, S. L., Dai, W., & Stephenson, F. A. (2015). APLP1 and APLP2, members of the APP family of proteins, behave similarly to APP in that they associate with NMDA receptors and enhance NMDA receptor surface expression. *Journal of Neurochemistry*, *133*(6). https://doi.org/10.1111/jnc.13063

Cousins, S. L., Hoey, S. E. A., Anne Stephenson, F., & Perkinton, M. S. (2009). Amyloid precursor protein 695 associates with assembled NR2A- and NR2B-containing NMDA receptors to result in the enhancement of their cell surface delivery. *Journal of Neurochemistry*, *111*(6). https://doi.org/10.1111/j.1471-4159.2009.06424.x

Creeley, C., Wozniak, D. F., Labruyere, J., Taylor, G. T., & Olney, J. W. (2006). Low doses of memantine disrupt memory in adult rats. *Journal of Neuroscience*, *26*(15). https://doi.org/10.1523/JNEUROSCI.4883-05.2006

Cui, H., Hung, A. C., Klaver, D. W., Suzuki, T., Freeman, C., Narkowicz, C., Jacobson, G. A., & Small, D. H. (2011). Effects of heparin and enoxaparin on APP processing and aβ production in primary cortical neurons from Tg2576 mice. *PLoS ONE*, *6*(7). https://doi.org/10.1371/journal.pone.0023007

Cupers, P., Orlans, I., Craessaerts, K., Annaert, W., & de Strooper, B. (2001). The amyloid precursor protein (APP)-cytoplasmic fragment generated by γ-secretase is rapidly degraded but distributes partially in a nuclear fraction of neurones in culture. *Journal of Neurochemistry*, *78*(5), 1168–1178. https://doi.org/10.1046/j.1471-4159.2001.00516.x

Dalva, M. B., McClelland, A. C., & Kayser, M. S. (2007). Cell adhesion molecules: Signalling functions at the synapse. In *Nature Reviews Neuroscience* (Vol. 8, Issue 3). https://doi.org/10.1038/nrn2075

Dalva, M. B., Takasu, M. A., Lin, M. Z., Shamah, S. M., Hu, L., Gale, N. W., & Greenberg, M. E. (2000). EphB receptors interact with NMDA receptors and regulate excitatory synapse formation. *Cell*, *103*(6). https://doi.org/10.1016/S0092-8674(00)00197-5

Danysz, W., & Parsons, C. G. (2003). The NMDA receptor antagonist memantine as a symptomatological and neuroprotective treatment for Alzheimer's disease: Preclinical evidence. *International Journal of Geriatric Psychiatry*, *18*(SUPPL. 1). https://doi.org/10.1002/gps.938

Das, U., Scott, D. A., Ganguly, A., Koo, E. H., Tang, Y., & Roy, S. (2013). Activity-induced convergence of app and bace-1 in acidic microdomains via an endocytosis-dependent pathway. *Neuron*, *79*(3). https://doi.org/10.1016/j.neuron.2013.05.035

Dawkins, E., & Small, D. H. (2014). Insights into the physiological function of the β-amyloid precursor protein: Beyond Alzheimer's disease. In *Journal of Neurochemistry* (Vol. 129, Issue 5). https://doi.org/10.1111/jnc.12675

Dawson, G. R., Seabrook, G. R., Zheng, H., Smith, D. W., Graham, S., O'Dowd, G., Bowery, B. J., Boyce, S., Trumbauer, M. E., Chen, H. Y., van der Ploeg, L. H. T., & Sirinathsinghji, D. J. S. (1999). Age-related cognitive deficits, impaired long-term potentiation and reduction in synaptic marker density in mice lacking the β-amyloid precursor protein. *Neuroscience*, *90*(1). https://doi.org/10.1016/S0306-4522(98)00410-2

de Coninck, D., Schmidt, T. H., Schloetel, J. G., & Lang, T. (2018). Packing Density of the Amyloid Precursor Protein in the Cell Membrane. *Biophysical Journal*, *114*(5). https://doi.org/10.1016/j.bpj.2018.01.009

de Roo, M., Klauser, P., Mendez, P., Poglia, L., & Muller, D. (2008). Activity-dependent PSD formation and stabilization of newly formed spines in hippocampal slice cultures. *Cerebral Cortex*, *18*(1). https://doi.org/10.1093/cercor/bhm041

del Prete, D., Lombino, F., Liu, X., & D'Adamio, L. (2014). APP is cleaved by bace1 in pre-synaptic vesicles and establishes a pre-synaptic interactome,

viaIts intracellular domain, with molecular complexes that regulate pre-synaptic vesicles functions. *PLoS ONE*, *9*(9). https://doi.org/10.1371/journal.pone.0108576

del Turco, D., Paul, M. H., Schlaudraff, J., Hick, M., Endres, K., Müller, U. C., & Deller, T. (2016). Region-specific differences in amyloid precursor protein expression in the mouse hippocampus. *Frontiers in Molecular Neuroscience*, *9*(NOV2016). https://doi.org/10.3389/fnmol.2016.00134

Delbove, C. E., Deng, X. Z., & Zhang, Q. (2018). The Fate of Nascent APP in Hippocampal Neurons: A Live Cell Imaging Study. *ACS Chemical Neuroscience*, *9*(9). https://doi.org/10.1021/acschemneuro.8b00226

Delport, A., & Hewer, R. (2022). The amyloid precursor protein: a converging point in Alzheimer's disease. In *Molecular Neurobiology* (Vol. 59, Issue 7, pp. 4501–4516). Springer. https://doi.org/10.1007/s12035-022-02863-x

Deyts, C., Vetrivel, K. S., Das, S., Shepherd, Y. M., Dupré, D. J., Thinakaran, G., & Parent, A. T. (2012). Novel Gα S-protein signaling associated with membrane-tethered amyloid precursor protein intracellular domain. *Journal of Neuroscience*, *32*(5). https://doi.org/10.1523/JNEUROSCI.5433-11.2012

Doody, R. S., Raman, R., Farlow, M., Iwatsubo, T., Vellas, B., Joffe, S., Kieburtz, K., He, F., Sun, X., Thomas, R. G., Aisen, P. S., Siemers, E., Sethuraman, G., & Mohs, R. (2013). A Phase 3 Trial of Semagacestat for Treatment of Alzheimer's Disease. *New England Journal of Medicine*, *369*(4). https://doi.org/10.1056/nejmoa1210951

Dudek, H., Ghosh, A., & Greenberg, M. E. (1998). Calcium Phosphate Transfection of DNA into Neurons in Primary Culture. *Current Protocols in Neuroscience*, *3*(1). https://doi.org/10.1002/0471142301.ns0311s03

Dumas, T. C. (2005). Developmental regulation of cognitive abilities: Modified composition of a molecular switch turns on associative learning. In *Progress in Neurobiology* (Vol. 76, Issue 3). https://doi.org/10.1016/j.pneurobio.2005.08.002

Durand, G. M., & Konnerth, A. (1996). Long-term potentiation as a mechanism of functional synapse induction in the developing hippocampus. *Journal of Physiology Paris*, *90*(5–6). https://doi.org/10.1016/S0928-4257(97)87905-3

Eason, M. G., Kurose, H., Holt, B. D., Raymond, J. R., & Liggett, S. B. (1992). Simultaneous coupling of α2-adrenergic receptors to two G-proteins with opposing effects: Subtype-selective coupling of α2C10, α2C4, and α2C2 adrenergic receptors to G(i) and G(s). *Journal of Biological Chemistry*, *267*(22).

Eckles-Smith, K., Clayton, D., Bickford, P., & Browning, M. D. (2000). Caloric restriction prevents age-related deficits in LTP and in NMDA receptor expression. *Molecular Brain Research*, *78*(1–2). https://doi.org/10.1016/S0169-328X(00)00088-7

Edbauer, D., Willem, M., Lammich, S., Steiner, H., & Haass, C. (2002). Insulin-degrading enzyme rapidly removes the β-amyloid precursor protein intracellular domain (AICD). *Journal of Biological Chemistry*, *277*(16). https://doi.org/10.1074/jbc.M111571200

Egan, M. F., Kost, J., Tariot, P. N., Aisen, P. S., Cummings, J. L., Vellas, B., Sur, C., Mukai, Y., Voss, T., Furtek, C., Mahoney, E., Harper Mozley, L., Vandenberghe, R., Mo, Y., & Michelson, D. (2018). Randomized Trial of Verubecestat for Mild-to-Moderate Alzheimer's Disease. *New England Journal of Medicine*, *378*(18). https://doi.org/10.1056/nejmoa1706441

Eggert, S., Paliga, K., Soba, P., Evin, G., Masters, C. L., Weidemann, A., & Beyreuther, K. (2004). The proteolytic processing of the amyloid precursor protein gene family members APLP-1 and APLP-2 involves α-, β-, γ-, and ε-Like cleavages: Modulation of APLP-1 processing by N-glycosylation. *Journal of Biological Chemistry*, *279*(18). https://doi.org/10.1074/jbc.M311601200

Eggert, S., Thomas, C., Kins, S., & Hermey, G. (2018). Trafficking in Alzheimer's Disease: Modulation of APP Transport and Processing by the Transmembrane Proteins LRP1, SorLA, SorCS1c, Sortilin, and Calsyntenin. In *Molecular Neurobiology* (Vol. 55, Issue 7). https://doi.org/10.1007/s12035-017-0806-x

Elias, G. M., Elias, L. A. B., Apostolides, P. F., Kriegstein, A. R., & Nicoll, R. A. (2008). Differential trafficking of AMPA and NMDA receptors by SAP102 and PSD-95 underlies synapse development. *Proceedings of the National Academy of Sciences of the United States of America*, *105*(52). https://doi.org/10.1073/pnas.0811025106

Erreger, K., Dravid, S. M., Banke, T. G., Wyllie, D. J. A., & Traynelis, S. F. (2005). Subunit-specific gating controls rat NR1/NR2A and NR1/NR2B NMDA channel kinetics and synaptic signalling profiles. *Journal of Physiology*, *563*(2). https://doi.org/10.1113/jphysiol.2004.080028

Fanutza, T., del Prete, D., Ford, M. J., Castillo, P. E., & D'Adamio, L. (2015). APP and APLP2 interact with the synaptic release machinery and facilitate transmitter release at hippocampal synapses. *ELife*, *4*(NOVEMBER2015). https://doi.org/10.7554/eLife.09743

Farber, S. A., Nitsch, R. M., Schulz, J. G., & Wurtman, R. J. (1995). Regulated secretion of β-amyloid precursor protein in rat brain. *Journal of Neuroscience*, *15*(11). https://doi.org/10.1523/jneurosci.15-11-07442.1995

Faria-Pereira, A., Temido-Ferreira, M., & Morais, V. A. (2022). BrainPhys Neuronal Media Support Physiological Function of Mitochondria in Mouse Primary Neuronal Cultures. *Frontiers in Molecular Neuroscience*, *15*. https://doi.org/10.3389/fnmol.2022.837448

Feilen, L. P., Haubrich, K., Strecker, P., Probst, S., Eggert, S., Stier, G., Sinning, I., Konietzko, U., Kins, S., Simon, B., & Wild, K. (2017). Fe65-PTB2 dimerization mimics Fe65-APP interaction. *Frontiers in Molecular Neuroscience*, *10*. https://doi.org/10.3389/fnmol.2017.00140

Ferreira, D. G., Temido-Ferreira, M., Miranda, H. V., Batalha, V. L., Coelho, J. E., Szegö, É. M., Marques-Morgado, I., Vaz, S. H., Rhee, J. S., Schmitz, M., Zerr, I., Lopes, L. v., & Outeiro, T. F. (2017). α-synuclein interacts with PrP C to induce cognitive impairment through mGluR5 and NMDAR2B. *Nature Neuroscience*, *20*(11). https://doi.org/10.1038/nn.4648

Ferreira, J. S., Papouin, T., Ladépêche, L., Yao, A., Langlais, V. C., Bouchet, D., Dulong, J., Mothet, J. P., Sacchi, S., Pollegioni, L., Paoletti, P., Richard Oliet,

S. H., & Groc, L. (2017). Co-agonists differentially tune GluN2B-NMDA receptor trafficking at hippocampal synapses. *ELife*, *6*. https://doi.org/10.7554/eLife.25492

Ferreira, J. S., Schmidt, J., Rio, P., Águas, R., Rooyakkers, A., Li, K. W., Smit, A. B., Craig, A. M., & Carvalho, A. L. (2015). GluN2B-containing NMDA receptors regulate AMPA receptor traffic through anchoring of the synaptic proteasome. *Journal of Neuroscience*, *35*(22). https://doi.org/10.1523/JNEUROSCI.3567-14.2015

Ferrer-Raventós, P., Puertollano-Martín, D., Querol-Vilaseca, M., Sánchez-Aced, É., Valle-Tamayo, N., Cervantes-Gonzalez, A., Nuñez-Llaves, R., Pegueroles, J., Dols-Icardo, O., Iulita, M. F., Aldecoa, I., Molina-Porcel, L., Sánchez-Valle, R., Fortea, J., Belbin, O., Sirisi, S., & Lleó, A. (2023). Amyloid Precursor Protein *β*CTF accumulates in synapses in sporadic and genetic forms of Alzheimer's disease. *Neuropathology and Applied Neurobiology*. https://doi.org/10.1111/nan.12879

Filser, S., Ovsepian, S. v., Masana, M., Blazquez-Llorca, L., Elvang, A. B., Volbracht, C., Müller, M. B., Jung, C. K. E., & Herms, J. (2015). Pharmacological inhibition of BACE1 impairs synaptic plasticity and cognitive functions. *Biological Psychiatry*, *77*(8). https://doi.org/10.1016/j.biopsych.2014.10.013

Fischer, W., Gage, F. H., & Björklund, A. (1989). Degenerative Changes in Forebrain Cholinergic Nuclei Correlate with Cognitive Impairments in Aged Rats. *European Journal of Neuroscience*, *1*(1). https://doi.org/10.1111/j.1460-9568.1989.tb00772.x

Flurkey, K., Currer, J. M., & Harrison, D. E. (2007). Mouse Models in Aging Research. In *The Mouse in Biomedical Research* (Vol. 3). https://doi.org/10.1016/B978-012369454-6/50074-1

Fonseca-Gomes, J., Jerónimo-Santos, A., Lesnikova, A., Casarotto, P., Castrén, E., Sebastião, A. M., & Diógenes, M. J. (2019). TrkB-ICD fragment, originating from BDNF receptor cleavage, is translocated to cell nucleus and phosphorylates nuclear and axonal proteins. *Frontiers in Molecular Neuroscience*, *12*. https://doi.org/10.3389/fnmol.2019.00004

Forrest, D., Yuzaki, M., Soares, H. D., Ng, L., Luk, D. C., Sheng, M., Stewart, C. L., Morgan, J. I., Connor, J. A., & Curran, T. (1994). Targeted disruption of NMDA receptor 1 gene abolishes NMDA response and results in neonatal death. *Neuron*, *13*(2). https://doi.org/10.1016/0896-6273(94)90350-6

Frandemiche, M. L., de Seranno, S., Rush, T., Borel, E., Elie, A., Arnal, I., Lanté, F., & Buisson, A. (2014). Activity-dependent tau protein translocation to excitatory synapse is disrupted by exposure to amyloid-beta oligomers. *Journal of Neuroscience*, *34*(17). https://doi.org/10.1523/JNEUROSCI.4261-13.2014

Freitas, C., Perez, J., Knobel, M., Tormos, J. M., Oberman, L., Eldaief, M., Bashir, S., Vernet, M., Peña-Gómez, C., & Pascual-Leone, A. (2011). Changes in cortical plasticity across the lifespan. *Frontiers in Aging Neuroscience*, *3*(APR). https://doi.org/10.3389/fnagi.2011.00005

Fukumoto, H., Rosene, D. L., Moss, M. B., Raju, S., Hyman, B. T., & Irizarry, M. C. (2004). β-Secretase Activity Increases with Aging in Human, Monkey, and Mouse Brain. *American Journal of Pathology*, *164*(2). https://doi.org/10.1016/S0002-9440(10)63159-8

Gambrill, A. C., & Barria, A. (2011). NMDA receptor subunit composition controls synaptogenesis and synapse stabilization. *Proceedings of the National Academy of Sciences of the United States of America*, *108*(14). https://doi.org/10.1073/pnas.1012676108

Gao, X., Pellois, J. P., Na, Y., Kim, Y., Gulari, E., & Zhou, X. (2004). High density peptide microarrays. In situ synthesis and applications. In *Molecular Diversity* (Vol. 8, Issue 3). https://doi.org/10.1023/B:MODI.0000036233.58271.25

Gao, Y., & Pimplikar, S. W. (2001). The γ-secretase-cleaved C-terminal fragment of amyloid precursor protein mediates signaling to the nucleus. *Proceedings of the National Academy of Sciences of the United States of America*, *98*(26). https://doi.org/10.1073/pnas.261463298

Garaschuk, O., Schneggenburger, R., Schirra, C., Tempia, F., & Konnerth, A. (1996). Fractional Ca2+ currents through somatic and dendritic glutamate receptor channels of rat hippocampal CA1 pyramidal neurones. *Journal of Physiology*, *491*(3). https://doi.org/10.1113/jphysiol.1996.sp021255

Ghosal, K., Vogt, D. L., Liang, M., Shen, Y., Lamb, B. T., & Pimplikar, S. W. (2009). Alzheimer's disease-like pathological features in transgenic mice expressing the APP intracellular domain. *Proceedings of the National Academy of Sciences of the United States of America*, *106*(43). https://doi.org/10.1073/pnas.0907652106

Goedert, M. (1987). Neuronal localization of amyloid beta protein precursor mRNA in normal human brain and in Alzheimer's disease. *The EMBO Journal*, *6*(12). https://doi.org/10.1002/j.1460-2075.1987.tb02694.x

Goldman-Rakic, P. S. (1987). Development of cortical circuitry and cognitive function. *Child Development*, *58*(3). https://doi.org/10.1111/j.1467-8624.1987.tb01404.x

Gómez de Salazar, M., Grau, C., Ciruela, F., & Altafaj, X. (2018). Phosphoproteomic Alterations of Ionotropic Glutamate Receptors in the Hippocampus of the Ts65Dn Mouse Model of Down Syndrome. *Frontiers in Molecular Neuroscience*, *11*. https://doi.org/10.3389/fnmol.2018.00226

Gonzalez-Lozano, M. A., Klemmer, P., Gebuis, T., Hassan, C., van Nierop, P., van Kesteren, R. E., Smit, A. B., & Li, K. W. (2016). Dynamics of the mouse brain cortical synaptic proteome during postnatal brain development. *Scientific Reports*, *6*. https://doi.org/10.1038/srep35456

Goodger, Z. v., Rajendran, L., Trutzel, A., Kohli, B. M., Nitsch, R. M., & Konietzko, U. (2009). Nuclear signaling by the APP intracellular domain occurs predominantly through the amyloidogenic processing pathway. *Journal of Cell Science*, *122*(20). https://doi.org/10.1242/jcs.048090

Grabrucker, A., Vaida, B., Bockmann, J., & Boeckers, T. M. (2009). Synaptogenesis of hippocampal neurons in primary cell culture. *Cell and Tissue Research*, *338*(3). https://doi.org/10.1007/s00441-009-0881-z

Grau, C., Arató, K., Fernández-Fernández, J. M., Valderrama, A., Sindreu, C., Fillat, C., Ferrer, I., de la Luna, S., & Altafaj, X. (2014). DYRK1A-mediated phosphorylation of GluN2A at ser1048 regulates the surface expression and channel activity of GluN1/GluN2A receptors. *Frontiers in Cellular Neuroscience*, *8*(OCT). https://doi.org/10.3389/fncel.2014.00331

Gray, J. A., Shi, Y., Usui, H., During, M. J., Sakimura, K., & Nicoll, R. A. (2011). Distinct Modes of AMPA Receptor Suppression at Developing Synapses by GluN2A and GluN2B: Single-Cell NMDA Receptor Subunit Deletion In Vivo. *Neuron*, *71*(6). https://doi.org/10.1016/j.neuron.2011.08.007

Grimm, M. O. W., Mett, J., Stahlmann, C. P., Haupenthal, V. J., Zimmer, V. C., & Hartmann, T. (2013). Neprilysin and Aβ clearance: Impact of the APP intracellular domain in NEP regulation and implications in Alzheimer's disease. In *Frontiers in Aging Neuroscience* (Vol. 5, Issue DEC). https://doi.org/10.3389/fnagi.2013.00098

Groc, L., & Choquet, D. (2020). Linking glutamate receptor movements and synapse function. In *Science* (Vol. 368, Issue 6496). https://doi.org/10.1126/science.aay4631

Groc, L., Choquet, D., Stephenson, F. A., Verrier, D., Manzoni, O. J., & Chavis, P. (2007). NMDA receptor surface trafficking and synaptic subunit composition are developmentally regulated by the extracellular matrix protein reelin. *Journal of Neuroscience*, *27*(38). https://doi.org/10.1523/JNEUROSCI.1772-07.2007

Groc, L., Heine, M., Cousins, S. L., Stephenson, F. A., Lounis, B., Cognet, L., & Choquet, D. (2006). NMDA receptor surface mobility depends on NR2A-2B subunits. *Proceedings of the National Academy of Sciences of the United States of America*, *103*(49). https://doi.org/10.1073/pnas.0605238103

Gruart, A., Muñoz, M. D., & Delgado-García, J. M. (2006). Involvement of the CA3-CA1 synapse in the acquisition of associative learning in behaving mice. *Journal of Neuroscience*, *26*(4). https://doi.org/10.1523/JNEUROSCI.2834-05.2006

Gu, Y., & Huganir, R. L. (2016). Identification of the SNARE complex mediating the exocytosis of NMDA receptors. *Proceedings of the National Academy of Sciences of the United States of America*, *113*(43). https://doi.org/10.1073/pnas.1614042113

Guénette, S., Chang, Y., Hiesberger, T., Richardson, J. A., Eckman, C. B., Eckman, E. A., Hammer, R. E., & Herz, J. (2006). Essential roles for the FE65 amyloid precursor protein-interacting proteins in brain development. *EMBO Journal*, *25*(2). https://doi.org/10.1038/sj.emboj.7600926

Gulisano, W., Melone, M., Li Puma, D. D., Tropea, M. R., Palmeri, A., Arancio, O., Grassi, C., Conti, F., & Puzzo, D. (2018). The effect of amyloid-β peptide on synaptic plasticity and memory is influenced by different isoforms, concentrations, and aggregation status. *Neurobiology of Aging*, *71*. https://doi.org/10.1016/j.neurobiolaging.2018.06.025

Guo, Q., Li, H., Gaddam, S. S. K., Justice, N. J., Robertson, C. S., & Zheng, H. (2012). Amyloid Precursor Protein Revisited. *Journal of Biological Chemistry*, *287*(4). https://doi.org/10.1074/jbc.m111.315051

Haapasalo, A., & Kovacs, D. M. (2011). The many substrates of presenilin/γ-secretase. In *Journal of Alzheimer's Disease* (Vol. 25, Issue 1). https://doi.org/10.3233/JAD-2011-101065

Haass, C., Kaether, C., Thinakaran, G., & Sisodia, S. (2012). Trafficking and proteolytic processing of APP. *Cold Spring Harbor Perspectives in Medicine*, *2*(5). https://doi.org/10.1101/cshperspect.a006270

Hajieva, P., Kuhlmann, C., Luhmann, H. J., & Behl, C. (2009). Impaired calcium homeostasis in aged hippocampal neurons. *Neuroscience Letters*, *451*(2). https://doi.org/10.1016/j.neulet.2008.11.068

Hall, B. J., Ripley, B., & Ghosh, A. (2007). NR2B signaling regulates the development of synaptic AMPA receptor current. *Journal of Neuroscience*, *27*(49). https://doi.org/10.1523/JNEUROSCI.3793-07.2007

Hampel, H., Hardy, J., Blennow, K., Chen, C., Perry, G., Kim, S. H., Villemagne, V. L., Aisen, P., Vendruscolo, M., Iwatsubo, T., Masters, C. L., Cho, M., Lannfelt, L., Cummings, J. L., & Vergallo, A. (2021). The Amyloid-β Pathway in Alzheimer's Disease. In *Molecular Psychiatry* (Vol. 26, Issue 10). https://doi.org/10.1038/s41380-021-01249-0

Hansen, K. B., Ogden, K. K., & Traynelis, S. F. (2012). Subunit-selective allosteric inhibition of glycine binding to NMDA receptors. *Journal of Neuroscience*, *32*(18). https://doi.org/10.1523/JNEUROSCI.5757-11.2012

Hardy, J. A., & Higgins, G. A. (1992). Alzheimer's disease: The amyloid cascade hypothesis. In *Science* (Vol. 256, Issue 5054). https://doi.org/10.1126/science.1566067

Hauck, B., Chen, L., & Xiao, W. (2003). Generation and characterization of chimeric recombinant AAV vectors. *Molecular Therapy*, *7*(3). https://doi.org/10.1016/S1525-0016(03)00012-1

Hawkins, L. M., Prybylowski, K., Chang, K., Moussan, C., Stephenson, F. A., & Wenthold, R. J. (2004). Export from the endoplasmic reticulum of assembled N-methyl-D-aspartic acid receptors is controlled by a motif in the C terminus of the NR2 subunit. *Journal of Biological Chemistry*, *279*(28). https://doi.org/10.1074/jbc.M402599200

Haytural, H., Lundgren, J. L., Köse, T. B., Jordà-Siquier, T., Kalcheva, M., Seed Ahmed, M., Winblad, B., Sundström, E., Barthet, G., Tjernberg, L. O., & Frykman, S. (2019). Non-specific Detection of a Major Western Blotting Band in Human Brain Homogenates by a Multitude of Amyloid Precursor Protein Antibodies. *Frontiers in Aging Neuroscience*, *11*. https://doi.org/10.3389/fnagi.2019.00273

Heber, S., Herms, J., Gajic, V., Hainfellner, J., Aguzzi, A., Rulicke, T., Kretzschmar, H., von Koch, C., Sisodia, S., Tremml, P., Lipp, H. P., Wolfer, D. P., & Muller, U. (2000). Mice with combined gene knock-outs reveal essential and partially redundant functions of amyloid precursor protein family members. *Journal of Neuroscience*, *20*(21). https://doi.org/10.1523/jneurosci.20-21-07951.2000

Hébert, S. S., Serneels, L., Tolia, A., Craessaerts, K., Derks, C., Filippov, M. A., Müller, U., & de Strooper, B. (2006). Regulated intramembrane proteolysis of

amyloid precursor protein and regulation of expression of putative target genes. *EMBO Reports*, *7*(7). https://doi.org/10.1038/sj.embor.7400704

Hee, J. C., Yan, H. H., Lau, L. F., & Huganir, R. L. (2004). Regulation of the NMDA receptor complex and trafficking by activity-dependent phosphorylation of the NR2B subunit PDZ ligand. *Journal of Neuroscience*, *24*(45). https://doi.org/10.1523/JNEUROSCI.0546-04.2004

Hefter, D., Kaiser, M., Weyer, S. W., Papageorgiou, I. E., Both, M., Kann, O., Müller, U. C., & Draguhn, A. (2016). Amyloid precursor protein protects neuronal network function after hypoxia via control of voltage-gated calcium channels. *Journal of Neuroscience*, *36*(32). https://doi.org/10.1523/JNEUROSCI.4130-15.2016

Herms, J., Anliker, B., Heber, S., Ring, S., Fuhrmann, M., Kretzschmar, H., Sisodia, S., & Müller, U. (2004). Cortical dysplasia resembling human type 2 lissencephaly in mice lacking all three APP family members. *EMBO Journal*, *23*(20). https://doi.org/10.1038/sj.emboj.7600390

Hick, M., Herrmann, U., Weyer, S. W., Mallm, J. P., Tschäpe, J. A., Borgers, M., Mercken, M., Roth, F. C., Draguhn, A., Slomianka, L., Wolfer, D. P., Korte, M., & Müller, U. C. (2015). Acute function of secreted amyloid precursor protein fragment APPsα in synaptic plasticity. *Acta Neuropathologica*, *129*(1). https://doi.org/10.1007/s00401-014-1368-x

Higgins, G. A., Lewis, D. A., Bahmanyar, S., Goldgaber, D., Gajdusek, D. C., Young, W. G., Morrison, J. H., & Wilson, M. C. (1988). Differential regulation of amyloid-β-protein mRNA expression within hippocampal neuronal subpopulations in Alzheimer disease. *Proceedings of the National Academy of Sciences of the United States of America*, *85*(4). https://doi.org/10.1073/pnas.85.4.1297

Hoe, H. S., Fu, Z., Makarova, A., Lee, J. Y., Lu, C., Feng, L., Pajoohesh-Ganji, A., Matsuoka, Y., Hyman, B. T., Ehlers, M. D., Vicini, S., Pak, D. T. S., & Rebeck, G. W. (2009). The effects of amyloid precursor protein on postsynaptic composition and activity. *Journal of Biological Chemistry*, *284*(13). https://doi.org/10.1074/jbc.M900141200

Hoefgen, S., Coburger, I., Roeser, D., Schaub, Y., Dahms, S. O., & Than, M. E. (2014). Heparin induced dimerization of APP is primarily mediated by E1 and regulated by its acidic domain. *Journal of Structural Biology*, *187*(1). https://doi.org/10.1016/j.jsb.2014.05.006

Hoey, S. E., Williams, R. J., & Perkinton, M. S. (2009). Synaptic NMDA receptor activation stimulates α-secretase amyloid precursor protein processing and inhibits amyloid-β Production. *Journal of Neuroscience*, *29*(14). https://doi.org/10.1523/JNEUROSCI.6017-08.2009

Holehonnur, R., Phensy, A. J., Kim, L. J., Milivojevic, M., Vuong, D., Daison, D. K., Alex, S., Tiner, M., Jones, L. E., Kroener, S., & Ploski, J. E. (2016). Increasing the GluN2A/GluN2B ratio in neurons of the mouse basal and lateral amygdala inhibits the modification of an existing fear memory trace. *Journal of Neuroscience*, *36*(36). https://doi.org/10.1523/JNEUROSCI.1743-16.2016

Hruska, M., Cain, R. E., & Dalva, M. B. (2022). Nanoscale rules governing the organization of glutamate receptors in spine synapses are subunit specific. *Nature Communications*, *13*(1). https://doi.org/10.1038/s41467-022-28504-4

Hsia, A. Y., Malenka, R. C., & Nicoll, R. A. (1998). Development of excitatory circuitry in the hippocampus. *Journal of Neurophysiology*, *79*(4). https://doi.org/10.1152/jn.1998.79.4.2013

Huh, K. H., & Wenthold, R. J. (1999). Turnover analysis of glutamate receptors identifies a rapidly degraded pool of the N-methyl-D-aspartate receptor subunit, NR1, in cultured cerebellar granule cells. *Journal of Biological Chemistry*, *274*(1). https://doi.org/10.1074/jbc.274.1.151

Hunter, S., & Brayne, C. (2012). Relationships between the amyloid precursor protein and its various proteolytic fragments and neuronal systems. In *Alzheimer's Research and Therapy* (Vol. 4, Issue 2). https://doi.org/10.1186/alzrt108

Huttenlocher, P. R., & Dabholkar, A. S. (1997). Regional differences in synaptogenesis in human cerebral cortex. *Journal of Comparative Neurology*, *387*(2). https://doi.org/10.1002/(SICI)1096-9861(19971020)387:2<167::AID-CNE1>3.0.CO;2-Z

Huttenlocher, P. R., de Courten, C., Garey, L. J., & van der Loos, H. (1982). Synaptogenesis in human visual cortex - evidence for synapse elimination during normal development. *Neuroscience Letters*, *33*(3). https://doi.org/10.1016/0304-3940(82)90379-2

Ishida, A., Furukawa, K., Keller, J. N., & Mattson, M. P. (1997). Secreted form of β-amyloid precursor protein shifts the frequency dependency for induction of LTD, and enhances LTP in hippocampal slices. *NeuroReport*, *8*(9–10). https://doi.org/10.1097/00001756-199707070-00009

Ishida, T., & Kinoshita, K. (2007). PrDOS: Prediction of disordered protein regions from amino acid sequence. *Nucleic Acids Research*, *35*(SUPPL.2). https://doi.org/10.1093/nar/gkm363

Isshiki, M., Tanaka, S., Kuriu, T., Tabuchi, K., Takumi, T., & Okabe, S. (2014). Enhanced synapse remodelling as a common phenotype in mouse models of autism. *Nature Communications*, *5*. https://doi.org/10.1038/ncomms5742

Ito, I., Futai, K., Katagiri, H., Watanabe, M., Sakimura, K., Mishina, M., & Sugiyama, H. (1997). Synapse-selective impairment of NMDA receptor functions in mice lacking NMDA receptor ε1 or ε2 subunit. *Journal of Physiology*, *500*(2). https://doi.org/10.1113/jphysiol.1997.sp022030

Jantzie, L. L., Talos, D. M., Jackson, M. C., Park, H. K., Graham, D. A., Lechpammer, M., Folkerth, R. D., Volpe, J. J., & Jensen, F. E. (2015). Developmental expression of N-methyl-d-aspartate (NMDA) receptor subunits in human white and gray matter: Potential mechanism of increased vulnerability in the immature brain. *Cerebral Cortex*, *25*(2). https://doi.org/10.1093/cercor/bht246

Jeyifous, O., Waites, C. L., Specht, C. G., Fujisawa, S., Schubert, M., Lin, E. I., Marshall, J., Aoki, C., de Silva, T., Montgomery, J. M., Garner, C. C., Green, W. N., Silva, T. de, & Johanna, M. (2009). SAP97 and CASK mediate sorting

of N-Methyl-D-Aspartate Receptors through a novel secretory pathway. *Nature …*, *12*(8).

Jiang, M., Deng, L., & Chen, G. (2004). High Ca2+-phosphate transfection efficiency enables single neuron gene analysis. *Gene Therapy*, *11*(17). https://doi.org/10.1038/sj.gt.3302305

Jonsson, T., Atwal, J. K., Steinberg, S., Snaedal, J., Jonsson, P. v., Bjornsson, S., Stefansson, H., Sulem, P., Gudbjartsson, D., Maloney, J., Hoyte, K., Gustafson, A., Liu, Y., Lu, Y., Bhangale, T., Graham, R. R., Huttenlocher, J., Bjornsdottir, G., Andreassen, O. A., … Stefansson, K. (2012). A mutation in APP protects against Alzheimer's disease and age-related cognitive decline. *Nature*, *488*(7409). https://doi.org/10.1038/nature11283

Jordà-Siquier, T., Petrel, M., Kouskoff, V., Smailovic, U., Cordelières, F., Frykman, S., Müller, U., Mulle, C., & Barthet, G. (2022). APP accumulates with presynaptic proteins around amyloid plaques: A role for presynaptic mechanisms in Alzheimer's disease? *Alzheimer's and Dementia*, *18*(11). https://doi.org/10.1002/alz.12546

Jouvenceau, A., Dutar, P., & Billard, J. M. (1998). Alteration of NMDA receptor-mediated synaptic responses in CA1 area of the aged rat hippocampus: Contribution of GABAergic and cholinergic deficits. *Hippocampus*, *8*(6). https://doi.org/10.1002/(SICI)1098-1063(1998)8:6<627::AID-HIPO5>3.0.CO;2-X

Kamal, A., Stokin, G. B., Yang, Z., Xia, C. H., & Goldstein, L. S. B. (2000). Axonal transport of amyloid precursor protein is mediated by direct binding to the kinesin light chain subunit of kinesin-I. *Neuron*, *28*(2). https://doi.org/10.1016/S0896-6273(00)00124-0

Kamenetz, F., Tomita, T., Hsieh, H., Seabrook, G., Borchelt, D., Iwatsubo, T., Sisodia, S., & Malinow, R. (2003). APP Processing and Synaptic Function. *Neuron*, *37*(6). https://doi.org/10.1016/S0896-6273(03)00124-7

Karakas, E., & Furukawa, H. (2014). Crystal structure of a heterotetrameric NMDA receptor ion channel. *Science*, *344*(6187). https://doi.org/10.1126/science.1251915

Karakas, E., Simorowski, N., & Furukawa, H. (2011). Subunit arrangement and phenylethanolamine binding in GluN1/GluN2B NMDA receptors. *Nature*, *475*(7355). https://doi.org/10.1038/nature10180

Kay, K. R., Smith, C., Wright, A. K., Serrano-Pozo, A., Pooler, A. M., Koffie, R., Bastin, M. E., Bak, T. H., Abrahams, S., Kopeikina, K. J., McGuone, D., Frosch, M. P., Gillingwater, T. H., Hyman, B. T., & Spires-Jones, T. L. (2013). Studying synapses in human brain with array tomography and electron microscopy. *Nature Protocols*, *8*(7). https://doi.org/10.1038/nprot.2013.078

Kedia, S., Ramakrishna, P., Netrakanti, P. R., Jose, M., Sibarita, J. B., Nadkarni, S., & Nair, D. (2020). Real-time nanoscale organization of amyloid precursor protein. *Nanoscale*, *12*(15). https://doi.org/10.1039/d0nr00052c

Kew, J. N. C., & Kemp, J. A. (2005). Ionotropic and metabotropic glutamate receptor structure and pharmacology. In *Psychopharmacology* (Vol. 179, Issue 1). https://doi.org/10.1007/s00213-005-2200-z

Kim, H.-S., Kim, E.-M., Lee, J.-P., Park, C. H., Kim, S., Seo, J.-H., Chang, K.-A., Yu, E., Jeong, S.-J., Chong, Y. H., & Suh, Y.-H. (2003). C-terminal fragments of amyloid precursor protein exert neurotoxicity by inducing glycogen synthase kinase-3β expression. *The FASEB Journal*, *17*(13). https://doi.org/10.1096/fj.03-0106fje

Kimura, A., Hata, S., & Suzuki, T. (2016). Alternative selection of site APP-cleaving enzyme 1 (BACE1) cleavage sites in amyloid β-protein precursor (APP) harboring protective and pathogenic mutations within the Aβ sequence. *Journal of Biological Chemistry*, *291*(46). https://doi.org/10.1074/jbc.M116.744722

Kirazov, E., Kirazov, L., Bigl, V., & Schliebs, R. (2001). Ontogenetic changes in protein level of amyloid precursor protein (APP) in growth cones and synaptosomes from rat brain and prenatal expression pattern of APP mRNA isoforms in developing rat embryo. *International Journal of Developmental Neuroscience*, *19*(3). https://doi.org/10.1016/S0736-5748(01)00012-0

Kirkwood, A., Rioult, M. G., & Bear, M. F. (1996). Experience-dependent modification of synaptic plasticity in visual cortex. *Nature*, *381*(6582). https://doi.org/10.1038/381526a0

Kjaergaard, M., & Kragelund, B. B. (2017). Functions of intrinsic disorder in transmembrane proteins. In *Cellular and Molecular Life Sciences* (Vol. 74, Issue 17). https://doi.org/10.1007/s00018-017-2562-5

Klevanski, M., Herrmann, U., Weyer, S. W., Fol, R., Cartier, N., Wolfer, X. P., Caldwell, J. H., Korte, M., & Müller, U. C. (2015). The APP intracellular domain is required for normalsynaptic morphology, synaptic plasticity, and hippocampus-dependent behavior. *Journal of Neuroscience*, *35*(49). https://doi.org/10.1523/JNEUROSCI.2009-15.2015

Kojro, E., & Fahrenholz, F. (2005). The non-amyloidogenic pathway: structure and function of alpha-secretases. In *Sub-cellular biochemistry* (Vol. 38). https://doi.org/10.1007/0-387-23226-5_5

Konietzko, U., Gersbacher, M. T., Streuli, J., Krüger, M., Thöni, S., Kins, S., & Nitsch, R. M. (2019). A fluorescent protein-readout for transcriptional activity reveals regulation of APP nuclear signaling by phosphorylation sites. *Biological Chemistry*, *400*(9). https://doi.org/10.1515/hsz-2019-0125

Konradi, C., & Heckers, S. (2003). Molecular aspects of glutamate dysregulation: Implications for schizophrenia and its treatment. In *Pharmacology and Therapeutics* (Vol. 97, Issue 2). https://doi.org/10.1016/S0163-7258(02)00328-5

Koo, E. H., & Squazzo, S. L. (1994). Evidence that production and release of amyloid β-protein involves the endocytic pathway. *Journal of Biological Chemistry*, *269*(26). https://doi.org/10.1016/s0021-9258(17)32449-3

Kral, A., & Pallas, S. L. (2011). Development of the auditory cortex. In *The Auditory Cortex*. https://doi.org/10.1007/978-1-4419-0074-6_21

Kuhn, P. H., Wang, H., Dislich, B., Colombo, A., Zeitschel, U., Ellwart, J. W., Kremmer, E., Roßner, S., & Lichtenthaler, S. F. (2010). ADAM10 is the physiologically relevant, constitutive α-secretase of the amyloid precursor

protein in primary neurons. *EMBO Journal*, *29*(17). https://doi.org/10.1038/emboj.2010.167

Kuhn, P.-H., Colombo, A. V., Schusser, B., Dreymueller, D., Wetzel, S., Schepers, U., Herber, J., Ludwig, A., Kremmer, E., Montag, D., Müller, U., Schweizer, M., Saftig, P., Bräse, S., & Lichtenthaler, S. F. (2016). Systematic substrate identification indicates a central role for the metalloprotease ADAM10 in axon targeting and synapse function. *ELife*, *5*. https://doi.org/10.7554/elife.12748

Kumar, A. (2015). NMDA receptor function during senescence: Implication on cognitive performance. In *Frontiers in Neuroscience* (Vol. 9, Issue DEC). https://doi.org/10.3389/fnins.2015.00473

Kumar, A., & Foster, T. C. (2013). Linking redox regulation of NMDAR synaptic function to cognitive decline during aging. *Journal of Neuroscience*, *33*(40). https://doi.org/10.1523/JNEUROSCI.2176-13.2013

Kumar, A., Thinschmidt, J. S., & Foster, T. C. (2019). Subunit contribution to NMDA receptor hypofunction and redox sensitivity of hippocampal synaptic transmission during aging. *Aging*, *11*(14). https://doi.org/10.18632/aging.102108

Kutsuwada, T., Sakimura, K., Manabe, T., Takayama, C., Katakura, N., Kushiya, E., Natsume, R., Watanabe, M., Inoue, Y., Yagi, T., Aizawa, S., Arakawa, M., Takahashi, T., Nakamura, Y., Mori, H., & Mishina, M. (1996). Impairment of suckling response, trigeminal neuronal pattern formation, and hippocampal LTD in NMDA receptor ∈2 subunit mutant mice. *Neuron*, *16*(2). https://doi.org/10.1016/S0896-6273(00)80051-3

Lara, A. H., & Wallis, J. D. (2015). The role of prefrontal cortex in working memory: A mini review. In *Frontiers in Systems Neuroscience* (Vol. 9, Issue DEC). https://doi.org/10.3389/fnsys.2015.00173

Laßek, M., Weingarten, J., Acker-Palmer, A., Bajjalieh, S., Muller, U., & Volknandt, W. (2014). Amyloid Precursor Protein Knockout Diminishes Synaptic Vesicle Proteins at the Presynaptic Active Zone in Mouse Brain. *Current Alzheimer Research*, *11*(10). https://doi.org/10.2174/1567205011666141107152458

Laßek, M., Weingarten, J., Einsfelder, U., Brendel, P., Müller, U., & Volknandt, W. (2013). Amyloid precursor proteins are constituents of the presynaptic active zone. *Journal of Neurochemistry*, *127*(1). https://doi.org/10.1111/jnc.12358

Lauritzen, I., Pardossi-Piquard, R., Bauer, C., Brigham, E., Abraham, J. D., Ranaldi, S., Fraser, P., St-George-Hyslop, P., le Thuc, O., Espin, V., Chami, L., Dunys, J., & Checler, F. (2012). The β-secretase-derived C-terminal fragment of βAPP, C99, but not Aβ, is a key contributor to early intraneuronal lesions in triple-transgenic mouse hippocampus. *Journal of Neuroscience*, *32*(46). https://doi.org/10.1523/JNEUROSCI.2775-12.2012

Lavezzari, G., McCallum, J., Dewey, C. M., & Roche, K. W. (2004). Subunit-specific regulation of NMDA receptor endocytosis. *Journal of Neuroscience*, *24*(28). https://doi.org/10.1523/JNEUROSCI.1890-04.2004

Law, A. J., Weickert, C. S., Webster, M. J., Herman, M. M., Kleinman, J. E., & Harrison, P. J. (2003). Expression of NMDA receptor NR1, NR2A and NR2B subunit mRNAs during development of the human hippocampal formation.

European Journal of Neuroscience, *18*(5). https://doi.org/10.1046/j.1460-9568.2003.02850.x

Lee, K. J., Moussa, C. E. H., Lee, Y., Sung, Y., Howell, B. W., Turner, R. S., Pak, D. T. S., & Hoe, H. S. (2010). Beta amyloid-independent role of amyloid precursor protein in generation and maintenance of dendritic spines. *Neuroscience*, *169*(1). https://doi.org/10.1016/j.neuroscience.2010.04.078

Lee, S. H., Kang, J., Ho, A., Watanabe, H., Bolshakov, V. Y., & Shen, J. (2020). APP Family Regulates Neuronal Excitability and Synaptic Plasticity but Not Neuronal Survival. *Neuron*, *108*(4). https://doi.org/10.1016/j.neuron.2020.08.011

Lester, R. A. J., Clements, J. D., Westbrook, G. L., & Jahr, C. E. (1990). Channel kinetics determine the time course of NMDA receptor-mediated synaptic currents. *Nature*, *346*(6284). https://doi.org/10.1038/346565a0

Li, M., Cui, Z., Niu, Y., Liu, B., Fan, W., Yu, D., & Deng, J. (2010). Synaptogenesis in the developing mouse visual cortex. *Brain Research Bulletin*, *81*(1). https://doi.org/10.1016/j.brainresbull.2009.08.028

Liao, D., Zhang, X., O'Brien, R., Ehlers, M. D., & Huganir, R. L. (1999). Regulation of morphological postsynaptic silent synapses in developing hippocampal neurons. *Nature Neuroscience*, *2*(1). https://doi.org/10.1038/4540

Lipton, S. A. (2006). Paradigm shift in neuroprotection by NMDA receptor blockade: Memantine and beyond. In *Nature Reviews Drug Discovery* (Vol. 5, Issue 2). https://doi.org/10.1038/nrd1958

Liu, P., Smith, P. F., & Darlington, C. L. (2008). Glutamate receptor subunits expression in memory-associated brain structures: Regional variations and effects of aging. *Synapse*, *62*(11). https://doi.org/10.1002/syn.20563

Liu, Q., Zerbinatti, C. v., Zhang, J., Hoe, H. S., Wang, B., Cole, S. L., Herz, J., Muglia, L., & Bu, G. (2007). Amyloid Precursor Protein Regulates Brain Apolipoprotein E and Cholesterol Metabolism through Lipoprotein Receptor LRP1. *Neuron*, *56*(1). https://doi.org/10.1016/j.neuron.2007.08.008

Liu, X. B., Murray, K. D., & Jones, E. G. (2004). Switching of NMDA receptor 2A and 2B subunits at thalamic and cortical synapses during early postnatal development. *Journal of Neuroscience*, *24*(40). https://doi.org/10.1523/JNEUROSCI.2476-04.2004

Löffler, J., & Huber, G. (1992). β-Amyloid Precursor Protein Isoforms in Various Rat Brain Regions and During Brain Development. *Journal of Neurochemistry*, *59*(4). https://doi.org/10.1111/j.1471-4159.1992.tb08443.x

Lopes, L. v., Cunha, R. A., & Ribeiro, J. A. (1999). Cross talk between A1 and A(2A) adenosine receptors in the hippocampus and cortex of young adult and old rats. *Journal of Neurophysiology*, *82*(6). https://doi.org/10.1152/jn.1999.82.6.3196

Lorent, K., Overbergh, L., Moechars, D., de Strooper, B., van Leuven, F., & van den Berghe, H. (1995). Expression in mouse embryos and in adult mouse brain of three members of the amyloid precursor protein family, of the alpha-2-macroglobulin receptor/low density lipoprotein receptor-related protein and of its ligands apolipoprotein E, lipoprotein lipase, alpha-2-macroglobulin and

the 40,000 molecular weight receptor-associated protein. *Neuroscience*, *65*(4). https://doi.org/10.1016/0306-4522(94)00555-J

Lü, W., Du, J., Goehring, A., & Gouaux, E. (2017). Cryo-EM structures of the triheteromeric NMDA receptor and its allosteric modulation. *Science*, *355*(6331). https://doi.org/10.1126/science.aal3729

Ludwig, M. (2017). How Your Brain Cells Talk to Each Other—Whispered Secrets and Public Announcements. *Frontiers for Young Minds*, *5*. https://doi.org/10.3389/frym.2017.00039

Lundgren, J. L., Vandermeulen, L., Sandebring-Matton, A., Ahmed, S., Winblad, B., di Luca, M., Tjernberg, L. O., Marcello, E., & Frykman, S. (2020). Proximity ligation assay reveals both pre- A nd postsynaptic localization of the APP-processing enzymes ADAM10 and BACE1 in rat and human adult brain. *BMC Neuroscience*, *21*(1). https://doi.org/10.1186/s12868-020-0554-0

Lüscher, C., & Malenka, R. C. (2012). NMDA receptor-dependent long-term potentiation and long-term depression (LTP/LTD). *Cold Spring Harbor Perspectives in Biology*, *4*(6). https://doi.org/10.1101/cshperspect.a005710

Lussier, M. P., Sanz-Clemente, A., & Roche, K. W. (2015). Dynamic regulation of N-methyl-D-aspartate (NMDA) and α-amino-3-hydroxy-5-methyl-4-isoxazolepropionic acid (AMPA) receptors by posttranslational modifications. *Journal of Biological Chemistry*, *290*(48). https://doi.org/10.1074/jbc.R115.652750

Lüthi, A., Schwyzer, L., Mateos, J. M., Gähwiler, B. H., & McKinney, R. A. (2001). NMDA receptor activation limits the number of synaptic connections during hippocampal development. *Nature Neuroscience*, *4*(11). https://doi.org/10.1038/nn744

Magnusson, K. R. (1995). Differential effects of aging on binding sites of the activated NMDA receptor complex in mice. *Mechanisms of Ageing and Development*, *84*(3). https://doi.org/10.1016/0047-6374(95)01658-9

Magnusson, K. R. (2000). Declines in mRNA expression of different subunits may account for differential effects of aging on agonist and antagonist binding to the NMDA receptor. *Journal of Neuroscience*, *20*(5). https://doi.org/10.1523/jneurosci.20-05-01666.2000

Magnusson, K. R., & Cotman, C. W. (1993). Age-related changes in excitatory amino acid receptors in two mouse strains. *Neurobiology of Aging*, *14*(3). https://doi.org/10.1016/0197-4580(93)90001-R

Magnusson, K. R., Nelson, S. E., & Young, A. B. (2002). Age-related changes in the protein expression of subunits of the NMDA receptor. *Molecular Brain Research*, *99*(1). https://doi.org/10.1016/S0169-328X(01)00344-8

Martinsson, I., Capetillo-Zarate, E., Faideau, M., Willén, K., Esteras, N., Frykman, S., Tjernberg, L. O., & Gouras, G. K. (2019). APP depletion alters selective pre- and post-synaptic proteins. *Molecular and Cellular Neuroscience*, *95*. https://doi.org/10.1016/j.mcn.2019.02.003

Matrone, C., Luvisetto, S., la Rosa, L. R., Tamayev, R., Pignataro, A., Canu, N., Yang, L., Barbagallo, A. P. M., Biundo, F., Lombino, F., Zheng, H., Ammassari-Teule, M., & D'Adamio, L. (2012). Tyr682 in the Aβ-precursor

protein intracellular domain regulates synaptic connectivity, cholinergic function, and cognitive performance. *Aging Cell*, *11*(6). https://doi.org/10.1111/acel.12009

May, P. C., Dean, R. A., Lowe, S. L., Martenyi, F., Sheehan, S. M., Boggs, L. N., Monk, S. A., Mathes, B. M., Mergott, D. J., Watson, B. M., Stout, S. L., Timm, D. E., LaBell, E. S., Gonzales, C. R., Nakano, M., Jhee, S. S., Yen, M., Ereshefsky, L., Lindstrom, T. D., … Audia, J. E. (2011). Robust central reduction of amyloid-β in humans with an orally available, non-peptidic β-secretase inhibitor. *Journal of Neuroscience*, *31*(46). https://doi.org/10.1523/JNEUROSCI.3647-11.2011

Mayadevi, M., Praseeda, M., Kumar, K. S., & Omkumar, R. v. (2002). Sequence determinants on the NR2A and NR2B subunits of NMDA receptor responsible for specificity of phosphorylation by CaMKII. *Biochimica et Biophysica Acta - Protein Structure and Molecular Enzymology*, *1598*(1–2). https://doi.org/10.1016/s0167-4838(02)00315-1

Mensch, M., Dunot, J., Yishan, S. M., Harris, S. S., Blistein, A., Avdiu, A., Pousinha, P. A., Giudici, C., Busche, M. A., Jedlicka, P., Willem, M., & Marie, H. (2021). Aη-α and Aη-β peptides impair LTP ex vivo within the low nanomolar range and impact neuronal activity in vivo. *Alzheimer's Research and Therapy*, *13*(1). https://doi.org/10.1186/s13195-021-00860-1

Mertens, J., Paquola, A. C. M., Ku, M., Hatch, E., Böhnke, L., Ladjevardi, S., McGrath, S., Campbell, B., Lee, H., Herdy, J. R., Gonçalves, J. T., Toda, T., Kim, Y., Winkler, J., Yao, J., Hetzer, M. W., & Gage, F. H. (2015). Directly Reprogrammed Human Neurons Retain Aging-Associated Transcriptomic Signatures and Reveal Age-Related Nucleocytoplasmic Defects. *Cell Stem Cell*, *17*(6). https://doi.org/10.1016/j.stem.2015.09.001

Michaluk, P., Mikasova, L., Groc, L., Frischknecht, R., Choquet, D., & Kaczmarek, L. (2009). Matrix metalloproteinase-9 controls NMDA receptor surface diffusion through integrin β1 signaling. *Journal of Neuroscience*, *29*(18). https://doi.org/10.1523/JNEUROSCI.5346-08.2009

Monyer, H., Burnashev, N., Laurie, D. J., Sakmann, B., & Seeburg, P. H. (1994). Developmental and regional expression in the rat brain and functional properties of four NMDA receptors. *Neuron*, *12*(3). https://doi.org/10.1016/0896-6273(94)90210-0

Moran, P. M., Higgins, L. S., Cordell, B., & Moser, P. C. (1995). Age-related learning deficits in transgenic mice expressing the 751-amino acid isoform of human β-amyloid precursor protein. *Proceedings of the National Academy of Sciences of the United States of America*, *92*(12). https://doi.org/10.1073/pnas.92.12.5341

Moreno, L., Rose, C., Mohanraj, A., Allinquant, B., Billard, J. M., Dutar, P., & Arancio, O. (2015). sAβPPα improves hippocampal NMDA-dependent functional alterations linked to healthy aging. *Journal of Alzheimer's Disease*, *48*(4). https://doi.org/10.3233/JAD-150297

Mosbacher, J., Schoepfer, R., Monyer, H., Burnashev, N., Seeburg, P. H., & Ruppersberg, J. P. (1994). A molecular determinant for submillisecond

desensitization in glutamate receptors. *Science*, *266*(5187). https://doi.org/10.1126/science.7973663

Mosser, S., Gerber, H., & Fraering, P. C. (2021). Identification of truncated C-terminal fragments of the Alzheimer's disease amyloid protein precursor derived from sequential proteolytic pathways. *Journal of Neurochemistry*, *156*(6). https://doi.org/10.1111/jnc.15143

Mucke, L., & Selkoe, D. J. (2012). Neurotoxicity of amyloid β-protein: Synaptic and network dysfunction. *Cold Spring Harbor Perspectives in Medicine*, *2*(7). https://doi.org/10.1101/cshperspect.a006338

Mulkey, R. M., Endo, S., Shenolikar, S., & Malenka, R. C. (1994). Involvement of a calcineurin/inhibitor-1 phosphatase cascade in hippocampal long-term depression. *Nature*, *369*(6480). https://doi.org/10.1038/369486a0

Mullan, M., Crawford, F., Axelman, K., Houlden, H., Lilius, L., Winblad, B., & Lannfelt, L. (1992). A pathogenic mutation for probable Alzheimer's disease in the APP gene at the N–terminus of β–amyloid. *Nature Genetics*, *1*(5). https://doi.org/10.1038/ng0892-345

Müller, T., Concannon, C. G., Ward, M. W., Walsh, C. M., Tirniceriu, A. L., Tribl, F., Kögel, D., Prehn, J. H. M., & Egensperger, R. (2007). Modulation of gene expression and cytoskeletal dynamics by the amyloid precursor protein intracellular domain (AICD). *Molecular Biology of the Cell*, *18*(1). https://doi.org/10.1091/mbc.E06-04-0283

Müller, T., Meyer, H. E., Egensperger, R., & Marcus, K. (2008). The amyloid precursor protein intracellular domain (AICD) as modulator of gene expression, apoptosis, and cytoskeletal dynamics-Relevance for Alzheimer's disease. In *Progress in Neurobiology* (Vol. 85, Issue 4). https://doi.org/10.1016/j.pneurobio.2008.05.002

Müller, T., Schrötter, A., Loosse, C., Pfeiffer, K., Theiss, C., Kauth, M., Meyer, H. E., & Marcus, K. (2013). A ternary complex consisting of AICD, FE65, and TIP60 down-regulates Stathmin1. *Biochimica et Biophysica Acta - Proteins and Proteomics*, *1834*(1). https://doi.org/10.1016/j.bbapap.2012.07.017

Müller, U. C., Deller, T., & Korte, M. (2017). Not just amyloid: Physiological functions of the amyloid precursor protein family. In *Nature Reviews Neuroscience* (Vol. 18, Issue 5). https://doi.org/10.1038/nrn.2017.29

Müller, U. C., & Zheng, H. (2012). Physiological functions of APP family proteins. *Cold Spring Harbor Perspectives in Medicine*, *2*(2). https://doi.org/10.1101/cshperspect.a006288

Munro, K. M., Nash, A., Pigoni, M., Lichtenthaler, S. F., & Gunnersen, J. M. (2016). Functions of the Alzheimer's Disease Protease BACE1 at the Synapse in the Central Nervous System. *Journal of Molecular Neuroscience*, *60*(3). https://doi.org/10.1007/s12031-016-0800-1

Muresan, V., & Ladescu Muresan, Z. (2015). Amyloid-β precursor protein: Multiple fragments, numerous transport routes and mechanisms. In *Experimental Cell Research* (Vol. 334, Issue 1). https://doi.org/10.1016/j.yexcr.2014.12.014

Murphy, J. A., Stein, I. S., Geoffrey Lau, C., Peixoto, R. T., Aman, T. K., Kaneko, N., Aromolaran, K., Saulnier, J. L., Popescu, G. K., Sabatini, B. L., Hell, J.

W., & Zukin, R. S. (2014). Phosphorylation of Ser1166 on GluN2B by PKA is critical to synaptic NMDA receptor function and Ca2+ signaling in spines. *Journal of Neuroscience*, *34*(3). https://doi.org/10.1523/JNEUROSCI.4538-13.2014

Nakazawa, T., Komai, S., Tezuka, T., Hisatsune, C., Umemori, H., Semba, K., Mishina, M., Manabe, T., & Yamamoto, T. (2001). Characterization of Fyn-mediated tyrosine phosphorylation sites on GluRε2 (NR2B) subunit of the N-methyl-D-aspartate receptor. *Journal of Biological Chemistry*, *276*(1). https://doi.org/10.1074/jbc.M008085200

Nalbantoglu, J., Tirado-Santiago, G., Lahsaïni, A., Poirier, J., Goncalves, O., Verge, G., Momoli, F., Welner, S. A., Massicotte, G., Julien, J. P., & Shapiro, M. L. (1997). Impaired learning and LTP in mice expressing the carboxy terminus of the Alzheimer amyloid precursor protein. *Nature*, *387*(6632). https://doi.org/10.1038/387500a0

NCBI. (n.d.). *Gene [Internet]. Bethesda (MD): National Library of Medicine (US), National Center for Biotechnology Information; 2004 – [cited 02 2023]. Available from: https://www.ncbi.nlm.nih.gov/gene/ (Gene ID: 351)*.

Newman, M. C., & Kaszniak, A. W. (2000). Spatial memory and aging: Performance on a human analog of the Morris water maze. *Aging, Neuropsychology, and Cognition*, *7*(2). https://doi.org/10.1076/1382-5585(200006)7:2;1-U;FT086

Nishimoto, I., Okamoto, T., Matsuura, Y., Takahashi, S., Okamoto, T., Murayama, Y., & Ogata, E. (1993). Alzheimer amyloid protein precursor complexes with brain GTP-binding protein Go. *Nature*, *362*(6415). https://doi.org/10.1038/362075a0

Nowak, L., Bregestovski, P., Ascher, P., Herbet, A., & Prochiantz, A. (1984). Magnesium gates glutamate-activated channels in mouse central neurones. *Nature*, *307*(5950), 462–465. https://doi.org/10.1038/307462a0

Oh, M. M., Oliveira, F. A., Waters, J., & Disterhoft, J. F. (2013). Altered calcium metabolism in aging CA1 hippocampal pyramidal neurons. *Journal of Neuroscience*, *33*(18). https://doi.org/10.1523/JNEUROSCI.5457-12.2013

Okabe, S. (2020). Imaging Synapse Formation and Remodeling In Vitro and In Vivo. In *Make Life Visible*. https://doi.org/10.1007/978-981-13-7908-6_19

Oliet, S. H. R., & Mothet, J. P. (2009). Regulation of N-methyl-d-aspartate receptors by astrocytic d-serine. In *Neuroscience* (Vol. 158, Issue 1). https://doi.org/10.1016/j.neuroscience.2008.01.071

Ott, M. O., & Bullock, S. L. (2001). A gene trap insertion reveals that amyloid precursor protein expression is a very early event in murine embryogenesis. *Development Genes and Evolution*, *211*(7). https://doi.org/10.1007/s004270100158

Ou-Yang, M. H., Kurz, J. E., Nomura, T., Popovic, J., Rajapaksha, T. W., Dong, H., Contractor, A., Chetkovich, D. M., Tourtellotte, W. G., & Vassar, R. (2018). Axonal organization defects in the hippocampus of adult conditional BACE1 knockout mice. *Science Translational Medicine*, *10*(459). https://doi.org/10.1126/scitranslmed.aao5620

Paoletti, P., & Neyton, J. (2007). NMDA receptor subunits: function and pharmacology. In *Current Opinion in Pharmacology* (Vol. 7, Issue 1). https://doi.org/10.1016/j.coph.2006.08.011

Papouin, T., Ladépêche, L., Ruel, J., Sacchi, S., Labasque, M., Hanini, M., Groc, L., Pollegioni, L., Mothet, J. P., & Oliet, S. H. R. (2012). Synaptic and extrasynaptic NMDA receptors are gated by different endogenous coagonists. *Cell*, *150*(3). https://doi.org/10.1016/j.cell.2012.06.029

Pardossi-Piquard, R., Petit, A., Kawarai, T., Sunyach, C., da Costa, C. A., Vincent, B., Ring, S., D'Adamio, L., Shen, J., Müller, U., Hyslop, P. S. G., & Checler, F. (2005). Presenilin-dependent transcriptional control of the Aβ-degrading enzyme neprilysin by intracellular domains of βAPP and APLP. *Neuron*, *46*(4). https://doi.org/10.1016/j.neuron.2005.04.008

Parsons, C. G., Stöffler, A., & Danysz, W. (2007). Memantine: a NMDA receptor antagonist that improves memory by restoration of homeostasis in the glutamatergic system - too little activation is bad, too much is even worse. In *Neuropharmacology* (Vol. 53, Issue 6). https://doi.org/10.1016/j.neuropharm.2007.07.013

Paschou, M., Liaropoulou, D., Kalaitzaki, V., Efthimiopoulos, S., & Papazafiri, P. (2023). Knockdown of Amyloid Precursor Protein Increases Ion Channel Expression and Alters Ca2+ Signaling Pathways. *International Journal of Molecular Sciences*, *24*(3), 2302. https://doi.org/10.3390/ijms24032302

Patneau, D. K., & Mayer, M. L. (1990). Structure-activity relationships for amino acid transmitter candidates acting at N-methyl-D-aspartate and quisqualate receptors. *Journal of Neuroscience*, *10*(7). https://doi.org/10.1523/jneurosci.10-07-02385.1990

Pegasiou, C. M., Zolnourian, A., Gomez-Nicola, D., Deinhardt, K., Nicoll, J. A. R., Ahmed, A. I., Vajramani, G., Grundy, P., Verhoog, M. B., Mansvelder, H. D., Perry, V. H., Bulters, D., & Vargas-Caballero, M. (2020). Age-dependent changes in synaptic NMDA receptor composition in adult human cortical neurons. *Cerebral Cortex*, *30*(7). https://doi.org/10.1093/CERCOR/BHAA052

Pérez-Otaño, I., & Ehlers, M. D. (2004). Learning from NMDA receptor trafficking: Clues to the development and maturation of glutamatergic synapses. In *NeuroSignals* (Vol. 13, Issue 4). https://doi.org/10.1159/000077524

Petit-Pedrol, M., & Groc, L. (2021). Regulation of membrane NMDA receptors by dynamics and protein interactions. In *Journal of Cell Biology* (Vol. 220, Issue 1). https://doi.org/10.1083/JCB.202006101

Petralia, R. S., Sans, N., Wang, Y. X., & Wenthold, R. J. (2005). Ontogeny of postsynaptic density proteins at glutamatergic synapses. *Molecular and Cellular Neuroscience*, *29*(3). https://doi.org/10.1016/j.mcn.2005.03.013

Philpot, B. D., Sekhar, A. K., Shouval, H. Z., & Bear, M. F. (2001). Visual experience and deprivation bidirectionally modify the composition and function of NMDA receptors in visual cortex. *Neuron*, *29*(1). https://doi.org/10.1016/S0896-6273(01)00187-8

Pietá Dias, C., Martins de Lima, M. N., Presti-Torres, J., Dornelles, A., Garcia, V. A., Siciliani Scalco, F., Rewsaat Guimarães, M., Constantino, L., Budni, P.,

Dal-Pizzol, F., & Schröder, N. (2007). Memantine reduces oxidative damage and enhances long-term recognition memory in aged rats. *Neuroscience*, *146*(4). https://doi.org/10.1016/j.neuroscience.2007.03.018

Piggott, M. A., Perry, E. K., Perry, R. H., & Court, J. A. (1992). [3H]MK-801 binding to the NMDA receptor complex, and its modulation in human frontal cortex during development and aging. *Brain Research*, *588*(2). https://doi.org/10.1016/0006-8993(92)91586-4

Pimplikar, S. W., & Suryanarayana, A. (2011). Detection of APP intracellular domain in brain tissue. *Methods in Molecular Biology*, *670*. https://doi.org/10.1007/978-1-60761-744-0_7

Pinho, J., Vale, R., Batalha, V. L., Costenla, A. R., Dias, R., Rombo, D., Sebastião, A. M., de Mendonça, A., & Diógenes, M. J. (2017). Enhanced LTP in aged rats: Detrimental or compensatory? *Neuropharmacology*, *114*. https://doi.org/10.1016/j.neuropharm.2016.11.017

Placanica, L., Zhu, L., & Yue-Ming, L. (2009). Gender- and age-dependent γ-secretase activity in mouse brain and its implication in sporadic Alzheimer disease. *PLoS ONE*, *4*(4). https://doi.org/10.1371/journal.pone.0005088

Plasticity lab, https://www. plasticitylab. com/methods. (n.d.). *Methods*. Retrieved February 2023.

Plattner, F., Hernández, A., Kistler, T. M., Pozo, K., Zhong, P., Yuen, E. Y., Tan, C., Hawasli, A. H., Cooke, S. F., Nishi, A., Guo, A., Wiederhold, T., Yan, Z., & Bibb, J. A. (2014). Memory enhancement by targeting Cdk5 regulation of NR2B. *Neuron*, *81*(5). https://doi.org/10.1016/j.neuron.2014.01.022

Pliássova, A., Canas, P. M., Xavier, A. C., da Silva, B. S., Cunha, R. A., & Agostinho, P. (2016). Age-Related Changes in the Synaptic Density of Amyloid-β Protein Precursor and Secretases in the Human Cerebral Cortex. *Journal of Alzheimer's Disease*, *52*(4). https://doi.org/10.3233/JAD-160213

Potier, B., Billard, J. M., Rivière, S., Sinet, P. M., Denis, I., Champeil-Potokar, G., Grintal, B., Jouvenceau, A., Kollen, M., & Dutar, P. (2010). Reduction in glutamate uptake is associated with extrasynaptic NMDA and metabotropic glutamate receptor activation at the hippocampal CA1 synapse of aged rats. *Aging Cell*, *9*(5). https://doi.org/10.1111/j.1474-9726.2010.00593.x

Pousinha, P. A., Mouska, X., Bianchi, D., Temido-Ferreira, M., Rajão-Saraiva, J., Gomes, R., Fernandez, S. P., Salgueiro-Pereira, A. R., Gandin, C., Raymond, E. F., Barik, J., Goutagny, R., Bethus, I., Lopes, L. v., Migliore, M., & Marie, H. (2019). The Amyloid Precursor Protein C-Terminal Domain Alters CA1 Neuron Firing, Modifying Hippocampus Oscillations and Impairing Spatial Memory Encoding. *Cell Reports*, *29*(2). https://doi.org/10.1016/j.celrep.2019.08.103

Pousinha, P. A., Mouska, X., Raymond, E. F., Gwizdek, C., Dhib, G., Poupon, G., Zaragosi, L. E., Giudici, C., Bethus, I., Pacary, E., Willem, M., & Marie, H. (2017). Physiological and pathophysiological control of synaptic GluN2B-NMDA receptors by the C-terminal domain of amyloid precursor protein. *ELife*, *6*. https://doi.org/10.7554/eLife.25659

Pressler, R., & Auvin, S. (2013). Comparison of brain maturation among species: An example in translational research suggesting the possible use of bumetanide in newborn. *Frontiers in Neurology*, *4 APR*. https://doi.org/10.3389/fneur.2013.00036

Probst, S., Krüger, M., Kägi, L., Thöni, S., Schuppli, D., Nitsch, R. M., & Konietzko, U. (2021). Fe65 is the sole member of its family that mediates transcription regulated by the amyloid precursor protein. *Journal of Cell Science*, *133*(17). https://doi.org/10.1242/jcs.242917

Prox, J., Bernreuther, C., Altmeppen, H., Grende, J., Glatze, M., D'Hooge, R., Stroobants, S., Ahmed, T., Balschun, D., Willem, M., Lammich, S., Isbrandt, D., Schweizer, M., Horré, K., de Strooper, B., & Saftig, P. (2013). Postnatal disruption of the disintegrin/metalloproteinase ADAM10 in brain causes epileptic seizures, learning deficits, altered spine morphology, and defective synaptic functions. *Journal of Neuroscience*, *33*(32). https://doi.org/10.1523/JNEUROSCI.5910-12.2013

Prybylowski, K., Chang, K., Sans, N., Kan, L., Vicini, S., & Wenthold, R. J. (2005). The synaptic localization of NR2B-containing NMDA receptors is controlled by interactions with PDZ proteins and AP-2. *Neuron*, *47*(6). https://doi.org/10.1016/j.neuron.2005.08.016

Puzzo, D., Privitera, L., Leznik, E., Fà, M., Staniszewski, A., Palmeri, A., & Arancio, O. (2008). Picomolar amyloid-β positively modulates synaptic plasticity and memory in hippocampus. *Journal of Neuroscience*, *28*(53). https://doi.org/10.1523/JNEUROSCI.2692-08.2008

Quinlan, E. M., Lebel, D., Brosh, I., & Barkai, E. (2004). A Molecular Mechanism for Stabilization of Learning-Induced Synaptic Modifications. *Neuron*, *41*(2). https://doi.org/10.1016/S0896-6273(03)00874-2

Quinlan, E. M., Olstein, D. H., & Bear, M. F. (1999). Bidirectional, experience-dependent regulation of N-methyl-D-aspartate receptor subunit composition in the rat visual cortex during postnatal development. *Proceedings of the National Academy of Sciences of the United States of America*, *96*(22). https://doi.org/10.1073/pnas.96.22.12876

Rachline, J., Perin-Dureau, F., le Goff, A., Neyton, J., & Paoletti, P. (2005). The micromolar zinc-binding domain on the NMDA receptor subunit NR2B. *Journal of Neuroscience*, *25*(2). https://doi.org/10.1523/JNEUROSCI.3967-04.2005

Radulescu, C. I., Cerar, V., Haslehurst, P., Kopanitsa, M., & Barnes, S. J. (2021). The aging mouse brain: cognition, connectivity and calcium. *Cell Calcium*, *94*. https://doi.org/10.1016/j.ceca.2021.102358

Radzimanowski, J., Simon, B., Sattler, M., Beyreuther, K., Sinning, I., & Wild, K. (2008). Structure of the intracellular domain of the amyloid precursor protein in complex with Fe65-PTB2. *EMBO Reports*, *9*(11). https://doi.org/10.1038/embor.2008.188

Rauner, C., & Köhr, G. (2011). Triheteromeric NR1/NR2A/NR2B receptors constitute the major N-methyl-D-aspartate receptor population in adult hippocampal synapses. *Journal of Biological Chemistry*, *286*(9). https://doi.org/10.1074/jbc.M110.182600

Reichard, R. R., White, C. L., Hladik, C. L., & Dolinak, D. (2003). Beta-amyloid precursor protein staining in nonhomicidal pediatric medicolegal autopsies. *Journal of Neuropathology and Experimental Neurology*, *62*(3). https://doi.org/10.1093/jnen/62.3.237

Reinhard, C., Hébert, S. S., & de Strooper, B. (2005). The amyloid-β precursor protein: Integrating structure with biological function. In *EMBO Journal* (Vol. 24, Issue 23). https://doi.org/10.1038/sj.emboj.7600860

Reisberg, B., Doody, R., Stöffler, A., Schmitt, F., Ferris, S., & Möbius, H. J. (2003). Memantine in Moderate-to-Severe Alzheimer's Disease. *New England Journal of Medicine*, *348*(14). https://doi.org/10.1056/nejmoa013128

Ring, S., Weyer, S. W., Kilian, S. B., Waldron, E., Pietrzik, C. U., Filippov, M. A., Herms, J., Buchholz, C., Eckman, C. B., Korte, M., Wolfer, D. P., & Müller, U. C. (2007). The secreted β-amyloid precursor protein ectodomain APPsα is sufficient to rescue the anatomical, behavioral, and electrophysiological abnormalities of APP-deficient mice. *Journal of Neuroscience*, *27*(29). https://doi.org/10.1523/JNEUROSCI.1026-07.2007

Sabo, S. L., Lanier, L. M., Ikin, A. F., Khorkova, O., Sahasrabudhe, S., Greengard, P., & Buxbaum, J. D. (1999). Regulation of β-amyloid secretion by FE65, an amyloid protein precursor-binding protein. *Journal of Biological Chemistry*, *274*(12). https://doi.org/10.1074/jbc.274.12.7952

Sakimura, K., Kutsuwada, T., Ito, I., Manabe, T., Takayama, C., Kushiya, E., Yagi, T., Shinichi, A., Inoue, Y., Sugiyama, H., & Mishina, M. (1995). Reduced hippocampal LTP and spatial learning in mice lacking NMDA receptor *ε*1 subunit. In *Nature* (Vol. 373, Issue 6510). https://doi.org/10.1038/373151a0

Salat, D. H., Kaye, J. A., & Janowsky, J. S. (2001). Selective preservation and degeneration within the prefrontal cortex in aging and Alzheimer disease. *Archives of Neurology*, *58*(9). https://doi.org/10.1001/archneur.58.9.1403

Sanderson, J. L., & Dell'Acqua, M. L. (2011). AKAP signaling complexes in regulation of excitatory synaptic plasticity. In *Neuroscientist* (Vol. 17, Issue 3). https://doi.org/10.1177/1073858410384740

Sanhueza, M., Fernandez-Villalobos, G., Stein, I. S., Kasumova, G., Zhang, P., Ulrich Bayer, K., Otmakhov, N., Hell, J. W., & Lisman, J. (2011). Role of the CaMKII/NMDA receptor complex in the maintenance of synaptic strength. *Journal of Neuroscience*, *31*(25). https://doi.org/10.1523/JNEUROSCI.1250-11.2011

Sans, N., Petralia, R. S., Wang, Y. X., Blahos, J., Hell, J. W., & Wenthold, R. J. (2000). A developmental change in NMDA receptor-associated proteins at hippocampal synapses. *Journal of Neuroscience*, *20*(3). https://doi.org/10.1523/jneurosci.20-03-01260.2000

Sanz-Clemente, A., Nicoll, R. A., & Roche, K. W. (2013). Diversity in NMDA receptor composition: Many regulators, many consequences. In *Neuroscientist* (Vol. 19, Issue 1). https://doi.org/10.1177/1073858411435129

Scheff, S. W., Price, D. A., Schmitt, F. A., & Mufson, E. J. (2006). Hippocampal synaptic loss in early Alzheimer's disease and mild cognitive impairment.

Neurobiology of Aging, *27*(10). https://doi.org/10.1016/j.neurobiolaging.2005.09.012

Schmittgen, T. D., & Livak, K. J. (2008). Analyzing real-time PCR data by the comparative C(T) methodSchmittgen, T.D., Livak, K.J., 2008. Analyzing real-time PCR data by the comparative C(T) method. Nat. Protoc. 3, 1101–1108.. *Nature Protocols*, *3*(6).

Scott, D. B., Michailidis, I., Mu, Y., Logothetis, D., & Ehlers, M. D. (2004). Endocytosis and degradative sorting of NMDA receptors by conserved membrane-proximal signals. *Journal of Neuroscience*, *24*(32). https://doi.org/10.1523/JNEUROSCI.0780-04.2004

Seabrook, G. R., Smith, D. W., Bowery, B. J., Easter, A., Reynolds, T., Fitzjohn, S. M., Morton, R. A., Zheng, H., Dawson, G. R., Sirinathsinghji, D. J. S., Davies, C. H., Collingridge, G. L., & Hilla, R. G. (1999). Mechanisms contributing to the deficits in hippocampal synaptic plasticity in mice lacking amyloid precursor protein. *Neuropharmacology*, *38*(3). https://doi.org/10.1016/S0028-3908(98)00204-4

Segev, A., Garcia-Oscos, F., & Kourrich, S. (2016). Whole-cell patch-clamp recordings in brain slices. *Journal of Visualized Experiments*, *2016*(112). https://doi.org/10.3791/54024

Setou, M., Nakagawa, T., Seog, D. H., & Hirokawa, N. (2000). Kinesin superfamily motor protein KIF17 and mLin-10 in NMDA receptor- containing vesicle transport. *Science*, *288*(5472). https://doi.org/10.1126/science.288.5472.1796

Shariati, S. A. M., & de Strooper, B. (2013). Redundancy and divergence in the amyloid precursor protein family. In *FEBS Letters* (Vol. 587, Issue 13). https://doi.org/10.1016/j.febslet.2013.05.026

Shen, J., & Kelleher, R. J. (2007). The presenilin hypothesis of Alzheimer's disease: Evidence for a loss-of-function pathogenic mechanism. In *Proceedings of the National Academy of Sciences of the United States of America* (Vol. 104, Issue 2). https://doi.org/10.1073/pnas.0608332104

Shi, S. H., Hayashi, Y., Petralia, R. S., Zaman, S. H., Wenthold, R. J., Svoboda, K., & Malinow, R. (1999). Rapid spine delivery and redistribution of AMPA receptors after synaptic NMDA receptor activation. *Science*, *284*(5421). https://doi.org/10.1126/science.284.5421.1811

Silva, M. M., Rodrigues, B., Fernandes, J., Santos, S. D., Carreto, L., Santos, M. A. S., Pinheiro, P., & Carvalho, A. L. (2019). MicroRNA-186-5p controls GluA2 surface expression and synaptic scaling in hippocampal neurons. *Proceedings of the National Academy of Sciences of the United States of America*, *116*(12). https://doi.org/10.1073/pnas.1900338116

Simón, A. M., Schiapparelli, L., Salazar-Colocho, P., Cuadrado-Tejedor, M., Escribano, L., López de Maturana, R., del Río, J., Pérez-Mediavilla, A., & Frechilla, D. (2009). Overexpression of wild-type human APP in mice causes cognitive deficits and pathological features unrelated to Aβ levels. *Neurobiology of Disease*, *33*(3). https://doi.org/10.1016/j.nbd.2008.11.005

Simons, M., Ikonen, E., Tienari, P. J., Cid-Arregui, A., Mönning, U., Beyreuther, K., & Dotti, C. G. (1995). Intracellular routing of human amyloid protein precursor: Axonal delivery followed by transport to the dendrites. *Journal of Neuroscience Research*, *41*(1). https://doi.org/10.1002/jnr.490410114

Singh-Manoux, A., Kivimaki, M., Glymour, M. M., Elbaz, A., Berr, C., Ebmeier, K. P., Ferrie, J. E., & Dugravot, A. (2012). Timing of onset of cognitive decline: Results from Whitehall II prospective cohort study. *BMJ (Online)*, *344*(7840). https://doi.org/10.1136/bmj.d7622

Sisodia, S. S. (1992). β-Amyloid precursor protein cleavage by a membrane-bound protease. *Proceedings of the National Academy of Sciences of the United States of America*, *89*(13). https://doi.org/10.1073/pnas.89.13.6075

Skeberdis, V. A., Chevaleyre, V., Lau, C. G., Goldberg, J. H., Pettit, D. L., Suadicani, S. O., Lin, Y., Bennett, M. V. L., Yuste, R., Castillo, P. E., & Zukin, R. S. (2006). Protein kinase A regulates calcium permeability of NMDA receptors. *Nature Neuroscience*, *9*(4). https://doi.org/10.1038/nn1664

Smith, D. L., Pozueta, J., Gong, B., Arancio, O., & Shelanski, M. (2009). Reversal of long-term dendritic spine alterations in Alzheimer disease models. *Proceedings of the National Academy of Sciences of the United States of America*, *106*(39). https://doi.org/10.1073/pnas.0908706106

Smith-Swintosky, V. L., Pettigrew, L. C., Craddock, S. D., Culwell, A. R., Rydel, R. E., & Mattson, M. P. (1994). Secreted forms of β-amyloid precursor protein protect against ischemic brain injury. *Journal of Neurochemistry*, *63*(2). https://doi.org/10.1046/j.1471-4159.1994.63020781.x

Soba, P., Eggert, S., Wagner, K., Zentgraf, H., Siehl, K., Kreger, S., Löwer, A., Langer, A., Merdes, G., Paro, R., Masters, C. L., Müller, U., Kins, S., & Beyreuther, K. (2005). Homo- and heterodimerization of APP family members promotes intercellular adhesion. *EMBO Journal*, *24*(20). https://doi.org/10.1038/sj.emboj.7600824

Sobczyk, A., Scheuss, V., & Svoboda, K. (2005). NMDA receptor subunit-dependent [Ca2+] signaling in individual hippocampal dendritic spines. *Journal of Neuroscience*, *25*(26). https://doi.org/10.1523/JNEUROSCI.1221-05.2005

Solà, C., Mengod, G., Probst, A., & Palacios, J. M. (1993). Differential regional and cellular distribution of β-amyloid precursor protein messenger RNAs containing and lacking the kunitz protease inhibitor domain in the brain of human, rat and mouse. *Neuroscience*, *53*(1). https://doi.org/10.1016/0306-4522(93)90304-X

Song, D. K., Won, M. H., Jung, J. S., Lee, J. C., Kang, T. C., Suh, H. W., Huh, S. O., Paek, S. H., Kim, Y. H., Kim, S. H., & Suh, Y. H. (1998). Behavioral and neuropathologic changes induced by central injection of carboxyl-terminal fragment of β-amyloid precursor protein in mice. *Journal of Neurochemistry*, *71*(2). https://doi.org/10.1046/j.1471-4159.1998.71020875.x

Song, X., Jensen, M. O., Jogini, V., Stein, R. A., Lee, C. H., McHaourab, H. S., Shaw, D. E., & Gouaux, E. (2018). Mechanism of NMDA receptor channel block by MK-801 and memantine. *Nature*, *556*(7702). https://doi.org/10.1038/s41586-018-0039-9

Sosa, L. J., Cáceres, A., Dupraz, S., Oksdath, M., Quiroga, S., & Lorenzo, A. (2017). The physiological role of the amyloid precursor protein as an adhesion molecule in the developing nervous system. In *Journal of Neurochemistry* (Vol. 143, Issue 1). https://doi.org/10.1111/jnc.14122

Stahl, R., Schihing, S., Soba, P., Rupp, C., Hartmann, T., Wagner, K., Merdes, G., Eggert, S., & Kins, S. (2014). Shedding of app limits its synaptogenic activity and cell adhesion properties. *Frontiers in Cellular Neuroscience*, *8*(DEC). https://doi.org/10.3389/fncel.2014.00410

Stanic, J., Carta, M., Eberini, I., Pelucchi, S., Marcello, E., Genazzani, A. A., Racca, C., Mulle, C., di Luca, M., & Gardoni, F. (2015). Rabphilin 3A retains NMDA receptors at synaptic sites through interaction with GluN2A/PSD-95 complex. *Nature Communications*, *6*. https://doi.org/10.1038/ncomms10181

Steigerwald, F., Schulz, T. W., Schenker, L. T., Kennedy, M. B., Seeburg, P. H., & Köhr, G. (2000). C-terminal truncation of NR2A subunits impairs synaptic but not extrasynaptic localization of NMDA receptors. *Journal of Neuroscience*, *20*(12). https://doi.org/10.1523/jneurosci.20-12-04573.2000

Steubler, V., Erdinger, S., Back, M. K., Ludewig, S., Fässler, D., Richter, M., Han, K., Slomianka, L., Amrein, I., Engelhardt, J., Wolfer, D. P., Korte, M., & Müller, U. C. (2021). Loss of all three APP family members during development impairs synaptic function and plasticity, disrupts learning, and causes an autism-like phenotype. *The EMBO Journal*, *40*(12). https://doi.org/10.15252/embj.2020107471

Steward, O., & Falk, P. M. (1991). Selective localization of polyribosomes beneath developing synapses: A quantitative analysis of the relationships between polyribosomes and developing synapses in the hippocampus and dentate gyrus. *Journal of Comparative Neurology*, *314*(3). https://doi.org/10.1002/cne.903140311

Strecker, P., Ludewig, S., Rust, M., Mundinger, T. A., Görlich, A., Krächan, E. G., Mehrfeld, C., Herz, J., Korte, M., Guénette, S. Y., & Kins, S. (2016). FE65 and FE65L1 share common synaptic functions and genetically interact with the APP family in neuromuscular junction formation. *Scientific Reports*, *6*. https://doi.org/10.1038/srep25652

Sun, D. G., Kang, H., Tetteh, H., Su, J., Lee, J., Park, S. W., He, J., Jo, J., Yang, S., & Yang, S. (2018). Long term potentiation, but not depression, in interlamellar hippocampus CA1. *Scientific Reports*, *8*(1). https://doi.org/10.1038/s41598-018-23369-4

Suzuki, T., & Nakaya, T. (2008). Regulation of amyloid β-protein precursor by phosphorylation and protein interactions. In *Journal of Biological Chemistry* (Vol. 283, Issue 44). https://doi.org/10.1074/jbc.R800003200

T. Ferreira., & Rasband, W. (2012). ImageJ User Guide - IJ 1.46r. In *IJ 1.46r*.

Tanaka, S., Shiojiri, S., Takahashi, Y., Kitaguchi, N., Ito, H., Kameyama, M., Kimura, J., Nakamura, S., & Ueda, K. (1989). Tissue-specific expression of three types of β-protein precursor mRNA: Enhancement of protease inhibitor-harboring types in Alzheimer's disease brain. *Biochemical and Biophysical Research Communications*, *165*(3). https://doi.org/10.1016/0006-291X(89)92760-5

Taylor, C. J., Ireland, D. R., Ballagh, I., Bourne, K., Marechal, N. M., Turner, P. R., Bilkey, D. K., Tate, W. P., & Abraham, W. C. (2008). Endogenous secreted amyloid precursor protein-α regulates hippocampal NMDA receptor function, long-term potentiation and spatial memory. *Neurobiology of Disease*, *31*(2). https://doi.org/10.1016/j.nbd.2008.04.011

Tcw, J., & Goate, A. M. (2017). Genetics of β-Amyloid Precursor Protein in Alzheimer's Disease. In *Cold Spring Harbor perspectives in medicine* (Vol. 7, Issue 6). https://doi.org/10.1101/cshperspect.a024539

Temido-Ferreira, M., Coelho, J. E., Pousinha, P. A., & Lopes, L. v. (2019). Novel Players in the Aging Synapse: Impact on Cognition. *Journal of Caffeine and Adenosine Research*, *9*(3). https://doi.org/10.1089/caff.2019.0013

Temido-Ferreira, M., Ferreira, D. G., Batalha, V. L., Marques-Morgado, I., Coelho, J. E., Pereira, P., Gomes, R., Pinto, A., Carvalho, S., Canas, P. M., Cuvelier, L., Buée-Scherrer, V., Faivre, E., Baqi, Y., Müller, C. E., Pimentel, J., Schiffmann, S. N., Buée, L., Bader, M., … Lopes, L. v. (2020). Age-related shift in LTD is dependent on neuronal adenosine A2A receptors interplay with mGluR5 and NMDA receptors. *Molecular Psychiatry*, *25*(8). https://doi.org/10.1038/s41380-018-0110-9

Tombaugh, G. C., Rowe, W. B., Chow, A. R., Michael, T. H., & Rose, G. M. (2002). Theta-frequency synaptic potentiation in CA1 in vitro distinguishes cognitively impaired from unimpaired aged Fischer 344 rats. *Journal of Neuroscience*, *22*(22). https://doi.org/10.1523/jneurosci.22-22-09932.2002

Tomé, S. O., Gomes, L. A., Li, X., Vandenberghe, R., Tousseyn, T., & Thal, D. R. (2021). TDP-43 interacts with pathological τ protein in Alzheimer's disease. In *Acta Neuropathologica* (Vol. 141, Issue 5). https://doi.org/10.1007/s00401-021-02295-2

Tovar, K. R., & Westbrook, G. L. (2002). Mobile NMDA receptors at hippocampal synapses. *Neuron*, *34*(2). https://doi.org/10.1016/S0896-6273(02)00658-X

Trapp, B. D., & Hauer, P. E. (1994). Amyloid precursor protein is enriched in radial glia: Implications for neuronal development. *Journal of Neuroscience Research*, *37*(4). https://doi.org/10.1002/jnr.490370413

Traynelis, S. F., Wollmuth, L. P., McBain, C. J., Menniti, F. S., Vance, K. M., Ogden, K. K., Hansen, K. B., Yuan, H., Myers, S. J., & Dingledine, R. (2010). Glutamate receptor ion channels: Structure, regulation, and function. In *Pharmacological Reviews* (Vol. 62, Issue 3). https://doi.org/10.1124/pr.109.002451

Tsien, J. Z., Huerta, P. T., & Tonegawa, S. (1996). The essential role of hippocampal CA1 NMDA receptor-dependent synaptic plasticity in spatial memory. *Cell*, *87*(7). https://doi.org/10.1016/S0092-8674(00)81827-9

Tyan, S. H., Shih, A. Y. J., Walsh, J. J., Maruyama, H., Sarsoza, F., Ku, L., Eggert, S., Hof, P. R., Koo, E. H., & Dickstein, D. L. (2012). Amyloid precursor protein (APP) regulates synaptic structure and function. *Molecular and Cellular Neuroscience*, *51*(1–2). https://doi.org/10.1016/j.mcn.2012.07.009

Ultanir, S. K., Kim, J. E., Hall, B. J., Deerinck, T., Ellisman, M., & Ghosh, A. (2007). Regulation of spine morphology and spine density by NMDA receptor signaling in vivo. *Proceedings of the National Academy of Sciences of the United States of America*, *104*(49). https://doi.org/10.1073/pnas.0704031104

van der Kant, R., & Goldstein, L. S. B. (2015). Cellular Functions of the Amyloid Precursor Protein from Development to Dementia. In *Developmental Cell* (Vol. 32, Issue 4). https://doi.org/10.1016/j.devcel.2015.01.022

Vicini, S., Wang, J. F., Li, J. H., Zhu, W. J., Wang, Y. H., Luo, J. H., Wolfe, B. B., & Grayson, D. R. (1998). Functional and pharmacological differences between recombinant N- methyl-D-aspartate receptors. *Journal of Neurophysiology*, *79*(2). https://doi.org/10.1152/jn.1998.79.2.555

Vieira, M., Yong, X. L. H., Roche, K. W., & Anggono, V. (2020). Regulation of NMDA glutamate receptor functions by the GluN2 subunits. In *Journal of Neurochemistry* (Vol. 154, Issue 2). https://doi.org/10.1111/jnc.14970

von Engelhardt, J., Doganci, B., Jensen, V., Hvalby, Ø., Göngrich, C., Taylor, A., Barkus, C., Sanderson, D. J., Rawlins, J. N. P., Seeburg, P. H., Bannerman, D. M., & Monyer, H. (2008). Contribution of Hippocampal and Extra-Hippocampal NR2B-Containing NMDA Receptors to Performance on Spatial Learning Tasks. *Neuron*, *60*(5). https://doi.org/10.1016/j.neuron.2008.09.039

von Koch, C. S., Zheng, H., Chen, H., Trumbauer, M., Thinakaran, G., van der Ploeg, L. H. T., Price, D. L., & Sisodia, S. S. (1997). Generation of APLP2 KO mice and early postnatal lethality in APLP2/APP double KO mice. *Neurobiology of Aging*, *18*(6). https://doi.org/10.1016/S0197-4580(97)00151-6

von Rotz, R. C., Kohli, B. M., Bosset, J., Meier, M., Suzuki, T., Nitsch, R. M., & Konietzko, U. (2004). The APP intracellular domain forms nuclear multiprotein complexes and regulates the transcription of its own precursor. *Journal of Cell Science*, *117*(19). https://doi.org/10.1242/jcs.01323

Wang, B., Hu, Q., Hearn, M. G., Shimizu, K., Ware, C. B., Liggitt, D. H., Jin, L. W., Cool, B. H., Storm, D. R., & Martin, G. M. (2004). Isoform-Specific Knockout of FE65 Leads to Impaired Learning and Memory. *Journal of Neuroscience Research*, *75*(1). https://doi.org/10.1002/jnr.10834

Wang, C. C., Held, R. G., Chang, S. C., Yang, L., Delpire, E., Ghosh, A., & Hall, B. J. (2011). A critical role for gluN2B-containing NMDA receptors in cortical development and function. *Neuron*, *72*(5). https://doi.org/10.1016/j.neuron.2011.09.023

Wang, P., Yang, G., Mosier, D. R., Chang, P., Zaidi, T., Gong, Y. D., Zhao, N. M., Dominguez, B., Lee, K. F., Gan, W. B., & Zheng, H. (2005). Defective neuromuscular synapses in mice lacking amyloid precursor protein (APP) and APP-like protein 2. *Journal of Neuroscience*, *25*(5). https://doi.org/10.1523/JNEUROSCI.4660-04.2005

Wang, Z., Wang, B., Yang, L., Guo, Q., Aithmitti, N., Songyang, Z., & Zheng, H. (2009). Presynaptic and postsynaptic interaction of the amyloid precursor protein promotes peripheral and central synaptogenesis. *Journal of Neuroscience*, *29*(35). https://doi.org/10.1523/JNEUROSCI.2132-09.2009

Warnet, X. L., Bakke Krog, H., Sevillano-Quispe, O. G., Poulsen, H., & Kjaergaard, M. (2021). The C-terminal domains of the NMDA receptor: How intrinsically disordered tails affect signalling, plasticity and disease. In *European Journal of Neuroscience* (Vol. 54, Issue 8). https://doi.org/10.1111/ejn.14842

Wasco, W., Gurubhagavatula, S., Paradis, M. D., Romano, D. M., Sisodia, S. S., Hyman, B. T., Neve, R. L., & Tanzi, R. E. (1993). Isolation and characterization of APLP2 encoding a homologue of the alzheimer's associated amyloid β protein precursor. *Nature Genetics*, *5*(1). https://doi.org/10.1038/ng0993-95

Wenk, G. L., Walker, L. C., Price, D. L., & Cork, L. C. (1991). Loss of NMDA, but not GABA-A, binding in the brains of aged rats and monkeys. *Neurobiology of Aging*, *12*(2). https://doi.org/10.1016/0197-4580(91)90047-N

Wessels, A. M., Lines, C., Stern, R. A., Kost, J., Voss, T., Mozley, L. H., Furtek, C., Mukai, Y., Aisen, P. S., Cummings, J. L., Tariot, P. N., Vellas, B., Dupre, N., Randolph, C., Michelson, D., Andersen, S. W., Shering, C., Sims, J. R., & Egan, M. F. (2020). Cognitive outcomes in trials of two BACE inhibitors in Alzheimer's disease. *Alzheimer's and Dementia*, *16*(11). https://doi.org/10.1002/alz.12164

Weyer, S. W., Klevanski, M., Delekate, A., Voikar, V., Aydin, D., Hick, M., Filippov, M., Drost, N., Schaller, K. L., Saar, M., Vogt, M. A., Gass, P., Samanta, A., Jäsignschke, A., Korte, M., Wolfer, D. P., Caldwell, J. H., & Müller, U. C. (2011). APP and APLP2 are essential at PNS and CNS synapses for transmission, spatial learning and LTP. *EMBO Journal*, *30*(11). https://doi.org/10.1038/emboj.2011.119

Weyer, S. W., Zagrebelsky, M., Herrmann, U., Hick, M., Ganss, L., Gobbert, J., Gruber, M., Altmann, C., Korte, M., Deller, T., & Müller, U. C. (2014). Comparative analysis of single and combined APP/APLP knockouts reveals reduced spine density in APP-KO mice that is prevented by APPsα expression. *Acta Neuropathologica Communications*, *2*(1). https://doi.org/10.1186/2051-5960-2-36

Willem, M., Tahirovic, S., Busche, M. A., Ovsepian, S. v., Chafai, M., Kootar, S., Hornburg, D., Evans, L. D. B., Moore, S., Daria, A., Hampel, H., Müller, V., Giudici, C., Nuscher, B., Wenninger-Weinzierl, A., Kremmer, E., Heneka, M. T., Thal, D. R., Giedraitis, V., … Haass, C. (2015). σ-Secretase processing of APP inhibits neuronal activity in the hippocampus. *Nature*, *526*(7573). https://doi.org/10.1038/nature14864

Williams, K. (1993). Ifenprodil discriminates subtypes of the N-methyl-D-aspartate receptor: Selectivity and mechanisms at recombinant heteromeric receptors. *Molecular Pharmacology*, *44*(4).

Williams, K., Russell, S. L., Shen, Y. M., & Molinoff, P. B. (1993). Developmental switch in the expression of NMDA receptors occurs in vivo and in vitro. *Neuron*, *10*(2). https://doi.org/10.1016/0896-6273(93)90317-K

Wilquet, V., & Strooper, B. de. (2004). Amyloid-beta precursor protein processing in neurodegeneration. In *Current Opinion in Neurobiology* (Vol. 14, Issue 5). https://doi.org/10.1016/j.conb.2004.08.001

Wright, P. E., & Dyson, H. J. (2015). Intrinsically disordered proteins in cellular signalling and regulation. In *Nature Reviews Molecular Cell Biology* (Vol. 16, Issue 1). https://doi.org/10.1038/nrm3920

Xiong, M., Jones, O. D., Peppercorn, K., Ohline, S. M., Tate, W. P., & Abraham, W. C. (2017). Secreted amyloid precursor protein-alpha can restore novel object location memory and hippocampal LTP in aged rats. *Neurobiology of Learning and Memory*, *138*. https://doi.org/10.1016/j.nlm.2016.08.002

Yashiro, K., Corlew, R., & Philpot, B. D. (2005). Visual deprivation modifies both presynaptic glutamate release and the composition of perisynaptic/extrasynaptic NMDA receptors in adult visual cortex. *Journal of Neuroscience*, *25*(50). https://doi.org/10.1523/JNEUROSCI.4362-05.2005

Yashiro, K., & Philpot, B. D. (2008). Regulation of NMDA receptor subunit expression and its implications for LTD, LTP, and metaplasticity. In *Neuropharmacology* (Vol. 55, Issue 7). https://doi.org/10.1016/j.neuropharm.2008.07.046

Young-Pearse, T. L., Bai, J., Chang, R., Zheng, J. B., Loturco, J. J., & Selkoe, D. J. (2007). A critical function for β-amyloid precursor protein in neuronal migration revealed by in utero RNA interference. *Journal of Neuroscience*, *27*(52). https://doi.org/10.1523/JNEUROSCI.4701-07.2007

Yu, H., Saura, C. A., Choi, S. Y., Sun, L. D., Yang, X., Handler, M., Kawarabayashi, T., Younkin, L., Fedeles, B., Wilson, M. A., Younkin, S., Kandel, E. R., Kirkwood, A., & Shen, J. (2001). APP processing and synaptic plasticity in presenilin-1 conditional knockout mice. *Neuron*, *31*(5). https://doi.org/10.1016/S0896-6273(01)00417-2

Zajaczkowski, W., Frankiewicz, T., Parsons, C. G., & Danysz, W. (1997). Uncompetitive NMDA receptor antagoists attenuate NMDA-induced impairment of passive avoidance learning and LTP. *Neuropharmacology*, *36*(7). https://doi.org/10.1016/S0028-3908(97)00070-1

Zamzow, D. R., Elias, V., Shumaker, M., Larson, C., & Magnusson, K. R. (2013). An increase in the association of GluN2B containing NMDA receptors with membrane scaffolding proteins was related to memory declines during aging. *Journal of Neuroscience*, *33*(30). https://doi.org/10.1523/JNEUROSCI.0312-13.2013

Zhang, T., Chen, D., & Lee, T. H. (2020). Phosphorylation signaling in APP processing in Alzheimer's disease. In *International Journal of Molecular Sciences* (Vol. 21, Issue 1). https://doi.org/10.3390/ijms21010209

Zhang, W., Ross, P. J., Ellis, J., & Salter, M. W. (2022). Targeting NMDA receptors in neuropsychiatric disorders by drug screening on human neurons derived from pluripotent stem cells. In *Translational Psychiatry* (Vol. 12, Issue 1). Springer Nature. https://doi.org/10.1038/s41398-022-02010-z

Zhang, Y. W., Wang, R., Liu, Q., Zhang, H., Liao, F. F., & Xu, H. (2007). Presenilin/γ-secretase-dependent processing of β-amyloid precursor protein regulates EGF receptor expression. *Proceedings of the National Academy of Sciences of the United States of America*, *104*(25). https://doi.org/10.1073/pnas.0703903104

Zhao, X., Rosenke, R., Kronemann, D., Brim, B., Das, S. R., Dunah, A. W., & Magnusson, K. R. (2009). The effects of aging on N-methyl-d-aspartate receptor subunits in the synaptic membrane and relationships to long-term spatial memory. *Neuroscience*, *162*(4). https://doi.org/10.1016/j.neuroscience.2009.05.018

Zheng, C. Y., Petralia, R. S., Wang, Y. X., Kachar, B., & Wenthold, R. J. (2010). Sap102 is a highly mobile maguk in spines. *Journal of Neuroscience*, *30*(13). https://doi.org/10.1523/JNEUROSCI.6108-09.2010

Zhou, B., Lu, J. G., Siddu, A., Wernig, M., & Südhof, T. C. (2022). *Synaptogenic effect of APP-Swedish mutation in familial Alzheimer's disease*. https://www.science.org

Zhu, J. J., & Malinow, R. (2002). Acute versus chronic NMDA receptor blockade and synaptic AMPA receptor delivery. *Nature Neuroscience*, *5*(6). https://doi.org/10.1038/nn0602-850

Zoladz, P. R., Campbell, A. M., Park, C. R., Schaefer, D., Danysz, W., & Diamond, D. M. (2006). Enhancement of long-term spatial memory in adult rats by the noncompetitive NMDA receptor antagonists, memantine and neramexane. *Pharmacology Biochemistry and Behavior*, *85*(2). https://doi.org/10.1016/j.pbb.2006.08.011

Zou, C., Crux, S., Marinesco, S., Montagna, E., Sgobio, C., Shi, Y., Shi, S., Zhu, K., Dorostkar, M. M., Müller, U. C., & Herms, J. (2016). Amyloid precursor protein maintains constitutive and adaptive plasticity of dendritic spines in adult brain by regulating D-serine homeostasis. *The EMBO Journal*, *35*(20). https://doi.org/10.15252/embj.201694085

6 Appendix

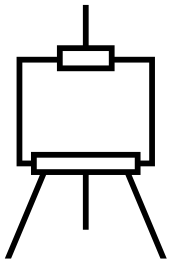

Publication related to this dissertation

Received: 2 August 2022 | Revised: 13 December 2022 | Accepted: 21 December 2022

DOI: 10.1111/acel.13778

Aging Cell WILEY

RESEARCH ARTICLE

Age-dependent NMDA receptor function is regulated by the amyloid precursor protein

Joana Rajão-Saraiva[1] | Jade Dunot[2] | Aurore Ribera[2] | Mariana Temido-Ferreira[1] | Joana E. Coelho[1] | Svenja König[3] | Sébastien Moreno[2] | Francisco J. Enguita[1] | Michael Willem[4] | Stefan Kins[3] | Hélène Marie[2] | Luísa V. Lopes[1] | Paula A. Pousinha[2]

[1]Instituto de Medicina Molecular João Lobo Antunes, Faculdade de Medicina de Lisboa, Universidade de Lisboa, Lisboa, Portugal

[2]University Côte d' Azur, Centre National de la Recherche Scientifique (CNRS) UMR 7275, Institut de Pharmacologie Moléculaire et Cellulaire (IPMC), Valbonne, France

[3]Division of Human Biology and Human Genetics, University of Kaiserslautern, Kaiserslautern, Germany

[4]Biomedical Center (BMC), Division of Metabolic Biochemistry, Faculty of Medicine, Ludwig-Maximilians-Universität München, Munich, Germany

Correspondence
Luísa V. Lopes, Instituto de Medicina Molecular, Av. Prof. Egas Moniz, 1649-028 Lisboa, Portugal.
Email: lvlopes@medicina.ulisboa.pt

Paula A. Pousinha, University Côte d' Azur, CNRS UMR 7275, IPMC, 660 Route des Lucioles, 06560 Valbonne, France.
Email: pousinha@ipmc.cnrs.fr

Funding information
Agence Nationale de la Recherche, Grant/Award Number: ANR257341; Alzheimer Forschung Initative (AFI), Grant/Award Number: DFG (KI 819/9-1); Santa Casa da Misericórdia de Lisboa, Grant/Award Number: MB-7-2018; Fundação para a Ciência e Tecnologia, Grant/Award Number: PTDC/MED-NEU/3890/2020

Abstract

N-methyl-D-aspartate receptors (NMDARs) are critical for the maturation and plasticity of glutamatergic synapses. In the hippocampus, NMDARs mainly contain GluN2A and/or GluN2B regulatory subunits. The amyloid precursor protein (APP) has emerged as a putative regulator of NMDARs, but the impact of this interaction to their function is largely unknown. By combining patch-clamp electrophysiology and molecular approaches, we unravel a dual mechanism by which APP controls GluN2B-NMDARs, depending on the life stage. We show that APP is highly abundant specifically at the postnatal postsynapse. It interacts with GluN2B-NMDARs, controlling its synaptic content and mediated currents, both in infant mice and primary neuronal cultures. Upon aging, the APP amyloidogenic-derived C-terminal fragments, rather than APP full-length, contribute to aberrant GluN2B-NMDAR currents. Accordingly, we found that the APP processing is increased upon aging, both in mice and human brain. Interfering with stability or production of the APP intracellular domain normalized the GluN2B-NMDARs currents. While the first mechanism might be essential for synaptic maturation during development, the latter could contribute to age-related synaptic impairments.

Abbreviations: 3xTg-AD, triple transgenic mouse model of Alzheimer's disease; AD, Alzheimer's disease; AICD, APP intracellular domain; APLP1, amyloid precursor-like protein 1; APLP2, amyloid precursor-like protein 2; APP, Amyloid precursor protein; APPswe, amyloid precursor protein with Swedish mutation; Aslow, amplitude of the slow component; Aβ, amyloid beta; BACE1, β-secretase 1; BI, β-secretase 1 inhibitor; Ca2+, Calcium; CTFs, APP C-terminal fragments; CTFα, APP C-terminal fragment α; CTFβ, APP C-terminal fragment β; cTKO, triple conditional knockout; DIV, days in vitro; EPSCs, excitatory postsynaptic currents; fEPSPs, field excitatory postsynaptic potentials; Ifen, ifenprodil; IPTG, Isopropyl β-D-1-thiogalactopyranoside; LTD, long-term depression; LTP, long-term potentiation; MAPT, microtubule-associated protein tau; NMDAR, N-methyl-D-aspartate receptors; NS1, nonsilencing sequence; pGluN2B, phosphorylated GluN2B; PSD, postsynaptic density; PSD-95, Postsynaptic density protein 95; PSEN1, presenilin-1; PTB1-p, PTB1 peptide; PTB2-p, PTB2 peptide; PVDF, polyvinylidene fluoride; ROI, region of interest; RT, room temperature; sAPPα, secreted APP α; sAPPβ, secreted APP β; SEM, standard error of the mean; shAPP, short-hairpin RNA against APP; shCTR, control short-hairpin RNA; shRNA, short-hairpin RNA; τweighted, weighted component.

Luísa V. Lopes and Paula A. Pousinha contributed equally as senior authors.

KEYWORDS
aging, AICD, Alzheimer's disease, APP, excitatory synapse, Fe65, GluN2B, hippocampus, NMDA receptor, postnatal development

1 | INTRODUCTION

The activation of N-methyl-D-aspartate receptors (NMDARs) at glutamatergic synapses results in calcium influx into neurons, activating downstream signaling pathways (Hardingham et al., 1999). Due to their voltage-dependent block by magnesium, NMDARs act as coincidence detectors for pre- and postsynaptic activity since receptor activation requires glutamate release and strong membrane depolarization (Nowak et al., 1984). This process is critical for the formation, maturation, maintenance, and plasticity of glutamatergic synapses, thereby contributing to development, learning, and memory processes (Gambrill & Barria, 2011; Morris et al., 1986). At the same time, NMDAR dysfunction is associated with several pathological conditions, including neurodevelopmental disorders (Burnashev & Szepetowski, 2015) and aged-related neurodegenerative diseases such as Alzheimer's disease (AD; Zhou & Sheng, 2013).

One of the main factors that determine NMDAR properties is their subunit composition. N-methyl-D-aspartate receptors are heterotetramers composed of two obligatory GluN1 subunits and two GluN2 (A–D) or GluN3 (A and B) subunits (Paoletti et al., 2013). In the hippocampus and cortex, NMDARs mainly contain GluN2A and/or GluN2B regulatory subunits (Monyer et al., 1994). GluN2B-NMDARs differ from the GluN2A subtype due to their slower deactivation kinetics, higher Ca^{2+} charge per unit of current, and specific intracellular interactors (Paoletti et al., 2013). Therefore, the synaptic GluN2B/GluN2A ratio determines the consequences of NMDAR activation, including total calcium influx and downstream signaling. This ratio is not static, changing not only in response to neuronal activity and sensory experience during postnatal development, but also in adult synapses (Paoletti et al., 2013).

During development, glutamatergic synaptic transmission in nascent synapses is mainly mediated by GluN2B-NMDARs (Bellone & Nicoll, 2007). When there is strong or synchronous neuronal activity, resulting in enough calcium entry through GluN2B-NMDARs (Adesnik et al., 2008), synapses undergo maturation, leading to alterations in the composition of postsynaptic receptors, namely a shift from a predominance of GluN2B to GluN2A-NMDARs (Williams et al., 1993; Bar-Shira et al., 2015). Upon adulthood, both NMDAR subtypes contribute for normal calcium signaling (Sobczyk et al., 2005), synaptic plasticity (Massey et al., 2004), and memory formation (von Engelhardt et al., 2008; Bannerman et al., 2008). However, these NMDAR-dependent processes become dysregulated upon aging, resulting in elevated postsynaptic calcium levels (Thibault et al., 2001), alterations in long-term potentiation/depression (LTP/LTD; Burke & Barnes, 2006; Temido-Ferreira et al., 2020) and memory deficits (Tombaugh et al., 2002). Based on this, NMDAR gain of function has emerged as a possible explanation for age-related synaptic impairments (Kumar, 2015). Accordingly, GluN2B present higher retention at aged synapses (al Abed et al., 2020; Zamzow et al., 2013) and an inverse correlation with memory performance (Zhao et al., 2009). Moreover, GluN2B-NMDAR overactivation and consequent excessive calcium influx are known to contribute to age-associated neurodegenerative disorders (Ferreira et al., 2017; Hanson et al., 2015). This hypothesis is counterintuitive, as the GluN2B subunit is thought to be the most affected by aging (Magnusson, 2012), showing a decline in expression levels (Magnusson, 2012; Zhao et al., 2009). Further knowledge by electrophysiological examination of functional changes in GluN2B-NMDARs during the aging process may be the key to understand aging cognitive disabilities.

The amyloid precursor protein (APP) has emerged as a putative NMDAR regulator, since it interacts with NMDARs in rodent brain lysates and in primary neuronal cultures (Cousins et al., 2009; Hoe et al., 2009). Also, we previously showed that in utero silencing of APP causes the loss of GluN2B synaptic contribution in infant mice (Pousinha et al., 2017). Studying the role of APP is not only challenging considering the functional redundancy with members of the same protein family, but also given the multiple APP fragments, generated by secretase cleavage, with specific cellular functions (Müller et al., 2017). The APP family is composed of three highly conserved transmembrane glycoproteins, the APP and amyloid precursor-like proteins 1 and 2 (APLP1 and APLP2), with overlapping functions (Müller & Zheng, 2012). Amyloid precursor protein undergoes extracellular cleavage mainly by α- or β-secretase (nonamyloidogenic or amyloidogenic pathway, respectively), resulting in the formation of large N-terminal extracellular fragments of secreted APP (sAPPα or sAPPβ, respectively) and smaller membrane-bound C-terminal fragments (Müller et al., 2017). Subsequently, the C-terminal fragments are subjected to an intramembranous scission by the γ-secretase complex (Wolfe et al., 1999) to generate the APP intracellular domain (AICD), which can be stabilized through its interaction to the PTB2 domain of Fe65 (Borg et al., 1996; Kimberly et al., 2001). The same cleavage step simultaneously releases p3 (after α-secretase cleavage) or the AD-related amyloid-β peptide (Aβ, after β-secretase cleavage). Therefore, APP has been mostly studied in the context of AD, while far less is known about its physiological role throughout life. Amyloid precursor protein levels reach their peak during brain development (Kirazov et al., 2001), when it has been suggested to participate in

synaptogenesis and clustering of synaptic proteins, as revealed by in vitro overexpression/knockdown studies (Baumkötter et al., 2012). Later in life, a role for APP in synaptic plasticity has been proposed, considering the impairments in LTP and cognitive behavioral performance observed in aged APP-knockout animals (>10 months), but not in earlier stages (2–4 months; Dawson et al., 1999).

We now explored the mechanism by which APP regulates NMDAR synaptic transmission at different life stages. Combining electrophysiological outputs and molecular approaches, we found a dual mechanism by which APP controls GluN2B-NMDARs. We identified the APP full-length protein as a new regulator of glutamatergic transmission in immature synapses, by controlling GluN2B synaptic content and mediated currents during development. In addition, we gathered strong evidence showing that AICD generated by the amyloidogenic pathway modifies NMDAR transmission, favoring the GluN2B synaptic contribution at later life stages. Our work highlights the importance of keeping APP processing under tight control, to ensure the normal functioning of glutamatergic synapses, being particularly relevant to understand age-related synaptic impairments and AD.

2 | RESULTS

2.1 | GluN2B-NMDAR synaptic contribution is increased in infant and aged mice

We recorded pharmacologically isolated NMDAR excitatory postsynaptic currents (EPSCs) in CA1 pyramidal cells in the hippocampus, evoked by electrical stimulation of Schaffer collaterals (Figure 1a) in C57BL/6 mice at different ages: infant (7–10 days), adult (10–16 weeks), and aged (18–20 months). To investigate whether age-mediated alterations of NMDAR currents were due to modifications of NMDAR subunit composition, we measured the time constant for the weighted component ($\tau_{weighted}$) of NMDAR EPSC deactivation kinetics. We found that NMDAR EPSC deactivation kinetics are age-dependent, since the $\tau_{weighted}$ was higher in infant (156.2 ms ± 4.20) and aged mice (177.0 ms ± 12.66), compared with the reference group of adults (126.3 ms ± 9.11; Figure 1b,c). We also found an increase in the relative amplitude of the slow component (A_{slow}) for infant and aged mice (Figure S1a).

Since GluN1/GluN2B heterodimers display slower deactivation kinetics than GluN1/GluN2A heteromers (Paoletti et al., 2013), this suggests that the GluN2B contribution to NMDAR EPSCs is higher at infant and aged life stages, when compared to adults. To test this hypothesis, we evaluated the effect of the selective GluN2B inhibitor, ifenprodil (5 μM), on NMDAR EPSCs. We found that the contribution of GluN2B to NMDAR EPSCs is of 50.88% ± 5.58 in infants, decreased to 14.20% ± 4.32 in adults, and increased to 33.11% ± 6.72 in aged mice, as depicted in Figure 1d–f.

We then correlated these effects with the GluN2B/GluN2A ratio measured in the postsynaptic density (PSD-enriched fractions; Figure 1g). The synaptic ratio of GluN2B/GluN2A was approximately four times higher in infant mice, than in adult and aged mice (Figure 1k), correlating with the increase in GluN2B synaptic contribution. A similar pattern was observed both in whole lysates (Figure 1f–i) and in PSD-95 immunoprecipitates (Figure 1j–m). The increase in GluN2B/A ratio in infants possibly reflects the lower expression levels of GluN2A at this age, while GluN2B synaptic levels reach their peak at this stage (Figure 1h–j; Figure S1b,c,f–m).

We also found that the levels of GluN2B phosphorylation (pGluN2B) at the Y1472 residue, known to enhance GluN2B-PSD95 binding (Rong et al., 2001), are reduced in infant mice and more stable in adult/aged stages (Figure 1d,e). When analyzing human postmortem tissue at different ages (21–89 years old), we found a tendency for an inverse correlation of total GluN2B levels with aging (Figure 1n,o).

These data demonstrate that NMDARs contribute to synaptic transmission in an age-dependent manner, whereby GluN2B contribution is higher in both infant and aged synapses.

2.2 | APP interacts and regulates GluN2B-NMDARs at immature synapses

There are several mechanisms and protein interactors able to regulate NMDAR synaptic transmission and GluN2B/A contribution. The APP has emerged as a potential candidate, following reports by our group and others that APP interacts, and regulates NMDAR surface levels and currents (Cousins et al., 2009; Hoe et al., 2009; Pousinha et al., 2017).

We detected APP in PSD-enriched fractions at all ages and observed a fivefold increase in infants compared with adults, whereas the APP postsynaptic levels remain low in aged synapses (Figure 2a,b; Figure S2a).

In addition, NMDARs co-immunoprecipitated with APP in whole lysates (Figure S2b), and isolated synaptosomes (Figure 2c) from infant, adult, and aged mice. This interaction is established with GluN2B over GluN2A during postnatal development, and occurs with both GluN2A and GluN2B in adult and aged animals (Figure 2c; Figure S2b–f). More importantly, this interaction was detected in human postmortem brain tissue (Figure 2d).

We previously reported that the loss of GluN2B synaptic contribution following in utero silencing of APP could be reverted by delivering the AICD peptide to the neurons (Pousinha et al., 2017), thus suggesting that APP—NMDR interaction occurs through AICD. We therefore interfered with APP—NMDAR interaction while recording NMDAR EPSCs, by introducing an APP C-terminal antibody (clone Y188, 2.5 nM) in the recording pipette (Figure 2e). We observed a reduction of 21.11 ± 4.47% in NMDAR EPSCs in infant mice, compared with the control condition (boiled Y188 antibody; as illustrated in Figure 2e–g), not amplified by increasing the Y188 antibody concentration to 5 nM (Figure S2g). This effect was not modified by preventing the APP processing through the oral administration of a β-secretase 1 (BACE 1; BI) inhibitor 12 h prior to patch-clamp recordings (LY2811376; 100 mg/kg; Figure 2g; Figure S2h).

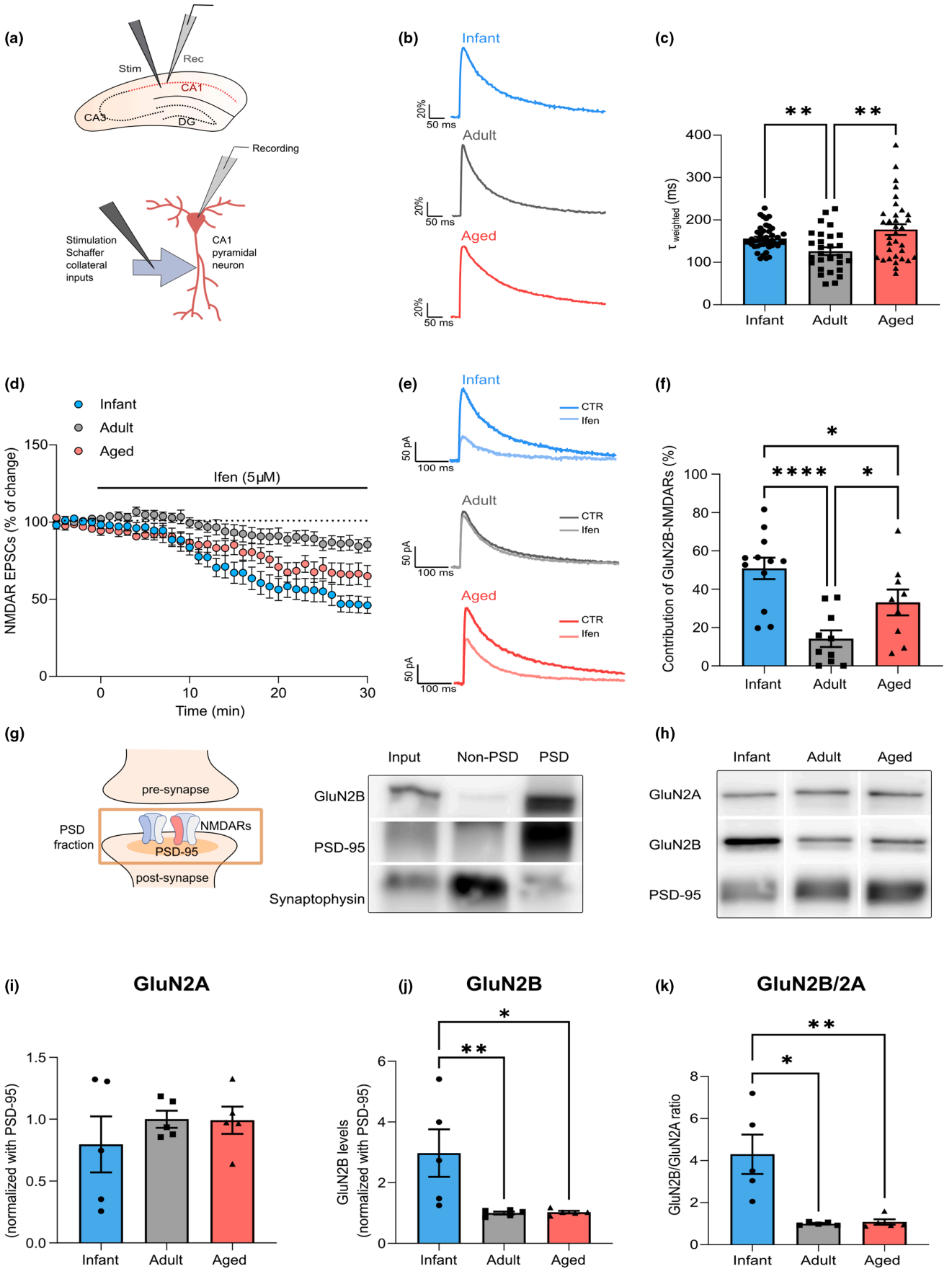

FIGURE 1 GluN2B-N-methyl-D-aspartate receptor (NMDAR) synaptic contribution is increased in infant and aged mice. (a) Schematic diagram showing the locations of stimulating and recording electrodes in the hippocampus and in a CA1 pyramidal neuron for whole-cell patch-clamp experiments. (b) Comparison of representative whole-cell patch-clamp recordings of pharmacologically isolated NMDAR EPSCs, normalized to the peak amplitude (in %), from infant (7–10 days), adult (10–16 weeks), and aged (18–20 months) C57BL/6 wild-type mice, illustrating differences in deactivation kinetics. (c) The weighted time constant (τweighted) was calculated using the relative contribution of both slow/fast components of NMDAR EPSCs and reflects the overall deactivation kinetics. Results are expressed as the mean ± SEM (Kruskal–Wallis, $p = 0.004$, Kruskal–Wallis statistic = 11.02, followed by uncorrected Dunn's multiple comparisons test, $^{**}p < 0.01$, $n = 28–44$). (d) Time course of ifenprodil (5 μM) effect on pharmacologically isolated NMDAR EPSC amplitude in CA1 pyramidal neurons, measured by whole-cell patch clamp in infant, adult, and aged C57BL/6 wild-type mice. Results are expressed as the mean ± SEM ($n = 9–12$). (e) Traces show NMDAR EPSCs recorded before (CTR) and after 30 min of Ifenprodil 5 μM perfusion (Ifen). (f) GluN2B contribution was calculated as the percentage of change in NMDAR EPSC amplitude after 30 min of ifenprodil perfusion. Results are expressed as the mean ± SEM (One-way ANOVA, $p = 0.0002$, $F(2, 28) = 11.37$, followed by uncorrected Fisher's LSD's multiple comparisons test, $^{*}p < 0.05$, $^{****}p < 0.0001$, $n = 9–12$). (g) Schematic representation and immunoblotting analysis of postsynaptic density (PSD)-enriched fractions from the hippocampal tissue of adult C57BL/6 wild-type mice. Membranes were immunoblotted with antibodies for GluN2B, PSD-95, and synaptophysin. PSD fractions are enriched in PSD-95, whereas non-PSD fractions contain high levels of synaptophysin. (h) Representative Western blot of hippocampal lysates subjected to biochemical fractionation to obtain PSD-enriched fractions from infant, adult, and aged C57BL/6 mice. Membranes were immunoblotted with antibodies for GluN2A, GluN2B, and PSD-95. (i, j) Results from PSD-enriched fractions blots as shown in h) were normalized with PSD-95 and are expressed as the mean ± SEM relative to the adult group. (i) One-way ANOVA, $p = 0.5735$, $F(2, 12) = 0.5825$, $n = 5$). (j) One-way ANOVA ($p = 0.014$, $F(2, 12) = 6.224$), followed by Uncorrected Fisher's LSD's multiple comparisons test, $^{*}p < 0.05$, $^{**}p < 0.01$, $n = 5$). (k) Results show the GluN2B/GluN2A in PSD-enriched fractions blots as shown in h) and are expressed as the mean ± SEM relative to the adult group (Kruskal–Wallis, $p = 0.0024$, Kruskal–Wallis statistic = 9.42, followed by Uncorrected Dunn's multiple comparisons test, $^{*}p < 0.05$, $^{**}p < 0.01$, $n = 5$). The full statistical analysis and Western Blot membranes are provided in the Supporting Information.

To test whether this response is mediated by GluN2B-NMDARs, we perfused hippocampal slices with a GluN2B selective antagonist, ifenprodil (5 μM), for 30 min at the end of the experiment (60–90 min; Figure 2h). As shown, the effect of ifenprodil was reduced in neurons previously incubated with the Y188 antibody, when comparing to the control condition (19.76 ± 3.29 vs. 46.82 ± 5.16%; Figure 2h–j). BY contrast, we found no alterations in NMDAR-mediated currents in adult and aged mice by blocking APP (Figure 2g).

In conclusion, these results show that APP interacts with GluN2B at immature synapses, thus regulating their contribution to NMDAR EPSCs.

2.3 | APP modulates the GluN2B-NMDAR synaptic content in immature synapses

The reported impact of APP on NMDAR transmission suggested a role for APP in regulating NMDARs during postnatal development. To assess the outcomes of APP depletion in immature neurons, we transfected primary neuronal cultures (7 days in vitro (DIV)) with a plasmid encoding a short-hairpin RNA (shRNA) sequence against APP (shAPP) or the respective control (shRNA with no silencing effect, shCTR). The APP knockdown was efficient, leading to a reduction of approximately 80% in APP immunoreactivity, when comparing to the control condition, evaluated 7 days post-transfection (14 DIV; Figure 3a,b).

Amyloid precursor protein-depleted neurons showed a significant reduction in the percentage of GluN2B clusters that co-localize with PSD-95 (postsynaptic marker; approximately 20%; Figure 3c,d). The GluN2B relative dendritic area, average particle size, and fluorescent density were not altered by APP depletion, indicating that GluN2B total levels/area and clustering remained constant (Figure 3c,e; Figure S3a,b).

Considering the impact of GluN2B on synaptic maturation, in which PSD-95 recruitment is a crucial step (Elias et al., 2008), we also evaluated whether this process is impaired in APP-depleted neurons. We found a reduction in PSD-95 dendritic area and average particle size (Figure 3c,f; Figure S3c), whereas the fluorescence density was not altered (Figure S3d).

These findings show that APP regulates GluN2B synaptic content and PSD-95 clustering in immature neurons.

2.4 | Age-related increase in βAPP processing contributes to higher GluN2B synaptic contribution

Since the increase in GluN2B contribution to NMDAR EPSCs in aged mice is not correlated with APP postsynaptic levels or APP-NMDAR interaction, we hypothesized that APP in its full-length form is not responsible for these alterations. In fact, we had previously reported that an APP-derived fragment, the AICD, has the ability to regulate synaptic GluN2B in CA1 pyramidal neurons (Pousinha et al., 2017).

We thus characterized APP processing throughout time in the hippocampus of wild-type C57BL/6 mice by detecting APP full-length (APP), APP C-terminal fragments (CTFs), and AICD. When compared to adults, aged mice displayed no alterations in the APP levels (Figure 4a,b), but instead, they exhibited an increase in APP processing products. Accordingly, the total CTFs levels in relation to APP, as well as the CTFs absolute values, exhibit an approximately 1.4-fold increase in aged mice (Figure 4a,c; Figure S4a). We found that the levels of AICD increased with aging, either in relation to APP or in absolute values (Figure 4a,d; Figure S4b).

We performed an approximate discrimination of the CTFs derived from α-secretase cleavage (CTFα, C83, and ≈9KDa) or β-secretase processing (CTFβ, C99, and ≈11 KDa) based on their molecular weight and using a triple transgenic mouse (3xTg-AD) as reference, since this model exhibits a predominant accumulation of CTFβ over the smaller CTFα (Lauritzen et al., 2012; Figure 4a). We found that the CTF β/α ratio increases upon aging (Figure 4a; Figure S4c). A similar tendency was observed for CTFβ (C99) detected with a specific antibody, although not reaching statistical significance (Figure 4e,f; Figure S4d).

To elucidate whether this age-related pattern of APP processing is also observed in the human brain, we prepared lysates from

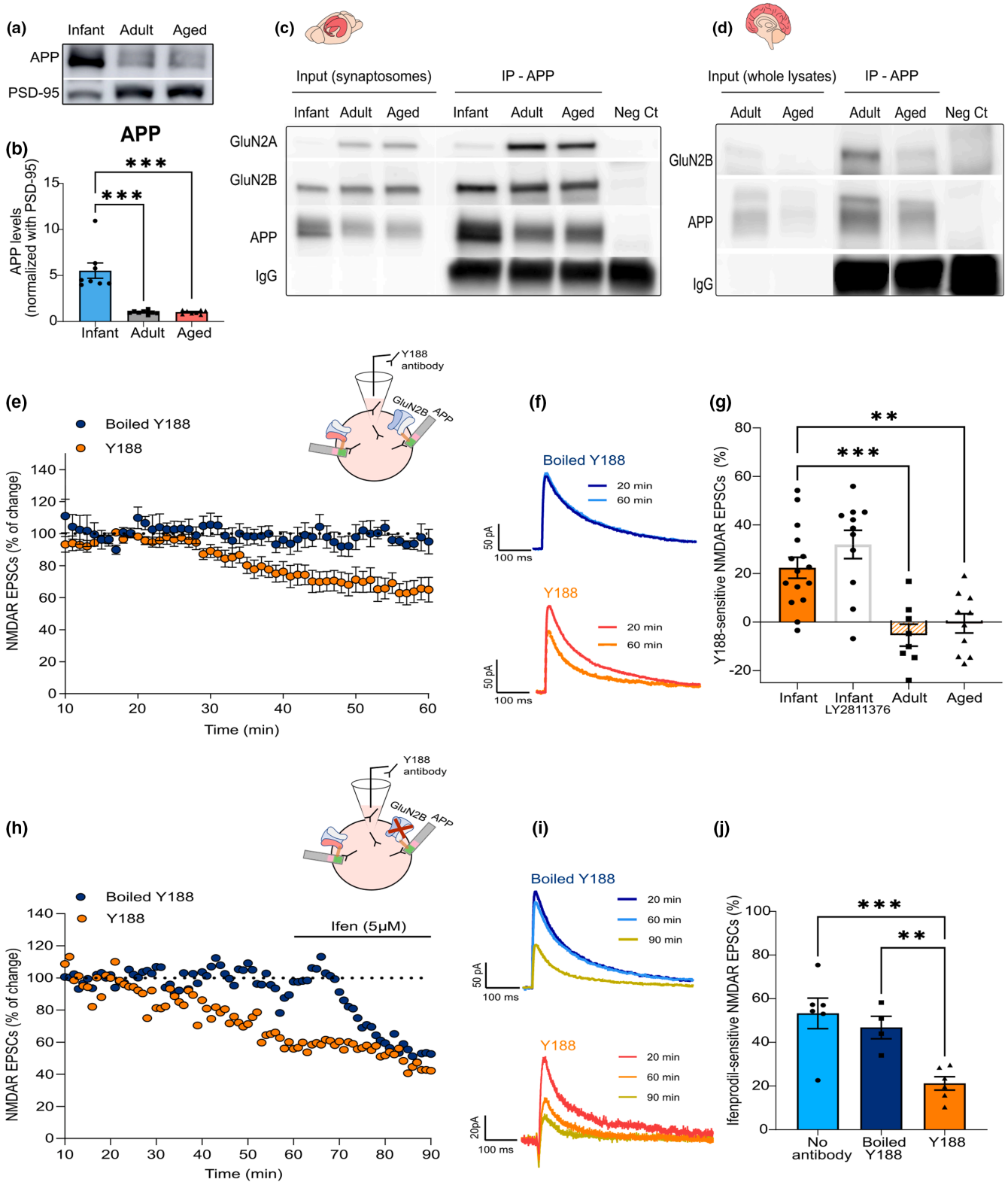

FIGURE 2 Amyloid precursor protein (APP) interacts and regulates GluN2B-N-methyl-D-aspartate receptors (NMDARs) at immature synapses. (a) Representative Western blot of hippocampal postsynaptic density (PSD)-enriched fractions from infant (7–10 days), adult (10–16 weeks), and aged (18–20 months) wild-type C57BL/6 mice. Membranes were immunoblotted with antibodies for APP and PSD-95. (b) Results from PSD-enriched fractions blots as shown in a) show APP levels normalized with PSD-95 and are expressed as the mean ± SEM relative to the adult group (Kruskal–Wallis, $p = 0.0005$, Kruskal–Wallis statistic = 15.37, followed by uncorrected Dunn's test, $^{***}p < 0.001$, $n = 8$). (c) Representative Western blot of synaptosome fractions from the hippocampi of infant, adult, and aged wild-type C57BL/6 mice immunoprecipitated for APP. Membranes were immunoblotted with antibodies for GluN2A, GluN2B, and APP. (d) Representative Western blot of postmortem brain tissue (prefrontal cortex) from human subjects (adult = 22 and aged = 89 years old) immunoprecipitated for APP. Membranes were immunoblotted with antibodies for GluN2B and APP. (e) Time course of NMDAR EPSC amplitude measured by whole-cell patch clamp in CA1 pyramidal neurons of infant C57BL/6 wild-type mice during 60 min of incubation with an antibody against the APP C-terminal (Y188). In the control condition, the antibody was heat-inactivated (boiled Y188). Results are expressed as the mean ± SEM ($n = 6$–10). The schematic diagram shows the strategy used to mask the APP C-terminal domain—the antibody was added to the intracellular solution in the patch pipette to diffuse into the intracellular space. (f) Traces show NMDAR EPSCs recorded at 20 min (baseline) and 60 min. The Y188 antibody was inside the patch pipette during the whole course of the experiment (60 min). (g) The percentage of Y188-sensitive NMDAR EPSCs was determined for infant mice with or without treatment with a BACE1 inhibitor (LY2811376, administration 12 h prior to patch-clamp recordings), adult, and aged C57BL/6 wild-type mice. The effect was calculated comparing the baseline amplitude (20 min) with the final amplitude (60 min) and normalized with the control condition (boiled Y188) for each age. Results are expressed as the mean ± SEM (One-way ANOVA, $p < 0.0001$, $F(3, 40) = 12.65$, followed by uncorrected Fisher's LSD's multiple comparisons test, $^{**}p < 0.01$, $^{***}p < 0.001$, $n = 8$–15). (h) Time course of NMDAR EPSC amplitude measured by whole-cell patch clamp in CA1 pyramidal neurons of infant C57BL/6 wild-type mice during 90 min of incubation with the Y188 antibody and perfusion with ifenprodil (5 μM) at 60–90 min. In the control condition, the antibody was heat-inactivated (boiled Y188; $n = 1$). The schematic diagram shows the strategy used to block APP (Y188 antibody in the patch pipette) and to inhibit GluN2B-NMDAR (ifenprodil perfusion). (i) Traces show NMDAR EPSCs recorded at 20 min (baseline), 60 min, and 90 min. The Y188 antibody was inside the patch pipette during the whole course of the experiment (90 min), whereas Ifenprodil perfusion occurred from 60 to 90 min. (j) The percentage of ifenprodil-sensitive NMDAR EPSCs in infant mice was calculated comparing the amplitude at 60 min with the final amplitude (90 min). The effect of ifenprodil on NMDAR EPSCs was calculated in neurons without antibody incubation (No antibody, used as reference), incubated with the Y188 antibody (Y188) or the heat-inactivated antibody (boiled Y188) for 90 min. Results are expressed as the mean ± SEM (one-way ANOVA, $p = 0.0019$, $F(2, 13) = 10.59$, followed by uncorrected Fisher's LSD multiple comparisons test, $^{***}p < 0.001$, $^{**}p < 0.01$, $n = 4$–6). The full statistical analysis and Western Blot membranes are provided in the Supporting Information.

human postmortem brain tissue (prefrontal cortex) of subjects with different ages (18–81 years old; Figure 4g). We found an inverse correlation between age and APP levels (Figure 4g,h), and a positive correlation in the production of CTFs and AICD from APP (Figure 4g,i,j). This is linked to an increase in the absolute levels of AICD, but not of CTFs (Figure S4e,f) or in the CTF β/α ratio (Figure S4g). We detected a similar pattern of APP levels/processing in samples from AD patients ($n = 4$, 65–81 years old) compared with aged controls (65–89 years old; Figure S4h–k), albeit more variable.

To test the hypothesis that APP amyloidogenic-derived fragments are involved in the changes of NMDA function, we treated aged mice with the BACE 1 (BI) inhibitor (LY2811376; 100 mg/kg) to inhibit APP β-processing (Figure 5a,b). The treated aged mice displayed a significant decrease in GluN2B synaptic contribution (Figure 5i–k) to a magnitude similar to that of untreated adult mice. We confirmed that the treatment was effective in reducing the levels of sAPPβ in the hippocampus (Figure 5c,f). This was accompanied by an increase in the sAPPα levels (Figure 5d,g), while the levels of APP full-length remained unaltered (Figure 5e,h).

We had previously implicated the $Y^{682}ENPTY^{687}$ sequence of AICD on the GluN2B-mediated effects in adult mice (Pousinha et al. 2017). The PTB2 domain of Fe65 (PTB2-p) is known to bind to the $Y^{682}ENPTY^{687}$ sequence (Feilen et al., 2017), thus interfering with AICD-Fe65 signaling. In hippocampal slices pre-incubated with PTB2-p for >3 h (Figure 5a,l), the aged GluN2B-NMDAR-mediated currents were rescued to adult-like levels (Figure 5m–o; Figure S5a,b), whereas the control PTB1 domain [PTB1-p; which does not bind either APP or AICD (Cao & Sudhof, 2001)] was devoid of effects, ruling out any nonspecific buffering effects of the PTBs domain.

We concluded that increased APP processing upon aging might lead to exacerbated AICD signaling, thus contributing to the aberrant NMDAR synaptic currents observed in aged cells.

3 | DISCUSSION

We show that synaptic GluN2B-NMDARs are regulated by APP in an age-dependent manner. During postnatal development, APP interacts with GluN2B at the synapse and modulates its synaptic content and evoked currents, possibly having an impact on synaptic maturation. On the contrary, APP-derived amyloidogenic fragments, namely AICD, contribute to increased GluN2B synaptic contribution upon aging, potentially underlying age-related synaptic impairments.

We found that the APP interaction regulates the GluN2B-NMDARs function during development, a life stage when the GluN2B subtype predominates, accounting for more than 50% of NMDAR EPSCs in the CA1 hippocampal region. The electrophysiological output reflected the synaptic NMDAR subunit composition, since infant mice exhibited a high GluN2B/GluN2A ratio in protein levels, according to the previously described NMDAR developmental switch (GluN2B to GluN2A) that occurs during postnatal

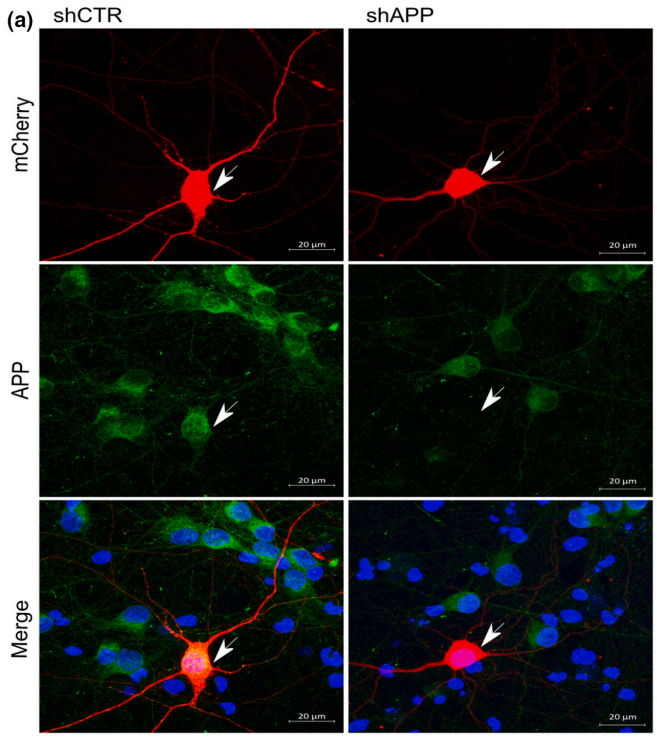

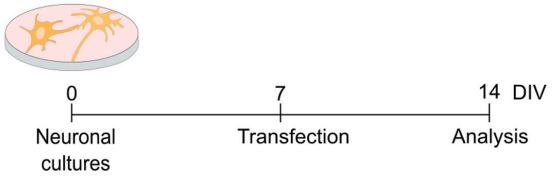

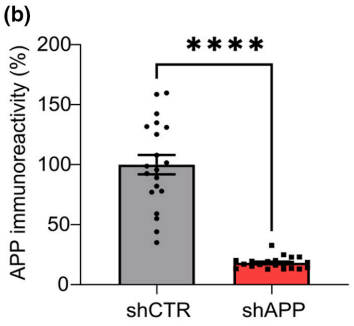

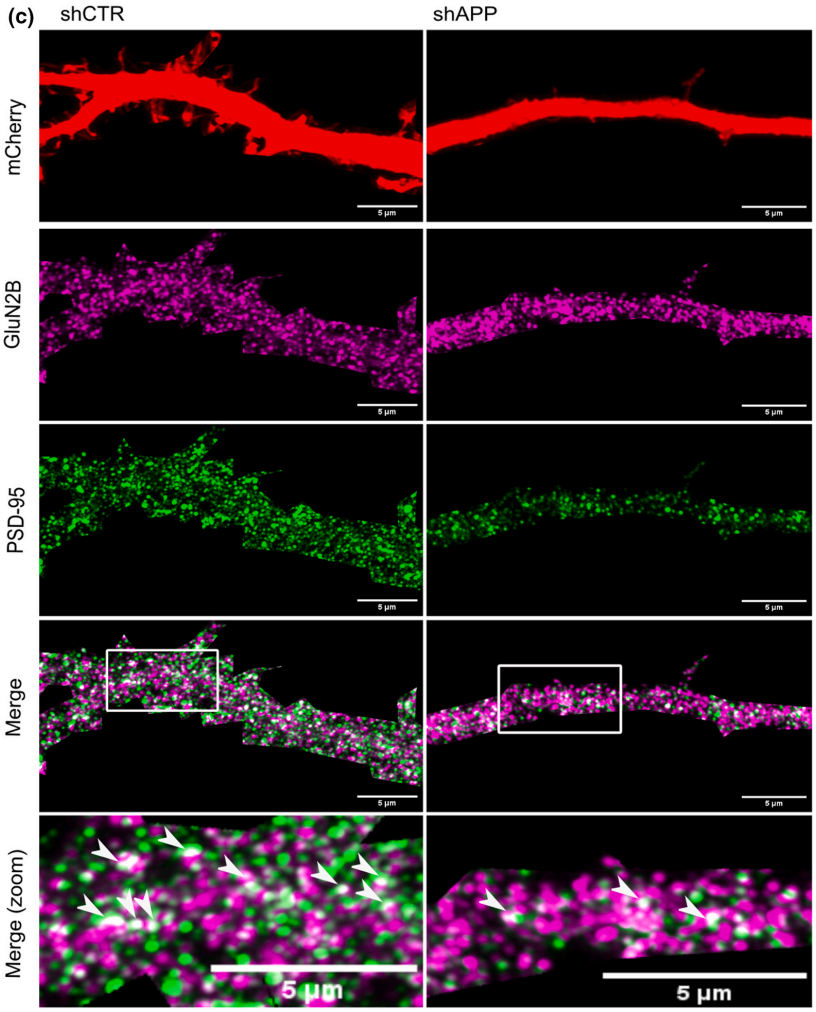

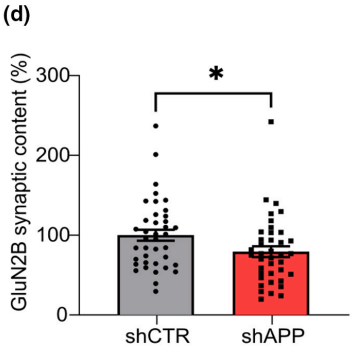

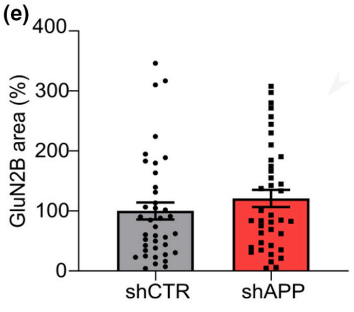

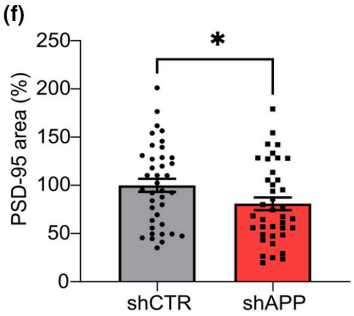

FIGURE 3 Amyloid precursor protein (APP) modulates the GluN2B-N-methyl-D-aspartate receptor (NMDAR) synaptic content in immature neurons. (a) Representative immunocytochemistry analysis of APP immunofluorescence in rat primary neuronal cultures (14 days in vitro (DIV)) transfected with shAPP or the respective control (shCTR) at DIV7, as indicated in the timeline. mCherry (reporter plasmid) is shown in red, APP is labeled in green and cell nuclei are stained with Hoechst in blue. Transfected neurons are indicated by arrows. Scale bars represent 20 μm. (b) APP immunoreactivity (%) in transfected neurons is expressed as the mean ± SEM, using the control condition as reference (Mann–Whitney test, $^{****}p < 0.0001$, $n = 20–21$ cells, three independent cultures). (c) Representative immunocytochemistry analysis of rat primary neuronal cultures (DIV14) transfected with shAPP or the respective control (shCTR) at DIV7. mCherry (reporter plasmid), labeled in red, was used to identify dendrites of transfected neurons. GluN2B is shown in magenta and postsynaptic density (PSD)-95 is labeled in green. Higher magnification images are shown at the bottom, with arrows indicating GluN2B/PSD95 co-localization. Scale bars represent 5 μm. (d and e) Results show GluN2B synaptic content and GluN2B total area in dendrites of transfected neurons. The synaptic content was calculated as the area of GluN2B-PSD co-localization normalized with the total area of GluN2B. Results are expressed as the mean ± SEM, using the control condition as reference (%; Mann–Whitney test, $^{*}p < 0.05$, $n = 39$, three independent cultures). (f) Results show PSD-95 total area in dendrites of transfected neurons. Results are expressed as the mean ± SEM, using the control condition as reference (%; Unpaired *t* test, $^{*}p < 0.05$, $n = 39$, 3 independent cultures). The full statistical analysis is provided in the Supporting Information.

development (Williams et al., 1993). These data indicate a crucial role for APP at the postsynapse, in contrast with most of the studies so far, which focused on APP function at the presynapse (Marquez-Sterling et al., 1997, Lyckman et al., 1998), given the low APP levels detected in PSD-enriched fractions from the adult brain (Kim et al., 1995).

We now found that APP subcellular localization is age-dependent, since we could observe abundant APP at the postsynapse in infant mice, whereas the levels decline in adulthood and aging, thus suggesting that the role of APP at the synapse shifts with age. Indeed, we proved that the presence of a monoclonal antibody against the APP C-terminal affects NMDAR-evoked currents during postnatal development. Importantly, this experimental strategy allows elucidating the role of APP at the postsynapse without interfering with the pre-synaptic compartment. The fact that preventing the APP β-processing did not modify this effect further reinforces the direct interaction between APP and NMDAR. It is likely that the kinetics of the action of the antibody is related to an alteration in the synaptic residency of NMDARs, a dynamic process that occurs within minute range (Groc et al., 2006), rather than to the turnover of the NMDAR subunits (half-life of 2–34 h; Huh & Wenthold, 1999).

The NMDAR-APP interaction was further investigated in rat hippocampal primary neuronal cultures at immature state (DIV 7–14), since this model recapitulates the synapse development process (Grabrucker et al., 2009) and the NMDAR developmental switch (Corbel et al., 2015), while providing appropriate imaging resolution to study synaptic proteins. Amyloid precursor protein-depleted neurons exhibited a decreased GluN2B synaptic content, thereby confirming that APP is crucial for NMDAR synaptic levels/activity in immature synapses. Considering the key role of GluN2B currents for synaptic maturation (Gray et al., 2011), we hypothesize that APP-NMDAR regulation is essential to achieve functional mature synapses. N-methyl-D-aspartate receptor activity has been associated with PSD-95 recruitment to new synapses (de Roo et al., 2008). This is consistent with our observations in APP-depleted neurons, in which the decreased GluN2B synaptic content is accompanied by a reduction in PSD-95 dendritic area and cluster size. However, we cannot discard the possibility that APP could directly regulate PSD-95 area and average particle size. In that case, the decline in GluN2B synaptic content might occur as an indirect response. The results obtained upon APP C-terminal disruption in infant mice show that it is possible to rapidly interfere with APP-NMDAR regulation, favoring the hypothesis of NMDAR synaptic stabilization rather than a structural role in PSD-95.

These data might seem contradictory with the observation that the APP KO model only presents synaptic deficits after 10 months of age (Dawson et al., 1999). This may result from the functional redundancy of APP and APP-like proteins (APLP1 and ALPL2). In accordance, constitutive triple knockout mice (TKO) die after birth (Heber et al., 2000), whereas Nex-Cre cTKO (conditional triple KO in excitatory forebrain neurons starting during embryonic development) present gross brain morphology alterations (Steubler et al., 2021), showing a crucial role for APP family members during development. Our combination of in vitro silencing and acute interference of the APP C-terminal domain ex vivo overcome a possible compensation by APP family members, while allowing to study APP specifically during postnatal developmental stages.

Considering that the antibody against the APP C-terminal had a significant effect on NMDAR-mediated currents in infant mice, this seems to be the domain responsible for interacting and regulating NMDARs at this stage. In particular, the YENPTY motif is highly conserved in APP family members and different species (Shariati & de Strooper, 2013) and known to interact with several proteins, such as Fe65 (van der Kant & Goldstein, 2015), possibly acting, directly or indirectly, as the interacting site for NMDARs. We had previously shown that neurons expressing a mutated form of AICD in the YENPTY motif lose their ability to modulate NMDA currents in the adult rat (Pousinha et al., 2017). Accordingly, mouse models in which the APP C-terminal domain is mutated (Matrone et al., 2012) or depleted (APPdCT15 knockin mice/APLP2 KO; Klevanski et al., 2015) show high postnatal lethality, impairments in synaptic plasticity, and memory in adult stages, which might be explained by NMDAR dysregulation, although this hypothesis has not been explored so far.

We could not affect NMDAR EPSCs in adult/aged animals when interfering with the APP C-terminal domain in a 60 min time window. Considering the technical approach we used, it is

possible that the accessibility of the APP C-terminal epitope at the postsynapse might be precluded in adult stages, due to the extensive alterations that occur in PSD structure and composition after postnatal development (Gonzalez-Lozano et al., 2016). However, we can also postulate that the APP regulation of NMDARs has indeed a higher impact during development, which is consistent with the marked decline of postsynaptic APP levels observed in adult stages. Moreover, it is possible that the APP-NMDAR regulation mainly occurs through GluN2B, whose synaptic contribution declines after development. Our observation of a reduced effect of ifenprodil on the neurons from infant mice exposed to the APP C-terminal antibody indicates that GluN2B-NMDARs are highly affected by disruption of APP C-terminal. Since APP interacts with both GluN2B and GluN2A in adult stages, it is extremely difficult to determine whether there is a subunit preferential binding, especially considering that triheteromeric complexes (GluN1/GluN2A/GluN2B) also exist in the hippocampus (Rauner & Köhr, 2011). Given the increased association of PSD-95 with NMDARs in mature synapses (Elias et al., 2008), we can postulate that the NMDAR synaptic clustering becomes APP-independent upon adulthood. However, the fact that the Camk2a-Cre cTKO mouse model (triple conditional knockout for APP family members in excitatory forebrain neurons starting at postnatal weeks 3–4) exhibits LTP impairments

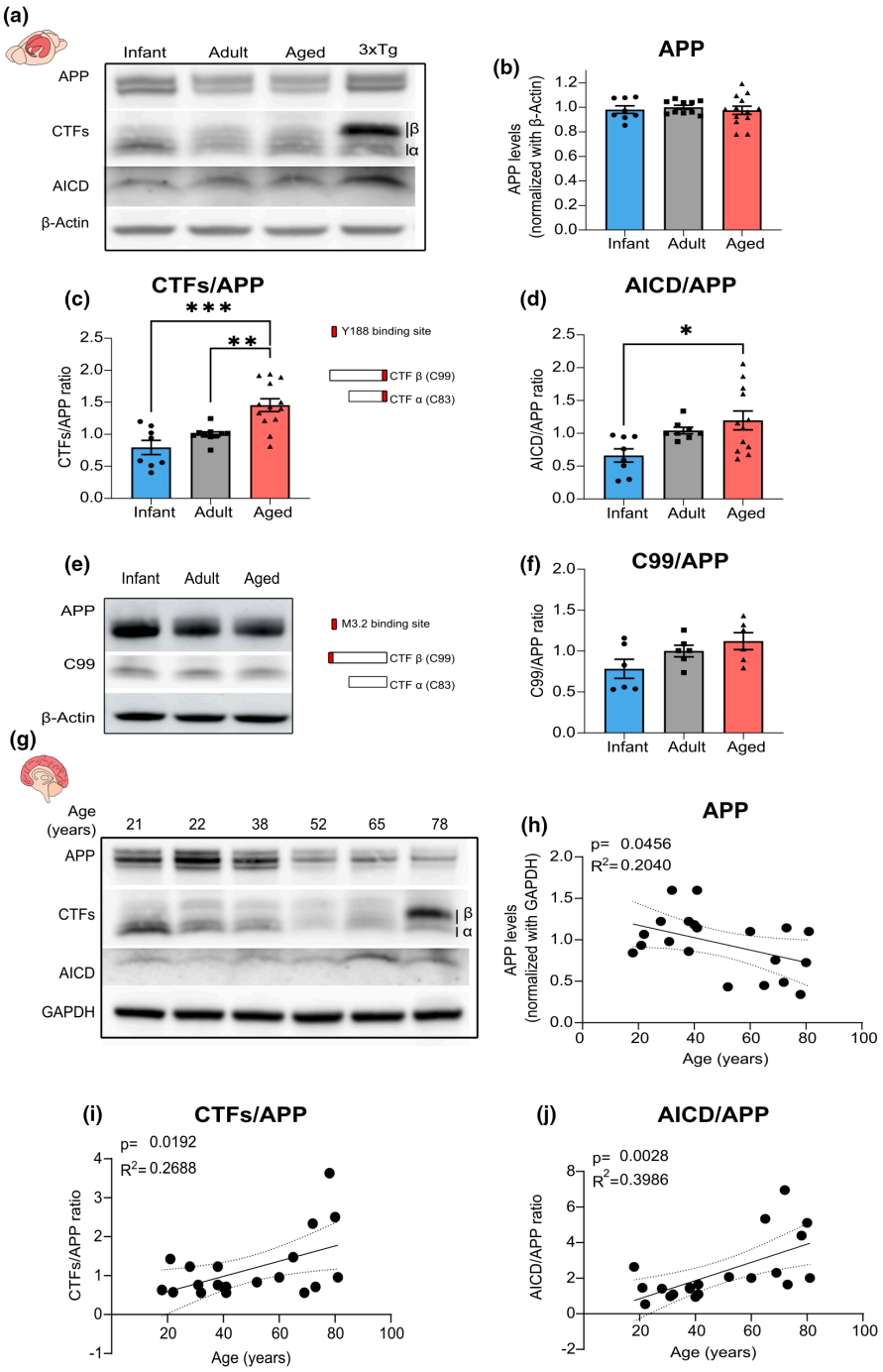

FIGURE 4 Age is associated with an increase in amyloid precursor protein (APP) processing in mice and humans. (a) Representative Western blot of hippocampal lysates from infant (7–10 days), adult (10–16 weeks), and aged (18–20 months) C57BL/6 wild-type mice. Membranes were immunoblotted with antibodies for APP C-terminal (to detect APP full-length (APP), APP C-terminal fragments (CTFs β and α), and the APP intracellular domain (AICD)) and β-actin. A female triple transgenic mouse (3xTg, 6 months) was used as a positive control for APP-derived fragments. (b) Results from blots shown in a) from mouse hippocampal lysates were normalized with β-actin and are expressed as the mean ± SEM relative to the adult group (one-way ANOVA, $p = 0.8263$, $F(2, 28) = 0.1921$, $n = 8–13$). (c) Results from blots shown in a) from mouse hippocampal lysates show the ratio between CTFs and APP are expressed as the mean ± SEM relative to the adult group (Kruskal–Wallis test, $p = 0.0008$, Kruskal–Wallis statistic = 14.21, followed by uncorrected Dunn's test, $^{**}p < 0.01$, $^{***}p < 0.001$, $n = 8–13$). The different CTFs detected with the Y188 antibody (CTFβ (C99) and CTFα (C83)) are schematically represented, with the antibody binding site illustrated in red. (d) Results from blots shown in a) from mouse hippocampal lysates show the ratio between AICD and APP and are expressed as the mean ± SEM relative to the adult group (One-way ANOVA, $p = 0.0143$, $F(2, 25) = 5.057$, followed by uncorrected Fisher's LSD's multiple comparisons test, $^{*}p < 0.05$, $n = 8–13$). (e) Representative Western blot of hippocampal lysates from infant, adult, and aged C57BL/6 wild-type mice. Membranes were immunoblotted with the M3.2 antibody to detect APP and CTFβ (C99) and probed for β-actin as the loading control. The binding site for the M3.2 antibody is represented in red, showing that it specifically detects CTFβ (C99). (f) Results from blots shown in (e) from mouse hippocampal lysates show the ratio between C99 and APP and are expressed as the mean ± SEM relative to the adult group (one-way ANOVA, $p = 0.0802$, $F(2, 15) = 3.000$, $n = 8–13$). (g) Representative Western blot of prefrontal cortex human samples (18 to 81 years old). Membranes were immunoblotted with antibodies for APP C-terminal (to detect APP, CTFs β and α, and AICD) and GAPDH as the loading control. (h) Linear regression graph calculated from blots as shown in (g) shows the variation in APP levels (normalized to GAPDH) depending on the age of human subjects. Statistical analysis was performed using Pearson's correlation (two-tailed *p*-value), $p = 0.0456$, $R2 = 0.204$, $n = 20$. Dotted lines represent the 95% confidence intervals. The values obtained for 20–25-year-old subjects were used as reference. (i) Linear regression graph calculated from blots as shown in (g) shows the variation in the ratio between APP-CTFs and APP depending on the age of human subjects. Statistical analysis was performed using Pearson's correlation (two-tailed *p*-value), $p = 0.0192$, $R2 = 0.2688$, $n = 20$. Dotted lines represent the 95% confidence intervals. The values obtained for 20–25-year-old subjects were used as reference. (j) Linear regression graph calculated from blots as shown in (g) shows the variation in the ratio between AICD and APP depending on the age of human subjects. Statistical analysis was performed using Pearson's correlation (two-tailed *p*-value), $p = 0.0028$, $R^2 = 0.3986$, $n = 20$. Dotted lines represent the 95% confidence intervals. The values obtained for 20–25-year-old subjects were used as reference. The full statistical analysis and Western Blot membranes are provided in the Supporting Information.

and reduced NMDAR-mediated responses in adult stages suggests that some form of NMDAR regulation by APP family members still occurs later in life (Lee et al., 2020).

We found that NMDAR deactivation kinetics become slower upon aging, possibly explaining the increased duration of NMDAR field excitatory postsynaptic potentials (fEPSPs) described previously in aged rodents (Jouvenceau et al., 1998). These data correlate with the augmented GluN2B contribution in aged mice, possibly reflecting the higher GluN2B synaptic retention reported in previous studies (al Abed et al., 2020; Zamzow et al., 2013). We postulate that APP contributes to these alterations, controlling NMDAR function in aged synapses. This hypothesis is supported by the synaptic plasticity and learning/memory deficits observed in APP KO-aged mice, but not at earlier stages (10 months vs. 4 months; Dawson et al., 1999).

Our findings suggest that the APP-NMDAR regulation in aged synapses occurs through APP-derived fragments rather than through the full-length protein. We detected a significant enhancement of APP processing into CTFs and AICD upon aging. Importantly, we observed the same profile in human brain samples, in which we established a positive correlation between APP processing and aging. Considering the previously described accumulation of CTFs (Burrinha et al., 2021) and increased BACE1 activity (Fukumoto et al., 2004) in aged mice, we postulate that this accumulation of APP-derived amyloidogenic fragments will eventually lead to alterations in NMDAR function. To test this hypothesis, we used a β-secretase 1 (BACE 1) inhibitor in aged animals to block the APP amyloidogenic processing, which resulted in a decrease in GluN2B synaptic contribution of about 20%, a magnitude closer to that obtained in adult mice.

Although we did not single out the APP amyloidogenic fragment responsible for this effect, the AICD has emerged as a potential target. This APP-derived fragment is affected by BACE1 inhibition, since the biologically active AICD form mainly derives from the amyloidogenic pathway (Goodger et al., 2009). We have previously shown that the overexpression of AICD in adult synapses leads to a NMDAR-GluN2B electrophysiological profile similar to the one we now report in aging (Pousinha et al., 2017). Concomitantly, we detect an increase in AICD levels upon aging. The fact that interfering with AICD-Fe65 interaction rescued the GluN2B contribution, further strengthens a role for AICD in the observed effects. Accordingly, the disruption of the AICD-Fe65 interaction normalized the GluN2B contribution to adult-like levels. The mechanism by which PTB2-p affects GluN2B-NMDAR-mediated currents may depend on direct binding of PTB2 to AICD after uptake in an endocytosis-dependent manner, as described for different cytosolic proteins, such as tau and alpha-synuclein (Peng et al., 2020) or by direct transmission over the membrane, as postulated for monomeric alpha-synuclein (Lee et al., 2008) or proteins carrying specific transmission sequences that resemble positively charged nuclear localization sequences (Suzuki, 2012). The AICD-Fe65 complex induces multiple signaling pathways (Augustin & Kins, 2021), as well as transcriptional activity in several target genes, including the one encoding for GluN2B (Grimm et al., 2013; Pousinha et al., 2017). The fact that we did not detect alterations in the synaptic levels of GluN2B by aging suggests that other transcriptional targets may be involved in the observed

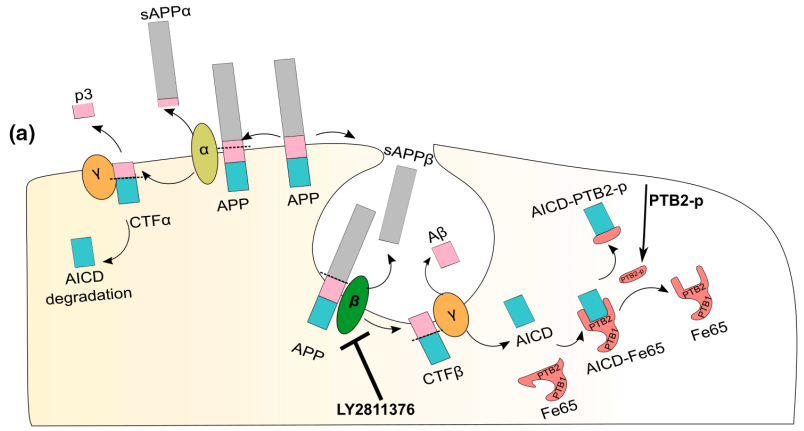

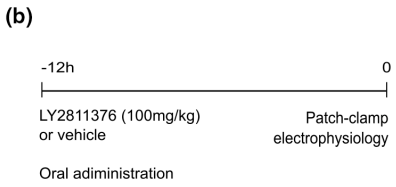

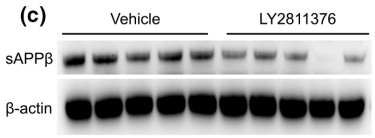

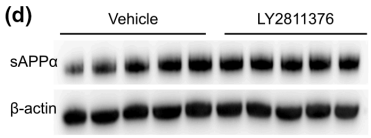

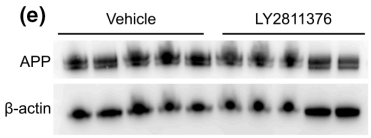

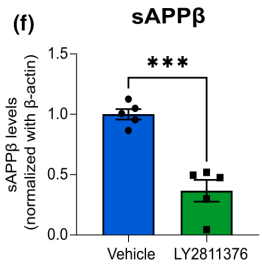

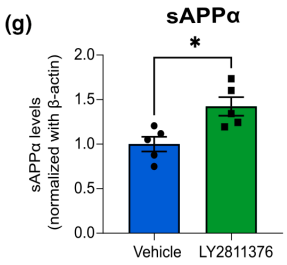

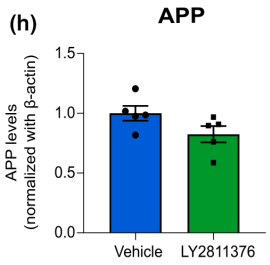

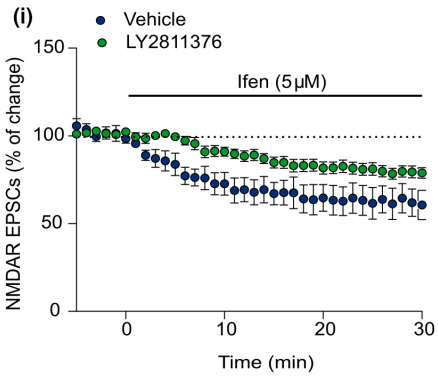

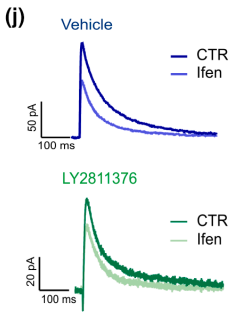

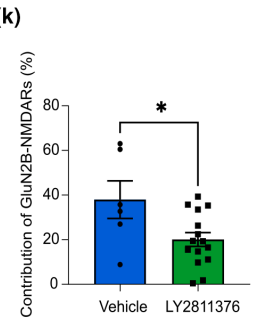

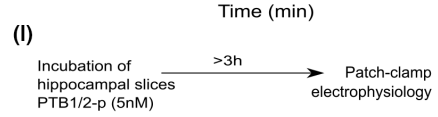

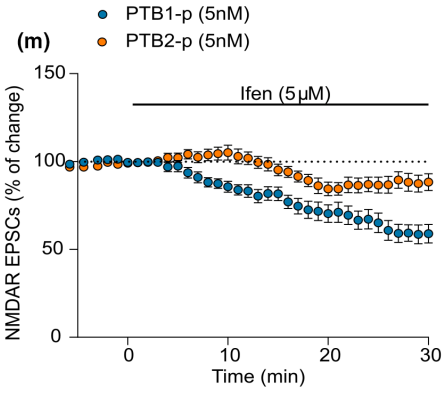

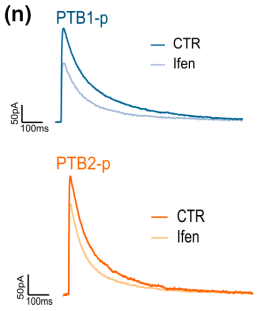

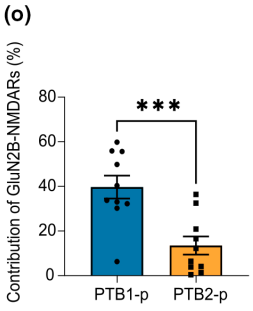

FIGURE 5 Age-related increase in βAPP processing contributes to enhanced GluN2B synaptic contribution. (a) Schematic diagram adapted from (Grimm et al., 2013; Müller et al., 2008) showing the experimental approaches to interfere with amyloid precursor protein (APP) processing or AICD signaling. The β-secretase inhibitor LY2811376 interferes with the APP amyloidogenic processing pathway, but not with the nonamyloidogenic pathway (α-secretase). The PTB2 peptide (PTB2-p) interferes with AICD interaction with Fe65 and respective signaling pathways. (b) Representation of the timeline for the β-secretase inhibitor (LY2811376) treatment in aged mice. (c) Representative Western blot of soluble fractions from hippocampal mouse tissue of aged wild-type C57BL/6 mice (18–20 months, vehicle vs. LY2811376, 12 h after the treatment). Membranes were immunoblotted with antibodies for sAPPβ and β-actin as the loading control. (d) Representative Western blot of soluble fractions from hippocampal mouse tissue of aged mice (vehicle vs. LY2811376, 12 h after the treatment). Membranes were immunoblotted with antibodies for sAPPα and β-actin as the loading control. (e) Representative Western blot of membrane/cytosolic fractions from hippocampal mouse tissue of aged mice (vehicle vs. LY2811376, 12 h after the treatment). Membranes were immunoblotted with antibodies for APP and β-actin as the loading control. (f) Results from blots of soluble fractions as shown in (c) show sAPPβ levels normalized with β-actin and are expressed as the mean ± SEM relative to the control condition (vehicle) unpaired *t* test, $^{***}p < 0.001$, $n = 5$. (g) Results from blots of soluble fractions as shown in (d) show sAPPα levels normalized with β-actin and are expressed as the mean ± SEM relative to the control condition (vehicle) unpaired *t* test, $^{*}p < 0.05$, $n = 5$. (h) Results from blots of membrane/cytosolic fractions as shown in (e) show APP levels normalized with β-actin and are expressed as the mean ± SEM relative to the control condition (vehicle), unpaired *t* test, $n = 5$. (i) Time course of ifenprodil (5 μM) effect on pharmacologically isolated NMDAR EPSC amplitude in CA1 pyramidal neurons, measured by whole-cell patch clamp in aged C57BL/6 wild-type mice (vehicle vs. LY2811376, administration 12 h prior to patch-clamp recordings). Results are expressed as the mean ± SEM ($n = 6$–15). (j) Traces show NMDAR EPSCs recorded before (CTR) and after 30 min of Ifenprodil 5 μM perfusion (Ifen). (k) GluN2B contribution was calculated as the percentage of change in NMDAR EPSCs after ifenprodil perfusion (for 30 min) in aged C57BL/6 wild-type mice (vehicle vs. LY2811376). Results are expressed as the mean ± SEM (Unpaired *t* test, $^{*}p < 0.05$, $n = 6$–15). (l) Representation of the timeline for the incubation of hippocampal slices from aged mice with PTB1-p or PTB2-p (5 nM, >3 h before patch-clamp recordings). (m) Time course of ifenprodil (5 μM) effect on pharmacologically isolated NMDAR EPSC amplitude in CA1 pyramidal neurons, measured by whole-cell patch clamp in aged C57BL/6 wild-type mice (PTB1-p vs. PTB2-p, incubation for >3 h prior to patch-clamp recordings). Results are expressed as the mean ± SEM ($n = 10$). (n) Traces show NMDAR EPSCs recorded before (CTR) and after 30 min of Ifenprodil 5 μM perfusion (Ifen). (o) GluN2B contribution was calculated as the percentage of change in NMDAR EPSCs after ifenprodil perfusion (for 30 min) in aged C57BL/6 wild-type mice (PTB1-p vs. PTB2-p). Results are expressed as the mean ± SEM (Unpaired *t* test, $^{***}p < 0.001$, $n = 10$). The full statistical analysis and Western blot membranes are provided in the Supporting Information.

effects, namely kinases/phosphatases that are known to regulate GluN2B phosphorylation status, Ca^{2+} permeability, or trafficking (Murphy et al., 2014).

Therefore, our findings could help to clarify an apparent paradox in the field: Although total NMDAR levels are known to decline in physiological aging and AD (Jacob et al., 2007; Magnusson, 2012), NMDAR antagonists such as memantine are effective in counteracting cognitive decline and approved for clinical use in AD (Reisberg et al., 2003). We show that the NMDARs that remain at aged synapses have altered properties from adulthood, staying open for longer times and being more dependent on the GluN2B subtype. An imbalance in subunit contribution toward GluN2B is expected to decrease the threshold for LTP (Yashiro & Philpot, 2008), possibly contributing to the LTD-LTP shift reported by our group in aged rats (Temido-Ferreira et al., 2020). Therefore, the increased contribution of GluN2B may lead to synaptic dysregulation in physiological aging, while increasing the susceptibility to neurodegeneration, in which GluN2B-NMDARs become overactivated (Li et al., 2011). This mechanism might be particularly relevant in AD, since the pathological accumulation of APP amyloidogenic fragments is expected to further enhance GluN2B contribution. More importantly, the now unraveled mechanism may explain the protective effect of the APP A6737 Icelandic variant in age-related cognitive decline and AD. This mutation decreases the affinity of APP for BACE1, reducing its cleavage activity by 40% (Jonsson et al., 2012), and possibly reducing the herein described GluN2B aberrant synaptic contribution.

In conclusion, we describe two alternative mechanisms by which APP controls GluN2B-NMDARs, depending on the age. We have discovered a new physiological role for APP at the postsynapse, being essential to maintain GluN2B synaptic content/currents in immature synapses. Moreover, we show that the age-related increase in APP processing contributes to a higher GluN2B synaptic contribution. While the first mechanism might play a crucial role in synaptic maturation, the latter could be involved in age-associated synaptic dysfunction.

4 | METHODS

4.1 | Human samples

The use of human samples was conducted in accordance with the Helsinki Declaration and National Ethical Guidelines. Protocols were approved by the Local Ethics Committee and the National Data Protection Committee. Samples of postmortem brain tissue from the prefrontal cortex were obtained from the National Institute of Legal Medicine and Forensic Sciences, Coimbra, Portugal, the Neuro-CEB Biological Resource Center (BRC), France, and the Newcastle Brain Tissue Resource, United Kingdom. Samples from human AD patients correspond to Braak Stage VI. The information about the gender and post-mortem delay is indicated in the Supporting Information.

4.2 | Animals

Male and female wild-type C57BL/6 mice at different ages were used: infant (7–10 days), adult (10–16 weeks), and aged

(18–20 months). A C7BL/6-129SvJ female mouse bearing three mutations (3xTg-AD) associated with familial AD (amyloid precursor protein [APPswe], presenilin-1 [PSEN1], and microtubule-associated protein tau [MAPT]; Mutant Mouse Research and Resource Center at The Jackson Laboratory) was used as control. The detailed procedures are described in the Supporting Information.

4.3 | BACE1 inhibitor

LY2811376 was obtained from Medchem Express (Sweden) and prepared in 10% DMSO, 40% PEG300, 5% Tween-80, and 45% saline. C57BL/6 infant (7–10 days) or aged mice (18–20 months) received LY2811376 at 100 mg/kg body weight by sucking reflex or oral gavage, respectively, as described in Filser et al. (2015). Animals treated with LY2811376 (infant: $n = 6$; aged: $n = 5$) or vehicle (infant: $n = 3$; aged: $n = 5$) were sacrificed ≈12 h after treatment.

4.4 | Expression and purification of His-tagged fusion proteins (PTB1-p and PTB2-p) in *Escherichia coli*

The recombinant fusion proteins were expressed in Escherichia coli BL21 (DE3) RIL cells transformed with the plasmid pET21d Fe65-PTB2 6xHis (Radzimanowski, Beyreuther et al., 2008) or pET24d Fe65-PTB1 6xHis (Radzimanowski, Ravaud et al., 2008). Transformed bacteria were cultivated at 37°C in 2xYT media containing 100 mg/L ampicillin (for Fe65-PTB2 6xHis) or 30 mg/L kanamycin (for Fe65-PTB1 6xHis). Twenty hours after inducing the protein expression via 1 mM IPTG (Isopropyl β-D-1-thiogalactopyranoside), the bacteria were sonicated five times with 10 pulses (Sonoplus HD 2200 sonicator, Bandelin) in lysis buffer (50 mM Tris/300 mM NaCl/10 mM Imidazole/pH 8), with EDTA-free protease inhibitor and 1 mM DTT. The lysate was centrifuged for 45 min at 11,300 *g* at 4°C. The proteins were purified using an Äkta Purifier 10 system (Cytiva) with a His-Trap HP column (GE Healthcare). After intense washing, the bound proteins were eluted in 50 mM Tris/300 mM NaCl/300 mM imidazole/pH 8. Using a PD-10 desalting column (Cytiva), the elution buffer was exchanged to HEPES buffer (20 mM HEPES/150 mM NaCl/pH 7.2).

4.5 | Patch-clamp electrophysiology

The whole-cell patch-clamp electrophysiology recordings to measure pharmacologically isolated evoked-NMDAR EPSCs were performed as described previously by our group (Pousinha et al. 2017). The detailed protocol is described in the Supporting Information.

For the analysis of NMDAR EPSCs deactivation kinetics, decay time was fitted with a double exponential function, using Clampfit software, to calculate both slow and fast decay time constants, τ_{fast} and τ_{slow}, respectively. The weighted time constant ($\tau_{weighted}$) was calculated using the relative contribution from each of these components, applying the formula: $\tau_w = [(a_f \cdot \tau_f) + (a_s \cdot \tau_s)]/(a_f + a_s)$, where a_f and a_s are the relative amplitudes of the two exponential components, and τ_f and τ_s are the corresponding time constants.

To calculate GluN2B-NMDAR contribution, NMDAR EPSCs were measured immediately before (5 min) and 25–20 min after ifenprodil (5 μM) perfusion to selectively block GluN2B-NMDARs.

To interfere with the APP-NMDAR interaction, the APP C-terminal antibody Y188 (ab32136, Abcam) was added to the intracellular solution to a final concentration of 0.4 μg/ml (2.57 nM). In the control condition, the same antibody was heat-inactivated by incubation at 98°C for 10 min. The percentage of reduction in NMDAR EPSCs due to the APP C-terminal antibody incubation was calculated comparing the baseline amplitude (15–20 min) with the final amplitude (55–60 min) and normalized with the control condition for each age.

To interfere with the AICD-Fe65, hippocampal slices from aged mice were preincubated prior to recording as indicated in each figure with either the PTB2-p or the respective control (PTB1-p) at a final concentration of 5 nM.

4.6 | Protein analysis

4.6.1 | Fractionation into PSD-enriched fractions

The fractionation protocol was adapted from Frandemiche et al. (2014). The integrity of non-PSD was verified by immunoblotting for synaptophysin, which was enriched in the non-PSD fraction, and the integrity of the PSD fraction was confirmed by the immunoblotting of PSD-95 enriched in this compartment. The detailed protocol is described in the Supporting Information.

4.6.2 | Synaptosomes preparation

The protocol for synaptosome preparation was adapted from Lopes et al. (1999). The detailed protocol is described in the Supporting Information.

4.6.3 | Extraction of soluble and membrane/cytosolic proteins

Soluble proteins were extracted from mouse hippocampal tissue with DEA buffer, whereas membrane/cytosolic proteins were extracted with RIPA buffer, as described in Willem et al. (2015). The detailed protocol is described in the Supporting Information.

4.6.4 | Co-immunoprecipitation

Mouse hippocampal or human postmortem cortical tissue was resuspended in immunoprecipitation buffer (50 mM Tris HCl pH 7.5;

150 mM NaCl; 2 mM EDTA; 1% Triton with protease and phosphatase inhibitors). The immunoprecipitation protocol was adapted from Tomé et al. (2021) using Dynabeads Protein A (10001D, Invitrogen), and the detailed protocol is described in the Supporting Information. At the end of the experiment, the immunoprecipitated samples were gently resuspended in 60 µl of preheated 2× sample buffer (140 mM Tris HCl pH 6.8, 4% SDS, 13.6% glycerol, 272 mM DTT, 0.004% Blue bromophenol) in RIPA (50 mM Tris, 1 mM EDTA, 150 mM NaCl, 0.1% SDS, 1% Tergitol-type NP-40, pH 8.0, and incubated for 10 min at 95°C). The supernatant was collected and used for Western blot analysis.

4.6.5 | Western blotting

Mouse and human frozen tissue samples were resuspended in A-EDTA buffer (10 mM HEPES-KOH pH 7.9, 10 mM KCl, 1.5 mM $MgCl_2$, 0.1 mM EDTA, and 0.3% NP-40 with protease and phosphatase inhibitors), as described in Pousinha et al. (2017).

For APP, APP-CTFs, and AICD analysis, optimal conditions for low molecular mass protein separation were used, as described in Willem et al. (2015). Proteins were separated using precast gradient Tricine Protein Gels (10–20%, 1 mm, Novex) in Tris-tricine buffer (1 M Tris, 1 M Tricine, 1% SDS). Samples were electrotransferred at 400 mA for 1 h to 0.2 µm nitrocellulose membranes using a Tris-glycine buffer (25 mM Tris, 190 mM glycine) with 20% ethanol. Proteins transferred to nitrocellulose membranes were additionally denatured by boiling the membrane in PBS for 5 min, acting as an antigen retrieval step to detect AICD, as described in Pimplikar & Suryanarayana (2011).

For the remaining proteins, electrophoresis was performed in Tris-glycine buffer with 10% SDS using 10–12% and 4% acrylamide resolving and stacking gels, respectively. Proteins were electrotransferred to 0.45 µm polyvinylidene fluoride (PVDF) membranes in Tris-glycine buffer with 20% methanol at 350 mA for 90 min.

After transfer, membranes were blocked with 3% BSA in TBS-T (20 mM Tris, 150 mM NaCl, 0.1% Tween-20) at room temperature (RT) for 1 h and incubated with primary antibodies (diluted in 3% BSA TBS-T) overnight at 4°C. After three washing steps with TBS-T, membranes were incubated with horseradish peroxidase-conjugated anti-mouse or anti-rabbit secondary antibodies for 1 h at RT. After three washing steps with TBS-T, chemiluminescent detection was performed with enhanced chemiluminescence (ECL) Western blotting detection reagent (GE Healthcare). For AICD detection, longer exposure times were applied.

For the analysis of soluble APP fragments (sAPPβ and α), DEA fractions were loaded in the gel, followed by electrophoresis in Tris-glycine buffer with 10% SDS. Following transfer, membranes were blocked in I-Block solution (1 g Topix I-Block, Thermo Fischer Scientific, in 500 ml PBS, 0.2% Tween 20) for 1 h at RT and incubated with primary antibodies diluted in I-Block solution overnight at 4°C. The washing steps were performed with PBS-Tween buffer and the secondary antibodies were diluted in I-Block solution and incubated for 1 h at RT. For ECL detection, membranes were incubated for 1 min at RT with peroxidase substrate (Western lightning ultra, PerkinElmer) and signals were captured with phospho-Fusion imager, Vilber Lourmat.

Optical density was determined with ImageJ, according to the software instructions (Ferreira & Rasband, 2012). The detailed protocols, as well as the full-length blots with the molecular weight standards (NZYColour Protein Marker I, NZYTech), are provided in the Supporting information.

4.6.6 | Primary neuronal cultures

Hippocampal neurons were cultured from 18-day Sprague–Dawley rat embryos, adapting the protocol from (Faria-Pereira et al., 2022). Cells were plated on poly-D-lysine-coated glass coverslips in 24-multiwell plates at a final density of 70,000 cells/coverslip, in neuronal plating media ((Minimum Essential Medium) supplemented with 10% horse serum, 0.6% glucose, and 100 U/ml Pen-Strep) and maintained at 37°C in a 5% CO_2-humidified incubator. After 4 hours, the plating medium was replaced for neuronal culture medium: Neurobasal medium (Gibco–Life Technologies) supplemented with B-27 supplement, 25 µM Glutamic acid, 0.5 mM Glutamine, and 20 U/ml penicillin/streptomycin. Cultures were maintained in the humidified incubator for 2 weeks, feeding the cells once per week with neuronal culture medium by replacing half of the medium per well. This protocol is associated with an enrichment in neuronal cells (NeuN-positive cells ≈80%) and a low number of glial cells (GFAP-positive cells ≈6%) at DIVs 11–14 (Faria-Pereira et al. 2022).

The detailed protocol is described in the Supporting Information.

4.6.7 | Neuronal transfection

Primary neuronal cultures were transiently transfected at DIV 7-8 using the calcium phosphate transfection protocol adapted from Silva et al. (2019); Jiang et al. (2004). The detailed protocol is described in the Supporting Information.

4.6.8 | Plasmid generation

Primary neuronal cultures were transfected with AAV-shRNA–mCherry plasmids, with a shRNA against APP or a shRNA control sequence.

The control plasmid was kindly provided by Dirk Grimm (University of Heidelberg) and corresponds to AAV-U6-NS1-CMV-mCherry plasmid, where NS1 is a nonsilencing sequence: GTAAC GACGCGACGACGTAA, with no identified targets in the rat genome, confirmed by NCBI Basic Local Alignment Search Tool (BLAST).

For the generation of the shRNA-APP construct, we used the following sequence: GCACTAACTTGCACGACTATG (Young-Pearse et al., 2007), which is complementary to the mRNA NCBI reference

sequence for rat APP (Rattus norvegicus amyloid beta precursor protein (App), NM_019288.2). This construct, which was provided by Tracy Young-Pearse (Harvard Medical School) in the pENTR-U6 vector, was then subcloned into an adeno-associated virus backbone (AAV-U6-shRNA empty-CMV-mCherry plasmid), kindly provided by Dirk Grimm, as described in the Supporting Information. Both plasmids were purified using the EndoFree Plasmid Maxi Kit (Qiagen) and verified by DNA sequencing (Primer 5′-GGGCCTATTTCCCATGATTCC-3′).

4.6.9 | Immunocytochemistry

The immunostaining protocol was adapted from Ferreira et al. (2017), as described in the Supporting Information.

4.6.10 | Microscopy imaging and analysis

All images were acquired in a Zeiss LSM 880 laser scanning confocal microscope using a Plan-Apochromat 63×/1.4 oil immersion objective.

For the analysis of APP immunofluorescence in transfected neurons, the APP (Alexa Fluor 488) relative fluorescence intensity was manually quantified using ImageJ, after maximum intensity projection. For each condition, seven transfected neurons were analyzed by defining regions of interest (ROI), which corresponded to the cell bodies using the mCherry channel. The average intensity of Alexa Fluor 488 was then determined for each ROI. All values were normalized to the average intensity in transfected neurons from the control condition (%).

For the analysis of GluN2B/PSD95 in dendrites of transfected neurons, the analysis of GluN2B/PSD95 in transfected neurons was performed using an in-house-developed macro for ImageJ.

4.7 | Statistical analysis

All statistical analyses were performed with GraphPad Prism software. Results are referred in the text as mean ± standard error of the mean (SEM), which is also represented in the graphs, together with dot blots with individual values. Statistical analyses were performed after evaluating normality using the Shapiro–Wilk test. When the distribution was normal in all groups, the statistical comparison included unpaired *t* test or one-way ANOVA followed by uncorrected Fisher's LSD's multiple comparisons test. When the distribution was not normal, the statistical comparison was performed by Mann–Whitney test or Kruskal–Wallis followed by uncorrected Dunn's multiple comparisons test. When the graphs represent relative levels, the values are expressed in relation to the reference group. Correlations between parameters were determined according to Pearson's correlation coefficient. Significance was determined according to the following criteria: $p > 0.05$ = not significant, $^{*}p < 0.05$, $^{**}p < 0.01$, $^{***}p < 0.001$, and $^{****}p < 0.0001$. The complete statistical analysis is provided in Supporting information.

AUTHOR CONTRIBUTIONS

JR-S has written the draft and performed the fractionation, co-immunoprecipitation, Western blotting, immunocytochemistry assays, and the primary neuronal cultures, assisted by MT-F and JEC. PAP performed the whole-cell patch-clamp recordings. FJE provided the tools to study APP-NMDAR interaction. MW provided tools to perform Western blot analysis of APP processing. LVL assisted with the analysis of Western blot of APP processing. HM and JR-S designed and cloned the shAPP plasmids. SKö expressed and purified the PTB1-p and PTB2-p under the supervision of SKi. AR and SM performed the in vivo pharmacological treatment of infant and aged mice, JD performed the respective fractionation and WB of APP processing and AR performed whole-cell patch-clamp recordings of treated infant mice. JRS, LVL, and PAP designed the experiments and wrote the manuscript. LVL and PAP coordinated the project. All authors revised the manuscript and discussed the experimental findings.

ACKNOWLEDGMENTS

JR-S is an FCT/PhD Fellow (IMM Lisbon BioMed PhD program; SFRH/BD/52228/2013); LVL is supported by Fundação para a Ciência e a Tecnologia. LVL is an FCT-CEEC Coordinator Investigator. LVL and PP were supported by Santa Casa da Misericórdia (MB-7-2018). PP was supported by ANR 257341. SM and HM were supported by the FLAG-ERA grant (MILEDI) by ANR. JD and AR are both recipients of a PhD fellowship from the Ministère de la Recherche, de l'Enseignement Supérieur et de l'Innovation. SKö and SKi were supported by Forschung Initiative e.V., DFG (KI 819/9–1). We would like to thank Dirk Grimm, Kathleen Börner (University of Heidelberg), and Tracy Young-Pearse (Harvard Medical School) for providing the plasmids, Frederic Checler for scientific discussion regarding APP processing inhibitors and APP fragments signaling. We would also like to acknowledge the Rodent and Bioimaging Facilities of Instituto de Medicina Molecular João Lobo Antunes for their technical support and the Biobanco-IMM, Lisbon Academic Medical Center, Lisbon, Portugal.

CONFLICT OF INTEREST

All the authors declare no known conflicts of interest associated with this publication, and there has been no significant financial support for this work that could have influenced its outcome. The manuscript has been read and approved by all named authors.

DATA AVAILABILITY STATEMENT

All the software used to data analysis is commercially available, and the respective information is provided in each respective section. The data that support the findings of this study are available from the corresponding authors upon request.

ORCID

Joana Rajão-Saraiva https://orcid.org/0000-0003-0970-8665
Luísa V. Lopes https://orcid.org/0000-0001-8367-3005
Paula A. Pousinha https://orcid.org/0000-0002-5992-9418

REFERENCES

Adesnik, H., Li, G., During, M. J., Pleasure, S. J., & Nicoll, R. A. (2008). NMDA receptors inhibit synapse unsilencing during brain development. *Proceedings of the National Academy of Sciences of the United States of America*, *105*(14), 5597–5602. https://doi.org/10.1073/pnas.0800946105

al Abed, A. S., Sellami, A., Potier, M., Ducourneau, E. G., Gerbeaud-Lassau, P., Brayda-Bruno, L., Lamothe, V., Sans, N., Desmedt, A., Vanhoutte, P., Bennetau-Pelissero, C., Trifilieff, P., & Marighetto, A. (2020). Age-related impairment of declarative memory: Linking memorization of temporal associations to GluN2B redistribution in dorsal CA1. *Aging Cell*, *19*(10), e13243. https://doi.org/10.1111/acel.13243

Augustin, V., & Kins, S. (2021). Fe65: A scaffolding protein of Actin regulators. *Cell*, *10*(7), 1599. https://doi.org/10.3390/cells10071599

Bannerman, D. M., Niewoehner, B., Lyon, L., Romberg, C., Schmitt, W. B., Taylor, A., Sanderson, D. J., Cottam, J., Sprengel, R., Seeburg, P. H., Köhr, G., & Rawlins, J. N. P. (2008). NMDA receptor subunit NR2A is required for rapidly acquired spatial working memory but not incremental spatial reference memory. *Journal of Neuroscience*, *28*(14), 3623–3630. https://doi.org/10.1523/JNEUROSCI.3639-07.2008

Bar-Shira, O., Maor, R., & Chechik, G. (2015). Gene expression switching of receptor subunits in human brain development. *PLoS Computational Biology*, *11*(12), e1004559. https://doi.org/10.1371/journal.pcbi.1004559

Baumkötter, F., Wagner, K., Eggert, S., Wild, K., & Kins, S. (2012). Structural aspects and physiological consequences of APP/APLP trans-dimerization. *Experimental Brain Research*, *217*(3–4), 389–395. https://doi.org/10.1007/s00221-011-2878-6

Bellone, C., & Nicoll, R. A. (2007). Rapid bidirectional switching of synaptic NMDA receptors. *Neuron*, *55*(5), 779–785. https://doi.org/10.1016/j.neuron.2007.07.035

Borg, J. P., Ooi, J., Levy, E., & Margolis, B. (1996). The phosphotyrosine interaction domains of X11 and FE65 bind to distinct sites on the YENPTY motif of amyloid precursor protein. *Molecular and Cellular Biology*, *16*(11), 6229–6241. https://doi.org/10.1128/mcb.16.11.6229

Burke, S. N., & Barnes, C. A. (2006). Neural plasticity in the ageing brain. *Nature Reviews Neuroscience*, *7*(1), 30–40. https://doi.org/10.1038/nrn1809

Burnashev, N., & Szepetowski, P. (2015). NMDA receptor subunit mutations in neurodevelopmental disorders. *Current Opinion in Pharmacology*, *20*, 73–82. https://doi.org/10.1016/j.coph.2014.11.008

Burrinha, T., Martinsson, I., Gomes, R., Terrasso, A. P., Gouras, G. K., & Almeida, C. G. (2021). Upregulation of APP endocytosis by neuronal aging drives amyloid-dependent synapse loss. *Journal of Cell Science*, *134*(9), jcs255752. https://doi.org/10.1242/jcs.255752

Cao, X., & Sudhof, T. C. (2001). A transcriptionally [correction of transcriptively] active complex of APP with Fe65 and histone acetyltransferase Tip60. *Science*, *293*(5527), 115–120.

Corbel, C., Hernandez, I., Wu, B., & Kosik, K. S. (2015). Developmental attenuation of N-methyl-D-aspartate receptor subunit expression by microRNAs. *Neural Development*, *10*(1), 20. https://doi.org/10.1186/s13064-015-0047-5

Cousins, S. L., Hoey, S. E. A., Anne Stephenson, F., & Perkinton, M. S. (2009). Amyloid precursor protein 695 associates with assembled NR2A- and NR2B-containing NMDA receptors to result in the enhancement of their cell surface delivery. *Journal of Neurochemistry*, *111*(6), 1501–1513. https://doi.org/10.1111/j.1471-4159.2009.06424.x

Dawson, G. R., Seabrook, G. R., Zheng, H., Smith, D. W., Graham, S., O'Dowd, G., Bowery, B. J., Boyce, S., Trumbauer, M. E., Chen, H. Y., van der Ploeg, L. H. T., & Sirinathsinghji, D. J. S. (1999). Age-related cognitive deficits, impaired long-term potentiation and reduction in synaptic marker density in mice lacking the β-amyloid precursor protein. *Neuroscience*, *90*(1), 1–13. https://doi.org/10.1016/S0306-4522(98)00410-2

de Roo, M., Klauser, P., Mendez, P., Poglia, L., & Muller, D. (2008). Activity-dependent PSD formation and stabilization of newly formed spines in hippocampal slice cultures. *Cerebral Cortex*, *18*(1), 151–161. https://doi.org/10.1093/cercor/bhm041

Elias, G. M., Elias, L. A. B., Apostolides, P. F., Kriegstein, A. R., & Nicoll, R. A. (2008). Differential trafficking of AMPA and NMDA receptors by SAP102 and PSD-95 underlies synapse development. *Proceedings of the National Academy of Sciences of the United States of America*, *105*(52), 20953–20958. https://doi.org/10.1073/pnas.0811025106

Faria-Pereira, A., Temido-Ferreira, M., & Morais, V. A. (2022). BrainPhys neuronal media support physiological function of mitochondria in mouse primary neuronal cultures. *Frontiers in Molecular Neuroscience*, *15*, 837448. https://doi.org/10.3389/fnmol.2022.837448

Feilen, L. P., Haubrich, K., Strecker, P., Probst, S., Eggert, S., Stier, G., Sinning, I., Konietzko, U., Kins, S., Simon, B., & Wild, K. (2017). Fe65-PTB2 dimerization mimics Fe65-APP interaction. *Frontiers in Molecular Neuroscience*, *10*, 140. https://doi.org/10.3389/fnmol.2017.00140

Ferreira, D. G., Temido-Ferreira, M., Miranda, H. V., Batalha, V. L., Coelho, J. E., Szegö, É. M., Marques-Morgado, I., Vaz, S. H., Rhee, J. S., Schmitz, M., Zerr, I., Lopes, L., & Outeiro, T. F. (2017). α-Synuclein interacts with PrP C to induce cognitive impairment through mGluR5 and NMDAR2B. *Nature Neuroscience*, *20*(11), 1569–1579. https://doi.org/10.1038/nn.4648

Ferreira, J. S., Papouin, T., Ladépêche, L., Yao, A., Langlais, V. C., Bouchet, D., Dulong, J., Mothet, J. P., Sacchi, S., Pollegioni, L., Paoletti, P., Richard Oliet, S. H., & Groc, L. (2017). Co-agonists differentially tune GluN2B-NMDA receptor trafficking at hippocampal synapses. *eLife*, *6*, e25492. https://doi.org/10.7554/eLife.25492

Ferreira, T., & Rasband, W. (2012). ImageJ User Guide - IJ 1.46r. *IJ 1.46r*. https://imagej.nih.gov/ij/docs/guide/146.html

Filser, S., Ovsepian, S., Masana, M., Blazquez-Llorca, L., Elvang, A. B., Volbracht, C., Müller, M. B., Jung, C. K. E., & Herms, J. (2015). Pharmacological inhibition of BACE1 impairs synaptic plasticity and cognitive functions. *Biological Psychiatry*, *77*(8), 729–739. https://doi.org/10.1016/j.biopsych.2014.10.013

Frandemiche, M. L., de Seranno, S., Rush, T., Borel, E., Elie, A., Arnal, I., Lanté, F., & Buisson, A. (2014). Activity-dependent tau protein translocation to excitatory synapse is disrupted by exposure to amyloid-beta oligomers. *Journal of Neuroscience*, *34*(17), 6084–6097. https://doi.org/10.1523/JNEUROSCI.4261-13.2014

Fukumoto, H., Rosene, D. L., Moss, M. B., Raju, S., Hyman, B. T., & Irizarry, M. C. (2004). β-Secretase activity increases with aging in human, monkey, and mouse brain. *American Journal of Pathology*, *164*(2), 719–725. https://doi.org/10.1016/S0002-9440(10)63159-8

Gambrill, A. C., & Barria, A. (2011). NMDA receptor subunit composition controls synaptogenesis and synapse stabilization. *Proceedings of the National Academy of Sciences of the United States of America*, *108*(14), 5855–5860. https://doi.org/10.1073/pnas.1012676108

Gonzalez-Lozano, M. A., Klemmer, P., Gebuis, T., Hassan, C., van Nierop, P., van Kesteren, R. E., Smit, A. B., & Li, K. W. (2016). Dynamics of the mouse brain cortical synaptic proteome during postnatal brain development. *Scientific Reports*, *6*, 35456. https://doi.org/10.1038/srep35456

Goodger, Z., Rajendran, L., Trutzel, A., Kohli, B. M., Nitsch, R. M., & Konietzko, U. (2009). Nuclear signaling by the APP intracellular domain occurs predominantly through the amyloidogenic processing pathway. *Journal of Cell Science*, *122*(20), 3703–3714. https://doi.org/10.1242/jcs.048090

Grabrucker, A., Vaida, B., Bockmann, J., & Boeckers, T. M. (2009). Synaptogenesis of hippocampal neurons in primary cell culture. *Cell and Tissue Research*, *338*(3), 333–341. https://doi.org/10.1007/s00441-009-0881-z

Gray, J. A., Shi, Y., Usui, H., During, M. J., Sakimura, K., & Nicoll, R. A. (2011). Distinct modes of AMPA receptor suppression at developing synapses by GluN2A and GluN2B: Single-cell NMDA receptor subunit deletion in vivo. *Neuron*, *71*(6), 1085–101. https://doi.org/10.1016/j.neuron.2011.08.007

Grimm, M. O. W., Mett, J., Stahlmann, C. P., Haupenthal, V. J., Zimmer, V. C., & Hartmann, T. (2013). Neprilysin and Aβ clearance: Impact of the APP intracellular domain in NEP regulation and implications in Alzheimer's disease. *Frontiers in Aging Neuroscience*, *5*, 98. https://doi.org/10.3389/fnagi.2013.00098

Groc, L., Heine, M., Cousins, S. L., Stephenson, F. A., Lounis, B., Cognet, L., & Choquet, D. (2006). NMDA receptor surface mobility depends on NR2A-2B subunits. *Proceedings of the National Academy of Sciences of the United States of America*, *103*(49), 18769–18774. https://doi.org/10.1073/pnas.0605238103

Hanson, J. E., Pare, J. F., Deng, L., Smith, Y., & Zhou, Q. (2015). Altered GluN2B NMDA receptor function and synaptic plasticity during early pathology in the PS2APP mouse model of Alzheimer's disease. *Neurobiology of Disease*, *74*, 254–262. https://doi.org/10.1016/j.nbd.2014.11.017

Hardingham, G. E., Chawla, S., Cruzalegui, F. H., & Bading, H. (1999). Control of recruitment and transcription-activating function of CBP determines gene regulation by NMDA receptors and L-type calcium channels. *Neuron*, *22*(4), 789–798. https://doi.org/10.1016/S0896-6273(00)80737-0

Heber, S., Herms, J., Gajic, V., Hainfellner, J., Aguzzi, A., Rulicke, T., Kretzschmar, H., von Koch, C., Sisodia, S., Tremml, P., Lipp, H. P., Wolfer, D. P., & Muller, U. (2000). Mice with combined gene knock-outs reveal essential and partially redundant functions of amyloid precursor protein family members. *Journal of Neuroscience*, *20*(21), 7951–7963. https://doi.org/10.1523/jneurosci.20-21-07951.2000

Hoe, H. S., Fu, Z., Makarova, A., Lee, J. Y., Lu, C., Feng, L., Pajooheshganji, A., Matsuoka, Y., Hyman, B. T., Ehlers, M. D., Vicini, S., Pak, D. T. S., & Rebeck, G. W. (2009). The effects of amyloid precursor protein on postsynaptic composition and activity. *Journal of Biological Chemistry*, *284*(13), 8495–8506. https://doi.org/10.1074/jbc.M900141200

Huh, K. H., & Wenthold, R. J. (1999). Turnover analysis of glutamate receptors identifies a rapidly degraded pool of the N-methyl-D-aspartate receptor subunit, NR1, in cultured cerebellar granule cells. *Journal of Biological Chemistry*, *274*(1), 151–7. https://doi.org/10.1074/jbc.274.1.151

Jacob, C. P., Koutsilieri, E., Bartl, J., Neuen-Jacob, E., Arzberger, T., Zander, N., Ravid, R., Roggendorf, W., Riederer, P., & Grünblatt, E. (2007). Alterations in expression of glutamatergic transporters and receptors in sporadic Alzheimer's disease. *Journal of Alzheimer's disease*, *11*, 97–116. https://doi.org/10.3233/JAD-2007-11113

Jiang, M., Deng, L., & Chen, G. (2004). High Ca^{2+}–phosphate transfection efficiency enables single neuron gene analysis. *Gene Therapy*, *11*(17), 1303–1311. https://doi.org/10.1038/sj.gt.3302305

Jonsson, T., Atwal, J. K., Steinberg, S., Snaedal, J., Jonsson, P., Bjornsson, S., Stefansson, H., Sulem, P., Gudbjartsson, D., Maloney, J., Hoyte, K., Gustafson, A., Liu, Y., Lu, Y., Bhangale, T., Graham, R. R., Huttenlocher, J., Bjornsdottir, G., Andreassen, O. A., … Stefansson, K. (2012). A mutation in APP protects against Alzheimer's disease and age-related cognitive decline. *Nature*, *488*(7409), 96–99. https://doi.org/10.1038/nature11283

Jouvenceau, A., Dutar, P., & Billard, J. M. (1998). Alteration of NMDA receptor-mediated synaptic responses in CA1 area of the aged rat hippocampus: Contribution of GABAergic and cholinergic deficits. *Hippocampus*, *8*(6), 627–637.

Kim, T. W., Wu, K., Xu, J. L., McAuliffe, G., Tanzi, R. E., Wasco, W., & Black, I. B. (1995). Selective localization of amyloid precursor-like protein 1 in the cerebral cortex postsynaptic density. *Molecular Brain Research*, *32*(1), 36–44. https://doi.org/10.1016/0169-328X(95)00328-P

Kimberly, W. T., Zheng, J. B., Guénette, S. Y., & Selkoe, D. J. (2001). The intracellular domain of the β-amyloid precursor protein is stabilized by Fe65 and Translocates to the nucleus in a notch-like manner. *Journal of Biological Chemistry*, *276*(43), 40288–40292. https://doi.org/10.1074/jbc.C100447200

Kirazov, E., Kirazov, L., Bigl, V., & Schliebs, R. (2001). Ontogenetic changes in protein level of amyloid precursor protein (APP) in growth cones and synaptosomes from rat brain and prenatal expression pattern of APP mRNA isoforms in developing rat embryo. *International Journal of Developmental Neuroscience*, *19*(3), 287–296. https://doi.org/10.1016/S0736-5748(01)00012-0

Klevanski, M., Herrmann, U., Weyer, S. W., Fol, R., Cartier, N., Wolfer, X. P., Caldwell, J. H., Korte, M., & Müller, U. C. (2015). The APP intracellular domain is required for normalsynaptic morphology, synaptic plasticity, and hippocampus-dependent behavior. *Journal of Neuroscience*, *35*(49), 16018–16033. https://doi.org/10.1523/JNEUROSCI.2009-15.2015

Kumar, A. (2015). NMDA receptor function during senescence: Implication on cognitive performance. *Frontiers in Neuroscience*, *9*, 473. https://doi.org/10.3389/fnins.2015.00473

Lauritzen, I., Pardossi-Piquard, R., Bauer, C., Brigham, E., Abraham, J. D., Ranaldi, S., Fraser, P., St-George-Hyslop, P., Le Thuc, O., Espin, V., Chami, L., Dunys, J., & Checler, F. (2012). The β-secretase-derived C-terminal fragment of βAPP, C99, but not Aβ, is a key contributor to early intraneuronal lesions in triple-transgenic mouse hippocampus. *Journal of Neuroscience*, *32*(46), 16243–1655a. https://doi.org/10.1523/JNEUROSCI.2775-12.2012

Lee, H. J., Suk, J. E., Bae, E. J., Lee, J. H., Paik, S. R., & Lee, S. J. (2008). Assembly-dependent endocytosis and clearance of extracellular α-synuclein. *International Journal of Biochemistry and Cell Biology*, *40*(9), 1835–1849. https://doi.org/10.1016/j.biocel.2008.01.017

Lee, S. H., Kang, J., Ho, A., Watanabe, H., Bolshakov, V. Y., & Shen, J. (2020). APP family regulates neuronal excitability and synaptic plasticity but not neuronal survival. *Neuron*, *108*(4), 676–690. https://doi.org/10.1016/j.neuron.2020.08.011

Li, S., Jin, M., Koeglsperger, T., Shepardson, N. E., Shankar, G. M., & Selkoe, D. J. (2011). Soluble a β oligomers inhibit long-term potentiation through a mechanism involving excessive activation of extrasynaptic NR2B-containing NMDA receptors. *Journal of Neuroscience*, *31*(18), 6627–6638. https://doi.org/10.1523/JNEUROSCI.0203-11.2011

Lopes, L., Cunha, R. A., & Ribeiro, J. A. (1999). Cross talk between A1 and a(2A) adenosine receptors in the hippocampus and cortex of young adult and old rats. *Journal of Neurophysiology*, *82*(6), 3196–3203. https://doi.org/10.1152/jn.1999.82.6.3196

Lyckman, A. W., Confaloni, A. M., Thinakaran, G., Sisodia, S. S., & Moya, K. L. (1998). Post-translational processing and turnover kinetics of presynaptically targeted amyloid precursor superfamily proteins in the central nervous system. *Journal of Biological Chemistry*, *273*(18), 11100–11106. https://doi.org/10.1074/jbc.273.18.11100

Magnusson, K. R. (2012). Aging of the NMDA receptor: From a mouses point of view. *Future Neurology*, *7*(5), 627–637. https://doi.org/10.2217/fnl.12.54

Marquez-Sterling, N. R., Lo, A. C. Y., Sisodia, S. S., & Koo, E. H. (1997). Trafficking of cell-surface β-amyloid precursor protein: Evidence that a sorting intermediate participates in synaptic vesicle recycling. *Journal of Neuroscience*, *17*(1), 140–151. https://doi.org/10.1523/jneurosci.17-01-00140.1997

Massey, P., Johnson, B. E., Moult, P. R., Auberson, Y. P., Brown, M. W., Molnar, E., Collingridge, G. L., & Bashir, Z. I. (2004). Differential

roles of NR2A and NR2B-containing NMDA receptors in cortical long-term potentiation and long-term depression. *Journal of Neuroscience*, *24*(36), 7821–7828. https://doi.org/10.1523/JNEUROSCI.1697-04.2004

Matrone, C., Luvisetto, S., la Rosa, L. R., Tamayev, R., Pignataro, A., Canu, N., Yang, L., Barbagallo, A. P. M., Biundo, F., Lombino, F., Zheng, H., Ammassari-Teule, M., & D'Adamio, L. (2012). Tyr682 in the Aβ-precursor protein intracellular domain regulates synaptic connectivity, cholinergic function, and cognitive performance. *Aging Cell*, *11*(6), 1084–1093. https://doi.org/10.1111/acel.12009

Monyer, H., Burnashev, N., Laurie, D. J., Sakmann, B., & Seeburg, P. H. (1994). Developmental and regional expression in the rat brain and functional properties of four NMDA receptors. *Neuron*, *12*(3), 529–540. https://doi.org/10.1016/0896-6273(94)90210-0

Morris, R. G. M., Anderson, E., Lynch, G. S., & Baudry, M. (1986). Selective impairment of learning and blockade of long-term potentiation by an N-methyl-D-aspartate receptor antagonist, AP5. *Nature*, *319*(6056), 774–776. https://doi.org/10.1038/319774a0

Müller, T., Meyer, H. E., Egensperger, R., & Marcus, K. (2008). The amyloid precursor protein intracellular domain (AICD) as modulator of gene expression, apoptosis, and cytoskeletal dynamics-relevance for Alzheimer's disease. *Progress in Neurobiology*, *85*(4), 393–406. https://doi.org/10.1016/j.pneurobio.2008.05.002

Müller, U. C., Deller, T., & Korte, M. (2017). Not just amyloid: Physiological functions of the amyloid precursor protein family. *Nature Reviews. Neuroscience*, *18*(5), 281–298. https://doi.org/10.1038/nrn.2017.29

Müller, U. C., & Zheng, H. (2012). Physiological functions of APP family proteins. *Cold Spring Harbor Perspectives in Medicine*, *2*(2), a006288. https://doi.org/10.1101/cshperspect.a006288

Murphy, J. A., Stein, I. S., Geoffrey Lau, C., Peixoto, R. T., Aman, T. K., Kaneko, N., Aromolaran, K., Saulnier, J. L., Popescu, G. K., Sabatini, B. L., Hell, J. W., & Zukin, R. S. (2014). Phosphorylation of Ser1166 on GluN2B by PKA is critical to synaptic NMDA receptor function and Ca^{2+} signaling in spines. *Journal of Neuroscience*, *34*(3), 869–879. https://doi.org/10.1523/JNEUROSCI.4538-13.2014

Nowak, L., Bregestovski, P., Ascher, P., Herbet, A., & Prochiantz, A. (1984). Magnesium gates glutamate-activated channels in mouse central neurones. *Nature*, *307*(5950), 462–465. https://doi.org/10.1038/307462a0

Paoletti, P., Bellone, C., & Zhou, Q. (2013). NMDA receptor subunit diversity: Impact on receptor properties, synaptic plasticity and disease. *Nature Reviews Neuroscience*, *14*(6), 383–400. https://doi.org/10.1038/nrn3504

Peng, C., Trojanowski, J. Q., & Lee, V. M. Y. (2020). Protein transmission in neurodegenerative disease. *Nature Reviews Neurology*, *16*(4), 199–212. https://doi.org/10.1038/s41582-020-0333-7

Pimplikar, S. W., & Suryanarayana, A. (2011). Detection of APP intracellular domain in brain tissue. *Methods in molecular biology*, *670*, 85–91. https://doi.org/10.1007/978-1-60761-744-0_7

Pousinha, P. A., Mouska, X., Raymond, E. F., Gwizdek, C., Dhib, G., Poupon, G., Zaragosi, L. E., Giudici, C., Bethus, I., Pacary, E., Willem, M., & Marie, H. (2017). Physiological and pathophysiological control of synaptic GluN2B-NMDA receptors by the C-terminal domain of amyloid precursor protein. *eLife*, *6*, e25659. https://doi.org/10.7554/eLife.25659

Radzimanowski, J., Beyreuther, K., Sinning, I., & Wild, K. (2008). Overproduction, purification, crystallization and preliminary X-ray analysis of human Fe65-PTB2 in complex with the amyloid precursor protein intracellular domain. *Acta Crystallographica Section F: Structural Biology and Crystallization Communications*, *64*(5), 409–412. https://doi.org/10.1107/S1744309108009524

Radzimanowski, J., Ravaud, S., Beyreuther, K., Sinning, I., & Wild, K. (2008). Mercury-induced crystallization and SAD phasing of the human Fe65-PTB1 domain. *Acta Crystallographica Section F: Structural Biology and Crystallization Communications*, *64*(5), 382–385. https://doi.org/10.1107/S174430910800835X

Rauner, C., & Köhr, G. (2011). Triheteromeric NR1/NR2A/NR2B receptors constitute the major N-methyl-D-aspartate receptor population in adult hippocampal synapses. *Journal of Biological Chemistry*, *286*(9), 7558–7566. https://doi.org/10.1074/jbc.M110.182600

Reisberg, B., Doody, R., Stöffler, A., Schmitt, F., Ferris, S., & Möbius, H. J. (2003). Memantine in moderate-to-severe Alzheimer's disease. *New England Journal of Medicine*, *348*(14), 1333–1341. https://doi.org/10.1056/nejmoa013128

Rong, Y., Lu, X., Bernard, A., Khrestchatisky, M., & Baudry, M. (2001). Tyrosine phosphorylation of ionotropic glutamate receptors by Fyn or Src differentially modulates their susceptibility to calpain and enhances their binding to spectrin and PSD-95. *Journal of Neurochemistry*, *79*(2), 382–390. https://doi.org/10.1046/j.1471-4159.2001.00565.x

Shariati, S. A. M., & de Strooper, B. (2013). Redundancy and divergence in the amyloid precursor protein family. *FEBS Letters*, *587*(13), 2036–2045. https://doi.org/10.1016/j.febslet.2013.05.026

Silva, M. M., Rodrigues, B., Fernandes, J., Santos, S. D., Carreto, L., Santos, M. A. S., Pinheiro, P., & Carvalho, A. L. (2019). MicroRNA-186-5p controls GluA2 surface expression and synaptic scaling in hippocampal neurons. *Proceedings of the National Academy of Sciences of the United States of America*, *116*(12), 5727–5736. https://doi.org/10.1073/pnas.1900338116

Sobczyk, A., Scheuss, V., & Svoboda, K. (2005). NMDA receptor subunit-dependent [Ca2+] signaling in individual hippocampal dendritic spines. *Journal of Neuroscience*, *25*(26), 6037–6046. https://doi.org/10.1523/JNEUROSCI.1221-05.2005

Steubler, V., Erdinger, S., Back, M. K., Ludewig, S., Fässler, D., Richter, M., Han, K., Slomianka, L., Amrein, I., Engelhardt, J., Wolfer, D. P., Korte, M., & Müller, U. C. (2021). Loss of all three APP family members during development impairs synaptic function and plasticity, disrupts learning, and causes an autism-like phenotype. *The EMBO Journal*, *40*(12), e107471. https://doi.org/10.15252/embj.2020107471

Suzuki, Y. (2012). Exploring transduction mechanisms of protein transduction domains (PTDs) in living cells utilizing single-quantum dot tracking (SQT) technology. *Sensors*, *12*(1), 549–572. https://doi.org/10.3390/s120100549

Temido-Ferreira, M., Ferreira, D. G., Batalha, V. L., Marques-Morgado, I., Coelho, J. E., Pereira, P., Gomes, R., Pinto, A., Carvalho, S., Canas, P. M., Cuvelier, L., Buée-Scherrer, V., Faivre, E., Baqi, Y., Müller, C. E., Pimentel, J., Schiffmann, S. N., Buée, L., Bader, M., … Lopes, L. V. (2020). Age-related shift in LTD is dependent on neuronal adenosine A2A receptors interplay with mGluR5 and NMDA receptors. *Molecular Psychiatry*, *25*(8), 1876–1900. https://doi.org/10.1038/s41380-018-0110-9

Thibault, O., Hadley, R., & Landfield, P. W. (2001). Elevated postsynaptic [CA2+]i and L-type calcium channel activity in aged hippocampal neurons: Relationship to impaired synaptic plasticity. *Journal of Neuroscience*, *21*(24), 9744–9756. https://doi.org/10.1523/jneurosci.21-24-09744.2001

Tombaugh, G. C., Rowe, W. B., Chow, A. R., Michael, T. H., & Rose, G. M. (2002). Theta-frequency synaptic potentiation in CA1 in vitro distinguishes cognitively impaired from unimpaired aged Fischer 344 rats. *Journal of Neuroscience*, *22*(22), 9932–9940. https://doi.org/10.1523/jneurosci.22-22-09932.2002

Tomé, S. O., Gomes, L. A., Li, X., Vandenberghe, R., Tousseyn, T., & Thal, D. R. (2021). TDP-43 interacts with pathological τ protein in Alzheimer's disease. *Acta Neuropathologica*, *141*(5), 795–799. https://doi.org/10.1007/s00401-021-02295-2

van der Kant, R., & Goldstein, L. S. B. (2015). Cellular functions of the amyloid precursor protein from development to dementia. *Developmental Cell*, *32*(4), 502–515. https://doi.org/10.1016/j.devcel.2015.01.022

von Engelhardt, J., Doganci, B., Jensen, V., Hvalby, Ø., Göngrich, C., Taylor, A., Barkus, C., Sanderson, D. J., Rawlins, J. N. P., Seeburg, P. H., Bannerman, D. M., & Monyer, H. (2008). Contribution of

hippocampal and extra-hippocampal NR2B-containing NMDA receptors to performance on spatial learning tasks. *Neuron*, *60*(5), 846–860. https://doi.org/10.1016/j.neuron.2008.09.039

Willem, M., Tahirovic, S., Busche, M. A., Ovsepian, S., Chafai, M., Kootar, S., Hornburg, D., Evans, L. D. B., Moore, S., Daria, A., Hampel, H., Müller, V., Giudici, C., Nuscher, B., Wenninger-Weinzierl, A., Kremmer, E., Heneka, M. T., Thal, D. R., Giedraitis, V., … Haass, C. (2015). σ-Secretase processing of APP inhibits neuronal activity in the hippocampus. *Nature*, *526*(7573), 443–447. https://doi.org/10.1038/nature14864

Williams, K., Russell, S. L., Shen, Y. M., & Molinoff, P. B. (1993). Developmental switch in the expression of NMDA receptors occurs in vivo and in vitro. *Neuron*, *10*(2), 267–278. https://doi.org/10.1016/0896-6273(93)90317-K

Wolfe, M. S., Xia, W., Ostaszewski, B. L., Diehl, T. S., Kimberly, W. T., & Selkoe, D. J. (1999). Two transmembrane aspartates in presenilin-1 required for presenilin endoproteolysis and γ-secretase activity. *Nature*, *398*(6727), 513–517. https://doi.org/10.1038/19077

Yashiro, K., & Philpot, B. D. (2008). Regulation of NMDA receptor subunit expression and its implications for LTD, LTP, and metaplasticity. *Neuropharmacology*, *55*(7), 1081–1094. https://doi.org/10.1016/j.neuropharm.2008.07.046

Young-Pearse, T. L., Bai, J., Chang, R., Zheng, J. B., Loturco, J. J., & Selkoe, D. J. (2007). A critical function for β-amyloid precursor protein in neuronal migration revealed by in utero RNA interference. *Journal of Neuroscience*, *27*(52), 14459–14469. https://doi.org/10.1523/JNEUROSCI.4701-07.2007

Zamzow, D. R., Elias, V., Shumaker, M., Larson, C., & Magnusson, K. R. (2013). An increase in the association of GluN2B containing NMDA receptors with membrane scaffolding proteins was related to memory declines during aging. *Journal of Neuroscience*, *33*(30), 12300–12305. https://doi.org/10.1523/JNEUROSCI.0312-13.2013

Zhao, X., Rosenke, R., Kronemann, D., Brim, B., Das, S. R., Dunah, A. W., & Magnusson, K. R. (2009). The effects of aging on N-methyl-d-aspartate receptor subunits in the synaptic membrane and relationships to long-term spatial memory. *Neuroscience*, *162*(4), 933–945. https://doi.org/10.1016/j.neuroscience.2009.05.018

Zhou, Q., & Sheng, M. (2013). NMDA receptors in nervous system diseases. *Neuropharmacology*, *74*, 69–75. https://doi.org/10.1016/j.neuropharm.2013.03.030

SUPPORTING INFORMATION

Additional supporting information can be found online in the Supporting Information section at the end of this article.

How to cite this article: Rajão-Saraiva, J., Dunot, J., Ribera, A., Temido-Ferreira, M., Coelho, J. E., König, S., Moreno, S., Enguita, F. J., Willem, M., Kins, S., Marie, H., Lopes, L. V., & Pousinha, P. A. (2022). Age-dependent NMDA receptor function is regulated by the amyloid precursor protein. *Aging Cell*, *00*, e13778. https://doi.org/10.1111/acel.13778